

# Physiological and Biochemical Aspects of 17 $\beta$ -Hydroxysteroid Dehydrogenase Type 2 and 3

**Inauguraldissertation**

zur

Erlangung der Würde eines Doktors der Philosophie  
vorgelegt der  
Philosophisch-Naturwissenschaftlichen Fakultät  
der Universität Basel

von

Roger Thomas Engeli  
aus Sulgen (TG), Schweiz

Basel, 2017

Originaldokument gespeichert auf dem Dokumentenserver der Universität Basel  
[edoc.unibas.ch](http://edoc.unibas.ch)



Dieses Werk ist lizenziert unter einer [Creative Commons Namensnennung-Nicht kommerziell 4.0 International Lizenz](https://creativecommons.org/licenses/by-nc/4.0/).

Genehmigt von der Philosophisch-Naturwissenschaftlichen Fakultät  
auf Antrag von Prof. Dr. Alex Odermatt und Prof. Dr. Rik Eggen

Basel, den 20.06.2017

---

Dekan  
Prof. Dr. Martin Spiess

# Table of Contents

<b>Table of Contents</b> .....	<b>3</b>
<b>Abbreviations</b> .....	<b>4</b>
<b>1. Summary</b> .....	<b>6</b>
<b>2. Introduction</b> .....	<b>8</b>
2.1 Steroid Hormones .....	8
2.2 Human Steroidogenesis.....	11
2.3 Hydroxysteroid Dehydrogenases .....	12
2.3.1 17 $\beta$ -Hydroxysteroid Dehydrogenases .....	13
<b>3. Project 1: 17<math>\beta</math>-Hydroxysteroid Dehydrogenase Type 2</b> .....	<b>14</b>
3.1 Introduction.....	14
3.2 Paper 1 (Vuorinen et al., 2014) .....	17
3.3 Paper 2 (Vuorinen/Engeli et al., 2017a) .....	31
3.4 Paper 3 (Vuorinen/Engeli et al., 2017b) .....	36
3.5 Paper 4 (Engeli et al., in preparation).....	47
3.7 Conclusion .....	62
<b>4. Project 2: 17<math>\beta</math>-Hydroxysteroid Dehydrogenase Type 3</b> .....	<b>64</b>
4.1 Introduction.....	64
4.2 Paper 5 (Engeli et al., 2016).....	66
4.3 Paper 6 (Ben Rhouma et al., 2017).....	75
4.4 Paper 7 (Engeli et al, submitted) .....	85
4.5 Conclusion .....	106
<b>5. Project 3: Murine Leydig Cell Lines</b> .....	<b>109</b>
5.1 Introduction.....	109
5.2 Paper 8 (Odermatt et al, 2016) .....	111
5.3 Paper 9 (Engeli et al, in preparation).....	125
5.4 Conclusion .....	152
<b>6. Acknowledgments</b> .....	<b>155</b>
<b>7. Appendix</b> .....	<b>155</b>
<b>8. References</b> .....	<b>157</b>

## Abbreviations

17 $\beta$ -HSD1:	17 $\beta$ -Hydroxysteroid Dehydrogenase type 1
17 $\beta$ -HSD2:	17 $\beta$ -Hydroxysteroid Dehydrogenase type 2
17 $\beta$ -HSD3:	17 $\beta$ -Hydroxysteroid Dehydrogenase type 3
17 $\beta$ -HSD5:	17 $\beta$ -Hydroxysteroid Dehydrogenase type 5
3 $\beta$ -HSD:	3 $\beta$ -Hydroxysteroid Dehydrogenase
AKR:	Aldo-keto Reductase
AR:	Androgen Receptor
CAIS:	Complete Androgen Insensitivity Syndrome
CYP:	Cytochrome P450
DHEA:	Dehydroepiandrosterone
DHT:	Dihydrotestosterone
DNA:	Deoxyribonucleic Acid
DSD:	Disorder of Sexual Development
EDC:	Endocrine Disrupting Chemical
ELISA:	Enzyme-linked Immunosorbent Assay
ER:	Endoplasmic Reticulum
ER $\alpha$ :	Estrogen Receptor Alpha
ER $\beta$ :	Estrogen Receptor Beta
GC-MS:	Gas Chromatography-mass Spectrometry
GR:	Glucocorticoid Receptor
hCG:	Human Chorionic Gonadotropin
HSD:	Hydroxysteroid Dehydrogenase
HPA:	Hypothalamic-pituitary-adrenal axis
LC-MS:	Liquid Chromatography-mass Spectrometry



LH:	Luteinizing Hormone
MR:	Mineralocorticoid Receptor
mRNA:	Messenger Ribonucleic Acid
NAD+:	Nicotinamide Adenine Dinucleotide
NADPH:	Nicotinamide Adenine Dinucleotide Phosphate
P450c17:	17 $\alpha$ -hydroxylase, 17,20 lyase
P450scc:	Cholesterol Side-Chain Cleavage Enzyme
PAIS:	Partial Androgen Insensitivity Syndrome
SAR:	Structure-activity Relationship
SDR:	Short-chain Dehydrogenase/Reductase
StAR:	Steroidogenic Acute Regulatory Protein
TBT:	Tributyltin
TPT:	Triphenyltin

## 1. Summary

Steroid hormones regulate a broad variety of physiological functions through the transcriptional regulation of target genes. The active steroid hormones discussed in this thesis largely elicit their physiological effects through the activation of nuclear receptors. Many of these receptors reside in their inactive form in the cytoplasm, translocate to the nucleus upon ligand binding and drive the transcription of target genes. The local interconversion of active and inactive steroid hormones is regulated by members of 17 $\beta$ -hydroxysteroid dehydrogenases/reductases (17 $\beta$ -HSDs). The enzyme 17 $\beta$ -HSD2 converts active estrogen estradiol and the potent androgen testosterone to its inactive keto-forms, whereas 17 $\beta$ -HSD3 mainly converts androstenedione into testosterone. The present thesis is split into three major projects that focus mainly on potential toxicological and therapeutic effects of inhibiting the enzyme 17 $\beta$ -HSD2 and biochemical aspects of the enzymes 17 $\beta$ -HSD3.

The first project was designed to develop a 17 $\beta$ -HSD2 pharmacophore model and subsequently use this model as a virtual screening tool to identify novel nonsteroidal 17 $\beta$ -HSD2 inhibitors. It has been hypothesized that pharmacological inhibition of the enzyme 17 $\beta$ -HSD2 expressed in osteoclasts could be a useful strategy to treat osteoporosis through increasing local concentrations of active sex hormones. Our approach was initiated through the development of a pharmacophore model that underwent several rounds of experimental validation and improvement. *In silico* screening of internal and external compound databases using the optimized pharmacophore model resulted in the identification of several novel nonsteroidal compounds that inhibit 17 $\beta$ -HSD2 at nanomolar concentrations *in vitro*. Furthermore, the virtual screening of a cosmetic ingredients database revealed several paraben compounds as potential 17 $\beta$ -HSD2 inhibitors. *In vitro* examinations revealed that all tested paraben compounds were found to significantly inhibit 17 $\beta$ -HSD2 at a concentration of 20  $\mu$ M. However, parabens are rapidly metabolized to *p*-hydroxybenzoic acid, which does not influence 17 $\beta$ -HSD2 activity. We reported a novel potential estrogenic effect of paraben compounds by inhibiting 17 $\beta$ -HSD2 although their estrogenic potential is unlikely to be of toxicological concern due to their rapid metabolism by esterases.

In the second project we biochemically analyzed six mutations in the *HSD17B3* gene that were associated to cause 17 $\beta$ -HSD3 deficiency in Egyptian and Tunisian patients with 46, XY disorder

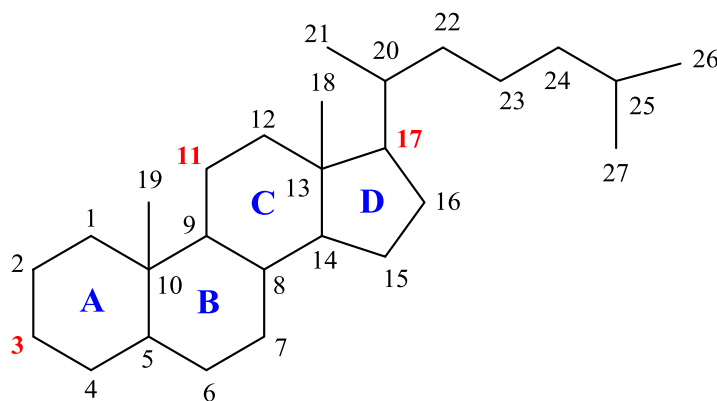
of sexual development (DSD). Patients with 17 $\beta$ -HSD3 deficiency are unable to synthesize sufficient amounts of testosterone during embryogenesis which leads to severe undervirilization of internal and external genitals. All tested mutations (G133R, C206X, T54A, M164T, and L194T) were confirmed to be nearly inactive *in vitro* and therefore unable to sufficiently convert androstenedione into testosterone. Further analyses showed that the G289S polymorphism exhibited a similar rate of testosterone formation as the wild type 17 $\beta$ -HSD3 enzyme and consequently cannot be causing the pathogenesis of 46, XY DSD. All *HSD17B3* mutations associated with 46, XY DSD in this project were predicted by an *in silico* 17 $\beta$ -HSD3 homology model (based on the structure of 17 $\beta$ -HSD1) to interfere with either cofactor (NADPH) or substrate (androstenedione) binding sites. The G289S polymorphism however, was located on the surface of the enzyme without eliciting any effects on the cofactor or substrate active sites. Besides its critical role in sexual differentiation, testosterone regulates a variety of physiological functions. The vast majority of testosterone is produced in testicular Leydig cells. The final project in the thesis focused on reviewing the *in vitro* models available for investigating androgen disruption by xenobiotics. Our *in vitro* investigations focused on validating the three most promising Leydig cell lines (MA-10, BLTK, TM3) for their potential to report androgen disruption by xenobiotic compounds through alteration of 17 $\beta$ -HSD3 activity and transcription. Our experiments revealed that these cell lines express minimal levels of 17 $\beta$ -HSD3 mRNA compared to freshly isolated mouse testes. Furthermore, the cell lines also exhibited a low rate of androstenedione to testosterone formation. In conclusion, all tested cell lines are not useful as screening tool to test androgen disruption by xenobiotic compounds due to the lack of endogenous 17 $\beta$ -HSD3.

Through the work described in this thesis, we have developed and optimized an *in silico* 17 $\beta$ -HSD2 pharmacophore model for the identification of inhibitors of the enzyme. We then confirmed and mechanistically evaluated mutations in the *HSD17B3* gene associated with 46, XY DSD and finally investigated Leydig cell models to test testosterone disruption by xenobiotic compounds. Altogether, these findings significantly expand the knowledge about physiological and biochemical aspects of the enzymes 17 $\beta$ -HSD2 and 17 $\beta$ -HSD3.

## 2. Introduction

### 2.1 Steroid Hormones

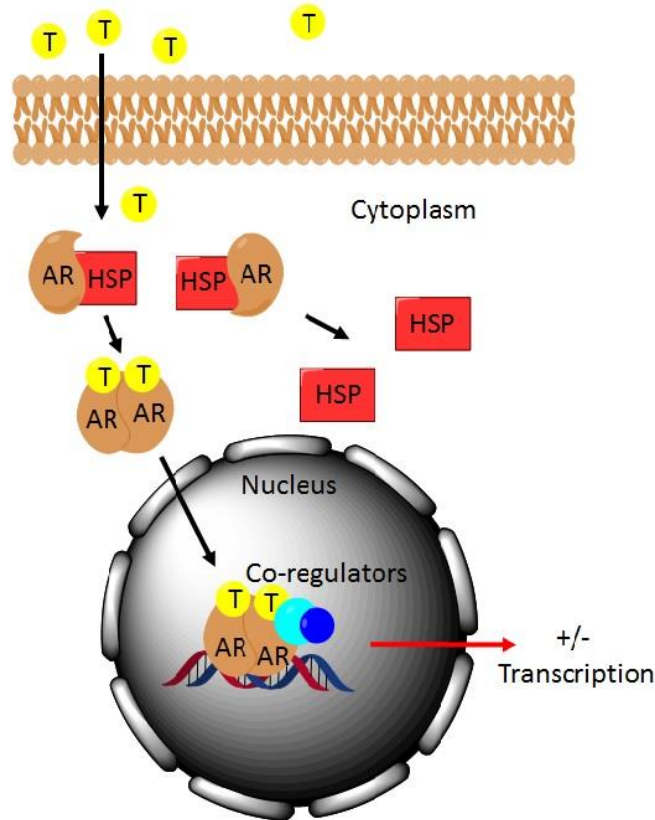
Steroid hormones are organic compounds with a broad variety of functions that are involved in almost every aspect of development and regulation of physiological processes[1, 2]. Most steroids act as signaling hormones on nuclear receptors in target tissues[3]. Upon steroid binding in the cytoplasm (Figure 2) or in the nucleus, nuclear receptors undergo conformational changes that lead to dissociation of accessory proteins[4]. Dissociated cytosolic nuclear receptors are able to translocate to the nucleus, where they bind to specific response elements (RE) located on deoxyribonucleic acid (DNA) and therefore initiating target gene transcription[5-7]. All steroids share a common planar basic sterane structure (Figure1), which is rigid and consists of three cyclohexane rings (A,B,C) and one cyclopentane ring fused together (D)[8].



**Figure 1.** Basic steroid chemical structure. (Carbons = numbers, rings = letters)

Generally, steroid hormones can be classified into five different groups; including progestogens, mineralocorticoids, glucocorticoids, androgens, and estrogens[9]. Progestogens, mineralocorticoids, and glucocorticoids consist of 21 carbon atoms, while androgens and estrogens consist of 19 and 18 carbons respectively[10, 11]. Steroid hormones bind and activate different nuclear receptors with different affinities[4, 12]. In order to activate their target nuclear receptors, steroid hormones have to be activated from their inactive forms, which allows for tight regulation[13]. Progestogens act on the progesterone receptor (PR) and are important for female reproduction[14]. Mineralocorticoids (mainly aldosterone) activate the mineralocorticoid receptor (MR) and regulate water retention in the kidneys by increasing sodium transport and potassium excretion[15]. Glucocorticoids (mainly cortisol) mediate their action through the

activation of the glucocorticoid receptor (GR), regulating many processes including the stress response, energy metabolism, and the immune system response[16-18]. In addition, glucocorticoids are able to activate the MR[19]. Hormonally active androgens initiate male development and maintain male physical characteristics through the activation of the androgen receptor (AR)[20]. Testosterone and dihydrotestosterone (DHT) are the most potent and predominant physiological active androgens in humans[21]. Estrogens belong to the sex hormones and induce the development of female sexual characteristics[22]. Estradiol is the most potent estrogen and induces its effect through activation of the estrogen receptor alpha (ER $\alpha$ ) and estrogen receptor beta (ER $\beta$ )[23]. All steroid hormones are derived from cholesterol, which is *de novo* synthesized in specific cells or absorbed from food[24]. The synthesis of steroid hormones occurs in specific cells in the gonads and the adrenals. Adrenal and gonadal steroidogenesis are under the control of the hypothalamus and pituitary gland, respectively[25, 26]. Luteinizing hormone (LH) secreted by the pituitary gland stimulates gonadal steroidogenesis. Systemic testosterone and estradiol levels independently control the secretion of hypothalamic LH releasing hormone by regulating negative feedback loops[27]. The pituitary gland releases LH following stimulation by LH releasing hormone[28]. Adrenal steroid homeostasis is controlled by the hypothalamic-pituitary-adrenal axis (HPA). Briefly, low circulating cortisol levels effect hypothalamic release of corticotropin-releasing hormone (CRH) through a negative feedback[29, 30]. CRH stimulates the release of adrenocorticotrophic hormone (ACTH) from the anterior pituitary gland into peripheral circulation[31]. Mineralo- and glucocorticoids are synthesized in the zona glomerulosa and the zona fasciculata of the adrenal cortex, respectively. However, local peripheral interconversion of active and inactive glucocorticoids by specific enzymes also plays a critical role in the regulation of physiological processes[32].

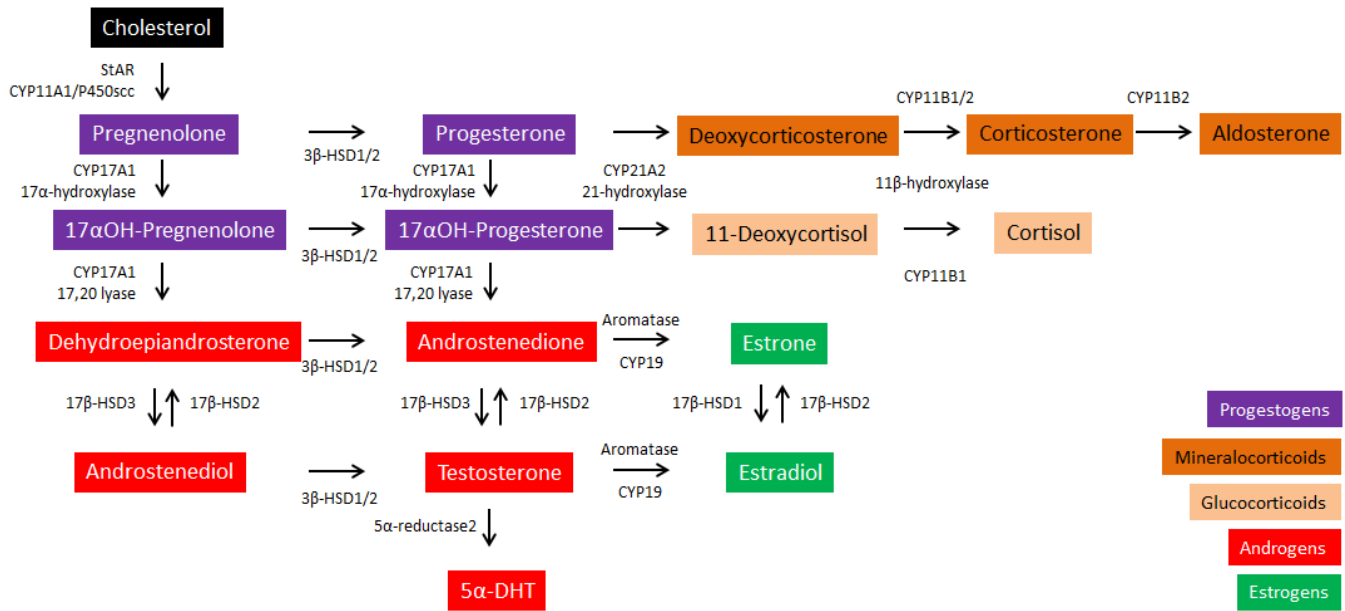


**Figure 2.** Nuclear signaling pathway of testosterone. Modified from Levin et al[4]. (AR = androgen receptor; T = testosterone; HSP = heat shock protein)

Additionally, the zona reticularis in the adrenal cortex produces the systemic sex hormone precursors DHEA and DHEA sulfate[33]. Generally, female and male sex hormones are produced in specific cells of the gonads. Men produce the majority of testosterone in testicular Leydig cells whilst females produce sex hormones in the ovarian theca and granulosa cells[34, 35]. However, the majority of systemic estrogens and androgens in females are produced in the peripheral tissues from the inactive adrenal precursors DHEA and DHEA sulfate[36]. It is noteworthy that intracrinological and peripheral steroid production have an enormous impact on systemic steroid hormone levels[37]. The majority of circulating sex steroids are bound to sex hormone-binding globulin, cortisol-binding globulin, and albumin with various binding affinities[17, 38, 39]. However, only free and weakly bound circulating steroids are considered to be biologically active[40]. Steroid hormones are eliminated mainly through the urine and to a lesser extent in the feces in various conjugated forms[41].

## 2.2 Human Steroidogenesis

Human steroidogenesis involves interactions of many crucial enzymes, cofactors, and regulators etc. A comprehensive overview of steroid synthesis is reported by Payne and Hales[42]. Figure 3 illustrates a brief overview of the most important human enzymes involved in steroid synthesis.



**Figure 3.** Overview of human steroid synthesis and their classification in five groups (Progestogens, mineralocorticoids, glucocorticoids, androgens, and estrogens). Modified from Häggström et al[43].

Generally, two types of protein classes are responsible for the biosynthesis of steroid hormones. The heme-containing cytochrome P450 enzymes (CYP) as well as the hydroxysteroid dehydrogenases (HSD)[44]. Steroidogenesis involves the biosynthesis of steroid hormones from the common precursor cholesterol[24]. Cholesterol is actively transported by the steroidogenic acute regulatory protein (StAR) into the inner mitochondrial membrane where it is converted by the cholesterol side-chain cleavage enzyme (P450scc) into pregnenolone[24]. Pregnenolone undergoes further metabolism in the endoplasmic reticulum (ER). Depending on the expression levels of specific enzymes in the ER, pregnenolone is converted into progesterone by 3β-hydroxysteroid dehydrogenase type 1 and 2 (3β-HSD1/2)[45, 46]. Progesterone itself is an active progestogen but can further be converted into the active mineralocorticoid aldosterone, by 21-

hydroxylase (*CYP21*, ER), 11-hydroxylase (*CYP21*, mitochondria) and finally aldosterone synthase (*CYP11B2*, mitochondria)[47-49]. For the biosynthesis of glucocorticoids, pregnenolone is converted into 17 $\alpha$ -hydroxy pregnenolone by the enzyme 17 $\alpha$ -hydroxylase, 17,20 lyase (P450c17, *CYP17A1*)[50]. For the final synthesis of cortisol, 3 $\beta$ -HSD1 or 2, 21-hydroxylase (*CYP21*), and 11-hydroxylase (*CYP11B1*) are involved[51]. Alternatively, to synthesize androgens and estrogens, 17-hydroxy pregnenolone is converted into dehydroepiandrosterone (DHEA) by P450c17. During this reaction, cytochrome b<sub>5</sub> acts as an allosteric effector of P450c17 to augment its 17,20 lyase activity[52]. DHEA is converted into the inactive androgen, androstenedione, by 3 $\beta$ -HSD1 or 2 in the ER[45, 46]. In order to activate the potent androgens, testosterone and DHT, the expression of 17 $\beta$ -hydroxysteroid dehydrogenase type 3 (17 $\beta$ -HSD3)[53] and 5 $\alpha$ -reductase type 2[54] is essential. Estrogens can be produced from androstenedione or testosterone by the enzyme aromatase (*CYP19*)[55]. Additionally, the interconversion of active and inactive steroid hormones and the intracrinological active steroid production from inactive precursors are regulated by many genes located in various peripheral tissues such as brain, fat tissue, liver, prostate, intestines and skin[56-62].

### **2.3 Hydroxysteroid Dehydrogenases**

The hydroxysteroid dehydrogenases, which catalyze the biosynthesis of steroids, belong to two protein superfamilies, the SDRs and aldo-keto reductases (AKRs)[63]. Most human HSDs belong in the SDR superfamily and play a major role in sex steroid synthesis. In humans, important HSDs of the AKR superfamily involved in steroidogenesis are AKR1C1 (20 $\alpha$ -HSD1), AKR1C2 (3 $\alpha$ -HSD3), AKR1C3 (17 $\beta$ -HSD5), and AKR1C4 (3 $\alpha$ -HSD1)[64, 65]. They share an overall sequence identity of about 86% and consist of a basic structure containing  $\alpha$ -helices and  $\beta$ -strands that repeats 8 times to form a barrel like tertiary structure[13]. In contrast, HSDs exhibit a very low sequence identity of less than 30% despite sharing characteristic conformational protein structures including a common Gly-XXX-Gly-X-Gly pattern in the cofactor binding site[66]. Additionally, the cofactor binding site of HSDs in the SDR superfamily contain a Rossmann fold. The Rossmann fold consists of up to seven parallel  $\beta$ -sheets surrounded by at least six  $\alpha$ -helices[67, 68]. The substrate binding



domain contained within SDRs, consists of a typical Asn-Ser-Tyr-Lys motif[68]. Important members of HSDs in steroidogenesis are 3 $\beta$ -HSD1 and 2, 11 $\beta$ -HSD1 and 2, and 17 $\beta$ -HSD1-3[68].

### 2.3.1 17 $\beta$ -Hydroxysteroid Dehydrogenases

Several members of the 17 $\beta$ -HSDs were of particular interest in this thesis. To date, 14 different subtypes of human 17 $\beta$ -HSDs have been identified[69, 70]. In addition, retinol dehydrogenase type 5 (RDH5) has been described in the literature which is also known as HSD17B9[71, 72]. The majority of enzymes investigated in this thesis belong to the SDR superfamily with the exception of 17 $\beta$ -HSD5 which is an AKR[73]. 17 $\beta$ -HSDs catalyze the interconversion of steroids,  $\beta$ -oxidation of fatty acids, retinoic metabolism and cholesterologenesis[71, 74-76]. However, many physiological functions of HSDs are still not well investigated. Bidirectional conversion properties of most of the 17 $\beta$ -HSDs impedes the evaluation of the physiological function *in vitro*[77]. Besides, 17 $\beta$ -HSDs are capable to convert various substrates on different carbon positions[70]. *In vitro* studies showed that some 17 $\beta$ -HSDs additionally possess 3  $\alpha/\beta$ , 20  $\alpha/\beta$ , or 21 activities[70, 78, 79]. This clearly indicates that enzymes have been classified as 17 $\beta$ -HSDs because of their capability to modify steroids at carbon position 17 without carefully investigating other potential major substrates. However, members of the HSDs have been reported to be potential prognostic cancer markers and potential drug targets[68]. Altered regulation of 17 $\beta$ -HSDs is associated with endocrine related cancer progression due to their ability to control intracellular active sex steroid hormones[80]. Additionally, the HSDs play an important role in regulating sexual differentiation and sexual development during embryogenesis and puberty[22, 81].

In conclusion, 17 $\beta$ -HSDs play a major role in the interconversion of sex steroid hormones. This thesis mainly focused on the identification of compounds that inhibit 17 $\beta$ -HSD2 and on the biochemical evaluation of mutations in the 17 $\beta$ -HSD3 enzyme.

## **3. Project 1: 17 $\beta$ -Hydroxysteroid Dehydrogenase Type 2**

### **3.1 Introduction**

This project is split into two major studies based on the enzyme 17 $\beta$ -HSD2. The first main study, describes three sub investigations, which focus on the identification of nonsteroidal compounds that inhibit the enzyme 17 $\beta$ -HSD2, as a novel potential approach to treat osteoporosis. The second major study, focuses on potential endocrine disrupting effects of paraben compounds targeting 17 $\beta$ -HSD1 and 2.

Several human 17 $\beta$ -HSD members play a pivotal role in the final biosynthesis of sex hormones[82]. The enzyme 17 $\beta$ -HSD2 primarily oxidizes the active estrogen estradiol and the active androgen testosterone into their inactive keto-forms estrone and androstenedione respectively, using nicotinamide adenine dinucleotide (NAD<sup>+</sup>) as cofactor. Additionally, 17 $\beta$ -HSD2 converts androstenediol into DHEA and the most potent androgen DHT into 5 $\alpha$ -androstenedione[83]. Generally, 17 $\beta$ -HSD2 protects specific tissues from excessive amounts of active sex hormones. The enzyme 17 $\beta$ -HSD2 consists of 387 amino acids, is located on chromosome 16, and is mainly expressed in the placenta, liver, bones, small intestines, endometrium, ovaries and prostate. [82, 84, 85]. The enzyme 17 $\beta$ -HSD2 is an endoplasmic reticulum (ER) membrane protein with its catalytic moiety facing the cytoplasm[86].

The conversion from estrone into estradiol is efficiently catalyzed by the enzyme 17 $\beta$ -HSD1 using nicotinamide adenine dinucleotide phosphate (NADPH) as cofactor. Additionally, 17 $\beta$ -HSD1 is able to convert androstenedione into testosterone but with less efficiency compared to the conversion of estrone into estradiol[87, 88]. The enzyme 17 $\beta$ -HSD1 consists of 328 amino acids, is a cytosolic homodimer, and is located in placenta, ovary, endometrium, and breast[89-92].

The inhibition of 17 $\beta$ -HSD1 may decrease the systemic and local concentration of estradiol which could affect the onset of osteoporosis. In the two major studies presented, every tested compound that significantly inhibited 17 $\beta$ -HSD2 (>70% inhibition at 20  $\mu$ M compared to DMSO control) was also tested against 17 $\beta$ -HSD1 to get first insights about their selectivity.

In the EU, the prevalence of people suffering from osteoporosis is high with estimated 27.5 million affected people in 2010[93]. Osteoporosis is a condition where decreased bone density and reduced bone mass results in increased risk of bone fractures[94]. The balance of osteoblast and osteoclast activity is crucial for maintenance of healthy bone homeostasis. In the elderly,

decreased bone density is linked to locally decreased concentrations of active estrogens and androgens[95-97]. In osteoclasts, estradiol and testosterone inhibit bone degradation[98]. To date, typical anti-osteoporosis drugs, such as selective estrogen modulators, bisphosphonates, or hormone replacement therapy bear several disadvantages and side effects[99, 100]. New therapeutic approaches are of particular interest. Local inhibition of 17 $\beta$ -HSD2 by specific nonsteroidal inhibitors increase estradiol and testosterone concentrations and therefore stimulate the reduction of bone resorption in osteoclasts. The potential of this treatment has recently been demonstrated in a study from Bagi et al., where they showed reduced bone resorption in ovariectomized cynomolgus monkeys treated with a 17 $\beta$ -HSD2 inhibitor[101].

The application of pharmacophore models was used to identify novel inhibitors of the enzyme 17 $\beta$ -HSD2. Virtual screening of pharmacophore models was applied to pre-screen several databases containing >200'000 chemical compounds. This screening method allows a cost-efficient and fast pre-selection of potential hit compounds[102]. The ligand-based 17 $\beta$ -HSD2 pharmacophore model was designed by Daniela Schuster and Anna Vuorinen using LigandScout[103]. Pharmacophore models characterize a three dimensional arrangement of chemical features and interactions of a specific substrate and its binding pocket. In the case of the 17 $\beta$ -HSD2 pharmacophore models, these features correspond to hydrogen bond donors, hydrogen bond acceptors, hydrophobic areas, and aromatic rings. Additionally, exclusion volumes were added that mimic steric limitations within the binding pocket. Originally, three ligand-based 17 $\beta$ -HSD2 pharmacophore models were designed and used for screening databases. These models were constantly improved using data generated from *in vitro* experiments from all tested compounds over the years. To date, model A has been shown to generate most of the active hit compounds and has been chosen as the standard 17 $\beta$ -HSD2 pharmacophore model to pre-screen databases.

The first sub investigation, of the first major project, focused on establishing a ligand-based pharmacophore model to identify potent nonsteroidal compounds that inhibit the enzyme 17 $\beta$ -HSD2. The second sub investigation was a follow up project focusing on improving the chemistry of identified compounds with respect to improving potency and eliminating potential side chains which are susceptible to metabolic modifications. The third sub investigation focused on the identification of natural products that inhibit 17 $\beta$ -HSD2 as potential lead compounds. In

summary, the focus of the first three sub investigations were to identify novel nonsteroidal 17 $\beta$ -HSD2 inhibitors. Inhibition of 17 $\beta$ -HSD2 in bone cells could lead to a local increase of sex hormones, eventually reducing bone resorption and therefore diminishing the onset of osteoporosis.

The focus on the second major study clearly differs from the first, since we investigated the potential consequences of inhibiting the enzyme 17 $\beta$ -HSD2. This study focused on potential endocrine disrupting effects of xenobiotics that inhibit 17 $\beta$ -HSD2. Screening a database containing ingredients of cosmetic products using the 17 $\beta$ -HSD2 pharmacophore model revealed several paraben compounds as potential inhibitors. Parabens have been proposed to possess endocrine disrupting properties[104-107]. Inhibition of 17 $\beta$ -HSD2 is suspected to contribute to endocrine disruption effects caused by parabens and was therefore further investigated in this study. Moreover, the human exposure to parabens is high due to its widespread use in cosmetic products, foods, and beverages[108, 109]. In total 10 parabens were chosen for biochemical *in vitro* evaluation.

### 3.2 Paper 1 (Vuorinen et al., 2014)

## Ligand-based pharmacophore modeling and virtual screening for the discovery of novel 17 $\beta$ -hydroxysteroid dehydrogenase 2 inhibitors

Anna Vuorinen, Roger T. Engeli, Arne Meyer, Fabio Bachmann, Ulrich J. Griesser, Daniela Schuster, Alex Odermatt

Published manuscript

**Contribution:** Provided the biochemical data of the lysate activity assays (Table 2 and 3). Drafting the materials and methods part on the activity assay description.

**Aims:** Identify novel non-steroidal 17 $\beta$ -HSD2 inhibitors using a ligand-based pharmacophore model as screening tool.

**Main Results:** The most potent hits identified, 12, 22 and 15, were selective over 17 $\beta$ -HSD1 and had IC<sub>50</sub> values of 240 nM, 1  $\mu$ M, and 1.5  $\mu$ M, respectively.

**Conclusion:** This study showed that the applied pharmacophore model is a powerful tool to predict novel selective 17 $\beta$ -HSD2 inhibitors from a screened library of compounds.

# Ligand-Based Pharmacophore Modeling and Virtual Screening for the Discovery of Novel 17 $\beta$ -Hydroxysteroid Dehydrogenase 2 Inhibitors

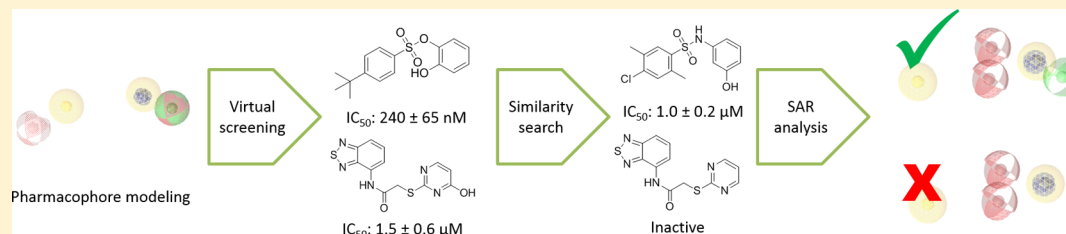
Anna Vuorinen,<sup>†</sup> Roger Engeli,<sup>‡</sup> Arne Meyer,<sup>‡</sup> Fabio Bachmann,<sup>‡</sup> Ulrich J. Griesser,<sup>§</sup> Daniela Schuster,<sup>\*†</sup> and Alex Odermatt<sup>\*‡</sup>

<sup>†</sup>Institute of Pharmacy/Pharmaceutical Chemistry and Center for Molecular Biosciences Innsbruck – CMBI, University of Innsbruck, Innrain 80/82, 6020 Innsbruck, Austria

<sup>‡</sup>Swiss Center for Applied Human Toxicology and Division of Molecular and Systems Toxicology, Department of Pharmaceutical Sciences, University of Basel, Klingelbergstrasse 50, 4056 Basel, Switzerland

<sup>§</sup>Institute of Pharmacy/Pharmaceutical Technology, University of Innsbruck, Innrain 52c, 6020 Innsbruck, Austria

## Supporting Information



**ABSTRACT:** 17 $\beta$ -Hydroxysteroid dehydrogenase 2 (17 $\beta$ -HSD2) catalyzes the inactivation of estradiol into estrone. This enzyme is expressed only in a few tissues, and therefore its inhibition is considered as a treatment option for osteoporosis to ameliorate estrogen deficiency. In this study, ligand-based pharmacophore models for 17 $\beta$ -HSD2 inhibitors were constructed and employed for virtual screening. From the virtual screening hits, 29 substances were evaluated in vitro for 17 $\beta$ -HSD2 inhibition. Seven compounds inhibited 17 $\beta$ -HSD2 with low micromolar IC<sub>50</sub> values. To investigate structure–activity relationships (SAR), 30 more derivatives of the original hits were tested. The three most potent hits, **12**, **22**, and **15**, had IC<sub>50</sub> values of 240 nM, 1  $\mu$ M, and 1.5  $\mu$ M, respectively. All but 1 of the 13 identified inhibitors were selective over 17 $\beta$ -HSD1, the enzyme catalyzing conversion of estrone into estradiol. Three of the new, small, synthetic 17 $\beta$ -HSD2 inhibitors showed acceptable selectivity over other related HSDs, and six of them did not affect other HSDs.

## INTRODUCTION

The worldwide prevalence of osteoporosis is high: already in 2006 it was estimated that over 200 million people suffered from this disease.<sup>1</sup> Osteoporosis is defined as a condition, where reduced bone mass and bone density lead to bone fragility and increased fracture risk.<sup>2</sup> Bone density is a result of the balance between osteoblast and osteoclast activities: while osteoblasts are responsible for the formation and mineralization of the bone, osteoclasts play an important role in bone degradation. Bone density is known to decrease in the elderly and is linked to decreased concentrations of sex steroids.<sup>3</sup> Postmenopausal estrogen deficiency promotes osteoporosis in women,<sup>4</sup> and an age-related decrease of testosterone has been associated with osteoporosis in men.<sup>5</sup> It has been shown that both estradiol and testosterone inhibit bone degradation, thereby providing an explanation for the age-related onset of osteoporosis.<sup>6</sup>

To date, there are only few treatment options for osteoporosis: bisphosphonates, which prevent bone loss, selective estrogen receptor modulators (SERMs) such as raloxifene, and hormone replacement therapy that increases circulating estrogen levels.<sup>7,8</sup>

However, all of these therapies have disadvantages. Bisphosphonates need to be orally administered at least 0.5 h before breakfast and any other medication, and the treatment has to be continued for at least three years, which diminishes the patient's compliance.<sup>8</sup> SERMs and hormone-replacement therapies have been associated with cardiovascular complications.<sup>7,8</sup> Besides, hormone replacement therapy increases the risk of breast cancer and is therefore only recommended for patients where a non-hormonal therapy is contraindicated.<sup>9</sup> Because of the limitations related to existing treatments, there is a great demand for novel therapies. One promising approach to overcome the cardiovascular complications and increased breast cancer risk is to increase estradiol concentrations locally in bone cells without altering systemic levels.

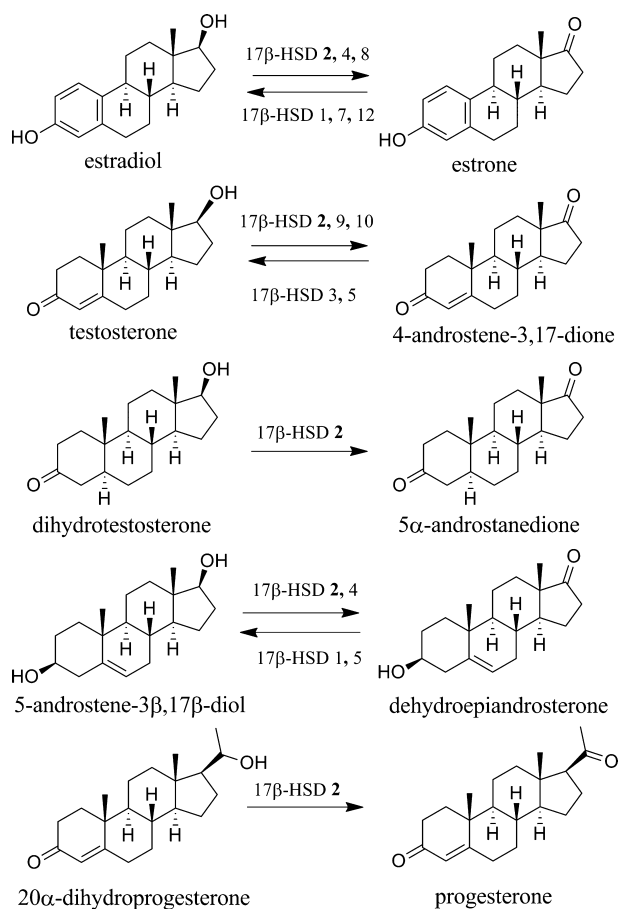
The activity of estrogen receptors is dependent on the local availability of active estradiol, which is regulated by the synthesis via aromatase, deconjugation by sulfatase, and conversion from

Received: February 21, 2014

Published: June 24, 2014

estrone by  $17\beta$ -hydroxysteroid dehydrogenase 1 ( $17\beta$ -HSD1).<sup>10</sup> Estradiol is primarily converted to the inactive estrone by  $17\beta$ -HSD2.<sup>11</sup> Besides its expression in bone cells,  $17\beta$ -HSD2 is localized only in a few tissues, including placenta,<sup>12</sup> endometrium,<sup>13</sup> prostate,<sup>14</sup> and small intestine epithelium.<sup>15</sup> Thus, inhibition of  $17\beta$ -HSD2 may be a suitable way to increase estradiol levels without raising breast cancer and cardiovascular risks. Indeed, there is support from *in vivo* studies that  $17\beta$ -HSD2 could be a target for the treatment of osteoporosis. In ovariectomized monkeys, oral administration of a  $17\beta$ -HSD2 inhibitor increased bone strength by elevating bone formation and decreasing bone resorption.<sup>16</sup>

In addition to the oxidative inactivation of estradiol to estrone,  $17\beta$ -HSD2 was reported to convert testosterone into 4-androstene-3,17-dione (androstenedione), dihydrotestosterone into  $5\alpha$ -androstenedione, and  $5\alpha$ -androstenediol into dehydroepiandrosterone (Figure 1).<sup>17,18</sup> It can also adopt 20-hydroxysteroids

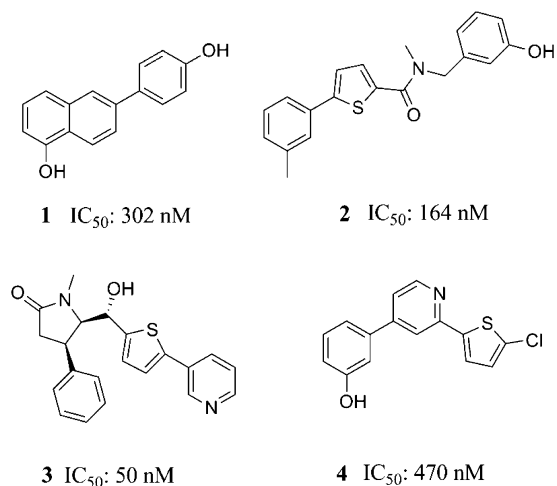


**Figure 1.** Sex steroid metabolism catalyzed by  $17\beta$ -HSD2 and other  $17\beta$ -HSDs.

as substrates and convert  $20\alpha$ -dihydroprogesterone into progesterone (Figure 1).<sup>17</sup>  $17\beta$ -HSD2 is an  $\text{NAD}^+$ -dependent microsomal membrane enzyme.<sup>18,19</sup> It belongs to the short-chain dehydrogenases (SDRs), an enzyme family of oxidoreductases comprising at least 72 different genes in humans.<sup>20,21</sup> Members of this family share a similar protein folding, the so-called "Rossmann-fold", where six or seven  $\beta$ -sheets are surrounded by three to four  $\alpha$ -helices.<sup>21</sup> Even though the sequence identities of SDRs are low, often less than 20%, they share a conserved glycine-rich area in the cofactor binding site and a Tyr-X-X-X-Lys motif in the active site. Despite the low sequence identities, the

SDRs are well superimposable in 3D and their active site structures are similar.<sup>21</sup> Thus, when developing inhibitors for one of the SDRs, the selectivity of the compounds over the other related enzymes should be evaluated.

In recent years, several potent and selective  $17\beta$ -HSD2 inhibitors (e.g., 1–4, Figure 2) have been reported.<sup>22–25</sup> Some of



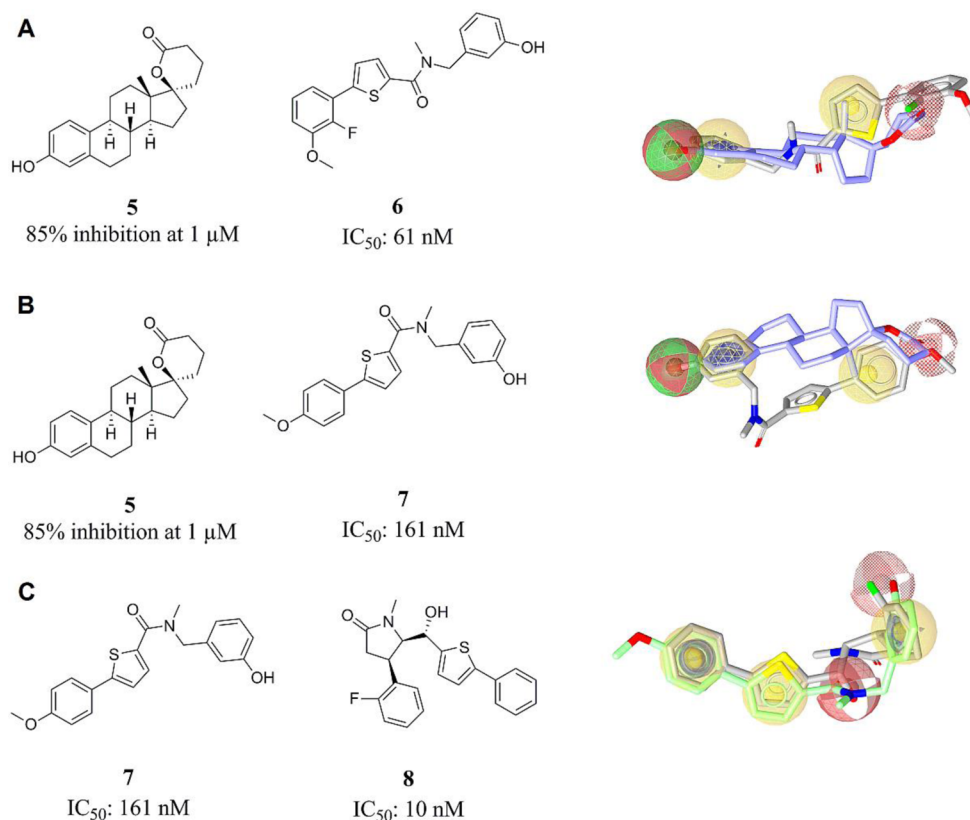
**Figure 2.** Previously reported  $17\beta$ -HSD2 inhibitors.<sup>22–25</sup>

these compounds (such as 4) have been discovered during the search for selective  $17\beta$ -HSD1 inhibitors by synthesizing estrone-mimicking compounds.<sup>25</sup> Most of these compounds were steroid mimetics or developed rationally by structure–activity-relationship (SAR) studies.<sup>22,23,26,27</sup> The starting structure for the SAR studies had been a previously developed inhibitor (3) or a promising scaffold such as flavonoids that represent the basis for compound 1.<sup>23</sup> Because most of the known inhibitors are based on estrone-mimicking compounds or previously developed inhibitors, they often are similar in size, are derived from the same scaffold, or include analogue bioisosteric groups. For this reason, there is a need for novel scaffolds and inhibitors that could serve as starting points for further drug development. We approached the search for novel, chemically diverse  $17\beta$ -HSD2 inhibitors by ligand-based pharmacophore modeling and virtual screening.

Pharmacophore models represent the 3D-arrangement of the chemical features and steric limitations that are necessary for a small molecule to interact with a specific target protein.<sup>28</sup> These features correspond to chemical functionalities such as hydrogen bond acceptors (HBAs), hydrogen bond donors (HBDs), hydrophobic areas (Hs), aromatic rings (ARs), positively/negatively ionizable groups (PIs/NIs), and exclusion volumes (XVOLs). Pharmacophore models are widely used as virtual screening filters.<sup>29</sup> A result of a virtual screening is a so-called hit list containing compounds with functional groups that map the pharmacophore model. These compounds are predicted to be active against a specific target. In this study, we report the development of a pharmacophore model for  $17\beta$ -HSD2 inhibitors and its use in a virtual screening campaign. From the virtual hit lists, 29 compounds were biologically evaluated, of which 7 showed activities in the low micromolar range. As follow-up, we focused on one scaffold and tested similar compounds to get insights into their SAR.

## RESULTS

Due to the lack of an experimentally determined 3D-structure of  $17\beta$ -HSD2, a ligand-based pharmacophore modeling approach



**Figure 3.** Pharmacophore models 1 (A), 2 (B), and 3 (C) for 17 $\beta$ -HSD2 inhibition with their training compounds. On the left-hand side, the training compounds are represented as 2D structures with their activities. On the right-hand side, the training compounds are aligned with the chemical features of the respective models. The pharmacophore features are color-coded: HBA, red; HBD, green; H, yellow; AR, blue. Optional features are shown in scattered style. For clarity, the XVOLs are not depicted.

was chosen. In this method, a model is based on the common chemical features of already known active compounds. After construction, the newly generated pharmacophore model is refined to recognize only the active compounds from a so-called test set, containing previously known active and inactive compounds. The theoretical model quality can be described quantitatively by its specificity and selectivity, which are defined by the retrieval of active and inactive compounds, respectively. Often an increase in specificity decreases the sensitivity: a model that finds all active compounds might also find multiple inactive compounds. Therefore, constructing a good pharmacophore model requires balancing between specificity and sensitivity. We aimed to overcome this fact by the parallel use of several restrictive models, complementing each other in their hit lists.<sup>30</sup> Using several restrictive models, we aimed to achieve the best overall enrichment of active compounds from the test set without finding a large number of inactive entries.

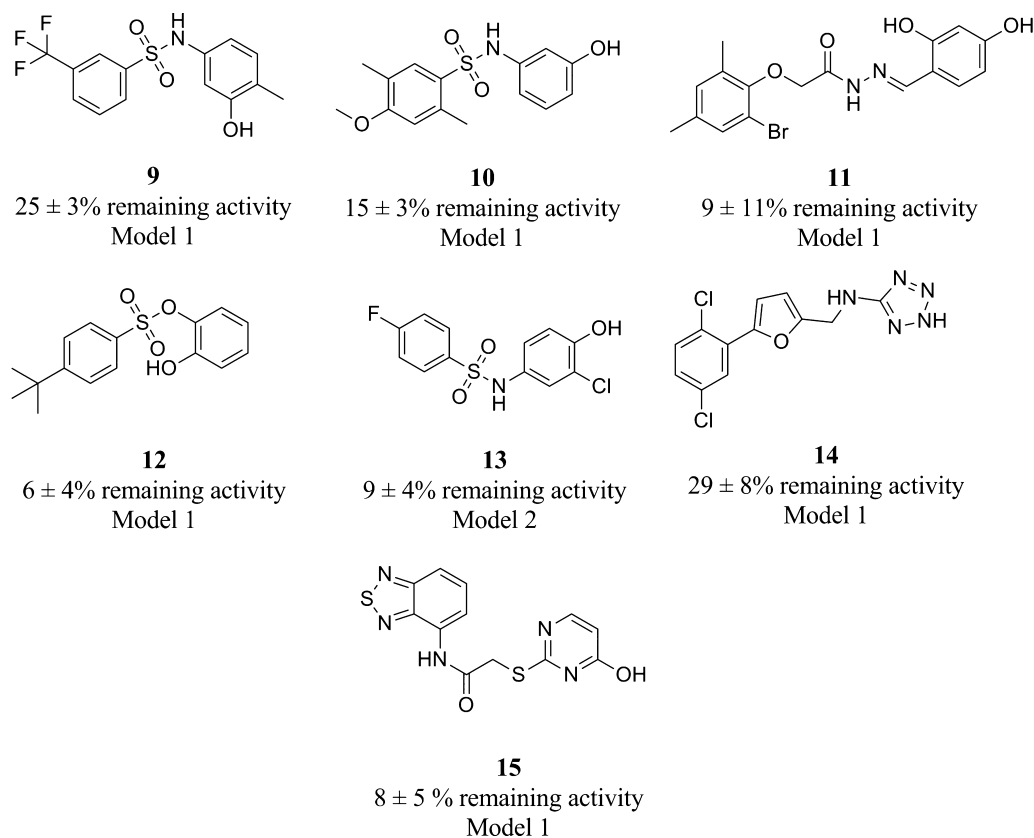
All generated models were based on the common chemical features of two training compounds, respectively, that were collected from the literature: model 1 on **5**<sup>31</sup> and **6**,<sup>22</sup> model 2 on **5** and **7**,<sup>22</sup> and model 3 on **7** and **8**,<sup>24</sup> respectively (Figure 3). The selection of these two molecules as training sets for each model was based on their structural diversity and potency. The automatically created common feature pharmacophore models were refined by removing features, adjusting the XVOL size, and setting features optional to correctly recognize the active compounds from the test set containing 15 active and 30 inactive compounds (Supporting Information, Table S1). The general workflow for model refinement has been described previously.<sup>32</sup>

Model 1 consisted of six features: two H, one HBD, one AR, and two HBAs, of which one was set optional, and 54 XVOLs (Figure 3A). This model was able to recognize eight active but no inactive compounds from the test set. Model 2 consisted of the same features as model 1, but with different spatial arrangement (Figure 3B). This model also recognized eight active compounds, of which five were common with model 1, but no inactive compounds from the test set. Model 3 consisted of seven features: three Hs, two ARs, two HBAs, of which one was set optional, and 56 XVOLs (Figure 3C). This model was more restrictive than the other two: it found six active but no inactive compounds from the test set screening. Together, these three models were able to correctly retrieve 13 active compounds from the test set, representing 87% of all the actives (overall sensitivity: 0.87. Sensitivity of models 1 and 2: 0.53, respectively, and model 3: 0.4). Remarkably, not a single inactive compound was found.

Because the combined retrieval of the active compounds from the test set was encouraging, the three models were employed for virtual screening of the SPECS database including 202 906 small molecules ([www.specs.net](http://www.specs.net)). Models 1, 2, and 3 returned 573, 825, and 318 hits, respectively. In total, 1716 hits were obtained, of which 185 molecules were found by two models. Without duplicates, our models retrieved 1531 hits, representing 0.75% of all the compounds in the database. To separate the druglike compounds from the others, all the hit lists were filtered using a modified Lipinski filter,<sup>33</sup> resulting in total of 1381 unique, druglike hits.

From each hit list, the ten top-ranked hits were considered for further analysis. However, these top hits often contained chemically very similar hits. To get more diverse hits for





**Figure 4.** Seven newly discovered 17β-HSD2 inhibitors with their activities and mapping pharmacophore models. Activities are given as remaining enzyme activity (% of control) at an inhibitor concentration of 20 μM in a cell-free assay.

**Table 1. Inhibitory Activities (IC<sub>50</sub>) of the Seven Newly Discovered Inhibitors against 17β-HSD2 and Related HSDs**

compd	17β-HSD2 lysate	17β-HSD2 intact	17β-HSD1 lysate	11β-HSD1 lysate	11β-HSD2 lysate	17β-HSD3 intact
9	7.1 ± 0.4 μM	n.d. <sup>a</sup>	n.i. <sup>b</sup>	n.i.	n.i.	n.i.
10	6.9 ± 3.5 μM	n.d.	n.i.	n.i.	n.i.	n.i.
11	4.1 ± 1.4 μM	23 ± 3 μM	52 ± 15% <sup>c</sup>	69 ± 2%	61 ± 3%	1.6 ± 0.8 μM
12	240 ± 65 nM	520 ± 210 nM	n.i.	2.1 ± 0.7 μM	n.i.	8.5 ± 3.5 μM
13	3.0 ± 1.5 μM	10 ± 1 μM	n.i.	n.i.	n.i.	3.9 ± 1.2 μM
14	33 ± 5 μM	n.d.	n.i.	n.i.	n.i.	n.i.
15	1.5 ± 0.6 μM	1.1 ± 0.1 μM	n.i.	n.i.	n.i.	n.i.

<sup>a</sup>n.d. = not determined. <sup>b</sup>n.i. = no inhibition (rest activity >70% at the concentration of 20 μM). <sup>c</sup>rest activity at 20 μM.

biological testing, for each hit list 10 clusters were calculated. Out of each cluster, the 3 best-ranked compounds were kept. The preferred compounds list finally contained 73 unique hits. Among them, 3 were consensus hits of two models and therefore selected for biological evaluation. The other compounds were selected based on their overall fit score and a preferentially high fit score within their cluster. Finally, the OSIRIS property explorer ([www.organic-chemistry.org/prog/peo](http://www.organic-chemistry.org/prog/peo)<sup>34</sup>) was used to predict druglikeness, mutagenicity, irritant, and tumorigenic effects of the compounds. Only compounds passing this filter were considered for further research. Giving preference for the best ranked compounds from the filtered hit lists, 2 consensus hits mapping the models 1 and 2, 10 compounds mapping model 1, 8 compounds fitting to model 2, and 9 compounds fitting model 3 were selected. In summary, the selection was based on compound druglikeness, pharmacophore fit score, chemical diversity, and availability. The chemical structures of all selected compounds with their pharmacophore fit scores and ranks in the hit lists are available in the Supporting Information, Table S2.

Next, the 17β-HSD2 inhibitory activities of the chosen hits were evaluated in a cell-free assay. The activities were first determined at an inhibitor concentration of 20 μM using lysates of transfected HEK-293 cells. In all experiments, vehicle was included as negative control and *N*-(3-methoxyphenyl)-*N*-methyl-5-*m*-tolylthiophene-2-carboxamide (compound 19 from ref 26) as positive control. Of the newly predicted 29 compounds, 7 showed more than 70% enzyme inhibition (Figure 4), which corresponds to a 24% true positive hit rate. The other compounds were inactive or weakly active (data not shown).

The seven active compounds (9–15) were further biologically evaluated. First, the IC<sub>50</sub> values were determined in the cell-free assay (Table 1). Irreversible inhibition was excluded by comparing enzyme activity upon preincubation of the enzyme preparation with the inhibitor of interest for 10 and 30 min with that after simultaneous incubation.<sup>35</sup> Promiscuous enzyme inhibition due to aggregate formation of the chemicals was excluded by comparing activities in the absence and presence of 0.1% Triton X-100.<sup>36</sup> Structurally, most of the active compounds

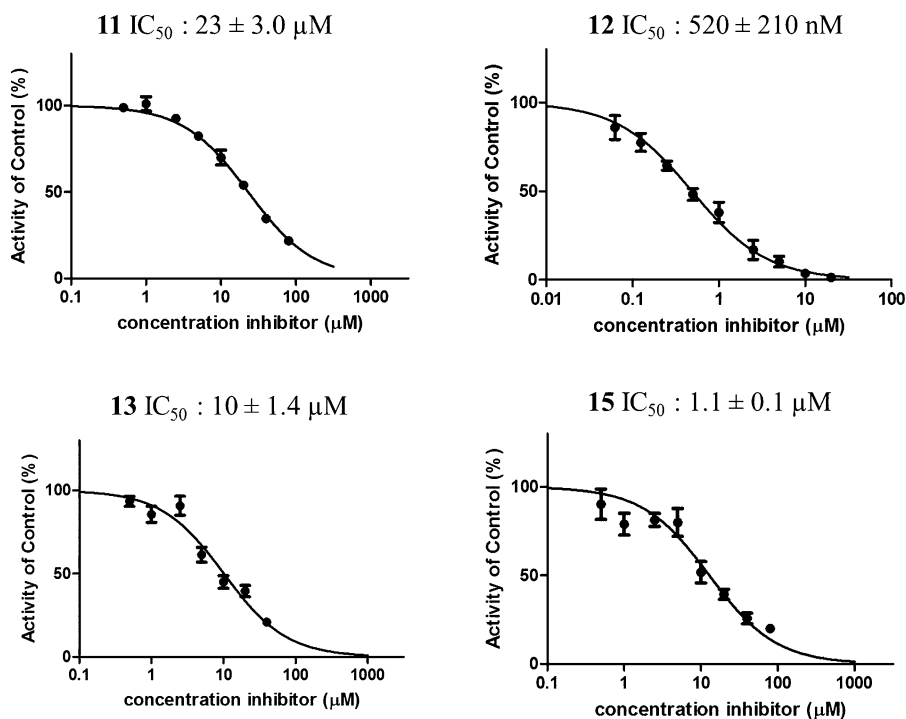


Figure 5.  $IC_{50}$  determinations for compounds 11–13 and 15 in intact cells ( $n = 3–5$ ).

shared a sulfonamide or sulfonic acid ester linker between two benzene rings. The remaining three active compounds represented other chemical classes. To the best of our knowledge, similar compounds or the same chemical scaffolds have not been reported previously as  $17\beta$ -HSD2 inhibitors.

The compounds with  $IC_{50}$  values below  $5 \mu M$  in lysed cells were tested in intact HEK-293 cells transfected with  $17\beta$ -HSD2. The four compounds (11, 12, 13, and 15) concentration-dependently inhibited  $17\beta$ -HSD2 (Figure 5). The two most potent inhibitors, 12 and 15, had  $IC_{50}$  values of  $520 \pm 210 nM$  and  $1.1 \pm 0.1 \mu M$ , respectively. Compound 15 had comparable  $IC_{50}$  values for  $17\beta$ -HSD2 in intact and in lysed cells. For compound 14, the initial enzyme inhibition tests at the concentration  $20 \mu M$  yielded a remaining activity of  $29 \pm 8\%$ . However, the  $IC_{50}$  for this compound was higher than the initial tests led to expect. The reason for this high  $IC_{50}$  value is unclear but may be due to limited solubility and/or stability of the compound.

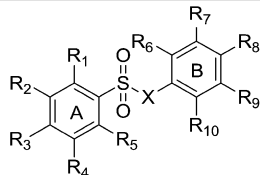
Because of the structural similarity to related HSDs and their common intracellular localization at the ER membrane, the seven most active compounds were evaluated for inhibitory activities against other HSDs: (i)  $17\beta$ -HSD1 catalyzing the conversion of estrone into estradiol (Figure 1), (ii)  $11\beta$ -HSD1 and -2 that are responsible for the interconversion of glucocorticoids,<sup>37</sup> and (iii)  $17\beta$ -HSD3 that converts androstenedione to testosterone (Figure 1).<sup>38</sup> The enzyme activity of  $17\beta$ -HSD3 was assessed in intact cells because the activity declines rapidly upon cell lysis; therefore, the relative inhibition of the compounds might be affected by their ability to enter the intact cell.  $IC_{50}$  values were determined for compounds with an inhibitory activity of at least 70% at a compound concentration of  $20 \mu M$ . Otherwise, the compound was considered as inactive. The results of the selectivity studies are presented in Table 1. Compounds 9, 10, 14, and 15 turned out to be selective over the other tested HSDs. Importantly, all compounds were selective over  $17\beta$ -HSD1. However, compound 12 inhibited  $11\beta$ -HSD1 and  $17\beta$ -HSD3

with  $IC_{50}$  values of  $2.1 \pm 0.7 \mu M$  and  $8.5 \pm 3.5 \mu M$ , respectively. Compounds 11 and 13 showed equal or more potent inhibition of  $17\beta$ -HSD3 with  $IC_{50}$  values below  $5 \mu M$ .

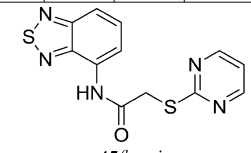
Inspired by the new inhibitors, we searched for compounds similar to the new  $17\beta$ -HSD2 inhibitors in the SPECS database, especially focusing on the phenylbenzenesulfonamide and phenylbenzenesulfonate scaffolds. The aim of the similarity search was to generate a SAR for this scaffold. The similarity search was approached from two ways: (i) plain 2D similarity search for all the new inhibitors without fitting the compounds into the pharmacophore models prior to purchasing them and (ii) search for similar compounds in the SPECS database via virtual screening using model 1, which found the originally active phenylbenzenesulfonamides and phenylbenzenesulfonates.

Altogether, 30 compounds were selected for the biological analysis (Table 2). Sixteen of them were selected just based on their structural similarity to active compounds, and 14 were picked from the virtual screening hits. From the 16 compounds that were selected because of plain 2D similarity, only one compound, 16, inhibited  $17\beta$ -HSD2 with an  $IC_{50}$  value of  $3.3 \pm 1.2 \mu M$ . The other tested compounds (17–19, 25–28, 21–24, 32–35, and 45–48), independent of their high structural similarity to the original hits (9–15), showed only weak or no activity (Table 2). However, among the compounds selected by model 1, several substances were active: five inhibited  $17\beta$ -HSD2 with  $IC_{50}$  values between 1 and  $15 \mu M$ , three had weak activity (50–70% inhibition at  $20 \mu M$ ), two were not tested because they were insoluble in commonly used solvents, and the remaining four compounds were inactive (Table 2).

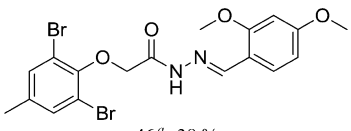
These active inhibitor-derivatives were also tested against other related HSDs (Table 3). Compound 22 was the only compound with weak activity on  $17\beta$ -HSD1; however, it was still 18-fold more active toward  $17\beta$ -HSD2. Compounds 20 and 23 were almost equipotent toward  $17\beta$ -HSD2 and  $11\beta$ -HSD1. Compounds 16 and 22 were weak  $17\beta$ -HSD3 inhibitors, while the other derivatives did not have effect on this enzyme.

Table 2. Phenylbenzenesulfonamides and -sulfonates with Their 17 $\beta$ -HSD2 Inhibitory Activities


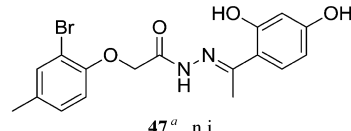
Comp.	X	R1	R2	R3	R4	R5	R6	R7	R8	R9	R10	IC <sub>50</sub>
9	NH	H	CF <sub>3</sub>	H	H	H	H	H	CH <sub>3</sub>	OH	H	7.1 $\mu$ M
10	NH	H	CH <sub>3</sub>	OCH <sub>3</sub>	H	CH <sub>3</sub>	H	OH	H	H	H	6.9 $\mu$ M
12	O	H	H	<i>Tert</i> -But	H	H	H	H	H	H	OH	240 nM
13	NH	H	H	F	H	H	H	H	OH	Cl	H	3.0 $\mu$ M
16 <sup>a</sup>	NH	CH <sub>3</sub>	H	CH <sub>3</sub>	CH <sub>3</sub>	H	H	OH	H	H	H	3.3 $\mu$ M
17 <sup>a</sup>	O	H	H	<i>Tert</i> -But	H	H	H	H	H	H	OCH <sub>3</sub>	51 % <sup>b</sup>
18 <sup>a</sup>	NH	H	H	F	H	H	H	H	H	Cl	H	n.i. <sup>c</sup>
19 <sup>a</sup>	NH	H	H	OCH <sub>3</sub>	H	H	H	H	CH <sub>3</sub>	OH	H	47 %
20	NH	H	H	OCH <sub>3</sub>	H	H	CH <sub>2</sub> CH <sub>2</sub> CH <sub>2</sub> C H <sub>2</sub>	H	OH	H	H	9.6 $\mu$ M
21	NH	H	H	Br	H	H	H	H	H	OH	H	4.9 $\mu$ M
22	NH	H	CH <sub>3</sub>	Cl	H	CH <sub>3</sub>	H	H	H	OH	H	1.0 $\mu$ M
23	NH	CH <sub>2</sub> CH <sub>2</sub> CH <sub>2</sub> C H <sub>2</sub>	H	OCH <sub>3</sub>	H	H	H	H	H	OH	H	15 $\mu$ M
24	NH	H	Br	H	H	H	H	H	CH <sub>3</sub>	OH	H	6.3 $\mu$ M
25 <sup>a</sup>	NH	CH <sub>3</sub>	H	H	CH <sub>3</sub>	H	H	H	OCH <sub>3</sub>	H	H	n.i.
26 <sup>a</sup>	NH	CH <sub>2</sub> C H <sub>3</sub>	H	H	CH <sub>2</sub> CH <sub>3</sub>	H	H	OCH <sub>3</sub>	H	H	OCH <sub>3</sub>	n.i.
27 <sup>a</sup>	NH	CH <sub>3</sub>	H	OCH <sub>3</sub>	CH <sub>3</sub>	H	H	H	COOH	H	H	n.i.
28 <sup>a</sup>	NH	CH <sub>3</sub>	H	OCH <sub>3</sub>	CH <sub>3</sub>	H	H	H	Cl	H	H	n.i.
29	NH	CH <sub>3</sub>	H	CH <sub>3</sub>	H	CH <sub>3</sub>	H	H	OH	H	H	33 %
30	NH	CH <sub>3</sub>	H	H	CH <sub>3</sub>	H	H	H	OH	H	H	39 %
31	NH	H	H	Cl	H	H	H	H	CH <sub>3</sub>	OH	H	45 %
32 <sup>a</sup>	NH	H	H	Cl	H	H	H	H	OH	H	H	55 %
33 <sup>a</sup>	NH	H	H	F	H	H	H	Cl	H	H	CH <sub>3</sub>	n.i.
34 <sup>a</sup>	NH	H	H	Cl	H	H	H	H	OCH <sub>3</sub>	H	H	n.i.
35 <sup>a</sup>	NH	H	CH <sub>3</sub>	F	H	H	H	Cl	H	H	OH	44 %
36	O	H	H	NHCO CH <sub>3</sub>	H	H	H	H	NCH <sub>2</sub> CH <sub>2</sub> CH <sub>2</sub>	H	H	n.i.
37	O	H	CH <sub>3</sub>	CH <sub>3</sub>	H	H	H	H	H	H	NHC OCH <sub>3</sub>	n.i.
38	O	H	H	NHCO CH <sub>3</sub>	H	H	H	H	H	H	OCH <sub>3</sub>	n.i.
39	O	H	H	NHCO CH <sub>3</sub>	H	H	H	H	COCH <sub>2</sub> CH <sub>3</sub>	H	H	67 %
40	NH	H	H	F	H	H	H	H	F	Cl	H	45 %
41	NH	H	H	Br	H	H	H	H	H	F	H	n.i.
42	NH	H	H	Cl	H	H	H	H	H	H	CH <sub>2</sub> OH	n.i.
43	NH	H	H	F	H	H	H	H	H	H	CHO HCH <sub>3</sub>	n.i.
44	NH	CH <sub>3</sub>	CH <sub>3</sub>	H	CH <sub>3</sub>	CH <sub>3</sub>	H	H	H	H	NHC OCH <sub>3</sub>	n.i.



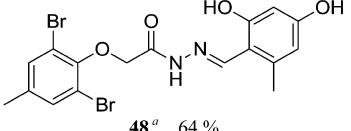
45<sup>a</sup> n.i.



46<sup>a</sup> 38 %



47<sup>a</sup> n.i.



48<sup>a</sup> 64 %

<sup>a</sup>Compound found by similarity search without fitting it to model 1. <sup>b</sup>17 $\beta$ -HSD2 rest activity given as % of control at an inhibitor concentration of 20  $\mu$ M. <sup>c</sup>n.i. = no inhibition (rest activity >70% at the concentration of 20  $\mu$ M).

With all the activity data from the phenylbenzenesulfonamides and -sulfonates, SAR rules were deduced. The SAR analysis confirmed that the HBD functionality is essential for the 17 $\beta$ -HSD2 inhibitory activity. In all the active compounds, except for

the weak inhibitors **39** and **46**, this functionality is a phenolic OH group that is an attractive metabolism site. Therefore, five other compounds (**40–44**) were purchased and biologically evaluated. In two of these compounds (**40** and **41**) the hydroxyl group was

**Table 3. Inhibitory Activities of Active Phenylbenzenesulfonamide and -sulfonate Derivatives Toward 17 $\beta$ -HSD2 and Related HSDs**

compd	17 $\beta$ -HSD2 lysate	17 $\beta$ -HSD1 lysate	11 $\beta$ -HSD1 lysate	11 $\beta$ -HSD2 lysate	17 $\beta$ -HSD3 intact
16	3.3 $\pm$ 1.2 $\mu$ M	n.i. <sup>a</sup>	n.i.	n.i.	43 $\pm$ 4% <sup>b</sup>
20	9.6 $\pm$ 0.4 $\mu$ M	n.i.	8.1 $\pm$ 1.9 $\mu$ M	n.i.	n.i.
21	4.9 $\pm$ 0.9 $\mu$ M	n.i.	n.i.	n.i.	n.i.
22	1.0 $\pm$ 0.2 $\mu$ M	18 $\pm$ 2 $\mu$ M	n.i.	n.i.	53 $\pm$ 4%
23	15 $\pm$ 2 $\mu$ M	53 $\pm$ 5%	13 $\pm$ 3 $\mu$ M	n.i.	n.i.
24	6.3 $\pm$ 1.1 $\mu$ M	58 $\pm$ 3%	n.i.	n.i.	n.i.

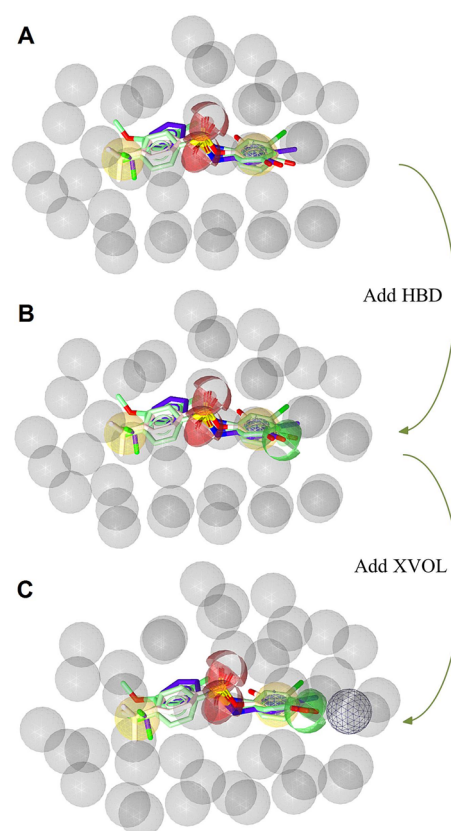
<sup>a</sup>n.i. = no inhibition (rest activity >70% at the concentration of 20  $\mu$ M). <sup>b</sup>% rest activity at 20  $\mu$ M.

replaced by fluorine, whereas the other three had a hydroxymethyl, 1-hydroxyethyl, or acetamide moiety. None of these compounds were active, which confirms the importance of the HBD feature being directly attached to ring B. Compounds **40** and **41**, where the HBD functionality was replaced by an HBA, were inactive and weakly active, in comparison to the active compounds **13** and **21**, in which the substitution pattern was otherwise identical with **40** and **41**. In case of the compounds **42–44**, the HBD functionality was present but not directly attached to the ring B. Unfortunately, no amine substitution of the OH group was available, so this option could not be tested. Either the inactivity of these compounds was caused by spacious substituents in ring B or was caused by different substitution patterns in ring A. To derive further information on this scaffold, a further medicinal chemistry study with a full synthesis series would be required.

In addition to just comparing the 2D-structures of the compounds, a ligand-based pharmacophore model from compounds **9**, **10**, **12**, and **13** was developed. The automatically generated model consisted of two Hs, one AR, two HBAs, and 42 XVOLs (Figure 6A). However, a comparison of the 2D-structures of the active compounds revealed that an HBD functionality on B-ring is essential for the activity. Fitting of the training compounds into the model also showed an overlay of hydroxyl groups in the respective area. Therefore, an HBD-feature was manually added to the model (Figure 6B). After fitting all the tested phenylbenzenesulfonamides and -sulfonates to this model, one new XVOL was placed near the HBD functionality to make the model more restrictive toward compounds with too spacious substituents (Figure 6C).

All the phenylbenzenesulfonamides and -sulfonates were fitted to the SAR models. As expected, the model without the HBD feature (Figure 6A) found 11 of the active but also all of the inactive and weakly active compounds. In comparison, the model where the HBD feature was manually added (Figure 6B) found 9 of the active hits, 2 weakly active and 2 inactive compounds. Once the new space restriction was added, (Figure 6C) 9 active and only 2 weakly active compounds fitted to the model. These results emphasized that phenylbenzenesulfonamides and -sulfonates need to have an HBD functionality attached to the B-benzene ring to inhibit 17 $\beta$ -HSD2. When the HBD is part of a more spacious substituent (e.g., in an amide), activity is decreased.

Finally, the quality of the original 17 $\beta$ -HSD2 pharmacophore models (models 1–3) was evaluated. Therefore, all 28 tested derivatives were fitted into the models to (i) evaluate the model qualities and (ii) to deduce and confirm activity rules from the obtained alignments with the models. In summary, model 1 found 15 phenylbenzenesulfonamides and -sulfonates, of which six (**19**, **20–24**) were active or weakly active. When screening without any space restrictions (XVOLs), compound **16** and



**Figure 6.** SAR models for 17 $\beta$ -HSD2 inhibiting phenylbenzenesulfonamides and -sulfonates. Automatically generated, ligand-based pharmacophore model (A), manually optimized model (B), and optimized model with space restrictions, added XVOL highlighted (C). Pharmacophore features are color coded: HBA, red; HBD, green; H, yellow; AR, blue; XVOL, gray.

three inactive compounds fitted into model 1 as well. Because model 1 performed well in finding active compounds, but also mapped a number of inactive ones, a possible refinement step could be an optimization of the space restrictions so that the specificity of the model improves. Model 2, in contrast, found the active compounds **16** and **22–24**. Additionally, one weakly active derivative and two inactive compounds mapped to this model. None of the derivatives fitted to model 3.

Because model 1 performed well in finding active compounds, but also mapped a number of inactive ones, it was chosen to be refined for higher specificity. For this purpose, the original test set comprising 15 active and 30 inactive compounds and the 13 active and 43 inactive compounds from the newly generated data were gathered to form a refinement database. All in all, model 1 correctly recognized 19 active compounds from the refinement database but found also 15 inactive compounds. The model's



specificity was then increased by adding new XVOLs as spatial restrictions to the model. In total, 7 new XVOLs were added in the regions, where the inactive molecules were located, but the actives did not protrude into this space. In the end, the refined model 1 found 19 active and 4 inactive compounds. To see how the model performed over a larger database, the SPECS database was screened again. The refined model returned 193 hits, in comparison to the 573 hits of the original model. Thus, the spatial refinement of model 1 drastically decreased the number of hits. This decreased number of hits may indicate an improvement in the models specificity and sensitivity and in its ability to enrich active compound from a database.

## DISCUSSION

This study aimed to identify new 17 $\beta$ -HSD2 inhibitors by ligand-based pharmacophore modeling. In the course of this study, three specific 17 $\beta$ -HSD2 pharmacophore models were developed and used in combination for prioritizing test compounds from the commercial SPECS database. Initially, 29 compounds from a total of 1381 hit molecules were selected for biological evaluation. Of these compounds, seven inhibited 17 $\beta$ -HSD2 activity more than 70% at a concentration of 20  $\mu$ M when assayed in lysed cells. In total, this yielded a 24% success rate for these pharmacophore models. A further search for similar compounds resulted in 30 small molecules, which were also tested against 17 $\beta$ -HSD2. Six of these compounds inhibited 17 $\beta$ -HSD2 by more than 70% at a concentration of 20  $\mu$ M, nine were weak inhibitors (40–69% inhibition at 20  $\mu$ M concentration), and the remaining compounds were inactive or insoluble. The remaining 28 compounds were then used to evaluate the pharmacophore model quality and derive an SAR model for phenylbenzenesulfonamide and -sulfonate type inhibitors of 17 $\beta$ -HSD2.

Because the original hit compounds were picked from the database by three separate models, the predictive power for each model was analyzed separately. Twelve of the biologically evaluated compounds were picked by model 1, and six of them turned out to be 17 $\beta$ -HSD2 inhibitors. This results in a success rate of 50%, which is very good for an unrefined model. In contrast, the predictive power of models 2 and 3 were moderate: one of the ten compounds selected by model 2 was active. None of the nine compounds picked by model 3 inhibited 17 $\beta$ -HSD2, yielding success rates of 10% and 0%, respectively.

The experimental validation of the models confirmed that the performance of model 1 was excellent, whereas that of models 2 and 3 should be improved if they will be used for further virtual screening studies. A further refinement of model 1 should render it more restrictive and thereby reduce the overall number of hits. However, in light of the obtained screening results, model 1 already showed good predictive power even within one scaffold. In addition, the results that most of the active compounds fit to model 1 and the structurally similar inactive derivatives do not supports the usage of pharmacophore modeling as a method for prioritizing compounds for in vitro assays.

During this study, 13 new 17 $\beta$ -HSD2 inhibitors were discovered. Two of these compounds were previously reported in the literature: **9** is a reagent in the preparation of translation initiation inhibitors,<sup>39</sup> and **20** is a substructure for protein kinase and angiogenesis inhibitors for cancer treatment.<sup>40</sup> For the other new 17 $\beta$ -HSD2 inhibitors, no references were found. The two studies mentioning compounds **9** and **20** described them as intermediate or substructures but not as actual endproducts, and no biological activity was reported for them. Eleven out of the 13 novel 17 $\beta$ -HSD2 inhibitors had IC<sub>50</sub> values lower than 10  $\mu$ M,

and the most potent hit **12** had a nanomolar IC<sub>50</sub> value. Because the first virtual screening revealed phenylbenzenesulfonates and phenylbenzenesulfonamides as promising hits, this scaffold was further explored and six additional 17 $\beta$ -HSD2 inhibitors were discovered. Therefore, a new validated scaffold for 17 $\beta$ -HSD2 inhibitors can be reported.

The similarities in the 3D-folding, functions, and intracellular location of related HSDs make it difficult to predict the selectivity of compounds active against an individual member of this enzyme family. Although the pharmacophore models were based on inhibitors that were selective against 17 $\beta$ -HSD1, the selectivity of the hits needed to be experimentally confirmed. Therefore, selectivity studies for the newly identified 17 $\beta$ -HSD2 inhibitors were performed. Twelve of the 13 discovered inhibitors were selective over 17 $\beta$ -HSD1, which is important regarding treatment of osteoporosis. The only hit that showed activity 17 $\beta$ -HSD1 activity, compound **22**, inhibited 17 $\beta$ -HSD1 with an IC<sub>50</sub> value of 18  $\mu$ M, thus being 18 times more active against 17 $\beta$ -HSD2. Compound **22** is similar to compound **10**, however, where **22** has chlorine, and **10** has a methoxy substituent. This suggests that 17 $\beta$ -HSD2 may tolerate more spacious groups in this region. Importantly, all compounds were selective over 11 $\beta$ -HSD2, an antitarget associated with cardiovascular complications such as hypertension and hypokalemia.<sup>37,41</sup> Unfortunately, the most active hit **12** inhibited 11 $\beta$ -HSD1 and 17 $\beta$ -HSD3, with 9-fold and 35-fold selectivity against 17 $\beta$ -HSD2, respectively. Because other compounds from the same scaffold (compounds **9**, **10**, **16**, **21**, and **24**) that were selective over the other tested HSDs were discovered, it may be possible to optimize the selectivity of **12**. In addition, compounds **20** and **23** were equipotent 17 $\beta$ -HSD2 and 11 $\beta$ -HSD1 inhibitors. However, 11 $\beta$ -HSD1 is considered as an antidiabetic target,<sup>42</sup> and its inhibition may actually have beneficial effects in patients suffering from osteoporosis.

Unfortunately, compound **11** turned out to be more active against 17 $\beta$ -HSD3 than 17 $\beta$ -HSD2 and **13** was equipotent toward these two enzymes. Compounds **16** and **26** showed weak activity on 17 $\beta$ -HSD3. 17 $\beta$ -HSD3 is responsible for gonadal testosterone production, and its proper function is essential for fetal development and during puberty.<sup>38</sup> Because osteoporosis usually arises among the elderly, inhibition of 17 $\beta$ -HSD3 may not lead to severe adverse effects. In addition, because this enzyme is expressed almost exclusively in testis<sup>43</sup> and in prostate cancer tissues,<sup>44</sup> its inhibition is not expected to cause adverse effects in postmenopausal patients.

The crystal structure of 17 $\beta$ -HSD2 is not known, but for 17 $\beta$ -HSD1, there are multiple crystal structures available in the Protein Data Bank (PDB, www.pdb.org,<sup>45</sup>). Therefore, the generated pharmacophore models and active compounds of this study were analyzed against the 17 $\beta$ -HSD1 structure (PDB code 3HB5<sup>46</sup>). Model 1 as well as the established SAR model aligned remarkably well with the cocrystallized estradiol derivative. The alignment of the phenylbenzenesulfonates and phenylbenzenesulfonamides with model 1 in the 17 $\beta$ -HSD1 binding pocket does not explain the compound's selectivities. Interestingly, in the binding site of 17 $\beta$ -HSD1, there are two hydrophobic residues, Leu149 and Val225, that may cause unfavorable interactions with the sulfonamide core of most 17 $\beta$ -HSD2-active compounds. However, this does not explain why compound **22** inhibits 17 $\beta$ -HSD1 but compound **10** does not. Precise conclusions regarding the selectivity cannot be drawn without a crystal structure or a high quality homology model of 17 $\beta$ -HSD2.

In the end, 13 novel 17 $\beta$ -HSD2 inhibitors were discovered during this study. Compound **15**, which was the most potent and

selective hit, was 5-fold less potent than the most active hit, making it a promising lead candidate. All of the identified 17 $\beta$ -HSD2 inhibitors are small molecules that can be easily optimized by ring substitution or bioisosteric replacements for better biological efficacy and/or selectivity.

Even though half of the in vitro evaluated derivatives were not active or were weak inhibitors, some precious information on our models and on the 17 $\beta$ -HSD2 binding site could be derived. Most of the inactive compounds did not fit to the pharmacophore models and especially model 1 was able to enrich the active compounds even within one scaffold. Structural analysis of the identified inhibitors and the derivatives suggested that the hydrogen bond donor functionality is essential for inhibitory activity. For example, compounds 12, 13, and 15 bore a hydroxyl-substituted benzene ring B and are active. In contrast, their derivatives, compounds 17, 22, and 45 either lacked this functionality or it was shielded by a methyl group to form an ether (compound 17). The same tendency was present among the phenylbenzenesulfonamides and -sulfonates in comparison with inactive compounds from the same scaffold (Table 2). In addition, substituents longer than two atoms in the benzene ring decreased the compounds inhibitory activity or rendered the compound inactive (compounds 36–39). Therefore, we observed that, ideally, 17 $\beta$ -HSD2 inhibitors contain an HBD feature directly linked to an aromatic ring B. The highest activity was gained when this functionality is in meta-position of the benzene ring, followed by ortho- and para-positions. The importance of this HBD feature was also confirmed with the SAR-pharmacophore model. Visual inspections of the substitution pattern of the A benzene ring suggested that hydrophobic substituents (*tert*-butyl, multiple methyl substituents) were well tolerated, whereas hydrogen-bond-forming functionalities decreased the activity.

To determine if our newly discovered 17 $\beta$ -HSD2 inhibitors could be unspecific, multitarget inhibitors interfering with many proteins, we applied a pan assay interference compounds (PAINS) filter.<sup>47</sup> This PAINS filter contains substructures that can possibly interfere with the biological assay by absorbing specific UV wavelengths, sticking to the unspecific binding sites, or interfering with singlet oxygen that is often transferred in certain high-throughput-screening assays. Two of our original hits, compounds 11 and 13, were recognized as potential PAINS.<sup>47</sup> Compound 11 hit filters 282:hzone\_phenol\_A(479) and 283:hzone\_phenol\_B(215), whereas compound 13 matched with filter 392:sulfonamideB(41). Both of these substructures are chromophores and therefore most likely predicted as PAINS. However, chromophoric compounds do not interfere with the biological assays used in this study. The enzyme activity was measured in the presence of the radiolabeled ligand, and the amounts of the substrate and product were detected by scintillation counting, measuring the <sup>3</sup>H activity. Therefore, the presence of a possible chromophore does not interfere with the assay, unlike in the HTS methods described by Baell and Holloway.<sup>47</sup> Moreover, compounds having the same substructures as 11 and 13 were also evaluated against 17 $\beta$ -HSD2 activity, and they were weakly active or inactive (such as 29 and 30, and 47 and 48). This also indicates that compounds 11 and 13 are true positive hits.

## CONCLUSION

In the present project, specific pharmacophore models for 17 $\beta$ -HSD2 inhibitors were developed. Using these models as virtual screening filters, 7 novel 17 $\beta$ -HSD2 inhibitors were discovered. An

additional search for structurally similar compounds resulted in the biological evaluation of 28 small molecules. In total, 13 new 17 $\beta$ -HSD2 inhibitors, from which 10 represented phenylbenzenesulfonamides and -sulfonates, were discovered. To the best of our knowledge, this scaffold has not been reported previously in the literature as 17 $\beta$ -HSD2 inhibitors. These inhibitors aided in the development of the SAR model and rules for this specific scaffold: in general, 17 $\beta$ -HSD2 inhibitors need to have an HBD functionality on the meta-position of one benzene ring, and hydrophobic substituents on the other.

This study proved that pharmacophore modeling is a powerful tool in predicting activities and setting priorities for virtual screening. However, quality evaluation of the pharmacophore models revealed that model 1 outperformed the other two models in finding actives. Therefore, model 1 will be further refined for better sensitivity and specificity and used for further virtual screening campaigns.

## MATERIALS AND METHODS

**Data Sets.** For the ligand-based pharmacophore modeling, a test set from the literature was collected. The aim was to collect structurally diverse, active compounds, which were shown to inhibit 17 $\beta$ -HSD2 in lysed cells. In contrast, all the inactive compounds had to be tested against 17 $\beta$ -HSD2 activity and be structurally similar to the actives. The final test set including the training molecules consisted of 15 17 $\beta$ -HSD2 inhibitors and 30 compounds that were inactive toward 17 $\beta$ -HSD2<sup>22–25,31,48–52</sup> (see Supporting Information Table S1 for structures and activities). The 2D structures of these compounds were drawn with ChemBioDraw Ultra 12.0.<sup>53</sup> For each molecule, a maximum of 500 conformations was generated with OMEGA-best settings (www.eyesopen.com,<sup>54–56</sup>) incorporated in LigandScout 3.03b (www.inteliland.com<sup>57</sup>).

For virtual screening campaigns, the SPECS database was downloaded from the SPECS Web site (www.specs.net). This commercial database is composed of small synthetic chemicals and consists of 202 906 compounds for which the company had at least 10 mg quantities in stock in January 2012. These compounds were transformed into a LigandScout database using the idbgen-tool of LigandScout. The database was generated using OMEGA-fast settings and calculating a maximum of 25 conformers/molecule (www.eyesopen.com,<sup>54–56</sup>). For the search for phenylbenzenesulfonamides and -sulfonates fitting model 1, the SPECS database version May 2013 ( $n = 197\,475$ ) was downloaded from the SPECS Web site and transformed into a multiconformational 3D database as described for the January 2012 version.

**Pharmacophore Modeling.** The pharmacophore models were constructed using LigandScout 3.0b (www.inteliland.com<sup>57</sup>). For the training set compounds, 500 conformations were created with OMEGA-best settings,<sup>54–56</sup> implemented in LigandScout. The program was set to create ten shared feature pharmacophore hypotheses from each of the training sets. In a shared feature pharmacophore model generation, LigandScout generates pharmacophore models from the chemical functionalities of the training compounds and aligns the molecules according to their pharmacophores.<sup>58</sup> Only features present in all training molecules are considered for model building. For the best alignment, common pharmacophore features are generated and assembled together, comprising the final pharmacophore model. The shared feature pharmacophore models contain only chemical features present in all the training molecules. The number of common chemical features naturally decreases when there are more training molecules, especially when using diverse ones. During this study, we started with larger training sets. However, when the training set contained more than two compounds, the obtained pharmacophore model became too general with only few features and low restrictivity, finding all the inactive compounds from the data set. The best of the generated hypotheses were selected for further refinement (removing features, setting features optional, adding XVOLs; for a general model refinement workflow, see ref 32), aiming to train each model to find only the active compounds and exclude the inactive ones from fitting. The quality of the

pharmacophore models was quantitatively evaluated by calculating the selectivity (eq 1) and specificity (eq 2) for each model separately and for a combination of multiple models.

$$\text{sensitivity} = \frac{\text{found actives}}{\text{all actives in the database}} \quad (1)$$

$$\text{specificity} = \frac{\text{found inactives}}{\text{all inactives in the database}} \quad (2)$$

**Virtual Screening and Selection of the Hits.** Virtual screening of the SPECS database ([www.specs.net](http://www.specs.net)) was performed using LigandScout 3.0b. The original hit lists were filtered using Pipeline Pilot<sup>59</sup> to reduce the number of hits. The modified Lipinski-filter was set to pass all the compounds with molecular weight 250–500 g/mol, AlogP 1–6, more than two rotatable bonds, more than two HBAs, and less than three HBDs. Then the hit lists were clustered using DiscoveryStudio 3.0 ([www.accelrys.com](http://www.accelrys.com))<sup>60</sup>. The program was set to create ten clusters for each hit list using function class fingerprints of maximum diameter 6 (FCFP<sub>6</sub>) fingerprints.

**Similarity Search.** The search for the similar compounds for each of the active hits found in the first screening run was performed within SciFinder,<sup>61</sup> using the Explore Substances–Similarity search tool. For each of the new inhibitors, the compounds with similarity score  $\geq 70$  were collected. From these compounds, the ones that were commercially available from SPECS and had a modified substitution pattern (such as methyl group into ether or hydroxyl to methyl ether) were purchased and biologically evaluated. For the search for phenylbenzenesulfonamides and -sulfonates fitting model 1, the SPECS database version May 2013 was virtually screened using LigandScout 3.0b with model 1 only.

**Screening against PAINS.** To evaluate virtual screening libraries against PAINS,<sup>47</sup> our original 29 compounds were screened against the PAINS filter using the program KNIME.<sup>62</sup> The PAINS filters in SMILES format were downloaded from <http://blog.rguha.net/?p=850>, and the KNIME script for PAINS filtering<sup>63</sup> from <http://www.myexperiment.org/workflows/1841.html>.

**Pharmacophore Model and Compound Alignments in 17 $\beta$ -HSD1.** The new 17 $\beta$ -HSD2 inhibitors, model 1, and the SAR were evaluated against the 17 $\beta$ -HSD1 structure (PDB code 3HBS).<sup>46</sup> All the alignments were performed using LigandScout3.0b. The ligand from the protein was copied to the “alignment view”, set as references, and aligned by features with model 1 or the SAR model. Then one of the models was set as reference structure, and all the active compounds were aligned to the model. After this, all the models and the compounds were copied into the ligand-binding pocket in the “structure-based view”. On the basis of these alignments, the models and the compounds were visually analyzed against the 17 $\beta$ -HSD1 structure.

**Literature Survey for Active Compounds.** To search whether or not our active hit molecules have been reported in the literature previously, a SciFinder search was performed. Each of the active compounds was drawn in the SciFinder Structure editor, and an exact structure search was performed. In case a compound already had references, these were downloaded and further investigated.

**Preparation of Inhibitors and Cytotoxicity Assessment.** Inhibitors were dissolved in DMSO to obtain 20 mM stock solutions. For solubility reasons, compound AH-487/15020191 (see Supporting Information Table S1 for structure) was dissolved in chloroform. Further dilutions to the end concentration of 200  $\mu$ M were prepared in TS2 buffer (100 mM NaCl, 1 mM EGTA, 1 mM EDTA, 1 mM MgCl<sub>2</sub>, 250 mM sucrose, 20 mM Tris-HCl, pH 7.4).

To exclude that decreased enzyme activity might be due to unspecific toxicity, all compounds were tested at a concentration of 20  $\mu$ M in intact HEK-293 cells for their effect on cell number, nuclear size, membrane permeability, and lysosomal mass. Cells grown in 96-well plates were incubated with compounds for 24 h, followed by addition of 50  $\mu$ L of staining solution (Dulbecco's modified Eagle medium (DMEM) containing 2.5  $\mu$ M Sytox-Green, 250 nM LysoTracker-Red, and 500 nM Hoechst-33342), rinsing twice with PBS and fixation with 4% paraformaldehyde. Plates were analyzed using a Cellomics ArrayScan high-content screening system using Bioapplication software according

to the manufacturer (Cellomics ThermoScientific, Pittsburgh, PA). None of the compounds altered these parameters.

**Preparation of Cell Lysates.** HEK-293 cells were transfected by the calcium phosphate precipitation method with plasmids for human 17 $\beta$ -HSD1, 17 $\beta$ -HSD2, or 11 $\beta$ -HSD2. Cells were cultivated for 48 h, washed with phosphate-buffered saline, and centrifuged for 4 min at 150g. After removal of the supernatants, cell pellets were snap frozen in dry ice and stored at  $-80$  °C until further use.

**17 $\beta$ -HSD1 and 17 $\beta$ -HSD2 Activity Measurements Using Cell Lysates.** Lysates of human embryonic kidney cells (HEK-293) expressing either 17 $\beta$ -HSD1 or 17 $\beta$ -HSD2 were incubated for 10 min at 37 °C in TS2 buffer in a final volume of 22  $\mu$ L containing either solvent (0.2% DMSO/chloroform) or the inhibitor at the respective concentration. *N*-(3-Methoxyphenyl)-*N*-methyl-5-*m*-tolylthiophene-2-carboxamide (compound 19 in ref 26) and apigenin<sup>50</sup> were used as positive controls for 17 $\beta$ -HSD1 and 17 $\beta$ -HSD2, respectively, in all experiments. 17 $\beta$ -HSD1 activity was measured in the presence of 190 nM unlabeled estrone, 10 nM radiolabeled estrone, and 500  $\mu$ M NADPH. In contrast, 17 $\beta$ -HSD2 activity was determined in the presence of 190 nM unlabeled estradiol, 10 nM radiolabeled estradiol, and 500  $\mu$ M NAD<sup>+</sup>. Reactions were stopped after 10 min by adding an excess of unlabeled estradiol and estrone (1:1, 2 mM in methanol). Possible promiscuous enzyme inhibition by aggregate formation of the chemicals was excluded by measuring the inhibition of the enzyme activity by the compounds in the presence of 0.1% Triton X-100.<sup>36</sup> The presence of the detergent did not affect the inhibitory effect of any of the compounds investigated. To exclude irreversible inhibition by the compounds investigated,<sup>35</sup> cell lysates were preincubated with the compounds for 0, 10, and 30 min, respectively, followed by measurement of the enzyme activity. Preincubation did not affect the inhibitory effects of any of the compounds investigated. The steroids were separated by TLC, followed by scintillation counting and calculation of substrate concentration. Data were collected from at least three independent measurements.

**11 $\beta$ -HSD1 and 11 $\beta$ -HSD2 Activity Measurements Using Cell Lysates.** The methods to determine 11 $\beta$ -HSD1 and -2 activity were performed as described previously.<sup>64</sup> Briefly, lysates of stably transfected cells, expressing either 11 $\beta$ -HSD1 or 11 $\beta$ -HSD2, were incubated for 10 min at 37 °C in TS2 buffer in a final volume of 22  $\mu$ L containing either solvent (0.2% DMSO) or the inhibitor at the respective concentration. The nonselective 11 $\beta$ -HSD inhibitor glycyrrhetic acid was used as positive control. Activity measurements of 11 $\beta$ -HSD1 were performed with 190 nM unlabeled cortisone, 10 nM radiolabeled cortisone, and 500  $\mu$ M NADPH. To measure 11 $\beta$ -HSD2 activity, lysates were incubated with 40 nM unlabeled cortisol, 10 nM radiolabeled cortisol, and 500  $\mu$ M NAD<sup>+</sup>. Reactions were stopped after 10 min by adding an excess of unlabeled cortisone and cortisol (1:1, 2 mM in methanol). The steroids were separated by TLC, followed by scintillation counting and calculation of substrate concentration. Data were collected from at least three independent measurements.

**17 $\beta$ -HSD2 and 17 $\beta$ -HSD3 Activity Measurement in Intact Cells.** Human embryonic kidney cells (HEK-293) were cultivated in DMEM containing 4.5 g/L glucose, 10% fetal bovine serum, 100 U/mL penicillin, 0.1 mg/mL streptomycin, 1 $\times$  MEM nonessential amino acids, and 10 mM HEPES buffer, pH 7.4. The cells were incubated at 37 °C until 80% confluency. The cells were transfected using the calcium phosphate method with expression plasmids for 17 $\beta$ -HSD2 and 17 $\beta$ -HSD3. After 24 h, the cells were trypsinized and seeded on poly-L-lysine-coated 96-well plates (15 000 cells/well).

The inhibitory activities were measured 24 h after seeding as follows: old medium was aspirated and replaced by 30  $\mu$ L of charcoal-treated DMEM (cDMEM). Ten microliters of inhibitor dissolved in cDMEM into the respective concentration was added, and mixtures were preincubated at 37 °C for 20 min. 17 $\beta$ -HSD2 inhibitory activities were measured in the presence of 190 nM unlabeled estradiol and 10 nM radiolabeled estradiol. *N*-(3-Methoxyphenyl)-*N*-methyl-5-*m*-tolylthiophene-2-carboxamide (compound 19 in ref 26) was used as positive control. The reaction mixtures were incubated for 20 min, and the reactions were stopped by adding an excess of estradiol and estrone (1:1, 2 mM in methanol) to the mixture.



17 $\beta$ -HSD3 inhibitory activities were measured in the presence of 190 nM unlabeled androstenedione and 10 nM radiolabeled androstenedione. Benzophenone-1 was used as positive control<sup>65</sup>. The reaction mixtures were incubated for 30 min, and the reactions were stopped by adding an excess of androstenedione and testosterone (1:1, 2 mM in methanol). The steroids were separated by TLC, followed by scintillation counting and calculation of substrate concentration. Data was obtained from three independent measurements.

**Characterization of Compounds 9–16 and 20–24.** The infrared spectra of the 13 active compounds were recorded with a Bruker ALPHA equipped with a PLATINUM-ATR unit (spectral range 4000–400 cm<sup>-1</sup>, 4 scans per cm<sup>-1</sup>, Opus 7 software). The melting behavior of the substances was observed with an Olympus BH2 polarization microscope (Olympus Optical, J) equipped with a Kofler hot stage (Reichert, Vienna, Austria). The temperature calibration of the hot stage was performed with a series of melting point standards such as azobenzene ( $T_{\text{fus}}$ : 68 °C), acetanilide ( $T_{\text{fus}}$ : 114.5 °C), benzanilide ( $T_{\text{fus}}$ : 163 °C), and saccharin ( $T_{\text{fus}}$ : 228 °C). The compound characterization data are available in the Supporting Information.

## ■ ASSOCIATED CONTENT

### ● Supporting Information

Compounds included in the test set and all the compounds tested for 17 $\beta$ -HSD2 activity during this study. For the active compounds additional data such as purity, melting points, calculated log*P* values, NMR, and LC-MS data as provided by the supplier as well as their infrared spectra are given. This material is available free of charge via the Internet at <http://pubs.acs.org>.

## ■ AUTHOR INFORMATION

### Corresponding Authors

\*(Computational) Phone: +43-512-507-58253. Fax: +43-512-507-58299. E-mail: Daniela.Schuster@uibk.ac.at.

\*(Biology) Phone: + 41 61 267 15 30. Fax: + 41 61 267 15 15. E-mail: Alex.Odermatt@unibas.ch.

### Notes

The authors declare no competing financial interest.

## ■ ACKNOWLEDGMENTS

A.V. is a recipient of the DOC-scholarship from the Austrian Academy of Sciences at the Institute of Pharmacy, University of Innsbruck. A.V. also thanks the TWF - Tiroler Wissenschaftsfond for financial support of this project. D.S. is grateful for her position in the Erika Cremer Habilitation Program and a Young Talents Grant by the University of Innsbruck. A.V. and D.S. thank InteLigand GmbH and OpenEye Inc. for providing LigandScout and OMEGA free of charge. This work was supported by the Swiss National Science Foundation (31003A\_140961) to A.O. and the Austrian Science Fund (FWF project P26782) to D.S. A.O. has a Chair for Molecular and Systems Toxicology by the Novartis Research Foundation. We are grateful to Rajarshi Guha for translating the PAINS filters from SMARTS codes into SMILES codes and providing them as well as the KNIME workflow in open access sources.

## ■ ABBREVIATIONS USED

AR, aromatic ring; H, hydrophobic feature; HSD, hydroxysteroid dehydrogenase; HBA, hydrogen bond acceptor; HBD, hydrogen bond donor; NI, negatively ionizable; PI, positively ionizable; SAR, structure–activity relationship; SDR, short chain reductase/dehydrogenase; XVOL, exclusion volume

## ■ REFERENCES

- (1) Reginster, J.-Y.; Burlet, N. Osteoporosis: A still increasing prevalence. *Bone* **2006**, *38*, S4–S9.
- (2) Glaser, D.; Kaplan, F. Osteoporosis. Definition and clinical presentation. *Spine (Philadelphia)* **1997**, *22* (24 suppl), 12S–16S.
- (3) Compston, J. E. Sex Steroids and Bone. *Phys. Rev.* **2001**, *81*, 419–447.
- (4) Riggs, B.; Khosia, S.; Melton, L. r. A unitary model for involuntional osteoporosis: Estrogen deficiency causes both type I and type II osteoporosis in postmenopausal women and contributes to bone loss in aging men. *J. Bone Miner. Res.* **1998**, *13*, 763–773.
- (5) Chin, K.-Y.; Ima-Nirwana, S. Sex steroids and bone health status in men. *Int. J. Endocrinol.* **2012**, *2012*, 208719.
- (6) Michael, H.; Härkönen, P. L.; Väänänen, H. K.; Hentunen, T. A. Estrogen and testosterone use different cellular pathways to inhibit osteoclastogenesis and bone resorption. *J. Bone Miner. Res.* **2005**, *20*, 2224–2232.
- (7) Kanis, J. A.; McCloskey, E. V.; Johansson, H.; Cooper, C.; Rizzoli, R.; Reginster, J.-Y. European guidance for the diagnosis and management of osteoporosis in postmenopausal women. *Osteoporosis Int.* **2012**, *24*, 23–57.
- (8) Lewiecki, E. Current and emerging pharmacologic therapies for the management of postmenopausal osteoporosis. *J. Womens Health* **2009**, *18*, 1615–1626.
- (9) Marjoribanks, J.; Farguhar, C.; Roberts, H.; Lethaby, A. Long term hormone therapy for perimenopausal and postmenopausal women. *Cochrane Database Syst. Rev.* **2012**, *11*, CD004143.
- (10) Janssen, J. M. F.; Bland, R.; Hewison, M.; Coughtrie, M. W. H.; Sharp, S.; Arts, J.; Pols, H. A. P.; van Leeuwen, J. P. T. M. Estradiol Formation by Human Osteoblasts via Multiple Pathways: Relation with Osteoblast Function. *J. Cell. Biochem* **1999**, *75*, S28–S37.
- (11) Dong, Y.; Qiu, Q. Q.; Debeer, J.; Lathrop, W. F.; Bertolini, D. R.; Tamburini, P. P. 17 $\beta$ -Hydroxysteroid dehydrogenases in human bone cells. *J. Bone Miner. Res.* **1998**, *13*, 1539–1546.
- (12) Takeyama, J.; Sasano, H.; Suzuki, T.; Iinuma, K.; Nagura, H.; Andersson, S. 17 $\beta$ -Hydroxysteroid dehydrogenase types 1 and 2 in human placenta: An immunohistochemical study with correlation to placental development. *J. Clin. Endocrinol. Metab.* **1998**, *83*, 3710–3715.
- (13) Mustonen, M. V.; Isomaa, V. V.; Vaskivuo, T.; Tapanainen, J.; Poutanen, M. H.; Stenbäck, F.; Vihko, R. K.; Vihko, P. T. Human 17 $\beta$ -hydroxysteroid dehydrogenase type 2 messenger ribonucleic acid expression and localization in term placenta and in endometrium during the menstrual cycle. *J. Clin. Endocrinol. Metab.* **1998**, *83*, 1319–1324.
- (14) Elo, J. P.; Akinola, L. A.; Poutanen, M.; Vihko, P.; Kyllönen, A. P.; Lukkarinen, O.; Vihko, R. Characterization of 17 $\beta$ -hydroxysteroid dehydrogenase isoenzyme expression in benign and malignant human prostate. *Int. J. Cancer* **1996**, *66*, 37–41.
- (15) Mustonen, M. V. J.; Poutanen, M. H.; Kellokumpu, S.; de Launoit, Y.; Isomaa, V. V.; Vihko, R. K.; Vihko, P. T. Mouse 17 $\beta$ -hydroxysteroid dehydrogenase type 2 mRNA is predominantly expressed in hepatocytes and in surface epithelial cells of the gastrointestinal and urinary tracts. *J. Mol. Endocrinol.* **1998**, *20*, 67–74.
- (16) Bagi, C. M.; Wood, J.; Wilkie, D.; Dixon, B. Effect of 17 $\beta$ -hydroxysteroid dehydrogenase type 2 inhibitor on bone strength in ovariectomized cynomolgus monkeys. *J. Musculoskeletal Neuronal Interact.* **2008**, *8*, 267–280.
- (17) Wu, L.; Einstein, M.; Geissler, W. M.; Chan, H. K.; Elliston, K. O.; Andersson, S. Expression cloning and characterization of human 17 $\beta$ -hydroxysteroid dehydrogenase type 2, a microsomal enzyme possessing 20 $\alpha$ -hydroxysteroid dehydrogenase activity. *J. Biol. Chem.* **1993**, *268*, 12964–12639.
- (18) Puranen, T. J.; Kurkela, R. M.; Lakkakorpi, J. T.; Poutanen, M. H.; Itäranta, P. V.; Melis, J. P. J.; Ghosh, D.; Vihko, R. K.; Vihko, P. T. Characterization of molecular and catalytic properties of intact and truncated human 17 $\beta$ -hydroxysteroid dehydrogenase type 2 enzymes: Intracellular localization of the wild-type enzyme in the endoplasmic reticulum. *Endocrinology* **1999**, *140*, 3334–3341.



- (19) Labrie, F.; Luu-The, V.; Lin, S.-X.; Labrie, C.; Simard, J.; Breton, R.; Bélanger, A. The key role of 17 $\beta$ -hydroxysteroid dehydrogenases in sex steroid biology. *Steroids* **1997**, *62*, 148–158.
- (20) Wu, X.; Lukacik, P.; Kavanagh, K. L.; Oppermann, U. SDR-type human hydroxysteroid dehydrogenases involved in steroid hormone action. *Mol. Cell. Endocrinol.* **2007**, *265–266*, 71–76.
- (21) Kavanagh, K. L.; Jörnvall, H.; Persson, B.; Oppermann, U. The SDR superfamily: Functional and structural diversity within a family of metabolic and regulatory enzymes. *Cell. Mol. Life Sci.* **2008**, *65*, 3895–3906.
- (22) Xu, K.; Al-Soud, Y. A.; Wetzel, M.; Hartmann, R. W.; Marchais-Oberwinkler, S. Triazole ring-opening leads to the discovery of potent nonsteroidal 17 $\beta$ -hydroxysteroid dehydrogenase type 2 inhibitors. *Eur. J. Med. Chem.* **2011**, *46*, 5978–5990.
- (23) Wetzel, M.; Marchais-Oberwinkler, S.; Hartmann, R. W. 17 $\beta$ -HSD2 inhibitors for the treatment of osteoporosis: Identification of a promising scaffold. *Bioorg. Med. Chem.* **2011**, *19*, 807–815.
- (24) Wood, J.; Bagi, C. M.; Akuche, C.; Bacchiocchi, A.; Baryza, J.; Blue, M.-L.; Brennan, C.; Campbell, A.-M.; Choi, S.; Cook, J. H.; Conrad, P.; Dixon, B. R.; Ehrlich, P. P.; Gane, T.; Gunn, D.; Joe, T.; Johnson, J. S.; Jordan, J.; Kramas, R.; Liu, P.; Levy, J.; Lowe, D. B.; McAlexander, I.; Natero, R.; Redman, A. M.; Scott, W. J.; Town, C.; Wang, M.; Wang, Y.; Zhang, Z. 4,5-Disubstituted *cis*-pyrrolidinones as inhibitors of type II 17 $\beta$ -hydroxysteroid dehydrogenase. Part 3. Identification of lead candidate. *Bioorg. Med. Chem. Lett.* **2006**, *16*, 4965–4968.
- (25) Oster, A.; Klein, T.; Werth, R.; Kruchten, P.; Bey, E.; Negri, M.; Marchais-Oberwinkler, S.; Frotscher, M.; Hartmann, R. W. Novel estrone mimetics with high 17 $\beta$ -HSD1 inhibitory activity. *Bioorg. Med. Chem.* **2010**, *18*, 3494–3505.
- (26) Marchais-Oberwinkler, S.; Xu, K.; Wetzel, M.; Perspicace, E.; Negri, M.; Meyer, A.; Odermatt, A.; Möller, G.; Adamski, J.; Hartmann, R. W. Structural optimization of 2,5-thiophene amides as highly potent and selective 17 $\beta$ -hydroxysteroid dehydrogenase type 2 inhibitors for the treatment of osteoporosis. *J. Med. Chem.* **2012**, *56*, 167–181.
- (27) Al-Soud, Y. A.; Marchais-Oberwinkler, S.; Frotscher, M.; Hartmann, R. W. Synthesis and biological evaluation of phenyl substituted 1H-1,2,4-triazoles as non-steroidal inhibitors of 17 $\beta$ -hydroxysteroid dehydrogenase type 2. *Arch. Pharm.* **2012**, *345*, 610–621.
- (28) Wermuth, C. G.; Ganellin, C. R.; Lindberg, P.; Mitscher, L. A. Glossary of terms used in medicinal chemistry (IUPAC Recommendations). *Pure Appl. Chem.* **1998**, *70*, 1129–1143.
- (29) Gao, Q.; Yang, L.; Zhu, Y. Pharmacophore based drug design approach as a practical process in drug discovery. *Curr. Comput.-Aided Drug Des.* **2010**, *6*, 37–49.
- (30) Schuster, D.; Waltenberger, B.; Kirchmair, J.; Distinto, S.; Markt, P.; Stuppner, H.; Rollinger, J. M.; Wolber, G. Predicting cyclooxygenase inhibition by three-dimensional pharmacophoric profiling. Part I: Model generation, validation and applicability in ethnopharmacology. *Mol. Inf.* **2010**, *1*, 79–90.
- (31) Bydal, P.; Auger, S.; Poirier, D. Inhibition of type 2 17 $\beta$ -hydroxysteroid dehydrogenase by estradiol derivatives bearing a lactone on the D-ring: Structure-activity relationships. *Steroids* **2004**, *69*, 325–342.
- (32) Vuorinen, A.; Nashev, L. G.; Odermatt, A.; Rollinger, J. M.; Schuster, D. Pharmacophore model refinement for 11 $\beta$ -hydroxysteroid dehydrogenase inhibitors: Search for modulators of intracellular glucocorticoid concentrations. *Mol. Inf.* **2014**, *33*, 15–25.
- (33) Lipinski, C. A.; Lombardo, F.; Dominy, B. W.; Feeney, P. J. Experimental and computational approaches to estimate solubility and permeability in drug discovery and development settings. *Adv. Drug Delivery Rev.* **2001**, *46*, 3–26.
- (34) Organic Chemistry Portal. *OSIRIS Property Explorer*; Actelion Pharmaceuticals Ltd., Gewerbestrasse 16, 4123 Allschwil, Switzerland.
- (35) Atanasov, A. G.; Tam, S.; Rocken, J. M.; Baker, M. E.; Odermatt, A. Inhibition of 11  $\beta$ -hydroxysteroid dehydrogenase type 2 by dithiocarbamates. *Biochem. Biophys. Res. Commun.* **2003**, *308*, 257–62.
- (36) McGovern, S. L.; Helfand, B. T.; Feng, B.; Shoichet, B. K. A Specific Mechanism of Nonspecific Inhibition. *J. Med. Chem.* **2003**, *46*, 4265–4272.
- (37) Odermatt, A.; Kratschmar, D. V. Tissue-specific modulation of mineralocorticoid receptor function by 11 $\beta$ -hydroxysteroid dehydrogenases: An overview. *Mol. Cell. Endocrinol.* **2012**, *350*, 168–86.
- (38) Geissler, W. M.; Davis, D. L.; Wu, L.; Bradshaw, K. D.; Patel, S.; Mendonca, B. B.; Elliston, K. O.; Wilson, J. D.; Russell, D. W.; Andersson, S. Male pseudohermaphroditism caused by mutations of testicular 17 $\beta$ -hydroxysteroid dehydrogenase 3. *Nat. Genet.* **1994**, *7*, 34–39.
- (39) Halperin, J. A.; Natarajan, A.; Aktas, H.; Fan, Y.-H. C., Preparation of 3-3-di-substituted oxindoles as inhibitors of translation initiation. Patent WO 2005080335 A1, January 9, 2005.
- (40) Xu, F.; Xu, H.; Wang, X.; Zhang, L.; Wen, Q.; Zhang, Y.; Xu, W. Discovery of N-(3-((7H-purin-6-yl)thio)-4-hydroxynaphthalen-1-yl)-sulfonamide derivatives as novel protein kinase and angiogenesis inhibitors for the treatment of cancer: Synthesis and biological evaluation. Part III. *Bioorg. Med. Chem.* **2014**, *22*, 1487–1495.
- (41) Kotelevtsev, Y.; Brown, R. W.; Fleming, S.; Kenyon, C.; Edwards, C. R. W.; Seckl, J. R.; Mullins, J. J. Hypertension in mice lacking 11 $\beta$ -hydroxysteroid dehydrogenase type 2. *J. Clin. Invest.* **1999**, *103*, 683–689.
- (42) Wang, M. Inhibitors of 11 $\beta$ -Hydroxysteroid Dehydrogenase Type 1 in Antidiabetic Therapy. In *Diabetes - Perspectives in Drug Therapy*; Schwanstecher, M., Ed.; Springer: Berlin, 2011; Vol. 203, pp 127–146.
- (43) Andersson, S.; Geissler, W. M.; Patel, S.; Wu, L. The molecular biology of androgenic 17 $\beta$ -hydroxysteroid dehydrogenases. *J. Steroid Biochem. Mol. Biol.* **1995**, *53*, 37–39.
- (44) Koh, E.; Noda, T.; Kanaya, J.; Namiki, M. Differential expression of 17 $\beta$ -hydroxysteroid dehydrogenase isozyme genes in prostate cancer and noncancer tissues. *Prostate* **2002**, *53*, 154–159.
- (45) Berman, H. M.; Westbrook, J.; Feng, Z.; Gilliland, G.; Bhat, T. N.; Weissig, H.; Shindyalov, I. N.; Bourne, P. E. The Protein Data Bank. *Nucl. Acids. Res.* **2000**, *28*, 235–242.
- (46) Mazumdar, M.; Fournier, D.; Zhu, D. W.; Cadot, C.; Poirier, D.; Lin, S. X. Binary and ternary crystal structure analyses of a novel inhibitor with 17 $\beta$ -HSD type 1: a lead compound for breast cancer therapy. *Biochem. J.* **2009**, *424*, 357–366.
- (47) Baell, J. B.; Holloway, G. A. New Substructure Filters for Removal of Pan Assay Interference Compounds (PAINS) from Screening Libraries and for Their Exclusion in Bioassays. *J. Med. Chem.* **2010**, *53*, 2719–2740.
- (48) Lilienkamp, A.; Karkola, S.; Alho-Richmond, S.; Koskimies, P.; Johansson, N.; Huhtinen, K.; Vihko, K.; Wähälä, K. Synthesis and biological evaluation of 17 $\beta$ -hydroxysteroid dehydrogenase type 1 (17 $\beta$ -HSD1) inhibitors based on a thieno[2,3-*d*]pyrimidin-4(3H)-one core. *J. Med. Chem.* **2009**, *52*, 6660–6671.
- (49) Allan, G. M.; Lawrence, H. R.; Cornet, J.; Bubert, C.; Fischer, D. S.; Vicker, N.; Smith, A.; Tutill, H. J.; Purohit, A.; Day, J. M.; Mahon, M. F.; Reed, M. J.; Potter, B. V. L. Modification of estrone at the 6, 16, and 17 positions: Novel potent inhibitors of 17 $\beta$ -hydroxysteroid dehydrogenase type 1. *J. Med. Chem.* **2006**, *49*, 1325–1345.
- (50) Schuster, D.; Nashev, L. G.; Kirchmair, J.; Laggner, C.; Wolber, G.; Langer, T.; Odermatt, A. Discovery of nonsteroidal 17 $\beta$ -hydroxysteroid dehydrogenase 1 inhibitors by pharmacophore-based screening of virtual compound libraries. *J. Med. Chem.* **2008**, *51*, 4188–4199.
- (51) Schuster, D.; Kowalik, D.; Kirchmair, J.; Laggner, C.; Markt, P.; Aebischer-Gumy, C.; Ströhle, F.; Möller, G.; Wolber, G.; Wilckens, T.; Langer, T.; Odermatt, A.; Adamski, J. Identification of chemically diverse, novel inhibitors of 17 $\beta$ -hydroxysteroid dehydrogenase type 3 and 5 by pharmacophore-based virtual screening. *J. Steroid Biochem. Mol. Biol.* **2011**, *125*, 148–161.
- (52) Fischer, D. S.; Allan, G. M.; Bubert, C.; Vicker, N.; Smith, A.; Tutill, H. J.; Purohit, A.; Wood, L.; Packham, G.; Mahon, M. F.; Reed, M. J.; Potter, B. V. L. E-ring modified steroids as novel potent inhibitors of 17 $\beta$ -hydroxysteroid dehydrogenase type 1. *J. Med. Chem.* **2005**, *48*, 5749–5770.

- (53) *ChemBioDraw Ultra*, 12.0; CambridgeSoft, 1986–2010.
- (54) *OMEGA*, 2.2.3; OpenEye Scientific Software, Santa Fe, NM.
- (55) Hawkins, P. C. D.; Skillman, A. G.; Warren, G. L.; Ellingson, B. A.; Stahl, M. T. Conformer generation with OMEGA: Algorithm and validation using high quality structures from the protein databank and Cambridge Structural Database. *J. Chem. Inf. Model* **2010**, *50*, 572–584.
- (56) Hawkins, P. C. D.; Nicholls, A. Conformer generation with OMEGA: Learning from the data set and the analysis of failures. *J. Chem. Inf. Model* **2012**, *52*, 2919–2936.
- (57) Wolber, G.; Langer, T. LigandScout: 3-D pharmacophores derived from protein-bound ligands and their use as virtual screening filters. *J. Chem. Inf. Model* **2005**, *45*, 160–169.
- (58) Wolber, G.; Dornhofer, A. A.; Langer, T. Efficient overlay of small organic molecules using 3D pharmacophores. *J. Comput.-Aided Mol. Des.* **2006**, *20*, 773–788.
- (59) *Pipeline Pilot*; Accelrys Software Inc., 2010.
- (60) *DiscoveryStudio*, 3.0; Accelrys Software Inc., 2005–2010.
- (61) *SciFinder*; American Chemical Society, 2013.
- (62) Berthold, M.; Cebon, N.; Dill, F.; Gabriel, T.; Kötter, T.; Meinel, T.; Ohl, P.; Sieb, C.; Thiel, K.; Wiswedel, B. KNIME: The Konstanz Information Miner. In *Data Analysis, Machine Learning and Applications*; Preisach, C.; Burkhardt, H.; Schmidt-Thieme, L.; Decker, R., Eds.; Springer: Berlin, 2008; pp 319–326.
- (63) Saubern, S.; Guha, R.; Baell, J. B. KNIME Workflow to Assess PAINS Filters in SMARTS Format. Comparison of RDKit and Indigo Cheminformatics Libraries. *Mol. Inf.* **2011**, *30*, 847–850.
- (64) Kratschmar, D. V.; Vuorinen, A.; Da Cunha, T.; Wolber, G.; Classen-Houben, D.; Doblhoff, O.; Schuster, D.; Odermatt, A. Characterization of activity and binding mode of glycyrrhetic acid derivatives inhibiting 11 $\beta$ -hydroxysteroid dehydrogenase type 2. *J. Steroid Biochem. Mol. Biol.* **2011**, *125*, 129–142.
- (65) Nashev, L. G.; Schuster, D.; Laggner, C.; Sodha, S.; Langer, T.; Wolber, G.; Odermatt, A. The UV-filter benzophenone-1 inhibits 17 $\beta$ -hydroxysteroid dehydrogenase type 3: Virtual screening as a strategy to identify potential endocrine disrupting chemicals. *Biochem. Pharmacol.* **2010**, *79*, 1189–1199.

### 3.3 Paper 2 (Vuorinen/Engeli et al., 2017a)

## Phenylbenzenesulfonates and –sulfonamide as 17 $\beta$ -hydroxysteroid dehydrogenase type 2 (17 $\beta$ -HSD2) inhibitors synthesis and SAR-analysis

Anna Vuorinen\*, Roger T. Engeli\*, Susanne Leugger, Christoph R. Kreutz, Alex Odermatt, Daniela Schuster, Barbara Matuszczak

Published manuscript

**Contribution:** Drafted the manuscript together with A. Vuorinen. First authorship was shared equally (\*). Providing the biochemical data for the activity experiments (Table 1 and 2).

**Aims:** In this project we tried to chemically improve the previously identified 17 $\beta$ -HSD2 inhibitors by replacing phenolic groups, which serve as an attractive target for intestinal and liver metabolizing enzymes.

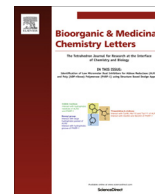
**Results:** The newly chemically altered compounds showed reduced potency and only inhibited 17 $\beta$ -HSD2 in low micro molar range.

**Conclusion:** Despite the fact that the newly chemically altered 17 $\beta$ -HSD2 inhibitors were less potent than the previously reported compounds, they do provide comprehensive evidence that the phenolic groups are critical for the structure activity relationship of these scaffolds.



Contents lists available at ScienceDirect

## Bioorganic &amp; Medicinal Chemistry Letters

journal homepage: [www.elsevier.com/locate/bmcl](http://www.elsevier.com/locate/bmcl)Phenylbenzenesulfonates and -sulfonamides as 17 $\beta$ -hydroxysteroid dehydrogenase type 2 inhibitors: Synthesis and SAR-analysisAnna Vuorinen<sup>a,b,d</sup>, Roger T. Engeli<sup>b,d</sup>, Susanne Leugger<sup>b</sup>, Christoph R. Kreutz<sup>c</sup>, Daniela Schuster<sup>a</sup>, Alex Odermatt<sup>b,\*</sup>, Barbara Matuszczak<sup>a,\*</sup><sup>a</sup> Institute of Pharmacy/Pharmaceutical Chemistry and Center for Molecular Biosciences Innsbruck (CMBI), University of Innsbruck, Innrain 80/82, 6020 Innsbruck, Austria<sup>b</sup> Division of Molecular and Systems Toxicology, Department of Pharmaceutical Sciences, University of Basel, Klingelbergstrasse 50, 4056 Basel, Switzerland<sup>c</sup> Institute of Organic Chemistry and Center for Molecular Biosciences (CMBI), University of Innsbruck, Innrain 80-82, 6020 Innsbruck, Austria

## ARTICLE INFO

## Article history:

Received 31 March 2017

Revised 1 May 2017

Accepted 3 May 2017

Available online xxxxx

## Keywords:

17 $\beta$ -HSD2

Inhibitor

Osteoporosis

Virtual screening

Estrogen

## ABSTRACT

17 $\beta$ -Hydroxysteroid dehydrogenase type 2 (17 $\beta$ -HSD2) converts the potent estrogen estradiol into the weakly active keto form estrone. Because of its expression in bone, inhibition of 17 $\beta$ -HSD2 provides an attractive strategy for the treatment of osteoporosis, a condition that is often caused by a decrease of the active sex steroids. Currently, there are no drugs on the market targeting 17 $\beta$ -HSD2, but in multiple studies, synthesis and biological evaluation of promising 17 $\beta$ -HSD2 inhibitors have been reported. Our previous work led to the identification of phenylbenzenesulfonamides and -sulfonates as new 17 $\beta$ -HSD2 inhibitors by ligand-based pharmacophore modeling and virtual screening. In this study, new molecules representing this scaffold were synthesized and tested *in vitro* for their 17 $\beta$ -HSD2 activity to derive more profound structure-activity relationship rules.

© 2017 Elsevier Ltd. All rights reserved.

The microsomal enzyme 17 $\beta$ -hydroxysteroid dehydrogenase 2 (17 $\beta$ -HSD2) regulates the intracellular concentrations of the sex steroid hormones estradiol and testosterone. It is responsible for the oxidative inactivation of estradiol into estrone and inactivation of testosterone into  $\Delta$ 4-androstene-3,17-dione (androstenedione), respectively (Fig. 1).<sup>1,2</sup> Additionally, 17 $\beta$ -HSD2 is involved in the inactivation of 5 $\alpha$ -dihydrotestosterone into 5 $\alpha$ -androstane-3-one and conversion of androstenediol into dehydroepiandrosterone.<sup>2,3</sup>

17 $\beta$ -HSD2 is expressed only in a few tissues: placenta,<sup>4</sup> endometrium,<sup>4,5</sup> prostate,<sup>6</sup> small intestine,<sup>7</sup> and bone.<sup>1</sup> Inhibition of 17 $\beta$ -HSD2 is an attractive way to increase local estradiol concentrations only in the target tissues, without affecting estrogen receptor signaling in tissues where it is not expressed. This is thought to be especially beneficial in the treatment of osteoporosis, a condition where reduced bone density increases the fracture risk. The onset of osteoporosis is often connected with the age-related decrease of estradiol in women and decrease of testosterone in men.<sup>8</sup> Currently, osteoporosis is treated by estrogen replacement therapy, bisphosphonates, monoclonal antibodies against receptor activator of nuclear factor kappa-B ligand (RANKL), and selective

estrogen receptor modulators (SERMs).<sup>9–11</sup> All of these treatments have their disadvantages: Hormone replacement therapies and SERMs have been associated with cardiovascular complications and bisphosphonate therapy suffers from low oral bioavailability.<sup>12</sup> Because of the challenges in the current treatment options, there is a considerable demand for novel therapies such as 17 $\beta$ -HSD2 inhibitors. In fact, there is evidence from a study in ovariectomized cynomolgus monkeys that 17 $\beta$ -HSD2 inhibition lowered bone resorption, although the effects were moderate and only observed at the highest dose tested (25 mg/kg/day).<sup>13</sup> Additionally, treatment with 17 $\beta$ -HSD2 inhibitor reversed the ovariectomy-dependent decrease in bone strength at 5 mg/kg and 25 mg/kg. Nevertheless, the selectivity of the inhibitor used as well as inhibitor concentration reached in the bone needs to be further assessed. To the best of our knowledge, there are currently no 17 $\beta$ -HSD2 inhibitors in clinical trials or already on the market. However, there are multiple studies on the discovery and development of 17 $\beta$ -HSD2 inhibitors.<sup>14–17</sup>

Our recently published study described 17 $\beta$ -HSD2 inhibitors that were discovered by ligand-based pharmacophore modeling and virtual screening.<sup>18</sup> In total, three pharmacophore models representing the common chemical features of 17 $\beta$ -HSD2 inhibitors were developed and used for virtual screening of the commercial SPECS database ([www.specs.net](http://www.specs.net)) containing about 200,000 small synthetic chemicals. From the hit molecules, 27 were purchased

\* Corresponding authors.

E-mail addresses: [Alex.Odermatt@unibas.ch](mailto:Alex.Odermatt@unibas.ch) (A. Odermatt), [Barbara.Matuszczak@uibk.ac.at](mailto:Barbara.Matuszczak@uibk.ac.at) (B. Matuszczak).<sup>d</sup> These authors contributed equally to the work.

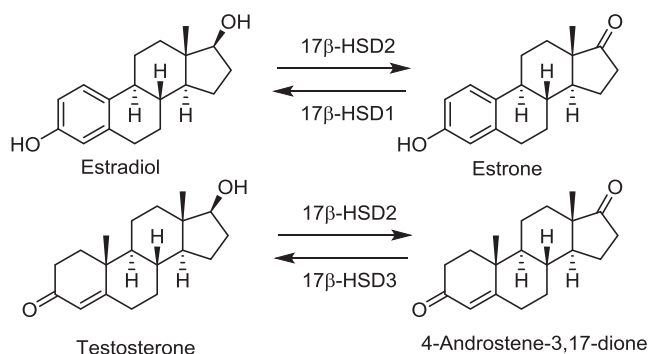


Fig. 1. Reactions catalyzed by 17 $\beta$ -HSD2.

and biologically evaluated for 17 $\beta$ -HSD2 inhibition. Seven of these compounds inhibited 17 $\beta$ -HSD2 by more than 70% at a concentration of 20  $\mu$ M. Four of these compounds represented the phenylbenzenesulfonate and -sulfonamide scaffold and were found by the most successful model (Fig. 2). To further explore the phenylbenzenesulfonamide and -sulfonate scaffold, 16 derivatives and additional 14 virtual hits representing this scaffold were purchased. From these compounds, six inhibited 17 $\beta$ -HSD2. In total, ten 17 $\beta$ -HSD2 inhibitors representing phenylbenzenesulfonamides and sulfonates were discovered. From these compounds, the most active ones are depicted in Fig. 3. The full series has been published previously.<sup>18</sup>

This follow-up study aims at a more comprehensive structure-activity relationship (SAR) analysis of this scaffold by synthesizing derivatives of the most active compounds. An additional aim was to replace the phenolic hydroxy group that is an attractive metabolic site and toxicologically not favorable.<sup>19,20</sup>

In total, 20 derivatives of the most active compounds shown in Fig. 3 were synthesized (Table 1) from the corresponding 1,2-phenyldiamine or 2-hydroxyaniline and 4-*tert*-butylbenzenesulfonylchloride (see Fig. 4). These compounds were tested for 17 $\beta$ -HSD2 inhibition in a cell-free radioligand binding assay using the same test system as reported in Vuorinen et al.<sup>18</sup> Ten of them

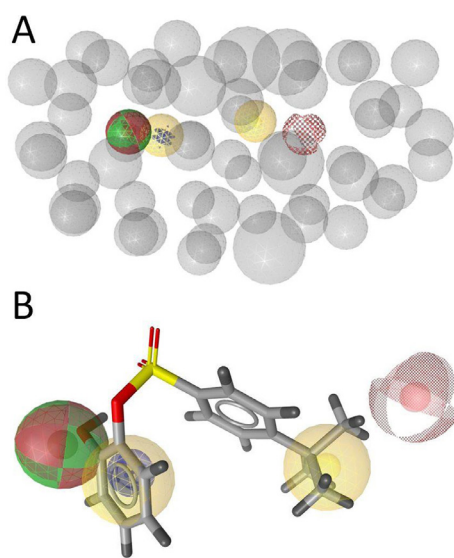


Fig. 2. (A) Pharmacophore model correctly predicting phenylbenzenesulfonamides and -sulfonates as 17 $\beta$ -HSD2 inhibitors. This model consists of six pharmacophore features: two hydrophobic areas (yellow), two hydrogen bond acceptors (red), of which one was optional (scattered representation), one hydrogen bond donor (green), an aromatic ring (blue rings), and 54 exclusion volumes (grey) mimicking spatial restrictions by the binding site. (B) Compound **1** fitted into the model.

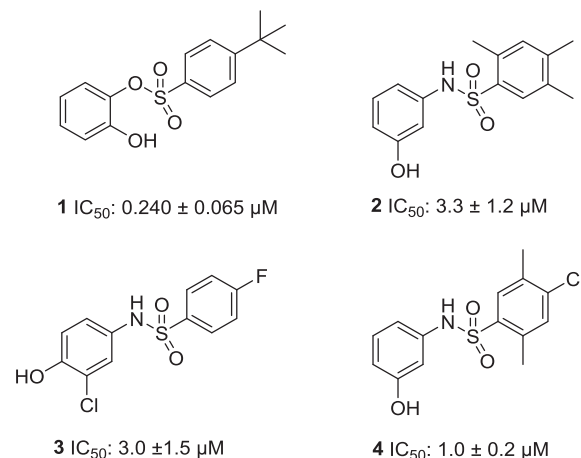
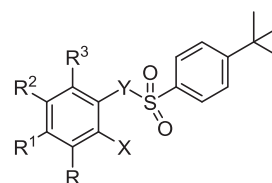


Fig. 3. The most active phenylbenzenesulfonamides and sulfonates from Vuorinen et al.<sup>18</sup> with their IC<sub>50</sub>-values.

Table 1

Structures and activities of the newly synthesized compounds.



Compound	X	Y	R	R <sup>1</sup>	R <sup>2</sup>	R <sup>3</sup>	Activity <sup>1</sup>
<b>5</b>	NH <sub>2</sub>	NH	H	H	H	H	46 ± 5%
<b>6</b>	NH <sub>2</sub>	O	H	CH <sub>3</sub>	H	H	37 ± 1%
<b>7</b>	NH <sub>2</sub>	O	H	H	H	H	33 ± 4%
<b>8</b>	NH <sub>2</sub>	NH	H	Cl	Cl	H	11 ± 4%
<b>9</b>	NH <sub>2</sub>	NH	H	CH <sub>3</sub>	CH <sub>3</sub>	H	4.65 ± 0.35 $\mu$ M
<b>10</b>	NH <sub>2</sub>	O	H	Cl	H	H	58 ± 7%
<b>11</b>	NH <sub>2</sub>	O	H	CH <sub>3</sub>	H	CH <sub>3</sub>	44 ± 2%
<b>12</b>	NH <sub>2</sub>	O	H	H	CH <sub>3</sub>	H	49 ± 3%
<b>13</b>	NH <sub>2</sub>	O	Bn		H	H	36 ± 3%
<b>14</b>	NH <sub>2</sub>	O	H	Ph	H	H	43 ± 1%
<b>15</b>	OH	NH	H	H	H	H	86 ± 3%
<b>16</b>	OH	NH	H	H	CH <sub>3</sub>	H	5 ± 3%
<b>17</b>	OH	NH	H	H	Cl	H	1.23 ± 0.35 $\mu$ M
<b>18</b>	OH	NH	CH <sub>3</sub>	H	CH <sub>3</sub>	H	13 ± 3%
<b>19</b>	OH	NH	H	CH <sub>3</sub>	H	H	4.09 ± 0.49 $\mu$ M
<b>20</b>	OH	NH	H	H	Ph	H	6 ± 4%
<b>21</b>	OH	NH	H	H	Bn	H	0.80 ± 0.22 $\mu$ M
<b>22</b>	NH <sub>2</sub>	NH	H	H	Cl	H	18 ± 7%
<b>23</b>	NH <sub>2</sub>	NH	H	Cl	H	H	5.19 ± 0.92 $\mu$ M
<b>24</b>	NH <sub>2</sub>	NH	H	F	H	H	22 ± 1%
<b>4</b> (positive control)							4.40 ± 0.79 $\mu$ M
							2 ± 2%
							1.25 ± 0.09 $\mu$ M
							7 ± 3%
							2.90 ± 0.69 $\mu$ M
							28 ± 6%
							5.58 ± 1.09 $\mu$ M
							35 ± 4%
							36 ± 2%
							10 ± 3%
							1.0 ± 0.2 $\mu$ M

<sup>1</sup> Given as remaining enzyme activity at a compound concentration of 20  $\mu$ M (%) or as IC<sub>50</sub>.

inhibited 17 $\beta$ -HSD2 by more than 70% at a concentration of 20  $\mu$ M, and IC<sub>50</sub> values were determined subsequently. These compounds inhibited 17 $\beta$ -HSD2 with low micromolar IC<sub>50</sub> values, with the most active compound **17** exhibiting an IC<sub>50</sub> of 0.80 ± 0.22  $\mu$ M.



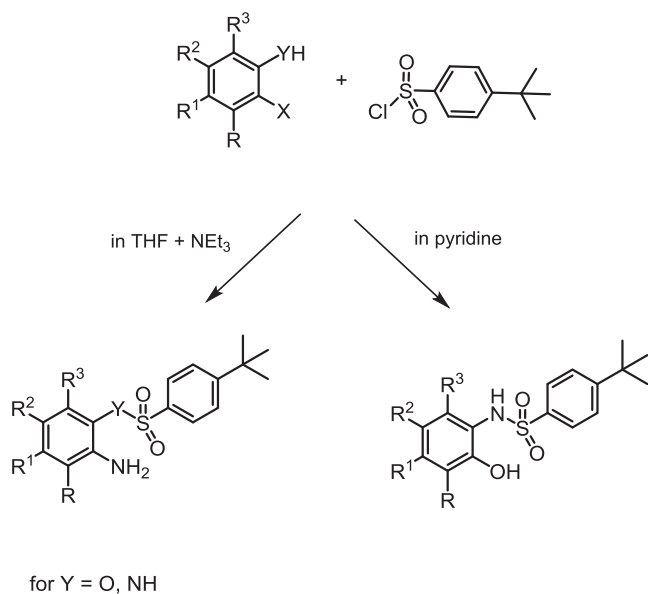


Fig. 4. Schematic synthesis of compounds 5–24.

As already observed in the previous publication, the phenolic hydroxyl group is advantageous for the activity. However, this functionality is an attractive site for metabolic modification<sup>19,20</sup> and therefore exchanging this feature with a bioisosteric group would be beneficial for the in vivo half-life of the molecule and may also address possible toxicological concerns. Nevertheless, replacing the phenolic hydroxy group by an amino group results in the formation of anilines, which also need to be evaluated for their toxic potential. The previous work revealed a decreased activity upon methylation of the phenol group, suggesting that a hydrogen bond donor is needed for the activity. Therefore, the hydroxy group was replaced by an amine. Unfortunately, the activity was decreased (compounds **5** and **7**). Introducing an electronegative substituent, such as chlorine or fluorine, to the sulfonamide compounds increased the activity, as can be concluded from the comparison of activities of the unhalogenated compound **5** and the corresponding halogenated derivatives **8**, **22**, **23** and **24**. In the sulfonamide series, methyl substituents in any position of the benzene ring reduced the inhibitory ability (compounds **16** and **18–19**) compared to compound **15**, however the activity was not completely lost. The position of the single methyl substituents did not make a significant difference in the activity of the compounds, as represented by their  $IC_{50}$  values. Interestingly, in the sulfonamide series, large aromatic ring substituents were tolerated by the enzyme (**20–21**); however, this was not the case in the sulfonate series. Whether the linker between the benzene rings was a sulfonamide or a sulfonate did not play a major role in the activity: Compounds **23** and **10** were equipotent. However, the sulfonate compound **1** was six times more active than the respective sulfonamide compound **15**. Still, compound **15** was more active than the sulfonamide **5** and the sulfonate **7**, respectively.

To demonstrate the observed SAR, a refined pharmacophore model representing the common chemical functionalities of our lead compound **1** and the most active compound from the new series (**17**) was generated. An addition of a phenyl and benzo annellation were tolerated (Fig. 5A and B), however, without significant effect on the potency of the compounds (compare compounds **7** vs. **13** and **15** vs. **21**). Substitution with a phenyl in para position to the amino group (position  $R^2$  in Table 1) was tolerated in the sulfonamide **20**. However, in the sulfonate **14**, a phenyl in the para position to the linker ( $R^1$  in Table 1) led to a loss of activity

(Fig. 5C). Therefore, the position of the phenyl substituent makes a difference in the activity. However, this loss of activity in compound **14** could also be caused by the hydroxyl-amino group exchange and by the different linker. It is speculated that the reason for the activity loss of **14** may lie in the spatial properties of the binding site in this position. Still, without structural data for 17 $\beta$ -HSD2, this remains an assumption. A chlorine substituent at position  $R^2$  in Table 1 is well tolerated, as compounds **15** and **17** are similarly active (Fig. 5D), and they both fit into the model well.

The previous report also depicted a predictive SAR-model for this scaffold.<sup>18</sup> The new compounds were fitted into this model as well. In fact, when the tolerance area of the hydrogen bond donor (HBD) functionality of the model was slightly increased by 0.15 Å, the following compounds could fit into the model: **15–17**, **19–20**, and **22** (Fig. 6A). Our previously published predictive SAR-model found most of the active compounds, but most remarkably, it was able to exclude the weakly active ones. The newly synthesized and biologically evaluated compounds were also fitted to our previously established pharmacophore model, the one that initially identified the scaffold. If screened without the exclusion volume spheres, three of the compounds: **15**, **16**, and **20** fitted into that model (Fig. 6B).

Additionally, the most active compounds were also tested against other HSDs (Table 2) that are structurally and functionally close to 17 $\beta$ -HSD2. Unfortunately, four of the new 17 $\beta$ -HSD2 inhibitors were also active on 17 $\beta$ -HSD1, the enzyme that is responsible for the reductive activation of estrone into estradiol.<sup>21</sup> Two of

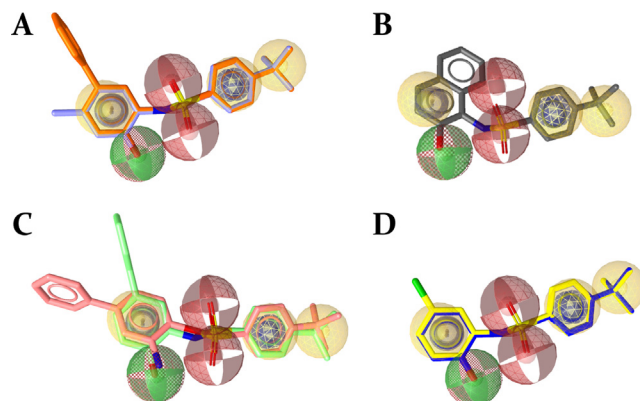


Fig. 5. New SAR-pharmacophore model with selected compounds: (A) **19** (light blue) and **20** (orange), (B) **21** (grey), (C) **14** (red) and **20** (green), (D) **15** (blue) and **17** (yellow). The pharmacophore features are color-coded: hydrogen bond acceptor – red, hydrogen bond donor green, aromatic ring – blue, hydrophobic – yellow. In case a feature is optional, it is depicted in a scattered style. Exclusion volumes were not generated.

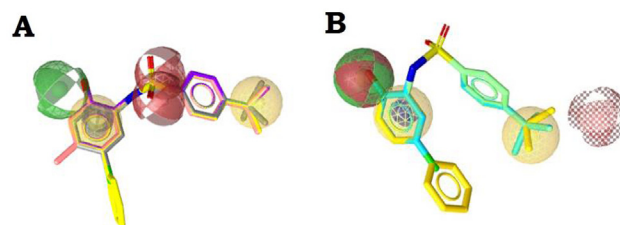


Fig. 6. (A) **15** (purple), **16** (green), **17** (blue), **19** (red), **20** (yellow), and **22** (grey) with the predictive SAR-model described previously.<sup>18</sup> (B) Compounds **16** (green), **17** (cyan), and **20** (yellow) fitted into the original pharmacophore model. The pharmacophore features are color coded: hydrogen bond acceptor – red, hydrogen bond donor green, aromatic ring – blue, hydrophobic – yellow. In case a feature is optional, it is depicted in a scattered style. Exclusion volumes are not shown for clarity.

**Table 2**  
Qualitative selectivity assessment of the active compounds represented as % of control at the inhibitor concentration of 20  $\mu$ M.

Compound	17 $\beta$ -HSD2	17 $\beta$ -HSD1	SI	11 $\beta$ -HSD1	SI	11 $\beta$ -HSD2	SI
<b>8</b>	11 $\pm$ 4%	23 $\pm$ 3% <sup>a</sup>	2.1	74 $\pm$ 4%	6.7	21 $\pm$ 11%	1.9
<b>15</b>	5 $\pm$ 3%	41 $\pm$ 6%	8.2	37 $\pm$ 5%	7.4	83 $\pm$ 9%	16.6
<b>16</b>	13 $\pm$ 3%	38 $\pm$ 6%	2.9	46 $\pm$ 2%	3.5	63 $\pm$ 12%	4.8
<b>17</b>	6 $\pm$ 4%	15 $\pm$ 6%	2.5	35 $\pm$ 3%	5.8	7 $\pm$ 4%	1.2
<b>18</b>	18 $\pm$ 7%	19 $\pm$ 8%	1.1	43 $\pm$ 2%	2.4	37 $\pm$ 10%	2.1
<b>19</b>	22 $\pm$ 1%	35 $\pm$ 9%	1.6	24 $\pm$ 4%	1.1	62 $\pm$ 9%	2.8
<b>20</b>	2 $\pm$ 2%	13 $\pm$ 3%	6.5	62 $\pm$ 5%	31	3 $\pm$ 3%	1.5
<b>21</b>	7 $\pm$ 3%	46 $\pm$ 7%	8.6	21 $\pm$ 4%	3	21 $\pm$ 4%	3
<b>22</b>	22 $\pm$ 6%	46 $\pm$ 10%	2.1	28 $\pm$ 7%	1.3	75 $\pm$ 8%	3.4
<b>24</b>	36 $\pm$ 2%	56 $\pm$ 11%	1.6	26 $\pm$ 8%	0.7	97 $\pm$ 4%	2.7
Positive controls (4)	10 $\pm$ 3%	11 $\pm$ 3% (apigenin) <sup>23</sup>		5 $\pm$ 1% (glycyrrhetic acid) <sup>24</sup>		7 $\pm$ 2% (glycyrrhetic acid) <sup>24</sup>	

<sup>a</sup> % residual enzyme activity compared to non-inhibited control at 20  $\mu$ M concentration. SI = selectivity index (residual HSD activity / residual 17 $\beta$ -HSD2 activity).

the compounds (**17** and **20**) also potently inhibited 11 $\beta$ -HSD2. This enzyme converts cortisol into cortisone in kidneys and is considered as an antitarget because its inhibition causes cardiovascular complications such as hypokalemia and hypertension.<sup>22</sup> Therefore, these compounds should be optimized for better selectivity. Compounds **19**, **21**, **22** and **24** inhibited 11 $\beta$ -HSD1, which activates cortisone to cortisol. Importantly, compound **15** could be considered as a relatively selective 17 $\beta$ -HSD2 inhibitor, indicating the feasibility to develop potent and selective compounds from this class.

In this study, 20 phenylbenzenesulfonamides and -sulfonates were synthesized and tested for 17 $\beta$ -HSD2 inhibition. In total, nine of them inhibited the enzyme with low micromolar IC<sub>50</sub> values. Even though none of these new compounds was more active than the parental compound **1**, they allowed establishing more comprehensive SAR-rules for this scaffold. In addition, these compounds provide also valuable information on the selectivity towards related enzymes.

## Acknowledgements

This study was supported by the Swiss National Science Foundation (31003A-159454 to A.O.) and the Novartis Research Foundation (A.O.).

## A. Supplementary data

Supplementary data associated with this article can be found, in the online version, at <http://dx.doi.org/10.1016/j.bmcl.2017.05.005>.

## References

- Dong Y, Qiu QQ, Debar J, Lathrop WF, Bertolini DR, Tamburini PP. 17 $\beta$ -Hydroxysteroid dehydrogenases in human bone cells. *J Bone Miner Res*. 1998;13:1539–1546.
- Puranen TJ, Kurkela RM, Lakkakorpi JT, et al. Characterization of molecular and catalytic properties of intact and truncated human 17 $\beta$ -hydroxysteroid dehydrogenase type 2 enzymes: intracellular localization of the wild-type enzyme in the endoplasmic reticulum. *Endocrinology*. 1999;140:3334–3341.
- Wu L, Einstein M, Geissler WM, Chan HK, Elliston KO, Andersson S. Expression cloning and characterization of human 17  $\beta$ -hydroxysteroid dehydrogenase type 2, a microsomal enzyme possessing 20  $\alpha$ -hydroxysteroid dehydrogenase activity. *J Biol Chem*. 1993;268:12964–12969.
- Takeyama J, Sasano H, Suzuki T, Iinuma K, Nagura H, Andersson S. 17 $\beta$ -Hydroxysteroid dehydrogenase types 1 and 2 in human placenta: an immunohistochemical study with correlation to placental development. *J Clin Endocrinol Metab*. 1998;83:3710–3715.
- Mustonen MV, Isomaa VV, Vaskivuo T, et al. Human 17 $\beta$ -hydroxysteroid dehydrogenase type 2 messenger ribonucleic acid expression and localization in term placenta and in endometrium during the menstrual cycle. *J Clin Endocrinol Metab*. 1998;83:1319–1324.
- Elo JP, Akinola LA, Poutanen M, et al. Characterization of 17 $\beta$ -hydroxysteroid dehydrogenase isoenzyme expression in benign and malignant human prostate. *Int J Cancer*. 1996;66:37–41.
- Mustonen M, Poutanen M, Kellokumpu S, et al. Mouse 17  $\beta$ -hydroxysteroid dehydrogenase type 2 mRNA is predominantly expressed in hepatocytes and in surface epithelial cells of the gastrointestinal and urinary tracts. *J Mol Endocrinol*. 1998;20:67–74.
- Cauley JA. Estrogen and bone health in men and women. *Steroids*. 2015;99:11–15.
- Kanis JA, McCloskey EV, Johansson H, Cooper C, Rizzoli R, Reginster JY. European guidance for the diagnosis and management of osteoporosis in postmenopausal women. *Osteoporos Int*. 2013;24:23–57.
- Lewiecki EM. Current and emerging pharmacologic therapies for the management of postmenopausal osteoporosis. *J Womens Health (Larchmt)*. 2009;18:1615–1626.
- Cummings SR, San Martin J, McClung MR, et al. Denosumab for prevention of fractures in postmenopausal women with osteoporosis. *N Engl J Med*. 2009;361:756–765.
- Ellis AJ, Hendrick VM, Williams R, Komm BS. Selective estrogen receptor modulators in clinical practice: a safety overview. *Expert Opin Drug Saf*. 2015;14:921–934.
- Bagi CM, Wood J, Wilkie D, Dixon B. Effect of 17 $\beta$ -hydroxysteroid dehydrogenase type 2 inhibitor on bone strength in ovariectomized cynomolgus monkeys. *J Musculoskelet Neuronal Interact*. 2008;8:267–280.
- Marchais-Oberwinkler S, Xu K, Wetzel M, et al. Structural optimization of 2,5-thiophene amides as highly potent and selective 17 $\beta$ -hydroxysteroid dehydrogenase type 2 inhibitors for the treatment of osteoporosis. *J Med Chem*. 2013;56:167–181.
- Wetzel M, Gargano EM, Hinsberger S, Marchais-Oberwinkler S, Hartmann RW. Discovery of a new class of bicyclic substituted hydroxyphenylmethanones as 17 $\beta$ -hydroxysteroid dehydrogenase type 2 (17 $\beta$ -HSD2) inhibitors for the treatment of osteoporosis. *Eur J Med Chem*. 2012;47:1–17.
- Wetzel M, Marchais-Oberwinkler S, Hartmann RW. 17 $\beta$ -HSD2 inhibitors for the treatment of osteoporosis: Identification of a promising scaffold. *Bioorg Med Chem*. 2011;19:807–815.
- Xu K, Al-Soud YA, Wetzel M, Hartmann RW, Marchais-Oberwinkler S. Triazole ring-opening leads to the discovery of potent nonsteroidal 17 $\beta$ -hydroxysteroid dehydrogenase type 2 inhibitors. *Eur J Med Chem*. 2011;46:5978–5990.
- Vuorinen A, Engeli R, Meyer A, et al. Ligand-based pharmacophore modeling and virtual screening for the discovery of novel 17 $\beta$ -hydroxysteroid dehydrogenase 2 inhibitors. *J Med Chem*. 2014;57:5995–6007.
- Hansch C, McKarns SC, Smith CJ, Doolittle DJ. Comparative QSAR evidence for a free-radical mechanism of phenol-induced toxicity. *Chem Biol Interact*. 2000;127:61–72.
- Moridani MY, Siraki A, O'Brien PJ. Quantitative structure toxicity relationships for phenols in isolated rat hepatocytes. *Chem Biol Interact*. 2003;145:213–223.
- Mindnich R, Moller G, Adamski J. The role of 17  $\beta$ -hydroxysteroid dehydrogenases. *Mol Cell Endocrinol*. 2004;218:7–20.
- Ferrari P. The role of 11 $\beta$ -hydroxysteroid dehydrogenase type 2 in human hypertension. *Biochim Biophys Acta*. 2010;1802:1178–1187.
- Schuster D, Nashev LG, Kirchmair J, et al. Discovery of nonsteroidal 17 $\beta$ -hydroxysteroid dehydrogenase 1 inhibitors by pharmacophore-based screening of virtual compound libraries. *J Med Chem*. 2008;51:4188–4199.
- Kratschmar DV, Vuorinen A, Da Cunha T, et al. Characterization of activity and binding mode of glycyrrhetic acid derivatives inhibiting 11 $\beta$ -hydroxysteroid dehydrogenase type 2. *J Biochem Mol Biol*. 2011;125:129–142.

### 3.4 Paper 3 (Vourinen/Engeli et al., 2017b)

## Potential Anti-osteoporotic Natural Products Lead Compounds that Inhibit 17 $\beta$ -Hydroxysteroid Dehydrogenase Type 2

Anna Vuorinen\*, Roger T. Engeli\*, Susanne Leugger, Fabio Bachmann, Muhammad Akram, Atanas G. Atanasov, Birgit Waltenberger, Veronika Temml, Hermann Stuppner, Liselotte Krenn, Sylvain B. Ateba, Dieudonné Njamé, Rohan A. Davis, Alex Odermatt, Daniela Schuster

Published manuscript

**Contribution:** Provided all data for the 17 $\beta$ -HSD1 and 17 $\beta$ -HSD2 activity assay experiments (Table 1-3). Co-wrote the paper manuscript. First authorship was shared equally (\*).

**Aims:** Identify natural products that inhibit 17 $\beta$ -HSD2 as potential lead structures to treat osteoporosis. Natural product databases were screened using the previously published ligand-based pharmacophore model.

**Results:** Several natural and semi-synthetic natural products were identified, which inhibit 17 $\beta$ -HSD2 with sub- and micromolar IC<sub>50</sub> values.

**Conclusion:** Identified natural products can be used as potential lead structures in medicinal chemistry studies to further improve the properties of the compounds.



## Potential Antiosteoporotic Natural Product Lead Compounds That Inhibit 17 $\beta$ -Hydroxysteroid Dehydrogenase Type 2

Anna Vuorinen,<sup>†,#</sup> Roger T. Engeli,<sup>†,#</sup> Susanne Leugger,<sup>†</sup> Fabio Bachmann,<sup>†</sup> Muhammad Akram,<sup>‡</sup> Atanas G. Atanasov,<sup>§,⊥</sup> Birgit Waltenberger,<sup>||</sup> Veronika Temml,<sup>||</sup> Hermann Stuppner,<sup>||</sup> Liselotte Krenn,<sup>§</sup> Sylvin B. Ateba,<sup>¶</sup> Dieudonné Njamen,<sup>¶</sup> Rohan A. Davis,<sup>□</sup> Alex Odermatt,<sup>\*,†</sup> and Daniela Schuster<sup>\*,†,⊙</sup>

<sup>†</sup>Division of Molecular & Systems Toxicology, University of Basel, Klingelbergstraße 50, 4056 Basel, Switzerland

<sup>‡</sup>Computer-Aided Molecular Design Group, Institute of Pharmacy/Pharmaceutical Chemistry and Center for Molecular Biosciences Innsbruck, and <sup>||</sup>Institute of Pharmacy/Pharmacognosy and Center for Molecular Biosciences Innsbruck, University of Innsbruck, Innrain 80-82, 6020 Innsbruck, Austria

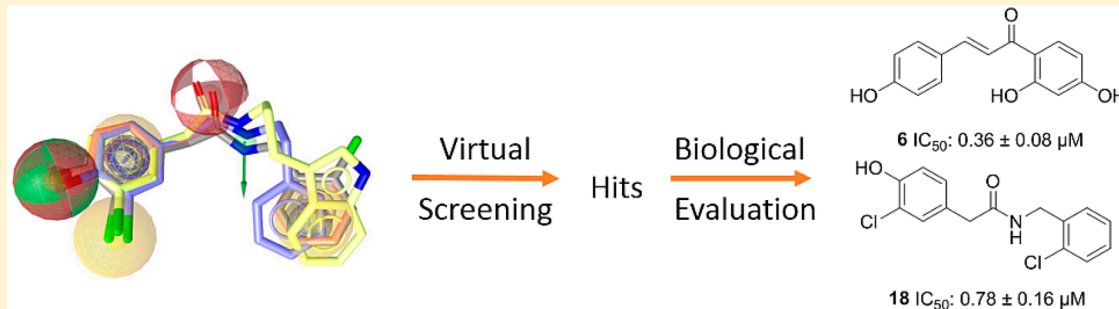
<sup>§</sup>Department of Pharmacognosy, University of Vienna, Althanstraße 14, 1090 Vienna, Austria

<sup>⊥</sup>Institute of Genetics and Animal Breeding of the Polish Academy of Sciences, Postępu 36A Street, 05-552, Jastrzebiec, Poland

<sup>¶</sup>Laboratory of Animal Physiology, Department of Animal Biology and Physiology, Faculty of Science, University of Yaounde I, P.O. Box 812, Yaounde, Cameroon

<sup>□</sup>Griffith Institute for Drug Discovery, Griffith University, Brisbane, QLD 4111, Australia

### Supporting Information



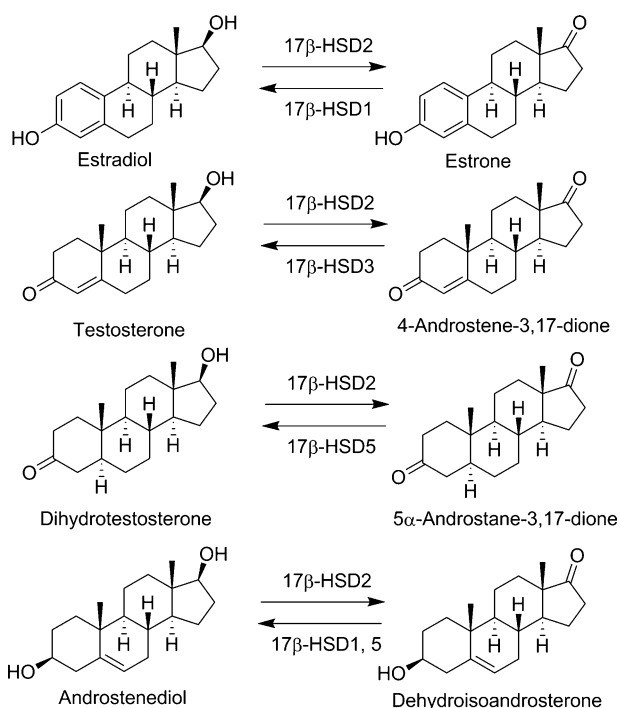
**ABSTRACT:** 17 $\beta$ -Hydroxysteroid dehydrogenase type 2 (17 $\beta$ -HSD2) converts the active steroid hormones estradiol, testosterone, and 5 $\alpha$ -dihydrotestosterone into their weakly active forms estrone,  $\Delta^4$ -androstene-3,17-dione, and 5 $\alpha$ -androstane-3,17-dione, respectively, thereby regulating cell- and tissue-specific steroid action. As reduced levels of active steroids are associated with compromised bone health and onset of osteoporosis, 17 $\beta$ -HSD2 is considered a target for antiosteoporotic treatment. In this study, a pharmacophore model based on 17 $\beta$ -HSD2 inhibitors was applied to a virtual screening of various databases containing natural products in order to discover new lead structures from nature. In total, 36 hit molecules were selected for biological evaluation. Of these compounds, 12 inhibited 17 $\beta$ -HSD2 with nanomolar to low micromolar IC<sub>50</sub> values. The most potent compounds, nordihydroguaiaretic acid (1), IC<sub>50</sub> 0.38 ± 0.04 μM, (–)-dihydroguaiaretic acid (4), IC<sub>50</sub> 0.94 ± 0.02 μM, isoliquiritigenin (6), IC<sub>50</sub> 0.36 ± 0.08 μM, and ethyl vanillate (12), IC<sub>50</sub> 1.28 ± 0.26 μM, showed 8-fold or higher selectivity over 17 $\beta$ -HSD1. As some of the identified compounds belong to the same structural class, structure–activity relationships were derived for these molecules. Thus, this study describes new 17 $\beta$ -HSD2 inhibitors from nature and provides insights into the binding pocket of 17 $\beta$ -HSD2, offering a promising starting point for further research in this area.

17 $\beta$ -Hydroxysteroid dehydrogenase type 2 (17 $\beta$ -HSD2) belongs to a large family of short-chain dehydrogenase/reductase (SDR) enzymes with the systematic name SDR9C2.<sup>1</sup> It is mainly expressed in the placenta, endometrium, breast, prostate, small intestine, liver, and bone.<sup>2–5</sup> This NAD<sup>+</sup>-dependent enzyme converts active sex steroid hormones such as estradiol, testosterone, and 5 $\alpha$ -dihydrotestosterone into their respective inactive forms, namely, estrone,  $\Delta^4$ -androstene-3,17-dione (androstenedione), and 5 $\alpha$ -androstane-3,17-dione (androstane-3,17-dione), thereby protecting tissues from excessive sex steroid hormone action (Figure 1).<sup>6,7</sup> Furthermore, 17 $\beta$ -HSD2

catalyzes the oxidation of  $\Delta^5$ -androstene-3 $\beta$ ,17 $\beta$ -diol (androstenediol) to dehydroepiandrosterone (DHEA). The enzyme shares considerable structural and functional similarity with other extensively studied SDR enzymes such as 17 $\beta$ -HSD1 and 17 $\beta$ -HSD3.<sup>8</sup> In contrast to 17 $\beta$ -HSD2, the enzymes 17 $\beta$ -HSD1, 17 $\beta$ -HSD3, and the aldo-keto-reductase 17 $\beta$ -HSD5 (also known as AKR1C3) are oxidoreductases converting the weak

Received: October 14, 2016

Published: March 20, 2017



**Figure 1.** Enzymatic reactions catalyzed by  $17\beta$ -HSD2 and reverse reactions catalyzed by other HSD enzymes.

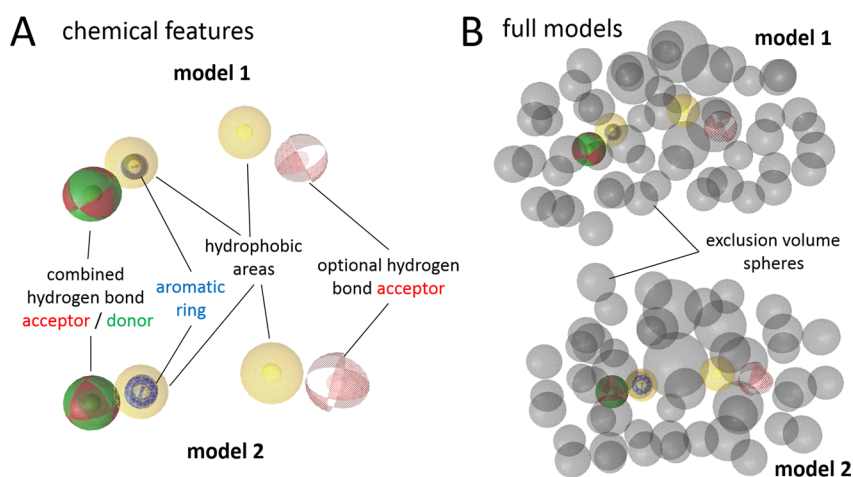
estrogen estrone to the potent estradiol and the weak androgens androstenedione and androstenedione to testosterone and  $5\alpha$ -dihydrotestosterone, respectively.<sup>9–11</sup> Whereas  $17\beta$ -HSD3 is responsible for the last step of testosterone synthesis in the testes,  $17\beta$ -HSD5 is responsible for the production of extratesticular testosterone and plays a crucial role in androgen maintenance in the elderly.<sup>9,10</sup>

Owing to its favorable localization and its role as a main contributor to the inactivation of estradiol, testosterone, and  $5\alpha$ -dihydrotestosterone in bone cells,<sup>2</sup>  $17\beta$ -HSD2 has been proposed as a promising target for the treatment of osteoporosis.<sup>12</sup> This condition, where decreased bone density leads to an increased fracture risk, is in the majority of cases

linked with the age-related decrease of sex steroid hormones.<sup>13</sup> The age-related onset of osteoporosis in postmenopausal women<sup>14</sup> and men with low testosterone levels<sup>15</sup> can be explained, at least in part, by a decline in the concentrations of estradiol and testosterone, which inhibit bone degradation.<sup>16</sup> Thus, by inhibiting  $17\beta$ -HSD2, the amount of active steroids can be locally increased in the bones, thereby improving bone health. This hypothesis is supported by an *in vivo* study, where a  $17\beta$ -HSD2 inhibitor was administered to ovariectomized cynomolgus monkeys.<sup>17</sup> In this study, the  $17\beta$ -HSD2 inhibitor was shown to improve bone strength by increasing bone formation and decreasing bone resorption, although the effects were rather weak and only observed at the highest dose of 25 mg/kg/day.

Although multiple synthetic  $17\beta$ -HSD2 inhibitors have already been reported,<sup>18–21</sup> natural products inhibiting this enzyme are currently underexplored. There are only a few reports on natural product inhibitors of  $17\beta$ -HSD2 and other steroid-metabolizing enzymes, and the majority of these compounds are flavonoids.<sup>22–24</sup> Flavonoids share certain functional similarities with steroids and can be considered as steroid mimetics (Figure S1, Supporting Information). However, most of these compounds are not selective. They also inhibit other members of the SDR enzyme family, and, additionally, they frequently show activity toward estrogen and androgen receptors. Nevertheless, natural compounds play an important role in providing new structures as potential lead candidates in drug discovery, and hence they are of high general interest.<sup>25,26</sup> Remarkably, from 1999 to 2008, 28% of all new FDA-approved, first-in-class small-molecule drugs were natural products or compounds derived thereof.<sup>27</sup>

Despite the fact that osteoporosis is not well represented among the conditions treated with plants and phytotherapy,<sup>28</sup> there are many other conditions related to bone homeostasis and fractures that are reported in the literature on ethnopharmacology. Interestingly, an ethnopharmacological study has been reported that shows that plants such as *Pholidota articulate* Lindl. and *Coelogyne cristata* Lindl. (both of the Orchidaceae family) contain several flavonoids that are used to treat bone fractures in India.<sup>29</sup> Even though part of the observed effects of these compounds may be due to direct



**Figure 2.** Pharmacophore models for  $17\beta$ -HSD2 inhibitors. (A) Chemical features of models 1 and 2 describing the types, locations, and tolerance spheres of inhibitory chemical functionalities. Pharmacophore features are colored as follows: red, hydrogen-bond acceptor; green, hydrogen-bond donor; yellow, hydrophobic; and blue, aromatic ring. Optional features are depicted in scattered style. (B) Full versions of models 1 and 2 with gray exclusion volumes as steric restraints for inhibitor size (forbidden areas). A 3D video view of model 1 is available as Supporting Information.

**Table 1. Active Hit Compounds of Natural Origin, Databases, Mapping Pharmacophore Models, and Activities against 17 $\beta$ -HSD2**

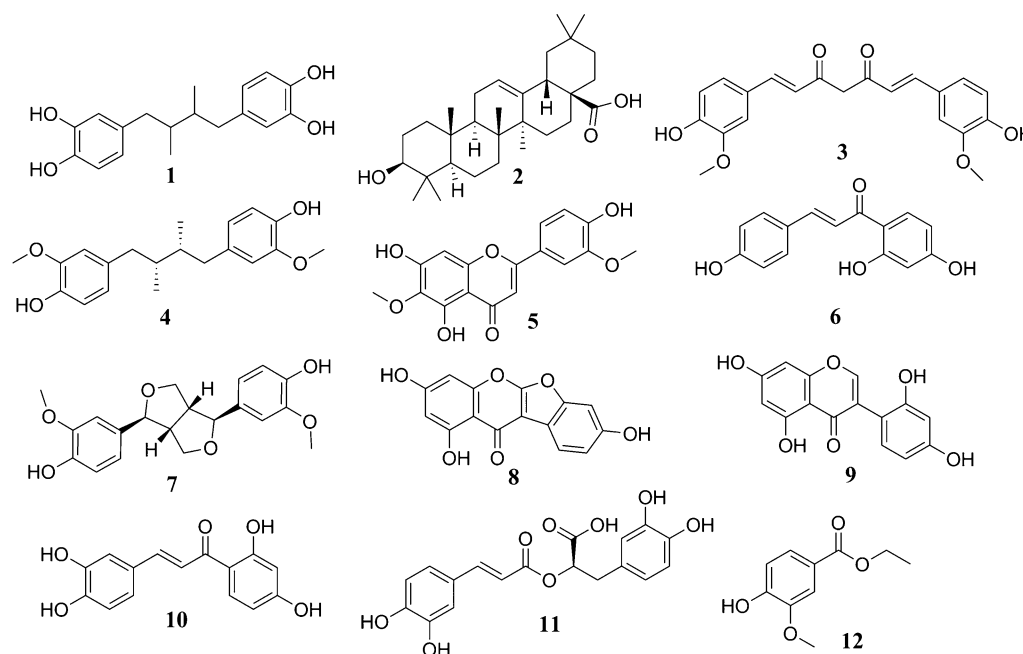
compound	database	pharmacophore models	remaining activity at 20 $\mu$ M (% of control) or IC <sub>50</sub>
nordihydroguaiaretic acid (1)	Atanasov	models 1 and 2	0.38 $\pm$ 0.04 $\mu$ M
oleanolic acid (2)	Atanosov	model 1 omf <sup>a</sup>	49 $\pm$ 6%
curcumin (3)	Atanosov	models 1 and 2 omf	1.73 $\pm$ 0.2 $\mu$ M
(-)-dihydroguaiaretic acid (4)	Davis	models 1 and 2	0.94 $\pm$ 0.02 $\mu$ M
jaceosidin (5)	Davis	models 1 and 2 omf	9.3 $\pm$ 2.3 $\mu$ M
isoliquiritigenin (6)	Davis	models 1 and 2	0.36 $\pm$ 0.08 $\mu$ M
pinosresinol (7)	Waltenberger	models 1 and 2	42 $\pm$ 5%
lupinalbin A (8)	Krenn	model 2 omf	1.52 $\pm$ 0.15 $\mu$ M
2'-hydroxygenistein (9)	Krenn	model 2 omf	2.03 $\pm$ 0.37 $\mu$ M
butein (10)	Sigma	model 1	7.3 $\pm$ 2.7 $\mu$ M
rosmarinic acid (11)	Sigma	model 1	3.72 $\pm$ 0.17 $\mu$ M
ethyl vanillate (12)	Sigma	model 1	1.28 $\pm$ 0.26 $\mu$ M

<sup>a</sup>omf, screening by allowing one omitted feature.

**Table 2. Active Semisynthetic Fungal Natural Products, Origin, Mapping Pharmacophore Models, and Activities against 17 $\beta$ -HSD2**

compound	database	pharmacophore models	remaining activity at 20 $\mu$ M (% of control) or IC <sub>50</sub>
2-(3-chloro-4-hydroxyphenyl)- <i>N</i> -phenethylacetamide (13)	Davis	model 1	1.57 $\pm$ 0.16 $\mu$ M
2-(3-chloro-4-hydroxyphenyl)- <i>N</i> -(2-methoxyethyl)acetamide (14)	Davis	model 1 omf <sup>a</sup>	37 $\pm$ 3%
<i>N</i> -butyl-2-(3-chloro-4-hydroxyphenyl)acetamide (15)	Davis	model 1	33 $\pm$ 6%
<i>N</i> -benzyl-2-(3-chloro-4-hydroxyphenyl)acetamide (16)	Davis	model 1	3.42 $\pm$ 0.74 $\mu$ M
<i>N</i> -(2-(1 <i>H</i> -indol-3-yl)ethyl)-2-(3-chloro-4-hydroxyphenyl)acetamide (17)	Davis	model 1	0.98 $\pm$ 0.24 $\mu$ M
2-(3-chloro-4-hydroxyphenyl)- <i>N</i> -(2-chlorobenzyl)acetamide (18)	Davis	model 1	0.78 $\pm$ 0.16 $\mu$ M

<sup>a</sup>omf, screening by allowing one omitted feature.

**Figure 3.** Structures of natural products identified in this study that inhibit 17 $\beta$ -HSD2.

modulation of estrogen and androgen receptor activities, the mechanism of action of these compounds in the treatment of bone-related conditions is largely unknown. Accordingly, 17 $\beta$ -HSD2 inhibition might well contribute to the effects of these herbal remedies.

As natural compounds represent a rich source of potential lead structures, novel 17 $\beta$ -HSD2 inhibitors of natural origin were searched using *in silico* methods. Previously, a procedure

to discover new synthetic chemicals that inhibit 17 $\beta$ -HSD2 was established.<sup>19</sup> In this previous study, pharmacophore models representing the chemical functionalities and steric requirements essential for the activity of small molecules toward 17 $\beta$ -HSD2 were constructed and employed for virtual screening of a commercial synthetic chemical database. From this previous experimental validation, the two pharmacophore models 1 and 2 (Figure 2) showed good predictive power, with positive hit

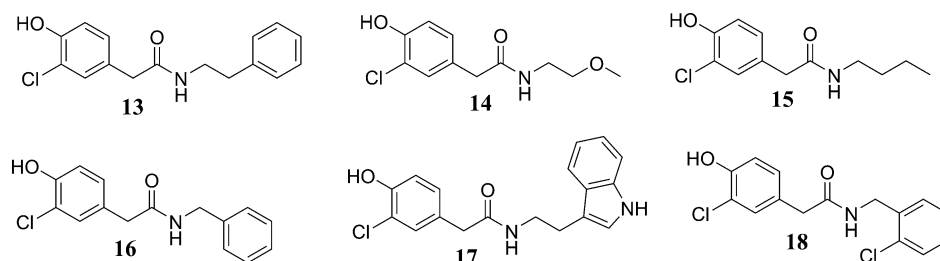


Figure 4. Semisynthetic fungal natural products that inhibit 17 $\beta$ -HSD2.

Table 3. Selectivity of the Most Active 17 $\beta$ -HSD2 Inhibitors toward 17 $\beta$ -HSD1

compound	17 $\beta$ -HSD2 activity (IC <sub>50</sub> )	17 $\beta$ -HSD1 activity (IC <sub>50</sub> or remaining activity at 20 $\mu$ M)	selectivity factor
nordihydroguaiaretic acid (1)	0.38 $\pm$ 0.04 $\mu$ M	5.5 $\pm$ 1.3 $\mu$ M	15
curcumin (3)	1.73 $\pm$ 0.20 $\mu$ M	52.2 $\pm$ 7.1%	~12
(-)-dihydroguaiaretic acid (4)	0.94 $\pm$ 0.02 $\mu$ M	7.7 $\pm$ 2.2 $\mu$ M	8
isoliquiritigenin (6)	0.36 $\pm$ 0.08 $\mu$ M	2.83 $\pm$ 0.80 $\mu$ M	8
lupinalbin A (8)	1.52 $\pm$ 0.15 $\mu$ M	0.049 $\pm$ 0.019 $\mu$ M	0.03
2'-hydroxygenistein (9)	2.03 $\pm$ 0.37 $\mu$ M	1.09 $\pm$ 0.06 $\mu$ M	0.5
rosmarinic acid (11)	3.72 $\pm$ 0.17 $\mu$ M	n.i. <sup>a</sup>	>5
ethyl vanillate (12)	1.28 $\pm$ 0.26 $\mu$ M	n.i.	>15
2-(3-chloro-4-hydroxyphenyl)- <i>N</i> -phenethylacetamide (13)	1.57 $\pm$ 0.16 $\mu$ M	n.i.	>12
<i>N</i> -benzyl-2-(3-chloro-4-hydroxyphenyl)acetamide (16)	3.42 $\pm$ 0.74 $\mu$ M	n.i.	>5
<i>N</i> -(2-(1 <i>H</i> -indol-3-yl)ethyl)-2-(3-chloro-4-hydroxyphenyl)acetamide (17)	0.98 $\pm$ 0.24 $\mu$ M	n.i.	>20
2-(3-chloro-4-hydroxyphenyl)- <i>N</i> -(2-chlorobenzyl)acetamide (18)	0.78 $\pm$ 0.16 $\mu$ M	54.8 $\pm$ 5.8%	~25

<sup>a</sup>n.i., no inhibition.

rates of 50% and 10%, respectively. Although the models are very similar in feature types and distribution, they differ slightly in feature location, which is why they may lead to somewhat different virtual hits. Thus, both of these models were selected for virtual screening of selected natural product databases.

## RESULTS AND DISCUSSION

In-house natural product databases based on input from several academic institutions (total of 439 entries) and the Sigma-Aldrich catalogue (Sigma-Aldrich, St. Louis, MO, USA), containing natural products and synthetic compounds, were screened virtually using the two pharmacophore models. The virtual screening procedure and its results are described in detail in the Supporting Information (text and Table S1). As the full models were quite restrictive, most databases were also screened in models where one omitted feature (omf) was applied during the pharmacophore mapping.

The 36 selected virtual hits were evaluated in an in vitro assay using lysates of cells expressing the recombinant human enzyme 17 $\beta$ -HSD2. Initially, all compounds were tested at a final concentration of 20  $\mu$ M. Compounds showing more than 50% inhibition at that concentration are shown in Tables 1 and 2 as well as Figures 3 and 4. For all compounds inhibiting 17 $\beta$ -HSD2 activity by at least 70% (remaining activity  $\leq$ 30% of vehicle control), IC<sub>50</sub> values were determined. The complete list of the compounds tested is provided in Table S2, Supporting Information.

From the selected 36 tested compounds, 12 were active with IC<sub>50</sub> values of  $<$ 5  $\mu$ M, six were moderately active showing at least 50% inhibition at a compound concentration of 20  $\mu$ M, and the remaining compounds were considered inactive. Altogether, this corresponds to a 50% hit rate, indicating that the pharmacophore models performed explicitly well, not only

for synthetic molecules but also for natural compounds. This is an important aspect, because natural products often differ from synthetic drug-like structures. From the 33 in-house database-derived test compounds, 10 fit into model 1 and four into model 2, respectively, without omitted features during the screening (Tables 1 and 2). Remarkably, all these hits were active in vitro. Additionally, the strategy of allowing one pharmacophore feature to be left out during the natural product database screening proved successful: The hits obtained by allowing one omitted feature additionally included the active compounds oleanolic acid (2), curcumin (3), jaceosidin (5), lupinalbin A (8), 2'-hydroxygenistein (9), and the semi-synthetic derivative 2-(3-chloro-4-hydroxyphenyl)-*N*-(2-methoxyethyl)acetamide (14). Although, admittedly, all inactive compounds from this study have also been identified in the screenings with one omitted feature, these additional active hits encourage this screening mode, when a wider range of chemically diverse 17 $\beta$ -HSD2 inhibitors is sought and a higher number of false positive virtual hits is acceptable.

For a possible therapeutic use of a 17 $\beta$ -HSD2 inhibitor, a compound must be selective over 17 $\beta$ -HSD1, which catalyzes the reverse reaction. Therefore, the most active newly identified 17 $\beta$ -HSD2 inhibitors were screened at a final concentration of 20  $\mu$ M in vitro using lysates of cells expressing the recombinant human 17 $\beta$ -HSD1 enzyme. For all compounds inhibiting 17 $\beta$ -HSD1 by 70% or more, IC<sub>50</sub> values and corresponding selectivity factors were determined. The results are shown in Table 3. Follow-up experiments should include additional SDR enzymes such as 11 $\beta$ -HSDs, 3 $\alpha$ / $\beta$ -HSDs, and retinol dehydrogenases as well as a careful assessment of the cytotoxic potential of the identified compounds.

Most of the active hits found in this study belong to compound classes associated with steroidogenic activities. This



includes the triterpene oleanolic acid (2), which belongs to a compound class containing several 11 $\beta$ -HSD inhibitors.<sup>30–33</sup> Compounds 5, 8, and 9 are flavonoids, a class known to have estrogenic activity. Nordihydroguaiaretic acid (1) is a lignan found at high concentrations in the leaves of *Larrea tridentata* (Sessé & Moc. ex DC.) Coville, a common shrub in the United States and in Mexico.<sup>34</sup> The leaves have been used in the preparation of a tea for the treatment of cancer, arthritis, and tuberculosis. Compound 1 is an antioxidant that also inhibits lipoxygenase, thus influencing the leukotriene cascade and suppressing ovulation in rats.<sup>35</sup> Thereby, it may pose a potential risk for reproductive toxicity if ingested in large amounts. Compound 1 was proposed to be converted into a phytoestrogen by gut flora.<sup>36</sup> In addition, it was shown to have estrogenic effects, being an ER $\alpha$ -agonist, with a tendency to be selective over ER $\beta$ .<sup>37</sup> Additionally, compound 1 was shown to inhibit the formation of  $\beta$ -amyloid fibrils in the central nervous system and the accumulation of  $\beta$ -peptides. These properties suggest that 1 is an interesting compound for the development of potential anti-Alzheimer disease (AD) pharmaceuticals.<sup>38</sup> Similar anti-amyloidogenic effects were also reported in studies with mice for 1, 3, and 11, supporting the potential preventive properties of these natural compounds against AD.<sup>39</sup>

Curcumin (3) is a tautomeric diarylheptanoid compound that is found in the roots of *Curcuma longa* L. and has a great variety of potential therapeutic activities.<sup>40,41</sup> It is one of the main ingredients of curry spice mixtures and is responsible for the yellow color.<sup>42</sup> Many papers have been published in the past few decades describing anti-inflammatory,<sup>43</sup> anticancer,<sup>44,45</sup> and antioxidant properties of 3.<sup>40</sup> In Asian medicine, 3 was used for topical or oral application to treat a variety of diseases for thousands of years. Despite the low bioavailability and rapid hepatic metabolism, 3 was shown to be therapeutically active against several diseases.<sup>46</sup> There is debate as to whether 3 may be an invalid bioactive compound because of its PAINS properties<sup>47–49</sup> or may still have some potential as a lead structure candidate for certain conditions.<sup>50</sup> According to the experiments and observations from this study, 3 directly and specifically inhibits 17 $\beta$ -HSD2 and 17 $\beta$ -HSD1. A detailed discussion on this issue is provided in the [Supporting Information](#) (p S9). Although 3 may not be a suitable lead compound for various reasons, it still reflects the ability of the virtual screening workflow to detect structurally diverse 17 $\beta$ -HSD2 inhibitors.

Dihydroguaiaretic acid (4) is another lignan that is present in various plant extracts, such as those derived from the bark of *Machilus thunbergii*<sup>51</sup> Siebold & Zucc. and the seeds of *Myristica fragrans* Houtt.<sup>52</sup> These plants are found predominantly in tropical and subtropical Asian countries. Compound 4 was reported to possess antibacterial,<sup>53</sup> antioxidative,<sup>54</sup> and potential anticancer properties.<sup>55</sup> Little is known about the potential interference of 4 with estrogen-metabolizing hormones. In 2001, Filleur et al. reported that 4 showed no effects on 17 $\beta$ -HSD activity in placenta microsomes.<sup>56</sup> This is in contrast with the potent inhibition (IC<sub>50</sub> 940  $\pm$  20 nM) of 17 $\beta$ -HSD2 by 4 found in the present study. The reason for this discrepancy is unclear but may be due to experimental differences, as in the present study recombinant human enzyme was used. In contrast, in the study by Filleur et al. placenta microsomes that also express other steroid-metabolizing enzymes were applied.

Isoliquiritigenin (6) is a hydroxylated chalcone found in *Glycyrrhiza uralensis* Fisch. ex DC.<sup>57</sup> and other various plant preparations. Many pharmacological effects of 6 have been described in the literature such as antitumor, antioxidative, and antibacterial properties.<sup>58</sup> Using a recombinant protein, it was reported that 6 inhibits aromatase activity with an IC<sub>50</sub> value of 3.8  $\mu$ M.<sup>59</sup> This would lower the amount of estrogens produced from androgens, which may aggravate osteoporosis. Nevertheless, 6 is a moderately potent inhibitor of aromatase, and efficient inhibition of 17 $\beta$ -HSD2 was achieved at concentrations 10 times lower. Importantly, 6 did not inhibit 17 $\beta$ -HSD1. Using yeast strains expressing human receptors, 6 was shown to bind to ER $\alpha$  (IC<sub>50</sub> to displace estradiol of 1.87  $\mu$ M) and ER $\beta$  (IC<sub>50</sub> of 269 nM), however, with much lower affinity than estradiol.<sup>60</sup>

Compounds 8 and 9 are major constituents contained in a methanolic extract of the aerial parts of *Eriosema laurentii* De Wild, which was shown to have protective effects against femur mass loss and significantly increased calcium and inorganic phosphorus content in the femur in ovariectomized rats.<sup>61,62</sup> Inhibition of 17 $\beta$ -HSD2 by these compounds may enhance local levels of estradiol, thereby potentiating estrogen receptor  $\alpha$  (ER $\alpha$ )-mediated signaling. However, some of these effects may be explained by direct effects of the compounds on steroid receptors and/or helix–loop–helix transcription factors. In yeast systems expressing the human ER $\alpha$  and the human aryl hydrocarbon receptor, 8 showed agonistic effects with EC<sub>50</sub> values of 21.4 nM and 1.34  $\mu$ M, respectively.<sup>63</sup> Additionally, 9 was reported to activate ER $\alpha$  with an EC<sub>50</sub> value of 6.1  $\mu$ M. Regarding 8 and 9, it needs to be noted that these compounds exert more potent inhibitory effects against 17 $\beta$ -HSD1 than 17 $\beta$ -HSD2. In fact, 8 potently inhibited 17 $\beta$ -HSD1 with an IC<sub>50</sub> of 49  $\pm$  19 nM and an approximately 30-fold selectivity over 17 $\beta$ -HSD2. This in vitro information suggests that 8 most potently activates ER $\alpha$  and potently inhibits estrone to estradiol conversion by 17 $\beta$ -HSD1 but shows weaker effects on 17 $\beta$ -HSD2-mediated estradiol inactivation. Depending on the tissue and cell type, ER $\alpha$  is expressed together with either 17 $\beta$ -HSD1 or 17 $\beta$ -HSD2, which may result in cell-specific estrogenic effects of 8.

Rosmarinic acid (11) was first isolated from an extract of *Rosmarinus officinalis* L.<sup>64</sup> This compound was studied for many years and showed antinociceptive and anti-inflammatory effects in animal studies.<sup>65</sup> In addition, several clinical trials showed positive effects of comfrey roots containing 11 as a topical treatment against pain.<sup>66</sup> Antinociceptive effects would clearly be beneficial in the treatment of osteoporosis because of increasing pain with progression of the disease. Compound 11 selectively inhibited 17 $\beta$ -HSD2 over 17 $\beta$ -HSD1, although with rather moderate activity. It therefore remains to be seen whether such concentrations can be reached in bone cells. Alternatively, paracrine effects from neighboring cells may affect estrogen availability and therefore bone metabolism.

Ethyl vanillate (12) is an antioxidative<sup>67</sup> compound that has been found in hedge mustard [*Sisymbrium officinale* (L.) Scop.] and also in Pinot noir wine.<sup>68</sup> Although 12 has been known for quite some time, due to its intense vanilla taste and its use as a flavoring additive, its biological properties remain poorly investigated.

Most of the newly discovered 17 $\beta$ -HSD2 inhibitors were already known as phytoestrogens or compounds that are converted into phytoestrogen by gut flora (e.g., pinoresinol (7) and 1).<sup>36</sup> The rationale why the pharmacophore model found

these ER-active compounds was that the substrate (estradiol) of 17 $\beta$ -HSD2 is the endogenous ER agonist, and thus the binding pockets of ER and 17 $\beta$ -HSD2 are obviously able to accommodate similar compounds that may be considered as steroid mimetics. This was reflected by the pharmacophore model that is based on the properties of compounds binding to 17 $\beta$ -HSD2: the compounds that share features needed for binding to 17 $\beta$ -HSD2 are likely to bind to ER $\alpha$  and ER $\beta$  as well.

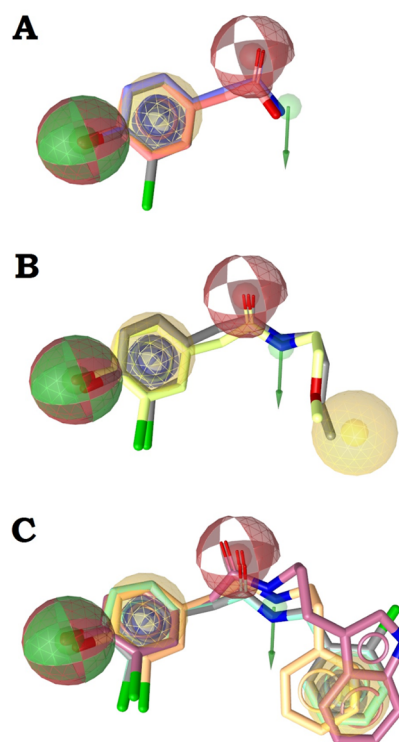
Many of the active hits share considerable structural similarity. Interestingly, the most active substance, **6**, has one phenolic hydroxy group less than **10**. This difference led to a drastic effect on the activity of these compounds: **6** gave an IC<sub>50</sub> value of 0.36  $\pm$  0.08  $\mu$ M, whereas **10** was 20-fold less active, with an IC<sub>50</sub> of 7.3  $\pm$  2.7  $\mu$ M. However, the difference in the overall lipophilicity of these compounds may also play a role in their different activities.

The semisynthetic fungal natural products (**13**–**18**)<sup>69</sup> followed a clear structure–activity relationship (SAR), with the activity shown to increase when a second aromatic ring was present. The parent compound (i.e., natural product) for this semisynthetic series, 2-(3-chloro-4-hydroxyphenyl)acetamide (**S11**), and the related natural products 2-(3-chloro-4-hydroxyphenyl)acetic acid (**S15**) and 2-(4-hydroxyphenyl)acetamide (**S16**) (see Table S1, Supporting Information, for their chemical structures), did not inhibit 17 $\beta$ -HSD2, whereas compounds 2-(3-chloro-4-hydroxyphenyl)-*N*-(2-methoxyethyl)acetamide (**14**) and *N*-butyl-2-(3-chloro-4-hydroxyphenyl)acetamide (**15**) were moderately active. The most active compounds from this series were 2-(3-chloro-4-hydroxyphenyl)-*N*-phenethylacetamide (**13**) and **16**–**18**, which all shared a similar interaction pattern (Figure 5A). However, if the acetamide fragment is extended with, for example, an *N*-butyl chain, the compound can form additional hydrophobic interactions with the enzyme, resulting in an increased activity (Figure 5B). In addition to the alkyl chain, the most active compounds have a second aryl ring that can form aromatic interactions with the enzyme (Figure 5C). On the basis of the activities of these compounds, it can be proposed that 17 $\beta$ -HSD2 has a hydrophobic ligand binding pocket and aromatic amino acid residues in the active site that may contribute to the affinities of these ligands.

Most of the tested compounds inhibited selectively 17 $\beta$ -HSD2 over 17 $\beta$ -HSD1, except for compounds **8** and **9**. The semisynthetic compounds **13** and **16**–**18** also showed good selectivity in terms of the inhibition of 17 $\beta$ -HSD2. The two most potent compounds, **1** and **6**, were 15 and 8 times more active toward 17 $\beta$ -HSD2 than 17 $\beta$ -HSD1. Both compounds are potential natural lead structures that could be used for the development of 17 $\beta$ -HSD2 drug candidates. Unlike many other related compounds that are possibly rapidly metabolized due to the presence of several hydroxy groups, 2-(3-chloro-4-hydroxyphenyl)-*N*-(2-chlorobenzyl)acetamide (**18**) has only a single hydroxy group and might therefore be less prone to rapid biotransformation. Compound **18** still potently and selectively inhibited 17 $\beta$ -HSD2 with an IC<sub>50</sub> of 0.78  $\pm$  0.16  $\mu$ M.

Among the most active compounds identified during these studies were also the flavonoids **5** and **9**. Schuster et al. earlier reported several flavonoids inhibiting 17 $\beta$ -HSD2. Taking the data together (Table 4),<sup>24</sup> a SAR model for the flavonoids that inhibit this enzyme could be established (Figure 6).

In general, the active flavonoids share a typical pharmacophore model containing hydrogen bond acceptors and donors

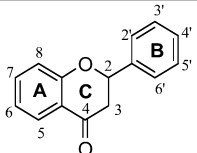
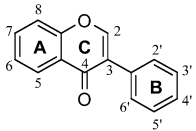


**Figure 5.** Illustration of the SAR of semisynthetic natural product derivatives (Table 3). (A) The core structure with compounds **S12** (gray), **S15** (red), and **S11** (blue) with a pharmacophore model illustrating the interaction pattern. (B) The moderately active compounds **14** (yellow) and **15** (gray) with the additional hydrophobic feature. (C) The most active compounds **13** (orange), *N*-benzyl-2-(3-chloro-4-hydroxyphenyl)acetamide (**16**, green), *N*-(2-(1*H*-indol-3-yl)ethyl)-2-(3-chloro-4-hydroxyphenyl) (**17**, purple), and **18** (gray) with the additional aromatic ring feature.

and hydrophobic and aromatic features (Figure 6A). The hydrogen bond acceptor in position C-3 (scaffold A) was found to be beneficial for activity, as the most active flavonoids, **30** and **31**, contain a hydroxy group at this position (Figure 6B). If this feature was absent, the activity decreased or the compound was inactive. Furthermore, the hydrogen bond acceptor unit at the C-4'-position is important and shared by all active compounds. If the hydrogen-bonding feature at this position was deleted, active and inactive compounds were no longer distinguished (Figure 6C).

To learn more about the general properties of 17 $\beta$ -HSD2 inhibitors, model 1 and the flavonoid model were aligned (Figure 7). Every model contains an aromatic ring feature next to a hydrogen bond donor/acceptor feature. Among the compounds mapped, this combination was often represented by a phenolic hydroxy group. Another common feature was the hydrophobic/aromatic group in a certain distance from the first feature group. Interestingly, in between these aligned hydrophobic/aromatic features, there were hydrogen bond acceptor features. These indicate that in the binding pocket there may be two hydrophobic regions that tolerate aromatic interactions, and in between these pockets, there was most likely a hydrogen-bonding partner. This feature arrangement is in line with the architecture of already crystallized 11 $\beta$ -HSD1 and 17 $\beta$ -HSD1, where inhibitors are anchored to the catalytically active amino acids by central hydrogen bonds and form further, adjacent hydrophobic contacts (e.g., the PDB structures 4c7j<sup>70</sup> and 3hb5<sup>71</sup>).

Table 4. Flavonoid Structures and Activities Used for Deriving a Flavonoid SAR Model of 17 $\beta$ -HSD2 Inhibitors

		 scaffold A (flavanone scaffold)		 scaffold B (isoflavone scaffold)			
compound	scaffold	ring A	ring B	ring C	inhibition of 17 $\beta$ -HSD2: % residual activity at 40 $\mu$ M or IC <sub>50</sub> ( $\mu$ M); mean $\pm$ SD	classification	
jaceosidin (5)	A	OH-5, OMe-6, OH-7	OMe-3', OH-4'	$\Delta^{2,3}$	9.27 $\pm$ 2.28 $\mu$ M	active	
2'-hydroxygenistein (9)	B	OH-5, OH-7	OH-2', OH-4'		2.03 $\pm$ 0.37 $\mu$ M	active	
flavanone (19)	A				70.7 $\pm$ 2.6 %	inactive <sup>24</sup>	
2'-hydroxyflavanone (20)	A		OH-2'		50.7 $\pm$ 0.5 %	inactive <sup>24</sup>	
4'-hydroxyflavanone (21)	A		OH-4'		63.6 $\pm$ 3.5 %	inactive <sup>24</sup>	
6-hydroxyflavanone (22)	A	OH-6			42.5 $\pm$ 1.8 %	inactive <sup>24</sup>	
naringenin (23)	A	OH-5, OH-7	OH-4'	2-(S)	14.4 $\pm$ 4.5 $\mu$ M	active <sup>24</sup>	
hesperetin (24)	A	OH-5, OH-7	OH-3', OMe-4'	2-(S)	36.4 $\pm$ 1.7 %	inactive <sup>24</sup>	
flavone (25)	A			$\Delta^{2,3}$	63.9 $\pm$ 0.6 %	inactive <sup>24</sup>	
7-hydroxyflavone (26)	A	OH-7		$\Delta^{2,3}$	23.1 $\pm$ 1.1 % (> 20 $\mu$ M)	weak <sup>24</sup>	
chrysin (27)	A	OH-5, OH-7		$\Delta^{2,3}$	32.8 $\pm$ 5.1 %	inactive <sup>24</sup>	
daidzein (28)	B	OH-7	OH-4'		58.3 $\pm$ 6.1 %	inactive <sup>24</sup>	
apigenin (29)	A	OH-5, OH-7	OH-4'	$\Delta^{2,3}$	25.2 $\pm$ 0.9 % (> 20 $\mu$ M)	weak <sup>24</sup>	
kaempferol (30)	A	OH-5, OH-7	OH-4'	$\Delta^{2,3}$ , OH-3	0.36 $\pm$ 0.04 $\mu$ M	active <sup>24</sup>	
quercetin (31)	A	OH-5, OH-7	OH-3', OH-4'	$\Delta^{2,3}$ , OH-3	1.54 $\pm$ 0.22 $\mu$ M	active <sup>24</sup>	
genistein (32)	B	OH-5, OH-7	OH-4'		16.5 $\pm$ 2.7 $\mu$ M	active <sup>24</sup>	
biochanin A (33)	B	OH-5, OH-7	OMe-4'		9.90 $\pm$ 1.87 $\mu$ M	active <sup>24</sup>	

The present virtual screening approach for the identification of natural products-derived 17 $\beta$ -HSD2 inhibitors was productive. Thus, only 38 compounds had to be tested to yield 17 active hits with sub- and low-micromolar IC<sub>50</sub> values. The most potent bioactive compound, **6**, exhibited an IC<sub>50</sub> value of 360  $\pm$  80 nM. Thus, the present approach had a success rate of 47% within the virtual hit lists. The fact that so many interesting 17 $\beta$ -HSD2 inhibitors were obtained within this relatively small natural product collection points toward the probable presence of more potent active compounds among other natural products.

Furthermore, SAR information was derived for two compound classes, providing more detailed insight into the binding pocket of the enzyme. Only **8** and **9**, which were identified by model 2 with one omitted feature, were not selective and even preferentially inhibited 17 $\beta$ -HSD1. Consequently, both compounds seem not to be suitable lead structures for further development as antiosteoporosis leads. All other newly discovered 17 $\beta$ -HSD2 inhibitors were preferentially selective over 17 $\beta$ -HSD1, and therefore they could serve as lead structures for further optimization. It needs to be noted that the activities of these compounds toward 17 $\beta$ -HSD2 are at least an order of magnitude lower than that of reported synthetic, chemically optimized compounds.<sup>18,20,21</sup> To further develop potential lead candidates, additional investigations into the bioavailability, metabolism, and tissue distribution of the identified natural compounds are needed. Inhibition of 17 $\beta$ -HSD2 is expected to result in tissue-specific elevated levels of estradiol, and potential adverse effects include endometrial hyperplasia and impaired growth control of the glandular epithelium of the breast.<sup>72–74</sup> Thus, compounds that are primarily active in the bone would be preferred for future drug development.

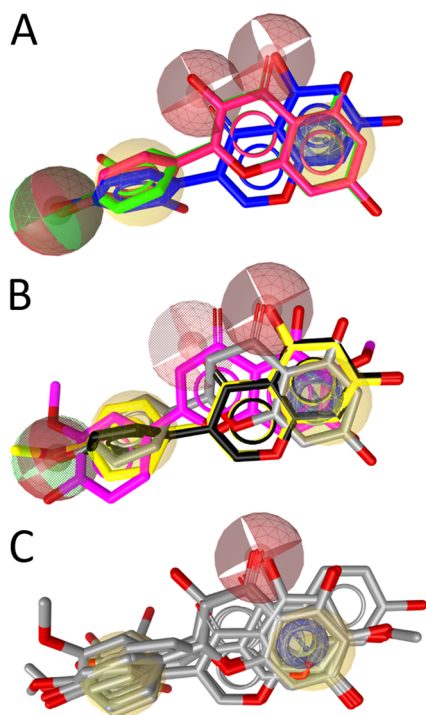
## EXPERIMENTAL SECTION

**Databases.** The Davis Compound Library (Griffith Institute for Drug Discovery, Griffith University) consisted of 352 compounds, of which the majority were obtained from Australian natural sources, such as endophytic fungi,<sup>75</sup> macrofungi,<sup>76</sup> plants,<sup>77</sup> and marine invertebrates.<sup>78,79</sup> Approximately 15% of the entries of this library were semisynthetic natural product analogues,<sup>80,76</sup> while a small percentage (~5%) are known commercial drugs or synthetic compounds inspired by natural products. The Atanasov and Krenn databases consisted of 51 and 13 in-house available natural products, respectively, from the Department of Pharmacognosy at the University of Vienna, Austria. From the University of Innsbruck, 23 selected plant- and lichen-derived compounds<sup>81–84,62</sup> available in-house at the Institute of Pharmacy/Pharmacognosy were collected in the Waltenberger database. Finally, the Sigma-Aldrich catalogue was also screened, as it includes some commercially available natural products.

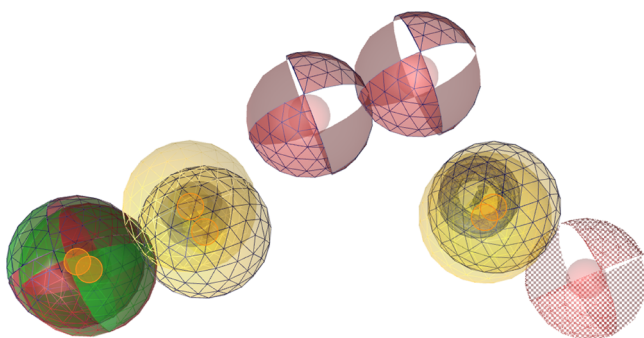
**Virtual Screening.** The databases were prepared for virtual screening by deleting counterions and generating multiconformational databases using OMEGA implemented in LigandScout 3.03b. For the relatively small in-house databases used, BEST settings were employed with a maximum of 500 conformers per molecule. For the larger Sigma-Aldrich database, FAST settings were used, which allowed for a maximum of 50 conformations per compound.

**Origin, Isolation, and Purification of the Natural Compounds.** All natural products from the Davis Compound Library were isolated from plants, marine invertebrates, or endophytic fungi archived at the Griffith Institute for Drug Discovery, Griffith University, Australia, or purchased from Sigma-Aldrich. The extraction and isolation of the natural products featured in this paper have been previously reported by Davis et al.<sup>69,85–88</sup> The synthesis and characterization of the semisynthetic fungal analogues **13–18** have also been previously reported in the literature.<sup>69</sup> All compounds from the Davis collection were analyzed for purity prior to screening and were shown by LC-MS or <sup>1</sup>H NMR analysis to have purities of >95%. The compounds from the Atanasov library were obtained from Sigma-Aldrich, except for **2**, **3**, and butyl gallate (**S3**), which were purchased from Fisher, Molekula, and ABCR GmbH & Co. KG, respectively. All





**Figure 6.** SAR of the flavonoids inhibiting 17 $\beta$ -HSD2. (A) The three most active compounds, **9** (2'-hydroxygenistein, blue), kaempferol (**30**, red), and quercetin (**31**, green), share a combined hydrogen bond acceptor/donor at position C-4', a hydrophobic (aromatic) ring (ring B), two neighboring hydrogen bond acceptors on rings A and C, and the aromatic ring A. (B) The moderately active inhibitors **5** (magenta), naringenin (**23**, gray), genistein (**32**, black), and biochanin A (**33**, yellow) fit into the SAR-pharmacophore illustrating the importance of the hydrogen bond acceptor features on the B and C rings, respectively. (C) For comparison, the general flavonoid model not distinguishing active from inactive compounds is shown with all 17 flavonoids from Table 4.



**Figure 7.** Alignment of the 17 $\beta$ -HSD2 inhibitor model 1 from Vuorinen et al.<sup>19</sup> and the SAR model (features highlighted by grid) for highly active flavonoids. The pharmacophore features are color-coded: hydrogen bond acceptor, red; hydrogen bond donor, green; hydrophobic, yellow; aromatic ring, blue. The alignment centers are indicated with orange spheres.

compounds were purchased at a purity of  $\geq 90\%$ . Compounds **8** and **9** were isolated in an activity-guided approach from a MeOH extract from *Eriosema laurentii* de Wild and unambiguously identified by following MS and NMR analysis. HPLC was applied to determine purity and resulted in 98.7% purity for **8** and 92.1% purity for **9**. The compounds from the Waltenberger library were isolated from different plant and lichen species in the course of the project "Drugs from Nature Targeting Inflammation" (DNIT).<sup>89</sup> Compound **7** was isolated

from a MeOH extract of the bark material of *Himatanthus succuba* (Spruce) Woodson as described elsewhere.<sup>62</sup> The purity of this compound was determined by HPLC and NMR experiments as  $>95\%$ .

**Activity Assays for 17 $\beta$ -HSD1 and 17 $\beta$ -HSD2 Using Cell Lysates.** The 17 $\beta$ -HSD1 and 17 $\beta$ -HSD2 activity assays were performed as described previously.<sup>19</sup> Briefly, lysates of human embryonic kidney cells (HEK-293, ATCC, Manassas, VA, USA) expressing either human 17 $\beta$ -HSD1 or human 17 $\beta$ -HSD2 were incubated for 10 min at 37 °C in TS2 buffer (100 mM NaCl, 1 mM EGTA, 1 mM EDTA, 1 mM MgCl<sub>2</sub>, 250 mM sucrose, 20 mM Tris-HCl, pH 7.4) in a final volume of 22  $\mu$ L containing either solvent (0.1% DMSO) or the inhibitor at the respective concentration. 17 $\beta$ -HSD1 activity was measured in the presence of 200 nM estrone, containing 50 nCi of [2,4,6,7-<sup>3</sup>H]-estrone, and 500  $\mu$ M NADPH. In contrast, 17 $\beta$ -HSD2 activity was determined in the presence of 200 nM estradiol, containing 50 nCi of [2,4,6,7-<sup>3</sup>H]-estradiol, and 500  $\mu$ M NAD<sup>+</sup>. Reactions were stopped after 10 min by adding an excess of unlabeled estradiol and estrone (2 mM of each in methanol). Unlabeled steroids and cofactors were purchased from Sigma-Aldrich and radiolabeled compounds from PerkinElmer (Boston, MA, USA). The steroids were separated by TLC, followed by scintillation counting and calculation of substrate conversion. Data were collected from at least three independent measurements. Compound **29**<sup>24</sup> was used as a positive control for 17 $\beta$ -HSD1 assays and compound **22** from Vuorinen et al.<sup>19</sup> as a positive control for 17 $\beta$ -HSD2 tests.

**Structure–Activity-Relationship Modeling.** The SAR models were generated using LigandScout 4.09 with default settings (Wolber 2005 JCIM;<sup>90</sup> LigandScout 4.09, 2005–2016, Inte:Ligand GmbH, Vienna, Austria, [www.inteligand.com](http://www.inteligand.com)). For all compounds, BEST conformational models using iCon (max 500 conformers per entry) were calculated and overlaid by chemical features using the pharmacophore-based alignment algorithm of the program.

## ■ ASSOCIATED CONTENT

### 📄 Supporting Information

The Supporting Information is available free of charge on the ACS Publications website at DOI: [10.1021/acs.jnatprod.6b00950](https://doi.org/10.1021/acs.jnatprod.6b00950).

Additional information (PDF)

3D video view of model 1 (AVI)

## ■ AUTHOR INFORMATION

### Corresponding Authors

\*Biochemistry: A. Odermatt, Tel: +41 (0)61 267 15 30. Fax: +41 (0)61 267 15 15. E-mail: [alex.odermatt@unibas.ch](mailto:alex.odermatt@unibas.ch).

\*Molecular modeling: D. Schuster, Tel: +43-512-507-58253. Fax: +43-512-507-58299. E-mail: [daniela.schuster@uibk.ac.at](mailto:daniela.schuster@uibk.ac.at).

### ORCID

Daniela Schuster: [0000-0002-9933-8938](https://orcid.org/0000-0002-9933-8938)

### Author Contributions

#A. Vuorinen and R. T. Engeli contributed equally to this work.

### Notes

The authors declare no competing financial interest.

## ■ ACKNOWLEDGMENTS

This study was supported by the Swiss National Science Foundation (31003A-159454 to A.O.), the Novartis Research Foundation (A.O.), the Austrian Science Fund (P26782 to D.S. and P25971-B23 to A.G.A.), the Hochschuljubiläumfond (H-297322/2014 to A.G.A.), the Ernst Mach Stipendium (to S.B.A.), the National Health and Medical Research Council (NHMRC) (APP1024314 to R.A.D.), and the Australian Research Council (ARC) (LE0668477, LE0237908, LP120200339 to R.A.D.). D.S. is an Ingeborg Hochmair professor of the University of Innsbruck. We thank P. Schuster



and G. Begg for help in preparing the manuscript and Inte:Ligand GmbH for providing LigandScout software free of charge.

## REFERENCES

- (1) Persson, B.; Kallberg, Y.; Bray, J. E.; Bruford, E.; Dellaporta, S. L.; Favia, A. D.; Duarte, R. G.; Jornvall, H.; Kavanagh, K. L.; Kedishvili, N.; Kisiela, M.; Maser, E.; Mindnich, R.; Orchard, S.; Penning, T. M.; Thornton, J. M.; Adamski, J.; Oppermann, U. *Chem.-Biol. Interact.* **2009**, *178*, 94–98.
- (2) Dong, Y.; Qiu, Q. Q.; Debear, J.; Lathrop, W. F.; Bertolini, D. R.; Tamburini, P. P. *J. Bone Miner. Res.* **1998**, *13*, 1539–1546.
- (3) Mustonen, M.; Poutanen, M.; Kellokumpu, S.; de Launoit, Y.; Isomaa, V.; Vihko, R.; Vihko, P. *J. Mol. Endocrinol.* **1998**, *20*, 67–74.
- (4) Mustonen, M. V.; Isomaa, V. V.; Vaskivuo, T.; Tapanainen, J.; Poutanen, M. H.; Stenback, F.; Vihko, R. K.; Vihko, P. T. *J. Clin. Endocrinol. Metab.* **1998**, *83*, 1319–1324.
- (5) Takeyama, J.; Sasano, H.; Suzuki, T.; Iinuma, K.; Nagura, H.; Andersson, S. *J. Clin. Endocrinol. Metab.* **1998**, *83*, 3710–3715.
- (6) Puranen, T. J.; Kurkela, R. M.; Lakkakorpi, J. T.; Poutanen, M. H.; Itaranta, P. V.; Melis, J. P.; Ghosh, D.; Vihko, R. K.; Vihko, P. T. *Endocrinology* **1999**, *140*, 3334–3341.
- (7) Wu, L.; Einstein, M.; Geissler, W. M.; Chan, H. K.; Elliston, K. O.; Andersson, S. *J. Biol. Chem.* **1993**, *268*, 12964–12969.
- (8) Lukacik, P.; Kavanagh, K. L.; Oppermann, U. *Mol. Cell. Endocrinol.* **2006**, *248*, 61–71.
- (9) Dufort, I.; Rheault, P.; Huang, X. F.; Soucy, P.; Luu-The, V. *Endocrinology* **1999**, *140*, 568–574.
- (10) Geissler, W. M.; Davis, D. L.; Wu, L.; Bradshaw, K. D.; Patel, S.; Mendonca, B. B.; Elliston, K. O.; Wilson, J. D.; Russell, D. W.; Andersson, S. *Nat. Genet.* **1994**, *7*, 34–39.
- (11) Ghosh, D.; Vihko, P. *Chem.-Biol. Interact.* **2001**, *130–132*, 637–650.
- (12) Soubhye, J.; Alard, I. C.; van Antwerpen, P.; Dufrasne, F. *Future Med. Chem.* **2015**, *7*, 1431–1456.
- (13) Compston, J. E. *Physiol. Rev.* **2001**, *81*, 419–447.
- (14) Riggs, B. L.; Khosla, S.; Melton, L. J. *J. Bone Miner. Res.* **1998**, *13*, 763–773.
- (15) Chin, K.-Y.; Ima-Nirwana, S. *Int. J. Endocrinol.* **2012**, *2012*, 208719.
- (16) Michael, H.; Härkönen, P. L.; Väänänen, H. K.; Hentunen, T. A. *J. Bone Miner. Res.* **2005**, *20*, 2224–2232.
- (17) Bagi, C. M.; Wood, J.; Wilkie, D.; Dixon, B. *J. Musculoskelet. Neuronal. Interact.* **2008**, *8*, 267–280.
- (18) Perspicace, E.; Cozzoli, L.; Gargano, E. M.; Hanke, N.; Carotti, A.; Hartmann, R. W.; Marchais-Oberwinkler, S. *Eur. J. Med. Chem.* **2014**, *83*, 317–337.
- (19) Vuorinen, A.; Engeli, R.; Meyer, A.; Bachmann, F.; Griesser, U. J.; Schuster, D.; Odermatt, A. *J. Med. Chem.* **2014**, *57*, 5995–6007.
- (20) Wetzell, M.; Marchais-Oberwinkler, S.; Perspicace, E.; Möller, G.; Adamski, J.; Hartmann, R. W. *J. Med. Chem.* **2011**, *54*, 7547–7557.
- (21) Xu, K.; Al-Soud, Y. A.; Wetzell, M.; Hartmann, R. W.; Marchais-Oberwinkler, S. *Eur. J. Med. Chem.* **2011**, *46*, 5978–5990.
- (22) Deluca, D.; Krazeisen, A.; Breitling, R.; Prehn, C.; Möller, G.; Adamski, J. *J. Steroid Biochem. Mol. Biol.* **2005**, *93*, 285–292.
- (23) Le Bail, J. C.; Laroche, T.; Marre-Fournier, F.; Habrioux, G. *Cancer Lett.* **1998**, *133*, 101–106.
- (24) Schuster, D.; Nashev, L. G.; Kirchmair, J.; Laggner, C.; Wolber, G.; Langer, T.; Odermatt, A. *J. Med. Chem.* **2008**, *51*, 4188–4199.
- (25) Atanasov, A. G.; Waltenberger, B.; Pferschy-Wenzig, E. M.; Linder, T.; Wawrosch, C.; Uhrin, P.; Temml, V.; Wang, L.; Schwaiger, S.; Heiss, E. H.; Rollinger, J. M.; Schuster, D.; Breuss, J. M.; Bochkov, V.; Mihovilovic, M. D.; Kopp, B.; Bauer, R.; Dirsch, V. M.; Stuppner, H. *Biotechnol. Adv.* **2015**, *33*, 1582–614.
- (26) Newman, D. J.; Cragg, G. M. *J. Nat. Prod.* **2012**, *75*, 311–335.
- (27) Eder, J.; Sedrani, R.; Wiesmann, C. *Nat. Rev. Drug Discovery* **2014**, *13*, 577–587.
- (28) Williamson, E. M.; Heinrich, M.; Jäger, A. K., Eds. *Ethnopharmacology*; John Wiley & Sons Ltd: Chichester, West Sussex, UK, 2015; pp 213–226.
- (29) Sharma, C.; Kumari, T.; Arya, K. R. *Int. J. Pharm. Res. Health Sci.* **2014**, *2*, 185–190.
- (30) Blum, A.; Favia, A. D.; Maser, E. *Mol. Cell. Endocrinol.* **2009**, *301*, 132–136.
- (31) Kratschmar, D. V.; Vuorinen, A.; Da Cunha, T.; Wolber, G.; Classen-Houben, D.; Doblhoff, O.; Schuster, D.; Odermatt, A. *J. Steroid Biochem. Mol. Biol.* **2011**, *125*, 129–142.
- (32) Rollinger, J. M.; Kratschmar, D. V.; Schuster, D.; Pfisterer, P. H.; Gumy, C.; Aubry, E. M.; Brandstötter, S.; Stuppner, H.; Wolber, G.; Odermatt, A. *Bioorg. Med. Chem.* **2010**, *18*, 1507–1515.
- (33) Vuorinen, A.; Seibert, J.; Papageorgiou, V. P.; Rollinger, J. M.; Odermatt, A.; Schuster, D.; Assimopoulou, A. N. *Planta Med.* **2015**, *81*, 525–532.
- (34) Lambert, J. D.; Zhao, D.; Meyers, R. O.; Kuester, R. K.; Timmermann, B. N.; Dorr, R. T. *Toxicol.* **2002**, *40*, 1701–1708.
- (35) Mikuni, M.; Yoshida, M.; Hellberg, P.; Peterson, C. A.; Edwin, S. S.; Brännström, M.; Peterson, C. M. *Biol. Reprod.* **1998**, *58*, 1211–1216.
- (36) Benassayag, C.; Perrot-Appianat, M.; Ferre, F. *J. Chromatogr. B: Anal. Technol. Biomed. Life Sci.* **2002**, *777*, 233–248.
- (37) Fujimoto, N.; Kohta, R.; Kitamura, S.; Honda, H. *Life Sci.* **2004**, *74*, 1417–1425.
- (38) Ono, K.; Hasegawa, K.; Yoshiike, Y.; Takashima, A.; Yamada, M.; Naiki, H. *J. Neurochem.* **2002**, *81*, 434–40.
- (39) Yamada, M.; Ono, K.; Hamaguchi, T.; Noguchi-Shinohara, M. *Adv. Exp. Med. Biol.* **2015**, *863*, 79–94.
- (40) Gupta, S. C.; Patchva, S.; Koh, W.; Aggarwal, B. B. *Clin. Exp. Pharmacol. Physiol.* **2012**, *39*, 283–299.
- (41) Manolova, Y.; Deneva, V.; Antonov, L.; Drakalska, E.; Momekova, D.; Lambov, N. *Spectrochim. Acta, Part A* **2014**, *132*, 815–820.
- (42) Eigner, D.; Scholz, D. *J. Ethnopharmacol.* **1999**, *67*, 1–6.
- (43) Ghosh, S.; Banerjee, S.; Sil, P. C. *Food Chem. Toxicol.* **2015**, *83*, 111–24.
- (44) Epstein, J.; Sanderson, I. R.; Macdonald, T. T. *Br. J. Nutr.* **2010**, *103*, 1545–1557.
- (45) Ko, E. Y.; Moon, A. *J. Cancer Prev.* **2015**, *20*, 223–231.
- (46) Anand, P.; Kunnumakara, A. B.; Newman, R. A.; Aggarwal, B. B. *Mol. Pharmacol.* **2007**, *4*, 807–818.
- (47) Baell, J. B. *J. Nat. Prod.* **2016**, *79*, 616–28.
- (48) Baell, J. B.; Holloway, G. A. *J. Med. Chem.* **2010**, *53*, 2719–40.
- (49) Bisson, J.; McAlpine, J. B.; Friesen, J. B.; Chen, S. N.; Graham, J.; Pauli, G. F. *J. Med. Chem.* **2016**, *59*, 1671–90.
- (50) Nelson, K. M.; Dahlin, J. L.; Bisson, J.; Graham, J.; Pauli, G. F.; Walters, M. A. *J. Med. Chem.* **2017**, *60*, 1620.
- (51) Ma, C. J.; Sung, S. H.; Kim, Y. C. *Planta Med.* **2004**, *70*, 79–80.
- (52) Kwon, H. S.; Kim, M. J.; Jeong, H. J.; Yang, M. S.; Park, K. H.; Jeong, T. S.; Lee, W. S. *Bioorg. Med. Chem. Lett.* **2008**, *18*, 194–198.
- (53) Favela-Hernandez, J. M.; Garcia, A.; Garza-Gonzalez, E.; Rivas-Galindo, V. M.; Camacho-Corona, M. R. *Phytother. Res.* **2012**, *26*, 1957–1960.
- (54) Yamauchi, S.; Masuda, T.; Sugahara, T.; Kawaguchi, Y.; Ohuchi, M.; Someya, T.; Akiyama, J.; Tominaga, S.; Yamawaki, M.; Kishida, T.; Akiyama, K.; Maruyama, M. *Biosci., Biotechnol., Biochem.* **2008**, *72*, 2981–2986.
- (55) Choi, M. S.; Jeong, H. J.; Kang, T. H.; Shin, H. M.; Oh, S. T.; Choi, Y.; Jeon, S. *Life Sci.* **2015**, *141*, 81–89.
- (56) Filleur, F.; Le Bail, J. C.; Duroux, J. L.; Simon, A.; Chulia, A. *J. Planta Med.* **2001**, *67*, 700–704.
- (57) Li, S.; Li, W.; Wang, Y.; Asada, Y.; Koike, K. *Bioorg. Med. Chem. Lett.* **2010**, *20*, 5398–401.
- (58) Peng, F.; Du, Q.; Peng, C.; Wang, N.; Tang, H.; Xie, X.; Shen, J.; Chen, J. *Phytother. Res.* **2015**, *29*, 969–977.
- (59) Ye, L.; Gho, W. M.; Chan, F. L.; Chen, S.; Leung, L. K. *Int. J. Cancer* **2009**, *124*, 1028–36.

- (60) Choi, S. Y.; Ha, T. Y.; Ahn, J. Y.; Kim, S. R.; Kang, K. S.; Hwang, I. K.; Kim, S. *Planta Med.* **2008**, *74*, 25–32.
- (61) Ateba, S. B.; Njamen, D.; Medjakovic, S.; Hobiger, S.; Mbanya, J. C.; Jungbauer, A.; Krenn, L. *J. Ethnopharmacol.* **2013**, *150*, 298–307.
- (62) Waltenberger, B.; Rollinger, J. M.; Griesser, U. J.; Stuppner, H.; Gelbrich, T. *Acta Crystallogr., Sect. C: Cryst. Struct. Commun.* **2011**, *67*, o409–12.
- (63) Ateba, S. B.; Njamen, D.; Medjakovic, S.; Zehl, M.; Kaehlig, H.; Jungbauer, A.; Krenn, L. *BMC Complementary Altern. Med.* **2014**, *14*, 294.
- (64) Petersen, M.; Simmonds, M. S. *Phytochemistry* **2003**, *62*, 121–125.
- (65) Boonyarikpunchai, W.; Sukrong, S.; Towiwat, P. *Pharmacol., Biochem. Behav.* **2014**, *124*, 67–73.
- (66) Staiger, C. *Phytother. Res.* **2012**, *26*, 1441–1448.
- (67) Tai, A.; Sawano, T.; Ito, H. *Biosci., Biotechnol., Biochem.* **2012**, *76*, 314–318.
- (68) Blazevic, I.; Radonic, A.; Mastelic, J.; Zekic, M.; Skocibusic, M.; Maravic, A. *Chem. Biodiversity* **2010**, *7*, 2023–2034.
- (69) Davis, R. A.; Pierens, G. K.; Parsons, P. G. *Magn. Reson. Chem.* **2007**, *45*, 442–445.
- (70) Goldberg, F. W.; Dossetter, A. G.; Scott, J. S.; Robb, G. R.; Boyd, S.; Groombridge, S. D.; Kemmitt, P. D.; Sjögren, T.; Gutierrez, P. M.; deSchoolmeester, J.; Swales, J. G.; Turnbull, A. V.; Wild, M. J. *J. Med. Chem.* **2014**, *57*, 970–986.
- (71) Mazumdar, M.; Fournier, D.; Zhu, D. W.; Cadot, C.; Poirier, D.; Lin, S. X. *Biochem. J.* **2009**, *424*, 357–366.
- (72) Gunnarsson, C.; Hellqvist, E.; Stal, O. *Br. J. Cancer* **2005**, *92*, 547–52.
- (73) Gunnarsson, C.; Olsson, B. M.; Stal, O. *Cancer Res.* **2001**, *61*, 8448–51.
- (74) Kitawaki, J.; Koshihara, H.; Ishihara, H.; Kusuki, I.; Tsukamoto, K.; Honjo, H. *J. Clin. Endocrinol. Metab.* **2000**, *85*, 3292–6.
- (75) Davis, R. A.; Carroll, A. R.; Andrews, K. T.; Boyle, G. M.; Tran, T. L.; Healy, P. C.; Kalaitzis, J. A.; Shivas, R. G. *Org. Biomol. Chem.* **2010**, *8*, 1785–1790.
- (76) Choomuenwai, V.; Andrews, K. T.; Davis, R. A. *Bioorg. Med. Chem.* **2012**, *20*, 7167–7174.
- (77) Levrier, C.; Balastrier, M.; Beattie, K. D.; Carroll, A. R.; Martin, F.; Choomuenwai, V.; Davis, R. A. *Phytochemistry* **2013**, *86*, 121–126.
- (78) Barnes, E. C.; Said, N. A. B. M.; Williams, E. D.; Hooper, J. N. A.; Davis, R. A. *Tetrahedron* **2010**, *66*, 283–287.
- (79) Liberio, M. S.; Sooraj, D.; Williams, E. D.; Feng, Y.; Davis, R. A. *Tetrahedron Lett.* **2011**, *52*, 6729–6731.
- (80) Barnes, E. C.; Choomuenwai, V.; Andrews, K. T.; Quinn, R. J.; Davis, R. A. *Org. Biomol. Chem.* **2012**, *10*, 4015–4023.
- (81) Atanasov, A. G.; Wang, J. N.; Gu, S. P.; Bu, J.; Kramer, M. P.; Baumgartner, L.; Fakhrudin, N.; Ladurner, A.; Malainer, C.; Vuorinen, A.; Noha, S. M.; Schwaiger, S.; Rollinger, J. M.; Schuster, D.; Stuppner, H.; Dirsch, V. M.; Heiss, E. H. *Biochim. Biophys. Acta, Gen. Subj.* **2013**, *1830*, 4813–9.
- (82) Bauer, J.; Waltenberger, B.; Noha, S. M.; Schuster, D.; Rollinger, J. M.; Boustie, J.; Chollet, M.; Stuppner, H.; Werz, O. *ChemMedChem* **2012**, *7*, 2077–2081.
- (83) Fakhrudin, N.; Ladurner, A.; Atanasov, A. G.; Heiss, E. H.; Baumgartner, L.; Markt, P.; Schuster, D.; Ellmerer, E. P.; Wolber, G.; Rollinger, J. M.; Stuppner, H.; Dirsch, V. M. *Mol. Pharmacol.* **2010**, *77*, 559–566.
- (84) Oettl, S. K.; Gerstmeier, J.; Khan, S. Y.; Wiechmann, K.; Bauer, J.; Atanasov, A. G.; Malainer, C.; Awad, E. M.; Uhrin, P.; Heiss, E. H.; Waltenberger, B.; Remias, D.; Breuss, J. M.; Boustie, J.; Dirsch, V. M.; Stuppner, H.; Werz, O.; Rollinger, J. M. *PLoS One* **2013**, *8*, e76929.
- (85) Barnes, E. C.; Kavanagh, A. M.; Ramu, S.; Blaskovich, M. A.; Cooper, M. A.; Davis, R. A. *Phytochemistry* **2013**, *93*, 162–166.
- (86) Baron, P. S.; Neve, J. E.; Camp, D.; Suraweera, L.; Lam, A.; Lai, J.; Jovanovic, L.; Nelson, C.; Davis, R. A. *Magn. Reson. Chem.* **2013**, *51*, 358–363.
- (87) Davis, R. A.; Barnes, E. C.; Longden, J.; Avery, V. M.; Healy, P. C. *Bioorg. Med. Chem.* **2009**, *17*, 1387–1392.
- (88) Healy, P. C.; Hocking, A.; Tran-Dinh, N.; Pitt, J. I.; Shivas, R. G.; Mitchell, J. K.; Kotiw, M.; Davis, R. A. *Phytochemistry* **2004**, *65*, 2373–2378.
- (89) Waltenberger, B.; Atanasov, A. G.; Heiss, E. H.; Bernhard, D.; Rollinger, J. M.; Breuss, J. M.; Schuster, D.; Bauer, R.; Kopp, B.; Franz, C.; Bochkov, V.; Mihovilovic, M. D.; Dirsch, V. M.; Stuppner, H. *Monatsh. Chem.* **2016**, *147*, 479–491.
- (90) Wolber, G.; Langer, T. *J. Chem. Inf. Model.* **2005**, *45*, 160–169.

### 3.5 Paper 4 (Engeli et al., in preparation)

## Interference of Paraben Compounds with Estrogen Metabolism by Inhibition of 17 $\beta$ -Hydroxysteroid Dehydrogenases

Roger T. Engeli, Simona R. Rohrer, Anna Vuorinen, Susanne Leugger, Daniela Schuster, Alex Odermatt

Manuscript in preparation

(Data not complete: *In vitro* results done, *in silico* SAR studies have not been performed yet)

**Contribution:** Drafted the paper manuscript. Providing Figures (1-4), analyzed data, and supervised the project.

**Aims:** Investigate the potential endocrine disrupting effects of parabens by disturbing the activity of estrogen metabolizing enzymes.

**Results:** All tested parabens, except the main metabolite *p*-hydroxybenzoic acid, decreased the activity of 17 $\beta$ -HSD2. Additionally, a size-dependent inhibition of 17 $\beta$ -HSD1 was found.

**Conclusion:** This study reports an additional endocrine disrupting effect of parabens.

## **Interference of Paraben Compounds with Estrogen Metabolism by Inhibition of 17 $\beta$ -Hydroxysteroid Dehydrogenases**

Roger T. Engeli <sup>1</sup>, Simona R. Rohrer <sup>1</sup>, Anna Vuorinen <sup>1</sup>, Susanne Leugger <sup>1</sup>, Daniela Schuster <sup>2\*</sup>, Alex Odermatt <sup>1\*\*</sup>

<sup>1</sup>Division of Molecular and Systems Toxicology, University of Basel, Klingelbergstr. 50, 4056 Basel, Switzerland

<sup>2</sup>Computer-Aided Molecular Design Group, Institute of Pharmacy / Pharmaceutical Chemistry and Center for Molecular Biosciences Innsbruck, University of Innsbruck, Innrain 80-82, 6020 Innsbruck, Austria

### **Correspondence**

\*Molecular Modeling: Daniela Schuster

Tel: +43-512-507-58253. Fax: +43-512-507-58299

E-mail: [daniela.schuster@uibk.ac.at](mailto:daniela.schuster@uibk.ac.at)

\*\*Biochemistry: Alex Odermatt

Tel: +41 (0)61 207 15 30 Fax: +41 (0)61 207 15 15

E-mail: [alex.odermatt@unibas.ch](mailto:alex.odermatt@unibas.ch)

## Abstract

**Background:** Parabens are effective preservatives widely used in cosmetic products and processed food, with high exposure to humans. Recent evidence suggested estrogenic effects of parabens. This study investigated the potential interference of parabens with the activities of 17 $\beta$ -hydroxysteroid dehydrogenase (17 $\beta$ -HSD) 1 and 2.

**Methods:** A ligand-based 17 $\beta$ -HSD2 pharmacophore model was applied to screen a cosmetic chemicals database. HEK-293 cells were transiently transfected with human 17 $\beta$ -HSD1 or 17 $\beta$ -HSD2 expression plasmids. Lysates of these cells were incubated for 10 min at 37°C with 200 nM radiolabeled substrates, 500  $\mu$ M co-factor NAD(PH) and paraben compounds. Steroids were separated using TLC and analyzed using scintillation counting.

**Results:** All tested parabens and paraben-like compounds, except their common metabolite *p*-hydroxybenzoic acid, inhibited 17 $\beta$ -HSD2 activity. Ethylparaben and ethyl vanillate inhibited 17 $\beta$ -HSD2 with an IC<sub>50</sub> of 4.64  $\pm$  0.83  $\mu$ M and 1.28  $\pm$  0.26  $\mu$ M. Besides, parabens size-dependently inhibited 17 $\beta$ -HSD1. Hexyl- and heptylparaben were most active and showed IC<sub>50</sub> values of 2.6  $\pm$  0.6  $\mu$ M and 1.8  $\pm$  0.3  $\mu$ M against 17 $\beta$ -HSD1.

**Conclusion:** Low micromolar concentrations of hexyl- and heptylparaben decreased *in vitro* activity of human 17 $\beta$ -HSD1 and ethylparaben and ethyl vanillate decreased *in vitro* activity of human 17 $\beta$ -HSD2. However, regarding their very rapid metabolism to the inactive metabolite *p*-hydroxybenzoic acid by esterases, it seems questionable whether micromolar concentrations of parabens are occurring in target cells to effectively disturb estrogen synthesis *in vivo*.

## Keywords

Paraben; 17 $\beta$ -hydroxysteroid dehydrogenase; endocrine disrupting chemical, estrogen; xenobiotic

## Introduction

Paraben compounds are widely used as additives in cosmetic products and processed food due to their broad spectrum preservative efficiency, low cost, and low toxicity[1, 2]. Additionally, parabens possess excellent chemical stability, are tasteless, inert, and biodegradable. Chemically, parabens are alkyl esters of *p*-hydroxybenzoic acid of which propyl- and methylparaben are the most frequently used parabens in cosmetic products[3, 4]. European Union (EU) authorities permit a paraben content in cosmetic products of 0.4% for one ester compound and 0.8% for mixtures of esters (EU Council Directive, Cosmetic Products, 76/768/EEC/M11). Generally, mixtures of parabens are used to increase preservative efficiency. Lately, the acceptance of the use of parabens has decreased among chemical and pharmaceutical companies, and despite their excellent properties they tend to replace parabens with other compounds[5].

Parabens can enter the systemic circulation via oral intake or by transdermal penetration, which was confirmed by the detection of systemic paraben concentrations upon exposure to these compounds [6-8]. However, parabens are very rapidly metabolized to *p*-hydroxybenzoic acid by esterases in the liver and in the skin, followed by excretion via the urine[9]. Parabens are mainly excreted as glycine, sulfate, and glucuronide conjugates [10]. The topical application of paraben containing products more likely contributes to the systemic paraben concentration than their oral intake due to the rapid intestinal and hepatic metabolism of parabens[11]. This assumption is supported by the fact that the main human paraben exposure is due to the extensive use of personal care products[12].

Estrogens are primary female sex hormones playing a central role in a variety of physiological actions in females and males. In females, estrogens primarily regulate sexual development of the reproductive tissues and development of secondary sexual characteristics at puberty[13]. Estrogens trigger target gene expression mainly by acting through estrogen receptors  $\alpha$  and  $\beta$  (ER $\alpha$ , ER $\beta$ )[14]. The 17 $\beta$ -hydroxysteroid dehydrogenase type 1 and 2 (17 $\beta$ -HSD1 and 17 $\beta$ -HSD2) regulate the local balance between potent and weakly active estrogens. While 17 $\beta$ -HSD1 converts the weakly active estrone (E1) into the most potent estrogen estradiol (E2), 17 $\beta$ -HSD2 catalyzes the opposite reaction and decreases the local concentrations of active estrogens [15]. A high 17 $\beta$ -HSD2 to 17 $\beta$ -HSD1 ratio in ER $\alpha$ -positive breast cancer patients has been shown to positively

correlate with survival in ER $\alpha$ -positive patients[16]. This finding illustrates the importance of proper 17 $\beta$ -HSD2 function.

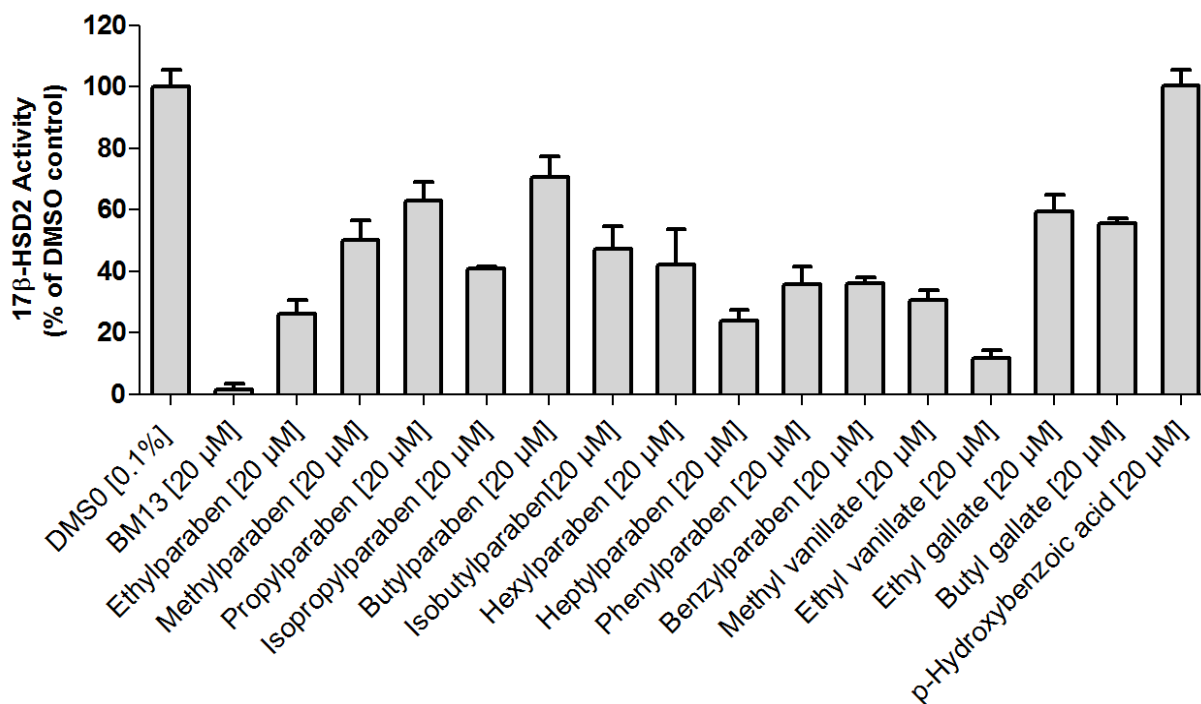
Potential estrogenic activities of parabens have been extensively investigated in the past decades[6, 9]. In 2004, Darbre et al. reported the detection of unconjugated parabens in breast cancer tissue, triggering further investigations into estrogenic activities of parabens[17]. Most of these studies focused on the effects of parabens on estrogen receptors. Possible interferences of parabens with pre-receptor control enzymes modulating endocrine functions, such as hydroxysteroid dehydrogenases (HSDs), remained to be investigated. Therefore, the present study addressed potential endocrine disrupting effects of parabens on estrogen homeostasis through inhibition of human estrogen metabolizing enzymes.

## Results

Virtual screening of a cosmetic chemical database using a 17 $\beta$ -HSD2 ligand-based pharmacophore model revealed parabens as possible 17 $\beta$ -HSD2 inhibitors. The chemical database contained around 75'000 chemical compounds that are used as additives in cosmetic products. Several paraben compounds were among the hits and this class of compounds was therefore subjected to biological testing. In total, ten parabens, its main metabolite *p*-hydroxybenzoic acid, and four paraben-like compounds were analyzed *in vitro*. All tested parabens as well as methyl vanillate, ethyl vanillate, ethyl gallate, and butyl gallate inhibited 17 $\beta$ -HSD2 at a concentration of 20  $\mu$ M (Figure 1). The common paraben metabolite *p*-hydroxybenzoic acid was inactive. For the two most potent compounds, IC<sub>50</sub> values were determined. Ethylparaben and ethyl vanillate inhibited 17 $\beta$ -HSD2 with an IC<sub>50</sub> of 4.64  $\pm$  0.83  $\mu$ M and 1.28  $\pm$  0.26  $\mu$ M, respectively (Figure S1, Supporting Information). A mixture of ethyl- (6  $\mu$ M) and hexylparaben (12  $\mu$ M) showed additive effects in terms of 17 $\beta$ -HSD2 inhibition compared to each individual compound (Figure 2).

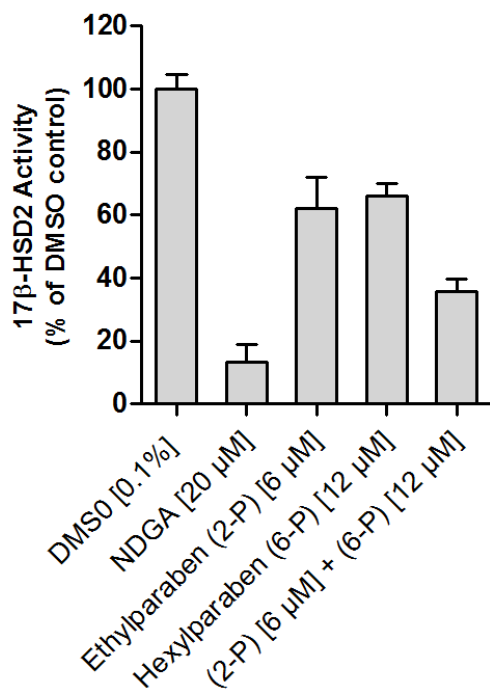
Additionally, effects of parabens and paraben-like compounds on the activity of 17 $\beta$ -HSD1 were analyzed. Small parabens such as the main metabolite *p*-hydroxybenzoic acid, methyl-, and ethylparaben did not inhibit 17 $\beta$ -HSD1. In contrast larger parabens, size-dependently inhibited 17 $\beta$ -HSD1 activity (Figure 3). Methyl vanillate, ethyl vanillate, ethyl gallate, and butyl gallate did not inhibit 17 $\beta$ -HSD1 (data not shown). IC<sub>50</sub> values were determined for the two most potent

parabens inhibiting 17 $\beta$ -HSD1. Hexyl- and heptylparaben showed IC<sub>50</sub> values of 2.6  $\pm$  0.6  $\mu$ M and 1.8  $\pm$  0.3  $\mu$ M, respectively, in 17 $\beta$ -HSD1 lysate assays. COV434 cells were used to determine IC<sub>50</sub> values of hexylparaben (3.5  $\pm$  1.3  $\mu$ M) and heptylparaben (4.9  $\pm$  0.6  $\mu$ M.) in intact cells expressing endogenous 17 $\beta$ -HSD1, indicating that parabens are able to penetrate cell membranes and inhibit the enzyme (Figure 4).

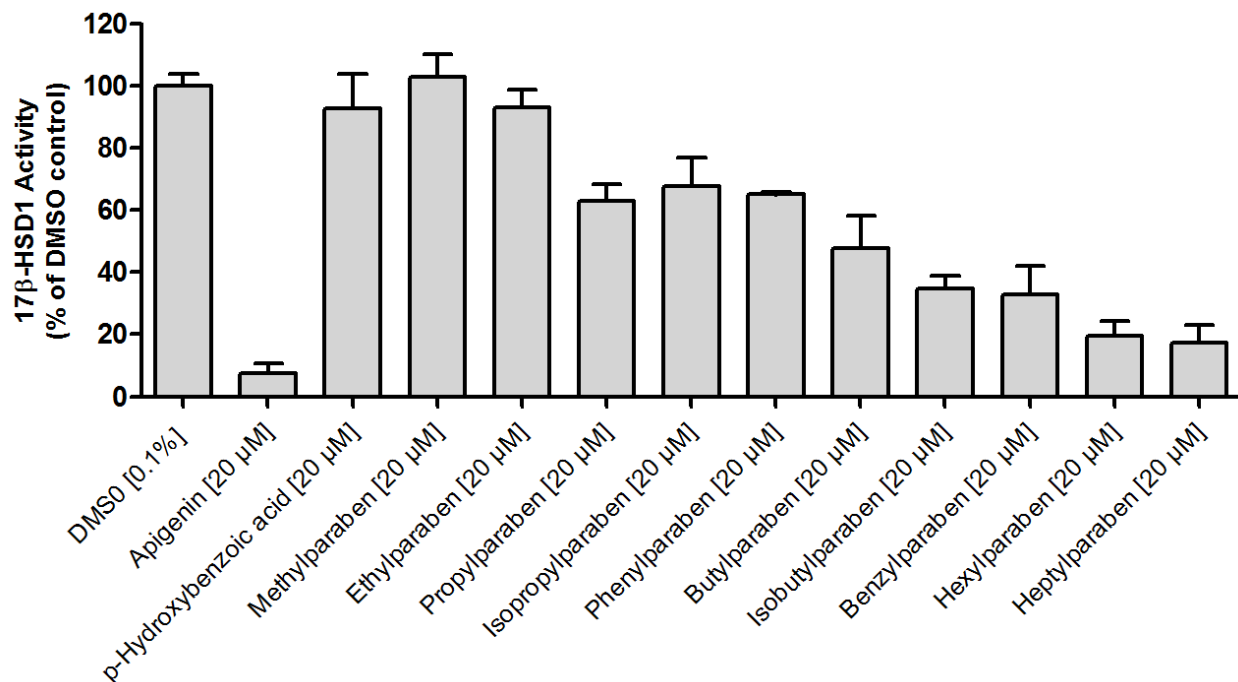


**Figure 1.** Estrone formation in HEK-293 cell lysates expressing human 17 $\beta$ -HSD2. HEK-293 cells were transiently transfected using the calcium phosphate method. Transfected cells were lysed and incubated with 200 nM radiolabeled estradiol and parabens or paraben-like compounds at a final concentration of 20  $\mu$ M for 10 min at 37 $^{\circ}$ C. Steroids were separated using TLC and the formation of estrone was determined using scintillation counting. Results represent mean  $\pm$  SD of three independent measurements. BM13 was used as positive control published in Vuorinen et al., (compound 22)[18].

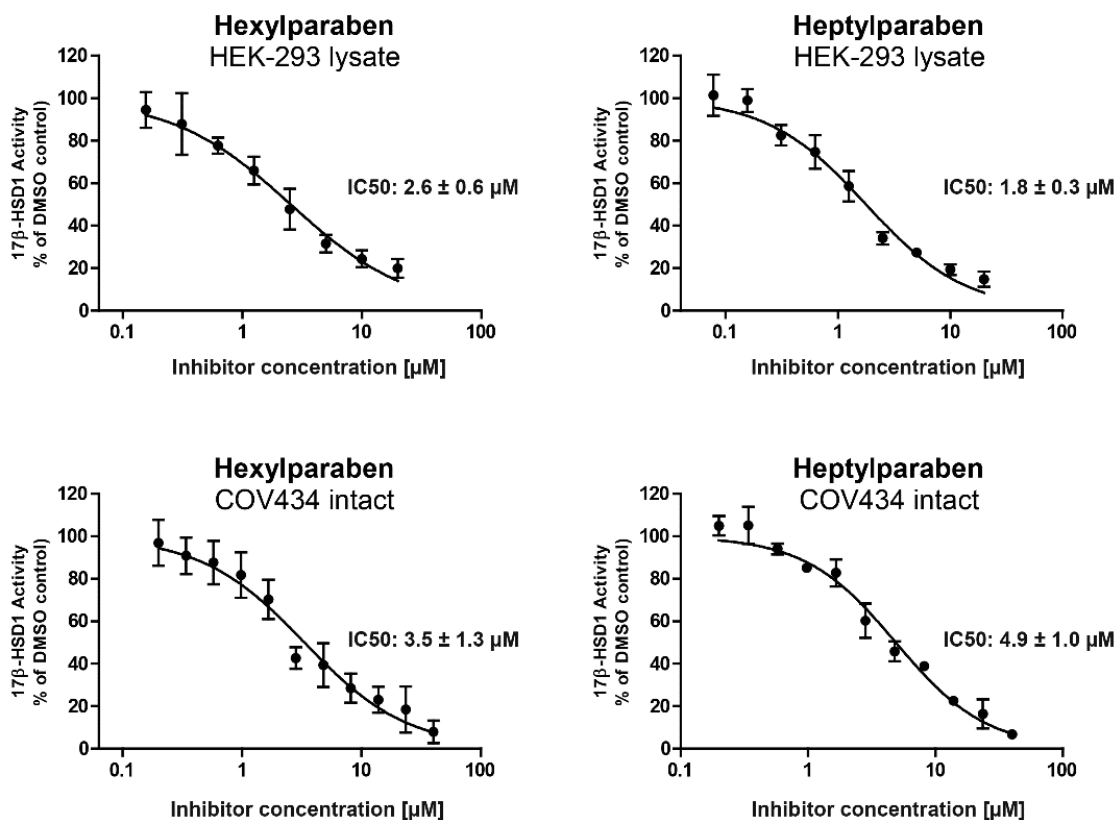




**Figure 2.** Additive effects of two parabens in terms of 17β-HSD2 activity. Lysates of transiently transfected HEK-293 cells were incubated with radiolabeled estradiol for 10 min at 37°C, containing 6 μM of ethyl- (2-P) or 12 μM of hexylparaben (6-P) or a mixture of both compounds. The 17β-HSD2 activity upon incubation with parabens was compared to that of the DMSO control. Steroids were separated using TLC and analyzed using scintillation counting. Experiments were performed three times independently.



**Figure 3.** Inhibition of 17β-HSD1 activity by parabens. HEK-293 cells were transiently transfected with 17β-HSD1 using the calcium phosphate method. Lysates were incubated together with radiolabeled estrone, 500 μM NADPH, as well as parabens at a final concentration of 20 μM, for 10 min at 37°C. Steroids were separated using TLC and estradiol formation was determined using scintillation counting. Experiments were performed three times independently and shown as mean ± SD.



**Figure 4.** Inhibition of 17 $\beta$ -HSD1 by hexyl- and heptylparaben measured in lysates and intact cells. Lysate assays were performed using HEK-293 cells transiently transfected with 17 $\beta$ -HSD1. Intact cell assays were performed using human COV434 granulosa cells endogenously expressing 17 $\beta$ -HSD1. Both assays were conducted using 200 nM radiolabeled estrone as substrate. The lysate assay additionally contained 500  $\mu$ M NADPH. Results represent mean  $\pm$  SD of three independent experiments.

## Discussion

In this study, we identified several parabens potentially interfering with local estrogen metabolism by inhibiting 17 $\beta$ -HSD1 and 17 $\beta$ -HSD2. Parabens have successfully been used as preservative additives for more than 50 years. However, in recent years, following the detection of parent paraben compounds in female breast tumors, possible estrogenic effects were extensively investigated[17]. The first weak estrogenic effects of parabens were reported by Routledge et al. using a yeast-based estrogen receptor (ER) assay[19]. Methyl-, ethyl-, propyl-, and butylparaben were found to have weak estrogenic effects. Butylparaben was the most potent

estrogenic paraben found, but still 10'000 times less potent than estradiol. Furthermore, Routledge et al. reported minor estrogenic effects of paraben *in vivo*. Subcutaneous application of high doses of butylparaben (600-1200 mg/kg/day) significantly increased uterotrophic response in rats. However, it was approximately 100'000 times less potent than the positive control estradiol (0.4 mg/kg/day). The oral administration of butylparaben failed to increase uterotrophic response[19]. This observation may be explained by highly abundant paraben metabolizing enzymes, located in the intestine and liver. Miller et al. showed estrogenic activity of benzyl-, butyl-, propyl-, ethyl-, and methylparaben in a yeast-based estrogen assay. Benzylparaben was reported to be the most active paraben despite being 4000-fold less potent than estradiol[20]. In the present study, benzylparaben inhibited 60% of 17 $\beta$ -HSD2 activity at a concentration of 20  $\mu$ M (Figure 1). The Benzylparaben concentration used in the activity assays of this study was 100 times in excess to the substrate concentration. Therefore, it can be assumed that the weak estrogenic effects of benzylparaben may be due to the inhibition of 17 $\beta$ -HSD2 and subsequently elevated estradiol concentrations rather than by a direct activation of the ER.

Byford et al. reported estrogenic effects of methyl-, ethyl-, propyl-, and butylparaben in estrogen-dependent MCF7 human breast cancer cells[21]. Parabens were able to competitively replace estradiol from binding to ER $\alpha$  in these cells. To replace estradiol from binding to its receptor a 1'000'000-fold molar excess of parabens was used. Additionally, parabens increased the proliferation of MCF7 cells, while in ER $\alpha$  receptor-negative MDA-MB-231 cells parabens showed no increase in proliferation at equal concentrations. In both cases butylparaben was the most active estrogenic paraben tested. Similar results were published by Okubo et al. showing ER-dependent proliferation of MCF7 cells treated with methyl-, ethyl-, propyl-, butyl-, isopropyl-, or isobutylparaben at concentrations that were 100'000 to 1'000'000 higher than estradiol[22]. However, the ER $\alpha$ -mediated estrogenic effects were not potent and it remains unclear whether these effects were indeed due to the activation of ER $\alpha$  or whether other pathways are involved.

The main metabolite of parabens, *p*-hydroxybenzoic acid, was reported by Pugazhendhi et al. to be slightly estrogenic [23]. They reported that *p*-hydroxybenzoic acid competitively displaced estradiol from ER $\alpha$  at a 10<sup>6</sup> to 10<sup>7</sup>-fold molar excess. Despite the fact that *p*-hydroxybenzoic acid is the main metabolite of all parabens and its presence in serum, the paraben concentrations needed to observe estrogenic effects are several orders of magnitude higher than the circulating

concentrations, questioning the concerns about their potential estrogenic properties in human. Besides, *p*-hydroxybenzoic acid is a highly hydrophilic compound with no evidence for bioaccumulation but rapid excretion via the urine[9].

Parabens were shown to inhibit sulfotransferases (SULTs) in human epidermal keratinocytes and skin cytosolic fractions and therefore block local estrogen inactivation[24]. It was suggested that a chronic application together with a potential accumulation of parabens in the skin might lead to increasing local estrogen concentrations due to the inhibition of SULTs. Butylparben was the most potent paraben tested with an  $IC_{50}$  of  $37 \pm 5 \mu M$ . Thus, parabens are thought to be rather weak inhibitors of SULTs; however, subcutaneous accumulation of parabens due to extensive use of dermally applied cosmetic products might actually lead to endocrine disruption due to the interference with estrogen sulfation by parabens. The inhibition of SULTs was the first study that showed estrogenic effects of paraben without direct modulation of ER activity.

Several studies showed that parabens can easily penetrate rat[25], rabbit[26] and human skin[7]. Daily application of cosmetic products for one-month led to an accumulation of methylparaben in the stratum corneum (SC) of the human fore arm. However, two days after stopping daily application, methylparaben in the SC was no longer detected[27]. These results indicate the possibility of local accumulation of parabens in the SC. However, only a daily and extensive use of products containing parabens will eventually lead to accumulation.

Despite the rapid metabolism of parabens to *p*-hydroxybenzoic acid, original parent paraben compounds can be detected in human plasma[28], seminal plasma[28], urine[10] and milk[29]. It is supposed that the detection of systemic paraben concentrations is due to dermal rather than oral application of products containing parabens because of highly active intestinal and liver esterase activities[6, 11]. This report showed additive effects of parabens (Figure 2). Often, a mixture of parabens is added to the cosmetic formulation to improve preservative efficiency. Studies showed that various parabens can be detected systemically, substantiating the importance of investigating potential additive effects[7]. Additive effects clearly increase their estrogenic potential and are important to take into account for further evaluation of the estrogenic potential of parabens.

## Conclusion

The present study identified several parabens inhibiting 17 $\beta$ -HSD1 and 17 $\beta$ -HSD2. Parabens can exert estrogenic effects by inhibiting 17 $\beta$ -HSD2. Inhibition of 17 $\beta$ -HSD2 prevents local inactivation of the active estrogen E2. All tested parabens and paraben-like structures, except the main metabolite *p*-hydroxybenzoic acid, interfered with the activity of 17 $\beta$ -HSD2 at a concentration of 20  $\mu$ M. The most potent compounds had IC<sub>50</sub> values in low micromolar range. The potential estrogenic effects reported in this study were observed at lower concentrations than those activating the ER or inhibiting SULTs as previously reported[8, 20-24]. Whereas most of the tested parabens were found to interfere with 17 $\beta$ -HSD2 activity, thereby increasing local E2 concentrations, only larger parabens were found to inhibit 17 $\beta$ -HSD1. The most frequently used parabens in cosmetic products are short parabens; therefore, inhibition of 17 $\beta$ -HSD1 by parabens used in cosmetic products is of minor relevance regarding health issues. Nevertheless, this study revealed a size-dependent 17 $\beta$ -HSD1 inhibition by parabens, and structure-activity relationship analyses should allow improving the previously established 17 $\beta$ -HSD1 pharmacophore models[30].

## Materials and Methods

Human embryonic kidney cells (HEK-293, ATCC, Manassas, VA, USA) were cultured in Dulbecco's modified Eagle's medium solution (DMEM, Sigma-Aldrich, St. Louis, MO, USA) supplemented with 10% fetal bovine serum (FBS, Connectorate, Dietikon, Switzerland), 100 U/mL penicillin, 100  $\mu$ g/mL streptomycin, 10 mM HEPES buffer (Gibco life technologies, Carlsbad, CA, USA) at pH 7.4, and 1% of non-essential amino acids solution (Sigma-Aldrich).

Endogenous 17 $\beta$ -HSD1 activity assays were performed in intact COV434 cells (Sigma-Aldrich). Cells were cultured under standard condition (5% CO<sub>2</sub>, 37°C) in DMEM (Sigma-Aldrich) supplemented with 100  $\mu$ g/mL streptomycin and 100 U/mL penicillin (Gibco life technologies), 10% FBS (Connectorate), and 2 mM L-glutamine (Sigma-Aldrich).

Lysate activity assays were performed as previously described. Briefly, HEK-293 cells (ATCC) were transiently transfected by the calcium phosphate precipitation method with plasmids for human 17 $\beta$ -HSD1 or 17 $\beta$ -HSD2. Lysates of HEK-293 expressing either 17 $\beta$ -HSD1 or 17 $\beta$ -HSD2 were

incubated for 10 min at 37 °C in TS2 buffer (100 mM NaCl, 1 mM EDTA, 1 mM EGTA, 250 mM sucrose, 1 mM MgCl<sub>2</sub>, 20 mM Tris-HCl, pH 7.4), containing either the inhibitor at the respective concentration or solvent (0.2% DMSO). 17 $\beta$ -HSD1 activity was determined in the presence of 200 nM estrone, including 50 nCi of [2,4,6,7-<sup>3</sup>H]-estrone and 500  $\mu$ M NADPH. Whereas, the 17 $\beta$ -HSD2 activity was performed in the presence of 200 nM estrone, including 50 nCi of [2,4,6,7-<sup>3</sup>H]-estradiol and 500  $\mu$ M NAD<sup>+</sup>.

To determine 17 $\beta$ -HSD1 activity in COV434 cells, cells were seeded (50'000) into 96-well plates and incubated for 90 min with 200 nM estrone, including 50 nCi of [2,4,6,7-<sup>3</sup>H]-estrone in serum-free charcoal treated media containing either the inhibitor at the respective concentration or solvent (0.1% DMSO). Both activity essays were stopped by adding a 1:1 ratio of 2 mM unlabeled E1 and E2 in methanol. Radiolabeled steroids were obtained from Perkin-Elmer (Boston, MA, USA) whereas normal steroids and cofactors were purchased from Sigma-Aldrich. Estrogens were separated by thin layer chromatography and samples were analyzed using scintillation counting. All data were collected from at least three independent measurements.

#### Author Contribution

Daniela Schuster and Alex Odermatt conceived and designed the experiments and wrote the paper. Simona R. Rohrer and Susanne Leugger performed all the *in vitro* experiments. Roger T. Engeli supervised the experiments, analyzed data, provided Figures, and wrote the paper. Anna Vuorinen provided all *in silico* data and modeling Figures.

1. Final amended report on the safety assessment of Methylparaben, Ethylparaben, Propylparaben, Isopropylparaben, Butylparaben, Isobutylparaben, and Benzylparaben as used in cosmetic products. International journal of toxicology, 2008. 27 Suppl 4: p. 1-82.
2. Daniel, J.W., Metabolic aspects of antioxidants and preservatives. Xenobiotica; the fate of foreign compounds in biological systems, 1986. 16(10-11): p. 1073-8.
3. Jackson, E.M., Moisturizers of today. J. Toxicol.-Cut. & Ocular Toxicol., 1992. 11(3): p. 173-184.
4. Soni, M.G., I.G. Carabin, and G.A. Burdock, Safety assessment of esters of p-hydroxybenzoic acid (parabens). Food and chemical toxicology : an international journal published for the British Industrial Biological Research Association, 2005. 43(7): p. 985-1015.
5. Sasseville, D., M. Alfalah, and J.P. Lacroix, "Parabenoia" Debunked, or "Who's Afraid of Parabens?". Dermatitis : contact, atopic, occupational, drug, 2015. 26(6): p. 254-9.



6. Darbre, P.D. and P.W. Harvey, Paraben esters: review of recent studies of endocrine toxicity, absorption, esterase and human exposure, and discussion of potential human health risks. *Journal of applied toxicology : JAT*, 2008. 28(5): p. 561-78.
7. Janjua, N.R., et al., Systemic uptake of diethyl phthalate, dibutyl phthalate, and butyl paraben following whole-body topical application and reproductive and thyroid hormone levels in humans. *Environmental science & technology*, 2007. 41(15): p. 5564-70.
8. Sandanger, T.M., et al., Plasma concentrations of parabens in postmenopausal women and self-reported use of personal care products: the NOWAC postgenome study. *J Expo Sci Environ Epidemiol*, 2011. 21(6): p. 595-600.
9. Boberg, J., et al., Possible endocrine disrupting effects of parabens and their metabolites. *Reproductive toxicology*, 2010. 30(2): p. 301-12.
10. Ye, X., et al., Quantification of the urinary concentrations of parabens in humans by on-line solid phase extraction-high performance liquid chromatography-isotope dilution tandem mass spectrometry. *Journal of chromatography. B, Analytical technologies in the biomedical and life sciences*, 2006. 844(1): p. 53-9.
11. Lakeram, M., et al., Paraben transport and metabolism in the biomimetic artificial membrane permeability assay (BAMPA) and 3-day and 21-day Caco-2 cell systems. *J Biomol Screen*, 2007. 12(1): p. 84-91.
12. Bledzka, D., J. Gromadzinska, and W. Wasowicz, Parabens. From environmental studies to human health. *Environ Int*, 2014. 67: p. 27-42.
13. Holst, J.P., et al., Steroid hormones: relevance and measurement in the clinical laboratory. *Clin Lab Med*, 2004. 24(1): p. 105-18.
14. Lin, C.Y., et al., Discovery of estrogen receptor alpha target genes and response elements in breast tumor cells. *Genome biology*, 2004. 5(9): p. R66.
15. Miller, W.L., Steroidogenic enzymes. *Endocrine development*, 2008. 13: p. 1-18.
16. Gunnarsson, C., E. Hellqvist, and O. Stal, 17beta-Hydroxysteroid dehydrogenases involved in local oestrogen synthesis have prognostic significance in breast cancer. *Br J Cancer*, 2005. 92(3): p. 547-52.
17. Darbre, P.D., et al., Concentrations of parabens in human breast tumours. *Journal of applied toxicology : JAT*, 2004. 24(1): p. 5-13.
18. Vuorinen, A., et al., Ligand-based pharmacophore modeling and virtual screening for the discovery of novel 17beta-hydroxysteroid dehydrogenase 2 inhibitors. *J Med Chem*, 2014. 57(14): p. 5995-6007.
19. Routledge, E.J., et al., Some alkyl hydroxy benzoate preservatives (parabens) are estrogenic. *Toxicol Appl Pharmacol*, 1998. 153(1): p. 12-9.
20. Miller, D., et al., Estrogenic activity of phenolic additives determined by an in vitro yeast bioassay. *Environ Health Perspect*, 2001. 109(2): p. 133-8.
21. Byford, J.R., et al., Oestrogenic activity of parabens in MCF7 human breast cancer cells. *J Steroid Biochem Mol Biol*, 2002. 80(1): p. 49-60.
22. Okubo, T., et al., ER-dependent estrogenic activity of parabens assessed by proliferation of human breast cancer MCF-7 cells and expression of ERalpha and PR. *Food Chem Toxicol*, 2001. 39(12): p. 1225-32.
23. Pugazhendhi, D., G.S. Pope, and P.D. Darbre, Oestrogenic activity of p-hydroxybenzoic acid (common metabolite of paraben esters) and methylparaben in human breast cancer cell lines. *J Appl Toxicol*, 2005. 25(4): p. 301-9.

24. Prusakiewicz, J.J., et al., Parabens inhibit human skin estrogen sulfotransferase activity: possible link to paraben estrogenic effects. *Toxicology*, 2007. 232(3): p. 248-56.
25. Bando, H., et al., Effects of skin metabolism on percutaneous penetration of lipophilic drugs. *J Pharm Sci*, 1997. 86(6): p. 759-61.
26. Pedersen, S., et al., In vitro skin permeation and retention of parabens from cosmetic formulations. *Int J Cosmet Sci*, 2007. 29(5): p. 361-7.
27. Ishiwatari, S., et al., Effects of methyl paraben on skin keratinocytes. *J Appl Toxicol*, 2007. 27(1): p. 1-9.
28. Frederiksen, H., N. Jorgensen, and A.M. Andersson, Parabens in urine, serum and seminal plasma from healthy Danish men determined by liquid chromatography-tandem mass spectrometry (LC-MS/MS). *J Expo Sci Environ Epidemiol*, 2011. 21(3): p. 262-71.
29. Schlumpf, M., et al., Exposure patterns of UV filters, fragrances, parabens, phthalates, organochlor pesticides, PBDEs, and PCBs in human milk: correlation of UV filters with use of cosmetics. *Chemosphere*, 2010. 81(10): p. 1171-83.
30. Schuster, D., et al., Discovery of nonsteroidal 17beta-hydroxysteroid dehydrogenase 1 inhibitors by pharmacophore-based screening of virtual compound libraries. *J Med Chem*, 2008. 51(14): p. 4188-99.

### 3.7 Conclusion

The goal of the studies in project 1 was to establish a ligand-based 17 $\beta$ -HSD2 pharmacophore model to identify specific novel nonsteroidal compounds that inhibit 17 $\beta$ -HSD2. The success of our first paper (Vuorinen et al., 2014) using this approach was the catalyst for three further projects. The pharmacophore model was constantly improved over the years and resulted in a remarkable predictive power of about 40-50% positive hit rate in the natural product paper (Vuorinen/Engeli et al., 2017b). Taking into account that no crystal structure of 17 $\beta$ -HSD2 is currently available and the pharmacophore model is just based on two active inhibitors, this positive hit rate is extraordinarily high. Additionally, it is noteworthy that the model predicts the selectivity over the enzyme 17 $\beta$ -HSD1 surprisingly well. In all projects, the selectivity over the enzyme 17 $\beta$ -HSD1 was evaluated. Enzymes of the HSD family share considerable structural similarity and therefore it is highly likely that other members of this family are also inhibited by the newly identified inhibitors. However, it is currently technically impossible to test the selectivity over all related enzymes. The physiological function of many HSDs is still not fully understood. Besides the use of pharmacophore models to identify new inhibitors, such models could also be applied to test potential interactions of new drugs candidates with selected targets in future work.

The focus in these studies was clearly on identifying novel compounds that inhibit 17 $\beta$ -HSD2. Metabolism, bioavailability, and distribution of the compounds were not tested. However, in the Vuorinen/Engeli et al., 2017a study, we had a strategy to attempt to minimize potential intestinal and liver metabolism of the compounds by replacing phenolic sides chains in the structure. Unfortunately, every chemically altered scaffold showed decreased activity. For any substance to be taken forward as a lead drug candidate ADME (absorption, distribution, metabolism and elimination) and many other preclinical tests need to be performed. To further develop 17 $\beta$ -HSD2 inhibitors as potential clinical drug candidates to treat osteoporosis, it has to be established if indeed 17 $\beta$ -HSD2 localized in bone tissues is actually accessible to the test compound. However, Bagi et al., showed that high doses of an orally administered 17 $\beta$ -HSD2 inhibitor (WH-9062) reduced bone resorption in ovariectomized cynomolgus monkeys relative to the control[101]. Additionally, the ovariectomized monkeys treated with 17 $\beta$ -HSD2 inhibitor regained ultimate

bone strength, substantiating that inhibition of 17 $\beta$ -HSD2 is an interesting potential osteoporosis target[110].

In contrast to the first major study within this project, the second major study focused on the evaluation of potential endocrine disruption effects of parabens by inhibiting 17 $\beta$ -HSD enzymes involved in estrogen metabolism. Parabens were identified as potential 17 $\beta$ -HSD2 inhibitors by virtual screening of a cosmetic chemical database using the 17 $\beta$ -HSD2 pharmacophore model and was therefore analyzed *in vitro* accordingly (Engeli et al. Manuscript in preparation 2017). Most of the parabens significantly decreased estrone formation by inhibiting 17 $\beta$ -HSD2, but none of the paraben compounds were able to potently inhibit 17 $\beta$ -HSD2. Besides, the major metabolite of all parabens, *p*-hydroxybenzoic acid, was not active at all. Interestingly, parabens inhibited 17 $\beta$ -HSD1 in a size-dependent matter. This finding will be used to perform a structure-activity relationship (SAR) study. This data will help to further improve the predictive power of the previously established 17 $\beta$ -HSD1 pharmacophore model[111]. In addition to the common lysate activity assay, 17 $\beta$ -HSD1 inhibition was also determined in COV434 cells which express endogenous 17 $\beta$ -HSD1. Parabens were able to penetrate cell membranes and also inhibited endogenous 17 $\beta$ -HSD1. This data demonstrates the capability of parabens to penetrate cell membranes and interfere with the intracellular activity of 17 $\beta$ -HSD1. However, it is very unlikely that parabens access cells expressing 17 $\beta$ -HSD1 or 2 at concentrations high enough to significantly disturb the activity of both enzymes since parabens are efficiently cleaved by esterases into *p*-hydroxybenzoic acid, rapidly metabolized in the liver, and excreted in urine[112]. This study revealed a novel endocrine disrupting effect of parabens. Although, the concentrations of parent paraben compounds needed to significantly disturb 17 $\beta$ -HSD enzymes activity will probably never be reached in target cells. However, potential estrogenic disrupting effects by parabens inhibiting 17 $\beta$ -HSD1 or 2 found in this study are more feasible than the previously reported ER $\alpha$  mediated estrogenic effects of paraben due to their very low potency towards ER $\alpha$ [104, 105, 107].

## 4. Project 2: 17 $\beta$ -Hydroxysteroid Dehydrogenase Type 3

### 4.1 Introduction

A human fetus exhibits no gender specific phenotypes until approximately the sixth week of gestation[113]. Male sexual differentiation is initiated by a complex interplay of androgens and essential sex determining genes located on the Y sex chromosome[114]. Androgens stimulate the development of internal and external male genitalia[115]. During embryogenesis, testosterone acts via the AR to stabilize the Wolffian ducts, which leads to the internal formation of the vas deferens, seminal vesicles, and epididymis[116]. Testosterone can further be reduced to the most potent androgen DHT, by the enzyme 5 $\alpha$ -reductase type 2[54]. DHT initiates the formation of external genitalia development (penis and scrotum) as well as the urethra and prostate[115]. Furthermore, Müllerian inhibitor hormone is produced by testicular Sertoli cells to regress the Müllerian duct development[117]. Mutations in both *HSD17B3* and *SRD5A2* genes result in severe 46, XY disorder of sexual development[118]. Currently, more than 40 different mutations (introns and exons) in the *HSD17B3* gene have been reported[119, 120]. So far, more than 50 mutations have been reported in the *SRD5A2* gene [121]. Proper function of the human 17 $\beta$ -HSD3 and 5 $\alpha$ -reductase type 2 enzymes is essential for prenatal androgen formation and male sexual differentiation[22].

The enzyme 17 $\beta$ -HSD3 is predominantly expressed in the testicular Leydig cells and mainly converts the inactive androgen androstenedione into its active form testosterone using NADPH as cofactor[53, 122]. Additionally, 17 $\beta$ -HSD3 converts the  $\Delta^5$ -steroid DHEA into androstenediol, which is further converted into testosterone[123]. Conversion of other substrates play a minor role. The 17 $\beta$ -HSD3 enzyme consists of 310 amino acids, with a molecular mass of 34.5 kDa and is located in the ER membrane facing the cytosol[86, 122]. Mutations in the *HSD17B3* gene (9q22) can result in lower testosterone concentrations during embryogenesis causing severe effects on male sexual development in affected patients[53, 124]. So called 17 $\beta$ -HSD3 deficiency is a rare autosomal recessive cause of 46, XY disorder of sexual development (46, XY DSD)[125]. Patients with such a disorder are XY individuals that characteristically show undervirilization at birth with an ambiguous or female genital phenotype[119]. Often the disorder is unnoticed at birth and patients are commonly raised as females. Typically, the disorder is recognized during puberty due to primary amenorrhea and occurring virilization[126]. Virilization is usually caused by increasing

systemic testosterone concentrations due to the appearance of 17 $\beta$ -HSD5 (at this specific stage of development) or residual 17 $\beta$ -HSD3 activity and can have severe effects on sex identity of the patient[127]. Several affected patients, who are usually raised as females, undergo sex change due to substantial masculinization at puberty[128]. Mutations in the *SRD5A2* gene can result in lower DHT levels in affected patients resulting in a very similar phenotype at birth, revealing that the most potent androgen DHT is also essential for male sex development[129].

In this chapter we biochemically investigated mutations in the *HSD17B3* gene of Tunisian and Egyptian patients that were associated with 46, XY DSD. A homology model of 17 $\beta$ -HSD3 based on the crystal structure of 17 $\beta$ -HSD1 was applied to further examine the structural changes caused by the mutations. All together five different 17 $\beta$ -HSD3 mutations, one polymorphism, and 20 patients were reported and analyzed.

## 4.2 Paper 5 (Engeli et al., 2016)

# **Biochemical analyses and molecular modeling explain the functional loss of 17 $\beta$ -hydroxysteroid dehydrogenase 3 mutant G133R in three Tunisian patients with 46, XY Disorders of Sex Development**

Roger T. Engeli\*, Bochra Ben Rhouma\*, Christoph P. Sager, Maria Tsachaki, Julia Birk, Faiza Fakhfakh, Leila Keskes, Neila Belguith, Alex Odermatt

Published manuscript

**Contribution:** Performed *in vitro* activity assays (Figure 2), western blot (Figure 3), immunolocalization experiments (Figure 4), and gene alignments (Figure 5). Co-wrote the paper manuscript. First authorship was shared equally (\*).

**Aims:** Biochemical analyses and explanation of the functional loss of 17 $\beta$ -HSD3 in Tunisian patients with G133R and C206X mutations causing 46, XY DSD.

**Results:** G133R and C206X mutations lead to a complete loss of 17 $\beta$ -HSD3 function despite normal protein expression levels.

**Conclusion:** Mutated arginine residue G133R, causes steric hindrance of the cofactor NADPH binding. The truncated C206X mutation causes inactivates 17 $\beta$ -HSD3 due to the loss of a specific section of the substrate binding site.





## Biochemical analyses and molecular modeling explain the functional loss of 17 $\beta$ -hydroxysteroid dehydrogenase 3 mutant G133R in three Tunisian patients with 46, XY Disorders of Sex Development



Roger T. Engeli<sup>a,1</sup>, Bochra Ben Rhouma<sup>b,1</sup>, Christoph P. Sager<sup>c</sup>, Maria Tsachaki<sup>a</sup>, Julia Birk<sup>a</sup>, Faiza Fakhfakh<sup>b</sup>, Leila Keskes<sup>b</sup>, Neila Belguith<sup>b,d,\*\*</sup>, Alex Odermatt<sup>a,\*</sup>

<sup>a</sup> Division of Molecular and Systems Toxicology, Department of Pharmaceutical Sciences, Pharmcenter, University of Basel, Basel, Switzerland

<sup>b</sup> Human Molecular Genetics Laboratory, Faculty of Medicine, University of Sfax, Sfax, Tunisia

<sup>c</sup> Molecular Modeling, Department of Pharmaceutical Sciences, Pharmcenter, University of Basel, Basel, Switzerland

<sup>d</sup> Department of Medical Genetics, HediChaker Hospital, Sfax, Tunisia

### ARTICLE INFO

#### Article history:

Received 24 June 2015

Received in revised form 21 October 2015

Accepted 29 October 2015

Available online 3 November 2015

#### Keywords:

46, XY DSD

17 $\beta$ -hydroxysteroid dehydrogenase  
HSD17B3

Testosterone

Mutation

Structure function relationship

Male sexual development

### ABSTRACT

Mutations in the *HSD17B3* gene resulting in 17 $\beta$ -hydroxysteroid dehydrogenase type 3 (17 $\beta$ -HSD3) deficiency cause 46, XY Disorders of Sex Development (46, XY DSD). Approximately 40 different mutations in *HSD17B3* have been reported; only few mutant enzymes have been mechanistically investigated. Here, we report novel compound heterozygous mutations in *HSD17B3*, composed of the nonsense mutation C206X and the missense mutation G133R, in three Tunisian patients from two non-consanguineous families. Mutants C206X and G133R were constructed by site-directed mutagenesis and expressed in HEK-293 cells. The truncated C206X enzyme, lacking part of the substrate binding pocket, was moderately expressed and completely lost its enzymatic activity. Wild-type 17 $\beta$ -HSD3 and mutant G133R showed comparable expression levels and intracellular localization. The conversion of  $\Delta$ 4-androstene-3,17-dione (androstenedione) to testosterone was almost completely abolished for mutant G133R compared with wild-type 17 $\beta$ -HSD3. To obtain further mechanistic insight, G133 was mutated to alanine, phenylalanine and glutamine. G133Q and G133F were almost completely inactive, whereas G133A displayed about 70% of wild-type activity. Sequence analysis revealed that G133 on 17 $\beta$ -HSD3 is located in a motif highly conserved in 17 $\beta$ -HSDs and other short-chain dehydrogenase/reductase (SDR) enzymes. A homology model of 17 $\beta$ -HSD3 predicted that arginine or any other bulky residue at position 133 causes steric hindrance of cofactor NADPH binding, whereas substrate binding seems to be unaffected. The results indicate an essential role of G133 in the arrangement of the cofactor binding pocket, thus explaining the loss-of-function of 17 $\beta$ -HSD3 mutant G133R in the patients investigated.

© 2015 Elsevier Ltd. All rights reserved.

### 1. Introduction

17 $\beta$ -hydroxysteroid dehydrogenase type 3 (17 $\beta$ -HSD3) deficiency is a rare autosomal recessive cause of 46, XY Disorders of Sex Development (46, XY DSD) described in 1971 [1]. It is caused by mutations in the *HSD17B3* gene (9q22) encoding the 17 $\beta$ -

HSD3 enzyme consisting of 310 amino acids [2,3]. 17 $\beta$ -HSD3 is predominantly expressed in the testes and utilizes NADPH as a cofactor [2,4]. 17 $\beta$ -HSD3 catalyzes the conversion of the  $\Delta$ 4-androstene-3,17-dione (androstenedione) to testosterone, which is responsible for the normal fetal development of male genitalia [5].

17 $\beta$ -HSD3 deficiency is characterized by a spectrum of clinical phenotypes due to a complete loss or residual activity of the mutated 17 $\beta$ -HSD3 enzyme in the testes [6], as well as differences in the degree of end-organ responsiveness and timing of exposure of external genitalia to androgens. The onset of the extra-testicular conversion of androstenedione to testosterone by 17 $\beta$ -HSD5 (also known as AKR1C3) is responsible for the observed virilization at puberty [1,7–9]. The characteristic phenotype at birth is an XY individual with undervirilization of the external genitalia, which often appear female with or without clitoromegaly and/or labial

\* Corresponding author at: Division of Molecular and Systems Toxicology, Department of Pharmaceutical Sciences, Pharmcenter, University of Basel, Klingelbergstrasse 50, 4056 Basel, Switzerland.

\*\* Corresponding author at: Human Molecular Genetics Laboratory, Faculty of Medicine, MagidaBoulila Street, 3029 Sfax, Tunisia.

E-mail addresses: [Neila.Belguith@fmsf.rnu.tn](mailto:Neila.Belguith@fmsf.rnu.tn) (N. Belguith), [alex.odermatt@unibas.ch](mailto:alex.odermatt@unibas.ch) (A. Odermatt).

<sup>1</sup> These authors contributed equally to the present study.

fusion and a blind-ending vagina [1,10]. Affected patients have testes and often have normal Wolffian duct derivatives. The diagnosis of 17 $\beta$ -HSD3 deficiency is based on an increased ratio of androstenedione to testosterone. It can be suspected in case of inguinal hernia or sexual ambiguity at early childhood and in case of severe virilization and primary amenorrhea at puberty age [11].

Here, we report on three Tunisian patients with 17 $\beta$ -HSD3 deficiency from two different non-consanguineous Tunisian families. Our results revealed novel compound heterozygous mutations, *i.e.*, the premature stop codon C206X and the missense mutation G133R, in the *HSD17B3* gene responsible for 17 $\beta$ -HSD3 deficiency. The impact of the missense mutations was studied by site-directed mutagenesis, expression of the recombinant proteins in HEK-293 cells and biochemical analysis of enzyme activity. In order to understand the loss of enzyme activity of mutant G133R, additional substitutions of G133 were investigated and a 17 $\beta$ -HSD3 homology model was generated using Modeller Version 9.11 [12–14].

## 2. Experimental procedures

### 2.1. Subjects and clinical history

Three Tunisian patients diagnosed with 46, XY Disorders of Sex Development (DSD) were studied. Since birth, all patients were raised as girls; patient P1 consulted at the age of 7 years for inguinal hernia, and the two remaining patients were sisters and consulted at puberty age for primary amenorrhea. For all patients, the physical examination revealed normal female external genitalia, and the karyotype analysis, performed using standard G-banding technique, revealed 46, XY. The magnetic resonance imaging of the pelvis and the abdomen showed no visualization of the uterus or vagina but revealed inguinal testes. The results of hormonal baseline testing of all patients are presented in Table 1.

### 2.2. Sequencing the HSD17B3 gene

Peripheral blood samples of the patients (P1, P2 and P3) and the parents of P1 were collected and genomic DNA was extracted using phenol-chloroform standard procedures [15]. All exons and flanking intron regions of the *HSD17B3* gene were tested for mutations by sequence analysis using the previously reported primers [16]. The PCR was performed using a thermal cycler (GenAmp PCR System 9700, Applied Biosystem, Waltham, MA) in a final volume of 50  $\mu$ L containing 50 ng genomic DNA, 0.2  $\mu$ M of each primer, 1 $\times$  PCR buffer, 1.2 mM MgCl<sub>2</sub>, 0.5 mM dNTP, and 1 U Taq DNA polymerase (Promega GoTaq DNA Polymerase, Fitchburg, WI). Direct sequencing of PCR products was performed using the ABI Prism BigDye Terminator Cycle Sequencing Ready Reaction Kit (ABI PRISM/Biosystems) and the products were resolved on an ABI PRISM.

**Table 1**  
Characterization of patients.

	Patient 1 (P1)	Patient 2 (P2)	Patient 3 (P3)
Age (years)	7	14	15
Height (cm)	155	–	–
Weight (kg)	45	–	–
Tanner stage	P1B1	P4B1	P5B1
Testosterone (ng/mL)	0.8	3	4
LH (IU/L)	12.5	–	–
FSH (IU/L)	4.7	40	42
Karyotype analysis	46, XY	46, XY	46, XY

References values: Luteinizing hormone (LH): 1.24–8.62 mIU/mL; follicle stimulating hormone (FSH): 1.27–19.26 mIU/mL; testosterone: 1.75–7.61 ng/mL.

### 2.3. Site-directed mutagenesis and construction of expression plasmids

A pCMV6 expression vector containing the full-length human 17 $\beta$ -HSD3 sequence was a kind gift of the late Prof. Dr. Stefan Andersson. The cDNA sequence from the ATG initiation codon to the stop codon, which was replaced by a FLAG epitope followed by a stop codon, was amplified by PCR and inserted into the pCDNA3.0 expression vector (Thermo Scientific, Rockford, IL, USA) between the restriction sites *Bam*H1 and *Xba*1 (Roche, Basel, Switzerland). This construct was used as a template to introduce the FLAG-tagged point mutations. Point mutations were introduced by site-directed mutagenesis using *Pfu* Polymerase (Promega, Madison, WI, USA) (for oligonucleotide primer sequences see Supporting information). All expression plasmids were verified by sequencing.

### 2.4. Cell culture and enzyme activity assay

Human Embryonic Kidney-293 cells (HEK-293, ATCC, Manassas, VA, USA) were cultured in Dulbecco's Modified Eagle Medium (DMEM, Sigma–Aldrich, St. Louis, MO, USA) supplemented with 10% fetal bovine serum (FBS, Connectorate, Dietikon, Switzerland), 100 U/mL penicillin, 100  $\mu$ g/mL streptomycin (Life Technologies, Grand Island, NY, USA), 10 mM HEPES buffer pH 7.4 (Life Technologies, Grand Island, NY, USA), and 1% MEM non-essential amino acid solution (Sigma–Aldrich). Cells were cultivated under standard conditions (37 °C, 5% CO<sub>2</sub>) in an incubator (Thermo Fisher Scientific, Waltham, MA, USA). HEK-293 cells ( $1.5 \times 10^6$ ) were seeded into 10 cm dishes, followed by transient transfection by the calcium phosphate precipitation method with 8  $\mu$ g of expression plasmid for wild-type 17 $\beta$ -HSD3 [17,18] or mutant 17 $\beta$ -HSD3 (see below). Transfected HEK-293 cells were incubated for 24 h at 37 °C, and 15,000 cells were seeded in 100  $\mu$ L medium in 96-well plates, pre-coated with poly-L-lysine (Sigma–Aldrich). After incubation for another 24 h, the medium was replaced by 50  $\mu$ L charcoal-treated DMEM and the 17 $\beta$ -HSD3 enzyme activity measurements were performed by adding androstenedione (Sigma–Aldrich) at a final concentration of 200 nM, containing 50 nCi [1,2,6,7-<sup>3</sup>H]-androstenedione (American Radiolabeled Chemicals, St. Louis, MO, USA). After 30 min reactions were stopped and cells lysed by adding 20  $\mu$ L of methanol containing 2 mM unlabeled androstenedione and 2 mM testosterone (Sigma–Aldrich). An amount of 20  $\mu$ L of lysate was loaded onto TLC plates (Macherey-Nagel, Oensingen, Switzerland) and steroids were separated using chloroform/ethyl acetate at a 4:1 ratio. Corresponding substrate and product concentrations were determined after scintillation counting (PerkinElmer, MA, USA).

### 2.5. Immunostaining

HEK-293 cells were seeded on glass coverslips and transiently transfected with plasmids for FLAG-tagged wild-type and mutant 17 $\beta$ -HSD3 constructs after 24 h. At 48 h post-transfection cells were washed with PBS, fixed with 4% paraformaldehyde and cell membranes were permeabilized for 5 min with 0.3% Triton X-100. After blocking with 2% defatted milk in PBS for 30 min, cells were incubated with the primary antibody at a dilution of 1:100 for 1 h at room temperature. Rabbit anti-FLAG (Sigma–Aldrich) and mouse anti-protein disulfide isomerase (PDI) antibodies (Abcam, Cambridge, UK) were used. Anti-PDI antibodies were used as control for a protein with an endoplasmic reticulum distribution. After washing, cells were incubated for 30 min at room temperature with goat anti-rabbit Alexa Fluor<sup>®</sup> 488 and goat anti-mouse Alexa Fluor<sup>®</sup> 555 IgG (Sigma–Aldrich) at a dilution of 1:300. After washing, samples were mounted in Mowiol 4-88 (Roth, Karlsruhe,

Germany) and analyzed using an Olympus Fluoview 1000 laser scanning confocal microscope (Olympus, Tokyo, Japan).

## 2.6. Western blot

HEK-293 cells (300,000) were seeded in 60 mm dishes. After 24 h, the calcium phosphate transfection method was used to transfect 5 µg of plasmid for FLAG-tagged wild-type and mutant enzymes. Medium was changed after 4 h and cells were incubated for another 48 h. Cells were lysed using RIPA buffer (Sigma–Aldrich), containing protease inhibitor cocktail (Roche, Basel, Switzerland), and centrifuged at  $14,000 \times g$  for 20 min at 4 °C. The supernatant was collected and protein concentrations were quantified using the Pierce<sup>®</sup> bicinchoninic acid protein assay kit (Thermo Scientific, Rockford, IL, USA). Samples were prepared in Laemmli solubilization buffer (LSB) (5 mM Tris–HCl, 10% glycerol, 0.2% sodium dodecyl sulfate, 0.04% bromophenol blue, pH 6.8), containing 5% β-mercaptoethanol (Promega, Madison, WI, USA) and boiled for 5 min. An amount of 35 µg of total protein was separated by sodium dodecyl sulfate-polyacrylamide gel electrophoresis (SDS–PAGE) on a 12% acrylamide gel and transferred to Immobilon-Blot<sup>®</sup> polyvinylidene difluoride (PVDF) membranes (Bio-Rad Laboratories, Hercules, CA, USA). For detection of the FLAG epitope, the membrane was blocked using 3% defatted milk in PBS for 30 min and incubated with the mouse monoclonal M2 antibody (Sigma–Aldrich) at a dilution of 1:750 in blocking solution overnight at 4 °C. After washing with Tris-buffered saline (20 mM Tris buffer, pH 7.4, 140 mM NaCl) containing 0.1% Tween-20 (TBS–T), the membrane was subsequently incubated with horseradish peroxidase-conjugated goat anti-mouse secondary antibody (Sigma–Aldrich) for 1 h at room temperature. For the detection of the house keeping control cyclophilin A, blocking was performed overnight at 4 °C using 3% defatted milk in PBS. Subsequently, the membrane was incubated with the rabbit anti-human cyclophilin A polyclonal antibody (Abcam, Cambridge, UK) at a dilution 1:2000 in blocking solution for 1 h at room

temperature. After washing with TBS–T, the membrane was subsequently incubated with horseradish peroxidase-conjugated goat anti-rabbit secondary antibody (Sigma–Aldrich) at a dilution 1:2000 in 3% defatted milk in PBS. After washing, the protein bands were visualized on a Fujifilm ImageQuant<sup>™</sup> LAS-4000 (GE Healthcare, Glattbrugg, Switzerland) using the Immobilon Western Chemiluminescent HRP substrate kit (Merck, Kenilworth, NJ, USA). The bands obtained for the FLAG-tagged wild-type and mutant 17β-HSD3 protein were subjected to densitometry analysis using ImageJ software. Signals were normalized to those of cyclophilin A house keeping control to correct for loading differences.

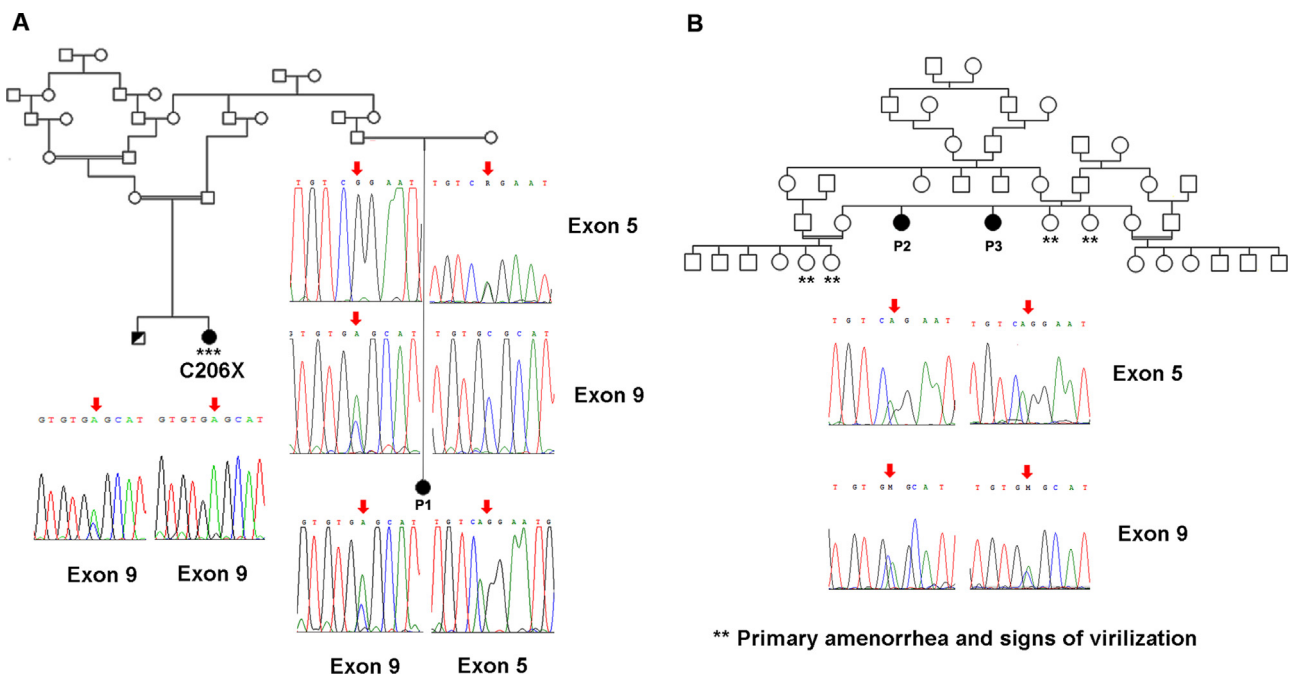
## 2.7. Molecular modeling

Protein sequences were aligned by multiple alignment using the Multiple Sequence Viewer implemented in Maestro [19]. A homology model of wild-type as well as of the G133R mutant of 17β-HSD3 were obtained by using the aligned sequences (see Supporting information) together with a crystal structure of 17β-hydroxysteroid dehydrogenase 1 (17β-HSD1, PDB code: 3DHE, 2.3 Å) as input for Modeller (Version 9.11), provided by the MPI Bioinformatics Toolkit [12–14].

SiteMap was used to predict the androstenedione binding site of the obtained homology model and was subsequently used as input for generating a Glide Docking Grid [20–24]. The Glide XP docking protocol was used to dock androstenedione to the generated rigid docking grid. The protein–ligand complex was refined using Prime [25–27]. Figures were produced by PyMOL [28].

## 2.8. Multiple protein alignment

Multiple protein alignment of relative 17β-HSDs was performed using ExPASy (<http://embnet.vital-it.ch/software/ClustalW.html>). Protein amino acid sequences of all tested 17β-HSDs



**Fig. 1.** Mutational analyses of 46, XY DSD patients.

Automated DNA sequencing of the *HSD17B3* gene for the three patients: the sequences revealed a heterozygous substitution (cDNA position 618, C > A) in exon 9 and a heterozygous substitution (cDNA position 397, G > A) in exon 5 of patients P1, P2 and P3. (A) Results of the mutational analysis of exon 9 and exon 5 for patient P1 and some of her family members. (B) Results of the mutational analysis of exon 9 and exon 5 for patients P2 and P3. Symbols indicate sex phenotype: circles represent females, squares represent males. Filled symbols indicate patients with mutated *HSD17B3* alleles and half-filled symbols indicate one mutated allele. Consanguineous marriage is indicated by a double line. \*\*\* indicates a patient homozygous for the C206X mutation. (For interpretation of the references to color in this figure legend, the reader is referred to the web version of this article.)

were collected from the gene database from the National Center of Biotechnology Information (<http://www.ncbi.nlm.nih.gov/gene/>).

### 3. Results

#### 3.1. 17 $\beta$ -HSD3 mutation G133R occurs in 46, XY DSD patients

The familial history of P1 recorded a paternal cousin with 17 $\beta$ -HSD3 deficiency due to a homozygous mutation (cDNA position 618, C > A) in exon 9 resulting in the substitution of the cysteine at position 206 to a premature stop codon (C206X) [29]. Therefore, the genomic DNA from patient P1 was analyzed for mutations in the *HSD17B3* gene. For patients P2 and P3, due to the signs of virilization observed at the age of puberty and the absence of a complete hormonal profile including an hCG stimulation test, two deficiencies were initially suspected: 5 $\alpha$ -reductase 2 deficiency with loss of function mutations in the *SRD5A2* gene or 17 $\beta$ -HSD3 deficiency. DNA analysis of the *SRD5A2* gene showed no abnormalities in the entire coding region and the adjacent intron/exon boundaries. Therefore, the genomic DNA of the patients was analyzed for mutations in *HSD17B3*. Patients P1, P2 and P3 were heterozygous for the previously described nonsense mutation C206X. In addition, they were also heterozygous for a novel missense mutation (cDNA position 397, G > A) in exon 5, resulting in the mutation G133R (Fig. 1A and B). The verification of the transmission of the mutations among the family of P1 showed that the mutation C206X was coded by a paternal allele and G133R by a maternal allele (Fig. 1A).

#### 3.2. Truncation C206X and substitution G133R cause abolished 17 $\beta$ -HSD3 activity

The mutation C206X, derived from the paternal allele, causes a truncation of the enzyme at position 206, only four amino acids downstream of the essential catalytic site (Y198 and K202) [30]. The truncated enzyme lacks a significant part of the substrate binding site. Enzyme activity measurements were performed in intact HEK-293 cells transfected with expression plasmids for either wild-type or mutant 17 $\beta$ -HSD3 enzymes. The formation of testosterone was examined after incubation of cells for 30 min with 200 nM androstenedione. No activity could be detected for mutant C206X, even after prolonged incubation time (not shown), and an almost complete loss of activity was obtained for mutant G133R (Fig. 2). Since the substitution of a glycine by an arginine residue alters both size and charge of the side chain, three additional mutant enzymes were constructed, i.e., G133A, G133Q and G133F. Enzymatic analysis revealed that substitution of glycine by the bulky phenylalanine and by the non-charged glutamine also almost completely abolished 17 $\beta$ -HSD3 activity, whereas mutant G133A retained approximately 70% of wild-type activity (Fig. 2).

Next, Western blotting of FLAG-tagged wild-type and mutant 17 $\beta$ -HSD3 proteins was conducted to investigate whether the loss of enzymatic activity of the mutant enzymes was due to impaired protein expression (Fig. 3). Wild-type and G133 mutant proteins yielded one specific band at about 35 kDa, as expected. Densitometry analyses of three independent experiments did not yield significant differences in the expression levels of wild-type and G133 mutant proteins (data not shown). A specific band for mutant C206X could be detected at about 18 kDa; however, the expression level seemed to be low and the band was visible only after prolonged exposure of the blot, which also led to the detection of several unspecific bands as shown by the empty vector control sample. Further investigation by immunofluorescence staining and confocal microscopy confirmed the typical endoplasmic reticulum (ER) membrane localization of FLAG-tagged wild-type and G133 mutant 17 $\beta$ -HSD3 enzymes (Fig. 4). No signs of dislocation

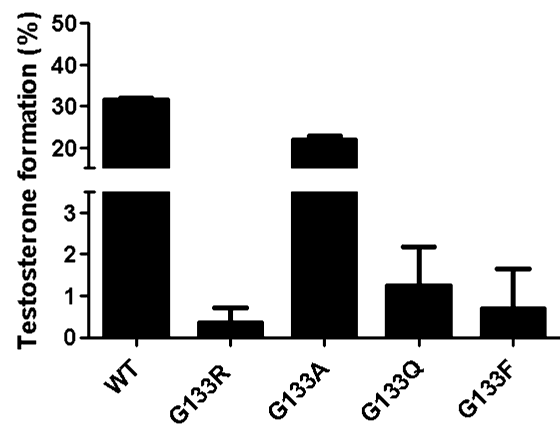


Fig. 2. Enzymatic activity of wild-type and mutant 17 $\beta$ -HSD3.

HEK-293 cells (15,000 cells per well of a 96-well plate) were transiently transfected with expression plasmids for wild-type human 17 $\beta$ -HSD3 and mutants G133R, G133A, G133Q and G133F. Enzymatic activity was measured by incubating cells for 30 min at 37 °C with androstenedione at a final concentration of 200 nM and containing 50 nCi [1,2,6,7-<sup>3</sup>H]-androstenedione, followed by analysis of the conversion of androstenedione to testosterone by scintillation counting. The percentage of testosterone formed from the initially supplied androstenedione is shown. Results represent mean  $\pm$  SD of four independent experiments.

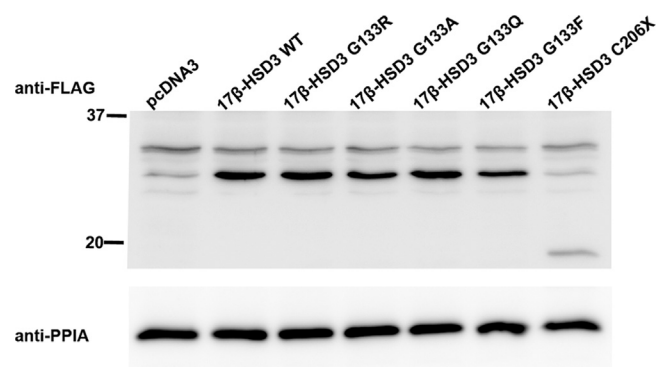


Fig. 3. Western blot of wild-type and mutant 17 $\beta$ -HSD3.

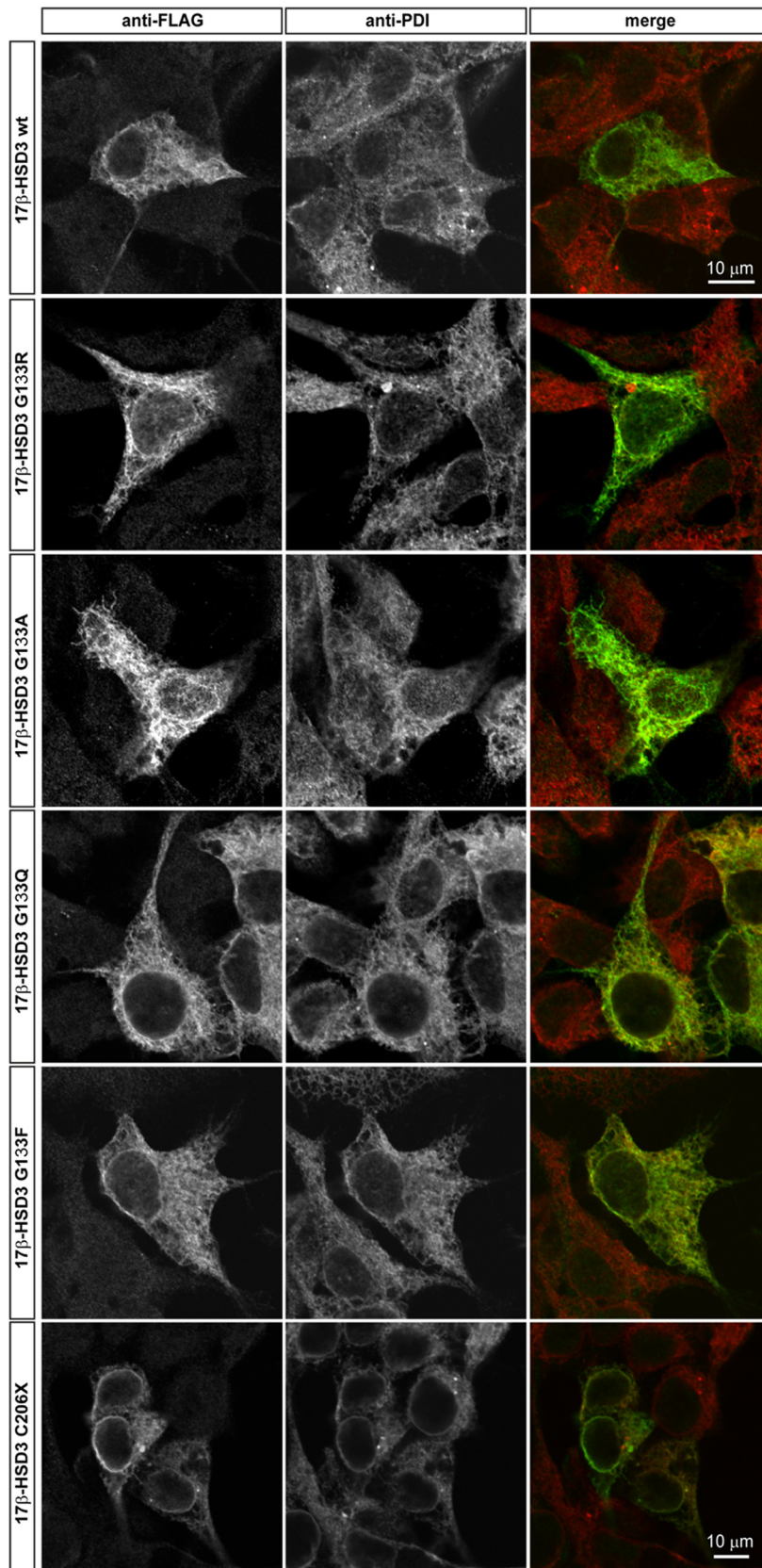
HEK-293 cells were transiently transfected with plasmids for C-terminally FLAG epitope-tagged wild-type and mutant 17 $\beta$ -HSD3. After an incubation time of 48 h, transfected cells were harvested and equal amounts of total protein were separated by SDS-PAGE and subjected to Western blotting using a mouse anti-FLAG antibody for detection. Cyclophilin A (PPIA) was used as a control and analyzed using an anti-PPIA antibody. One out of three similar experiments is shown.

or degradation of the G133 mutant enzymes were observed. In contrast, for mutant C206X, despite its moderate signal, signs of aggregated protein could be detected, suggesting impaired folding.

#### 3.3. G133 is conserved among 17 $\beta$ -HSD enzymes

A sequence alignment of human 17 $\beta$ -HSD3 with 17 $\beta$ -HSD3 of other species revealed that G133 is highly conserved (not shown). More importantly, alignment with sequences from related 17 $\beta$ -HSD enzymes corresponding to the region of the turn between  $\beta$ 4– $\alpha$ 5 on 17 $\beta$ -HSD3 showed that the glycine residue is highly conserved (Fig. 5). All of the 13 analyzed 17 $\beta$ -HSD enzymes of the short-chain dehydrogenase/reductase family (17 $\beta$ -HSD1–14, with the exception of 17 $\beta$ -HSD5 that belongs to the family of aldo-keto reductases (AKR) and was therefore not included in the alignment [31]) possess a glycine at this position. The glycine is the last residue of a cluster of seven conserved amino acids with the consensus sequence (I/V)(I/L/V)(I/V)NN(A/V)G. These residues are forming the turn between the 4th  $\beta$ -sheet and the 5th  $\alpha$ -helix of the conserved SDR structure. A glycine corresponding to position 133 on 17 $\beta$ -HSD3 is also found in





**Fig. 4.** Immunolocalization of wild-type and mutant 17 $\beta$ -HSD3.

HEK-293 cells were transiently transfected with plasmids for FLAG-tagged wild-type 17 $\beta$ -HSD3 and FLAG-tagged mutants G133R, G133A, G133Q, G133F and C206X, respectively. After an additional incubation time of 48 h, transfected cells were stained with rabbit anti-FLAG (green) and mouse anti-protein disulfide isomerase (PDI, red). Wild-type and mutant enzymes showed an endoplasmic reticular localization pattern similar to that of the control PDI. Anti-FLAG, anti-PDI and both stainings merged are shown. Pearson's correlation coefficients were calculated by the inbuilt Olympus Fluoview 1000 software for the images shown: 0.52 for wild-type 17 $\beta$ -HSD3, 0.75 for G133R, 0.78 for G133Q, 0.82 for G133A, 0.91 for G133F, 0.76 for C206X. (For interpretation of the references to color in this figure legend, the reader is referred to the web version of this article.)

		G133 ↓	
17β-HSD3	117	KEKLAGLEIGILVNNV	GMLPNLLPS
17β-HSD1	77	RERVTEGRVDV	LVLCNAGLGLLGP
17β-HSD2	153	AAMLQDRGLWAV	INNAGVLGFPTDG
17β-HSD4	85	TALDAFGRIDV	VVNNAGILRDRSFA
17β-HSD6	98	KEHVGDRGLWG	LVNNAGILTPITLC
17β-HSD7	76	ELKQRFQRLDCI	YLVNAGIMPNPQLN
17β-HSD8	89	VQACFSRPPSV	VVSCAGITQDEFLL
17β-HSD9	97	EMHVKEAGLFG	LVNNAGVAGIIGPT
17β-HSD10	77	LAKGKFGRRVD	VAVNCAGIAVASKTY
17β-HSD11	106	KVKAIEIGDVS	ILVNNAGVVYTSDF
17β-HSD12	119	KTGLAGLEIGI	LVNNVGMSEYYPEY
17β-HSD13	70	KVKKEVGDVTV	VVNNAGTVYPADLL
17β-HSD14	75	ETIRRFGRGLDC	VVNNAGHHPPPQRP
Consensus		(I/V) (I/L/V) (I/V) NN (A/V) G	

**Fig. 5.** Alignment of the region containing G133 on 17β-HSD3 with other 17β-HSDs.

Sequences of 17β-HSD enzymes belonging to the SDR family and corresponding to the region of the turn between the 4th β-sheet and the 5th α-helix of 17β-HSD3 were aligned. The alignment shows that the glycine at position 133 in 17β-HSD3 (marked and indicated with an arrow) is highly conserved among related 17β-HSD enzymes. Several amino acids upstream of the glycine residue are also conserved. Three hydrophobic amino acid residues are followed by two asparagine residues, an alanine or a valine, and the glycine, suggesting that the conserved residues of the β4–α5 turn have a role in the arrangement of the cofactor binding pocket.

many other SDR enzymes; however, to our knowledge no other substitution of this specific glycine residue has been reported so far in any of the other SDR members.

### 3.4. Molecular modeling

To begin to understand the loss-of-function of the G133R substitution, homology modeling was performed. The available crystal structures of the related enzyme 17β-HSD1 (see Supporting information for PDB codes) suggested that the glycine residue corresponding to position 133 in 17β-HSD3 lies in the cofactor binding pocket and that its mutation to an arginine might interfere with the binding of NADPH. Because no crystal structures of 17β-HSD3 are yet available, homology modeling was employed. Two models were built, the first represents the wild-type enzyme, and the second contains the G133R mutation. Both models are based on a crystal structure of 17β-HSD1 (PDB code: 3DHE, 2.3 Å) [12]. The wild-type 17β-HSD3 homology model suggests that the first four amino acids (127–130; ILVN) of the cluster of conserved amino acid residues lie at the end of the 4th β-sheet and the last three amino

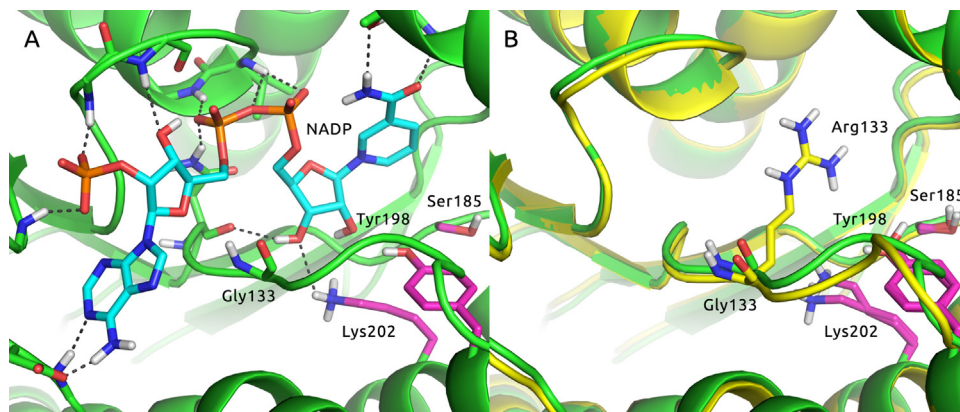
acids (131–133; NVG) at the start of the 5th α-helix, close to the NADPH binding pocket.

Superimposing the obtained models with a crystal structure of 17β-HSD1 complexed with cofactor NADP<sup>+</sup> (PDB code: 1QYV, 1.8 Å [32]) reveals the inherent inability of the G133R mutant to accommodate NADP<sup>+</sup>. The homology model of wild-type 17β-HSD3 supported this conclusion and showed that the wild-type enzyme is able to bind the cofactor (Fig. 6). Furthermore, the highly conserved N131 is involved in hydrogen bonding to NADP<sup>+</sup> and stabilization of the β1α2 turn that features the classical TGxxxGxG cofactor binding motif of related SDRs [33,34]. Docking of androstenedione to the homology model of wild-type 17β-HSD3 and mutant G133R and subsequent refinement yielded a pose of the steroid slightly tilted towards N240 in comparison to bound ligands of 17β-HSD1 crystal structures. Three hydrogen bonds were observed from androstenedione to S185, Y198 and N240 (wild-type 17β-HSD3: 1.8 Å, 1.8 Å and 1.8 Å, respectively; G133R mutant: 2.0 Å, 2.3 Å and 1.8 Å, respectively) as well as Van der Waals contacts to L135, I187, W192, Y195, Y198, Y229 and C266 (Fig. 7).

### 4. Discussion

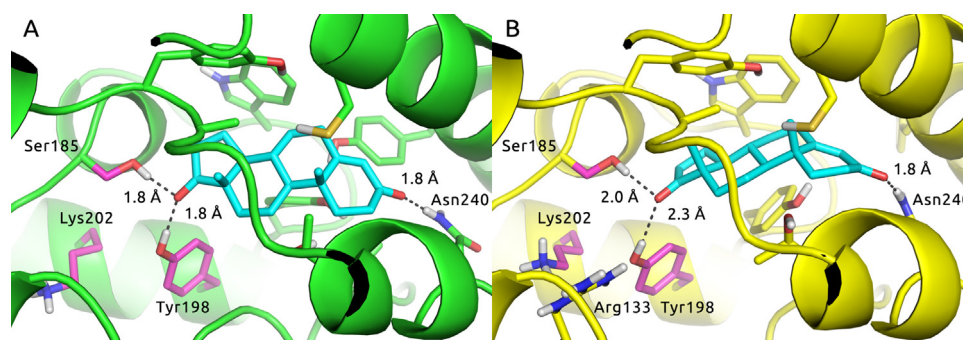
17β-HSD3 deficiency is a rare autosomal recessive disease, which is prevalent in the adolescent and adult 46, XY DSD population [3]. It is frequently unnoticed at birth and misdiagnosed during childhood and puberty, unless there is a complete hormonal profile including an hCG stimulation test. For our patients, the hypothesis of 17β-HSD3 deficiency was made on the basis of the family history of P1 and the observed signs of virilization at puberty age for P2 and P3. Initially, exon 9 of the *HSD17B3* gene was sequenced, revealing the previously described substitution C>A at cDNA position 618, which leads to the substitution of a cysteine by a premature stop codon (C206X) [29]. Then, further mutational analysis of the remaining exons and their flanking intron regions revealed a novel heterozygous mutation G>A at cDNA position 397 in exon 5, causing the mutation G133R.

To date, approximately 40 different mutations have been identified in the *HSD17B3* gene; most of them are homozygous mutations (<http://hgmd.cf.ac.uk>; [11]). Massanyi et al. reported a case of compound heterozygous mutations of the *HSD17B3* gene with a mutation corresponding to the cDNA position 277+4, A>T causing a splicing defect and skipping of exons 4–9 on one allele, and a 25.4 kb amplification of a region containing exon 3 to exon 10 on the second allele [35]. Another case of compound heterozygous mutations, i.e., cDNA position 277+2, T>G and 277+4, A>T, both located within the intron 3 splice donor site of



**Fig. 6.** Impaired cofactor binding of mutant G133.

(A) Homology model of wild-type 17β-HSD3 (green) with bound NADP<sup>+</sup> (cyan) and the catalytic triad (magenta). (B) Superimposed wild-type 17β-HSD3 (green) and mutant G133R (yellow) homology models; the side-chain of R133 protrudes into the cofactor binding pocket and causes steric hindrance. One conformation of many possible rotational isomers is shown. (For interpretation of the references to color in this figure legend, the reader is referred to the web version of this article.)



**Fig. 7.** Binding of androstenedione in mutant G133.

(A) Androstenedione (cyan) docked to the homology model of wild-type 17 $\beta$ -HSD3 (green), and (B) docked to the homology model of mutant G133R (yellow). The catalytic triad is highlighted in magenta; hydrogen bonds are shown by dashed lines (gray). (For interpretation of the references to color in this figure legend, the reader is referred to the web version of this article.)

the *HSD17B3* gene, was described by Castro et al. [11]. In the present work, we report the first case of compound heterozygous point mutations consisting of the known nonsense mutation C206X and the novel missense mutation G133R in *HSD17B3* gene responsible for 17 $\beta$ -HSD3 deficiency.

The prevalence of 17 $\beta$ -HSD3 deficiency is especially high in the Arab population, ranging from 1:100 to 1:300, due to a high frequency of consanguineous marriages [11]. So far, four Tunisian patients with 17 $\beta$ -HSD3 deficiency have been described [29]. However, the rate of this etiology is expected to be high in Tunisia because of many facts. First, we currently have many other cases with suspected 17 $\beta$ -HSD3 deficiency under investigation. Second, a high consanguinity rate is observed in Tunisia, which raises the frequency of homozygous mutations and, therefore, affected patients. Finally, the cultural habits and taboos often prevent families from exchanging information about sexual disorders among their children and reporting them to their physicians [29]. Thus, the number of affected patients may be underestimated because some of them are not brought to medical attention.

Expression analyses of G133R and the additional substitutions indicated that the mutant enzymes were expressed at levels comparable to that of wild-type 17 $\beta$ -HSD3. There were no signs of dislocation or degradation. Enzymatic analyses revealed almost completely abolished activity of mutants G133R, G133Q and G133F, whereas mutant G133A retained comparable activity to wild-type 17 $\beta$ -HSD3. Expression levels of mutant C206X were moderate, with signs of aggregation, and this mutant enzyme was devoid of activity.

These results suggest that the 17 $\beta$ -HSD3 deficiency causing 46, XYDSD in the three Tunisian patients is caused by the inactivity of the truncation mutation C206X from one allele and the loss of activity due to steric hindrance of NADPH binding by the bulky arginine residue of the G133R mutation from the other allele. Regarding the G133R mutant, the positive charge of the arginine side-chain seems not to be responsible for the enzyme inactivation, since amino acids with uncharged, similarly bulky side-chains such as glutamine and phenylalanine equally abolished enzyme activity, predicted by molecular modeling to be due to interference with NADPH binding. However, wild-type 17 $\beta$ -HSD3 and mutant G133A, containing the two smallest amino acids glycine and alanine, showed similar ability to form testosterone, indicating proper NADPH binding.

Mutations within the highly conserved residues from V127 to G133 are likely to affect 17 $\beta$ -HSD3 activity. The importance of these residues is emphasized by the finding of Moghrabi et al. who showed that the mutation N130S led to an abolished activity of 17 $\beta$ -HSD3, resulting in 46, XY DSD [36]. Due to the high level of conservation of G133 and the motif containing residues V127 to G133, mutations in other SDR enzymes can be expected to affect their enzyme activity by interfering with cofactor binding.

Docking studies using the homology models showed similar poses for both wild-type 17 $\beta$ -HSD3 and mutant G133R, suggesting a binding mode where the 3-position of androstenedione forms a hydrogen bond with N240. This interesting finding clearly needs further experimental investigation. Furthermore, overlapping of the 17 $\beta$ -HSD3 homology models with crystal structures of 17 $\beta$ -HSD1 revealed that the G133R mutation had no or only minor effect on the arrangement of the amino acids involved in the catalytic triad (S185, Y198, and K202). Therefore, it seems likely that the abolished activity of the G133R mutant enzyme is caused by a loss of NADPH binding due to steric hindrance.

## 5. Conclusions

Genetic analyses revealed the novel compound heterozygous mutations G133R and C206X, causing 46, XY DSD in three Tunisian patients. The mutation C206X was shown to be completely inactive, and G133R was completely devoid of enzymatic activity despite normal expression levels and intracellular localization. Biochemical analyses and molecular modeling suggest that the loss of activity is due to steric hindrance of NADPH binding by the bulky arginine side-chain of mutant G133R. Furthermore, amino acid sequence alignment revealed that G133 is located in a motif highly conserved among 17 $\beta$ -HSDs and other SDR members, indicating the importance of this residue for the arrangement of the cofactor binding pocket. The screening for the two mutations identified in the present study could help in the rapid diagnosis of 17 $\beta$ -HSD3 deficiency in the Tunisian population. The genetic confirmation of mutations in the *HSD17B3* gene provides crucial information for genetic counseling and prenatal diagnosis.

## Acknowledgments

We thank the patients and their families for their cooperation in this study and for giving informed consent. We thank all the physicians who contributed to the clinical investigation.

This work was supported by the Ministry of Higher Education and Scientific Research in Tunisia and the Swiss National Science Foundation Nos. 31003A\_159454 and 316030\_133859. There is no conflict of interest that could be perceived as prejudicing the impartiality of the research reported.

## Appendix A. Supplementary data

Supplementary data associated with this article can be found, in the online version, at <http://dx.doi.org/10.1016/j.jsbmb.2015.10.023>.



## References

- [1] M.M. George, M.I. New, S. Ten, C. Sultan, A. Bhargoo, The clinical and molecular heterogeneity of 17 $\beta$ -HSD3 enzyme deficiency, *Horm. Res. Paediatr.* 74 (2010) 229–240.
- [2] W.M. Geissler, D.L. Davis, L. Wu, K.D. Bradshaw, S. Patel, B.B. Mendonca, K.O. Elliston, J.D. Wilson, D.W. Russell, S. Andersson, Male pseudohermaphroditism caused by mutations of testicular 17 $\beta$ -hydroxysteroid dehydrogenase 3, *Nat. Genet.* 7 (1994) 34–39.
- [3] N. Phelan, E.L. Williams, S. Cardamone, M. Lee, S.M. Creighton, G. Rumsby, G.S. Conway, Screening for mutations in 17 $\beta$ -hydroxysteroid dehydrogenase and androgen receptor in women presenting with partially virilised 46, XY disorders of sex development, *Eur. J. Endocrinol.* 172 (2015) 745–751.
- [4] V. Luu-The, Analysis and characteristics of multiple types of human 17 $\beta$ -hydroxysteroid dehydrogenase, *J. Steroid Biochem. Mol. Biol.* 76 (2001) 143–151.
- [5] F. Labrie, V. Luu-The, S.X. Lin, J. Simard, C. Labrie, Role of 17 $\beta$ -hydroxysteroid dehydrogenases in sex steroid formation in peripheral intracrine tissues, *Trends Endocrinol. Metab.* 11 (2000) 421–427.
- [6] S. Andersson, N. Moghrabi, Physiology and molecular genetics of 17 $\beta$ -hydroxysteroid dehydrogenases, *Steroids* 62 (1997) 143–147.
- [7] R. Mindnich, G. Moller, J. Adamski, The role of 17 $\beta$ -hydroxysteroid dehydrogenases, *Mol. Cell. Endocrinol.* 218 (2004) 7–20.
- [8] I. Dufort, P. Rheault, X.F. Huang, P. Soucy, V. Luu-The, Characteristics of a highly labile human type 5 17 $\beta$ -hydroxysteroid dehydrogenase, *Endocrinology* 140 (1999) 568–574.
- [9] S.M. MacKenzie, S.S. Huda, N. Sattar, R. Fraser, J.M. Connell, E. Davies, Depot-specific steroidogenic gene transcription in human adipose tissue, *Clin. Endocrinol. (Oxford)* 69 (2008) 848–854.
- [10] S. Andersson, W.M. Geissler, L. Wu, D.L. Davis, M.M. Grumbach, M.I. New, H.P. Schwarz, S.L. Blethen, B.B. Mendonca, W. Bloise, S.F. Witchel, G.B. Cutler Jr., J.E. Griffin, J.D. Wilson, D.W. Russell, Molecular genetics and pathophysiology of 17 $\beta$ -hydroxysteroid dehydrogenase 3 deficiency, *J. Clin. Endocrinol. Metab.* 81 (1996) 130–136.
- [11] C.C. Castro, G. Guaragna-Filho, F.L. Calais, F.B. Coeli, I.R. Leal, E.F. Cavalcante-Junior, I.L. Monlleo, S.R. Pereira, R.B. Silva, J.R. Gabiatti, A.P. Marques-de-Faria, A.T. Maciel-Guerra, M.P. Mello, G. Guerra-Junior, Clinical and molecular spectrum of patients with 17 $\beta$ -hydroxysteroid dehydrogenase type 3 (17 $\beta$ -HSD3) deficiency, *Arq. Bras. Endocrinol. Metab.* 56 (2012) 533–539.
- [12] Q. Han, R.L. Campbell, A. Gangloff, Y.W. Huang, S.X. Lin, Dehydroepiandrosterone and dihydrotestosterone recognition by human estrogenic 17 $\beta$ -hydroxysteroid dehydrogenase. C-18/c-19 steroid discrimination and enzyme-induced strain, *J. Biol. Chem.* 275 (2000) 1105–1111.
- [13] A. Sali, L. Potterton, F. Yuan, H. van Vlijmen, M. Karplus, Evaluation of comparative protein modelling by MODELLER, *Proteins* 23 (1995) 318–326.
- [14] A. Biegert, C. Mayer, M. Remmert, J. Soding, A.N. Lupas, The MPI bioinformatics toolkit for protein sequence analysis, *Nucl. Acids Res.* 34 (2006) W335–W339.
- [15] H.A. Lewin, J.A. Stewart-Haynes, A simple method for DNA extraction from leukocytes for use in PCR, *Biotechniques* 13 (1992) 522–524.
- [16] S. Andersson, D.W. Russell, J.D. Wilson, 17 $\beta$ -Hydroxysteroid dehydrogenase 3 deficiency, *Trends Endocrinol. Metab.* 7 (1996) 121–126.
- [17] B. Legeza, Z. Balazs, L.G. Nashev, A. Odermatt, The microsomal enzyme 17 $\beta$ -hydroxysteroid dehydrogenase 3 faces the cytoplasm and uses NADPH generated by glucose-6-phosphate dehydrogenase, *Endocrinology* 154 (2013) 205–213.
- [18] L.G. Nashev, D. Schuster, C. Laggner, S. Sodha, T. Langer, G. Wolber, A. Odermatt, The UV-filter benzophenone-1 inhibits 17 $\beta$ -hydroxysteroid dehydrogenase type 3: virtual screening as a strategy to identify potential endocrine disrupting chemicals, *Biochem. Pharmacol.* 79 (2010) 1189–1199.
- [19] Maestro, version 10.0, Schrödinger, LLC, New York, NY (2014).
- [20] SiteMap, version 3.3, Schrödinger, LLC, New York, NY (2014).
- [21] R.A. Friesner, R.B. Murphy, M.P. Repasky, L.L. Frye, J.R. Greenwood, T.A. Halgren, P.C. Sanschagrin, D.T. Mainz, Extra precision glide: docking and scoring incorporating a model of hydrophobic enclosure for protein–ligand complexes, *J. Med. Chem.* 49 (2006) 6177–6196.
- [22] T.A. Halgren, R.B. Murphy, R.A. Friesner, H.S. Beard, L.L. Frye, W.T. Pollard, J.L. Banks, Glide: a new approach for rapid, accurate docking and scoring. 2. Enrichment factors in database screening, *J. Med. Chem.* 47 (2004) 1750–1759.
- [23] R.A. Friesner, J.L. Banks, R.B. Murphy, T.A. Halgren, J.J. Klicic, D.T. Mainz, M.P. Repasky, E.H. Knoll, M. Shelley, J.K. Perry, D.E. Shaw, P. Francis, P.S. Shenkin, Glide: a new approach for rapid, accurate docking and scoring. 1. Method and assessment of docking accuracy, *J. Med. Chem.* 47 (2004) 1739–1749.
- [24] Glide, version 6.5, Schrödinger, LLC, New York, NY (2014).
- [25] M.P. Jacobson, R.A. Friesner, Z. Xiang, B. Honig, On the role of the crystal environment in determining protein side-chain conformations, *J. Mol. Biol.* 320 (2002) 597–608.
- [26] M.P. Jacobson, D.L. Pincus, C.S. Rapp, T.J. Day, B. Honig, D.E. Shaw, R.A. Friesner, A hierarchical approach to all-atom protein loop prediction, *Proteins* 55 (2004) 351–367.
- [27] Prime, version 3.8, Schrödinger, LLC, New York, NY (2014).
- [28] The PyMOL Molecular Graphics System, Version 1.6 Schrödinger, LLC.
- [29] B. Ben Rhouma, N. Belguith, M.F. Mniif, T. Kamoun, N. Charfi, M. Kamoun, F. Abdelhedi, M. Hachicha, H. Kamoun, M. Abid, F. Fakhfakh, A novel nonsense mutation in HSD17B3 gene in a Tunisian patient with sexual ambiguity, *J. Sex Med.* 10 (2013) 2586–2589.
- [30] K.I. Varughese, N.H. Xuong, P.M. Kiefer, D.A. Matthews, J.M. Whiteley, Structural and mechanistic characteristics of dihydropteridine reductase: a member of the Tyr-(Xaa) 3-Lys-containing family of reductases and dehydrogenases, *Proc. Natl. Acad. Sci. U. S. A.* 91 (1994) 5582–5586.
- [31] X. Wu, P. Lukacik, K.L. Kavanagh, U. Oppermann, SDR-type human hydroxysteroid dehydrogenases involved in steroid hormone activation, *Mol. Cell. Endocrinol.* 265–266 (2007) 71–76.
- [32] R. Shi, S.X. Lin, Cofactor hydrogen bonding onto the protein main chain is conserved in the short chain dehydrogenase/reductase family and contributes to nicotinamide orientation, *J. Biol. Chem.* 279 (2004) 16778–16785.
- [33] W.L. Duax, J. Thomas, V. Pletnev, A. Addlagatta, R. Huether, L. Habegger, C.M. Weeks, Determining structure and function of steroid dehydrogenase enzymes by sequence analysis, homology modeling, and rational mutational analysis, *Ann. N.Y. Acad. Sci.* 1061 (2005) 135–148.
- [34] K.L. Kavanagh, H. Jornvall, B. Persson, U. Oppermann, Medium- and short-chain dehydrogenase/reductase gene and protein families: the SDR superfamily: functional and structural diversity within a family of metabolic and regulatory enzymes, *Cell Mol. Life Sci.* 65 (2008) 3895–3906.
- [35] E.Z. Massanyi, J.P. Gearhart, L.A. Kolp, C.J. Migeon, Novel mutation among two sisters with 17 $\beta$ -hydroxysteroid dehydrogenase type 3 deficiency, *Urology* 81 (2013) 1069–1071.
- [36] N. Moghrabi, I.A. Hughes, A. Dunaif, S. Andersson, Deleterious missense mutations and silent polymorphism in the human 17 $\beta$ -hydroxysteroid dehydrogenase 3 gene (HSD17B3), *J. Clin. Endocrinol. Metab.* 83 (1998) 2855–2860.

#### 4.3 Paper 6 (Ben Rhouma et al., 2017)

### Novel cases of Tunisian patients with mutations in the gene encoding 17 $\beta$ -hydroxysteroid dehydrogenase type 3 and a founder effect

Bochra Ben Rhouma, Fakhri Kallabi, Nadia Mahfoudh, Afif Ben Mahmoud, Roger T. Engeli,  
Hassen Kamoun, Leila Keskes, Alex Odermatt, Neila Belguith

Published manuscript

**Contribution:** Carefully reviewing the manuscript.

**Aims:** Case report of novel cases of 46, XY DSD in Tunisian patients. Haplotyping was performed to investigate the common p.C206X mutation in the region of Sfax.

**Results:** Haplotyping revealed a founder effect for the p.C206X mutations in Tunisian families. The carrier frequency in the region of Sfax was estimated as 1 in 40.

**Conclusion:** The identified haplotype will contribute to rapid diagnosis of 17 $\beta$ -HSD3 deficiency.



## Review

## Novel cases of Tunisian patients with mutations in the gene encoding 17 $\beta$ -hydroxysteroid dehydrogenase type 3 and a founder effect



Bochra Ben Rhouma<sup>a,\*\*</sup>, Fakhri Kallabi<sup>a</sup>, Nadia Mahfoudh<sup>b</sup>, Afif Ben Mahmoud<sup>a</sup>, Roger T. Engeli<sup>c</sup>, Hassen Kamoun<sup>d</sup>, Leila Keskes<sup>a</sup>, Alex Odermatt<sup>c,\*</sup>, Neila Belguith<sup>a,d</sup>

<sup>a</sup> Human Molecular Genetic Laboratory, Faculty of Medicine of Sfax, 3030, University of Sfax, Tunisia

<sup>b</sup> Department of Immunology, Hedi Chaker Hospital, 3029 Sfax, Tunisia

<sup>c</sup> Division of Molecular and Systems Toxicology, Department of Pharmaceutical Sciences, Pharmacenter, University of Basel, Basel, Switzerland

<sup>d</sup> Department of Medical Genetics, Hedi Chaker Hospital, 3029 Sfax, Tunisia

## ARTICLE INFO

## Article history:

Received 8 December 2015

Received in revised form 13 February 2016

Accepted 3 March 2016

Available online 5 March 2016

## Keywords:

46, XY disorders of sex development

17 $\beta$ -hydroxysteroid dehydrogenase

Mutation

HSD17B3

Founder effect

Male sexual development

## ABSTRACT

17 $\beta$ -Hydroxysteroid dehydrogenase type 3 (17 $\beta$ -HSD3) is expressed almost exclusively in the testis and converts  $\Delta$ 4-androstene-3,17-dione to testosterone. Mutations in the *HSD17B3* gene causing 17 $\beta$ -HSD3 deficiency are responsible for a rare recessive form of 46, XY Disorders of Sex Development (46, XY DSD). We report novel cases of Tunisian patients with 17 $\beta$ -HSD3 deficiency due to previously reported mutations, *i.e.* p.C206X and p.G133R, as well as a case with the novel compound heterozygous mutations p.C206X and p.Q176P. Moreover, the previously reported polymorphism p.G289S was identified in a heterozygous state in combination with a novel non-coding variant c.54G > T, also in a heterozygous state, in a male patient presenting with micropenis and low testosterone levels. The identification of four different mutations in a cohort of eight patients confirms the generally observed genetic heterogeneity of 17 $\beta$ -HSD3 deficiency. Nevertheless, analysis of DNA from 272 randomly selected healthy controls from the same geographic area (region of Sfax) revealed a high carrier frequency for the p.C206X mutation of approximately 1 in 40. Genotype reconstruction of the affected pedigree members revealed that all p.C206X mutation carriers harbored the same haplotype, indicating inheritance of the mutation from a common ancestor. Thus, the identification of a founder effect and the elevated carrier frequency of the p.C206X mutation emphasize the importance to consider this mutation in the diagnosis and genetic counseling of affected 17 $\beta$ -HSD3 deficiency pedigrees in Tunisia.

© 2016 Elsevier Ltd. All rights reserved.

## Contents

1. Introduction	87
2. Subjects and methods	87
2.1. Subjects	87
2.2. Controls	87
2.3. Methods	87
2.3.1. Analysis of <i>HSD17B3</i> mutations	87
2.3.2. Computational analyses	87
2.3.3. SNP typing and microsatellite analysis	87
3. Results	88
3.1. Clinical investigation of the patients	88
3.2. Mutational analysis of the <i>HSD17B3</i> gene and identification of three different mutations, a polymorphism and a novel silent variant	88
3.3. Haplotype reconstruction and c.618C> frequency calculation	91

\* Corresponding author.

\*\* Corresponding author.

E-mail addresses: [bochra.benrhouma@gmail.com](mailto:bochra.benrhouma@gmail.com) (B. Ben Rhouma), [alex.odermatt@unibas.ch](mailto:alex.odermatt@unibas.ch) (A. Odermatt).

<http://dx.doi.org/10.1016/j.jsbmb.2016.03.007>

0960-0760/© 2016 Elsevier Ltd. All rights reserved.

4. Discussion .....	91
5. Conclusion .....	93
Conflict of interest .....	93
Acknowledgments .....	93
References .....	94

## 1. Introduction

46, XY Disorders of Sex Development (46, XY DSD) is defined by the presence of female or incompletely virilized external genitalia in a 46, XY individual. 46, XY DSD can be classified in three main groups: (1) gonad development disorders (ovotesticular DSD and gonadal dysgenesis), (2) testosterone synthesis disorders (e.g. CYP11A1 deficiency, 3 $\beta$ -hydroxysteroid dehydrogenase type 2 (3 $\beta$ -HSD2) deficiency, 17 $\beta$ -hydroxysteroid dehydrogenase type 3 (17 $\beta$ -HSD3) deficiency, defects in luteinizing hormone receptor (LHR loss-of-function), and (3) disorders of testosterone action (Androgen Insensitivity Syndromes AIS) or metabolism (5 $\alpha$ -reductase type 2 deficiency) [1].

17 $\beta$ -HSD3 deficiency (OMIM: 264300) is a rare autosomal recessive cause of 46, XY DSD described in 1971 and resulting from loss-of-function mutations in 17 $\beta$ -HSD3 [2–4]. The enzymatic defect results in decreased conversion of  $\Delta$ 4-androstene-3,17-dione (androstenedione) to testosterone in the testes (testosterone/androstenedione ratio <0.8), and, as a consequence, diminished testosterone secretion and abnormal male sexual development [2].

The characteristic phenotype of 17 $\beta$ -HSD3 deficiency at birth is an XY individual with undervirilization of the external genitalia, which often appear female with or without clitoromegaly and/or labial fusion and a blind-ending vagina [2]. Less often, ambiguous external genitalia, male genitalia with micropenis or hypospadias are reported [2]. Affected patients have testes and often show normal Wolffian duct derivatives [2].

17 $\beta$ -HSD3 is composed of 310 amino acids, uses NADPH as cofactor and is expressed predominantly in the testes. It is encoded by the *HSD17B3* gene, mapped to 9q22 and composed of 11 exons. To date, about 40 mutations have been reported in the *HSD17B3* gene; comprising homozygous or compound heterozygous mutations, including intronic splice site mutations, exonic deletions, duplications of exons, as well as missense and nonsense mutations [5,6].

In an earlier report, we described a novel homozygous nonsense mutation, p.C206X, in a Tunisian patient with sexual ambiguity [7]. Later, we reported on another three Tunisian cases with 17 $\beta$ -HSD3 deficiency due to compound heterozygous mutations in the *HSD17B3* gene [8]. Here, we present additional cases of Tunisian patients with 17 $\beta$ -HSD3 deficiency. We performed mutational analyses and investigated the frequency of one of the newly identified mutations as well as the presence of a possible founder effect.

## 2. Subjects and methods

### 2.1. Subjects

Seven patients admitted to the Hedi Chaker hospital in Sfax, Tunisia, and belonging to five unrelated Tunisian families, were investigated. Patients P1 and P3 consulted for sexual ambiguity, patient P4 presented with inguinal hernia, and patients P2, P5, P6 and P7 were referred to the hospital due to primary amenorrhea and hirsutism. Since birth, all patients have been raised as girls; pelvic exams for all patients showed bilateral inguinal masses consistent with testes. The magnetic resonance imaging of the

pelvis and the abdomen showed no visualization of the vagina or uterus. The karyotype was determined by standard G banding technique and showed a 46, XY formula for all patients. The corresponding data from the clinical assessment are presented in Table 1. The parents of patients P1 and P4, the mother of P3 and the brother of P1 were also recruited.

In addition, patient P8, a boy, consulted at age 11 for micropenis in the Pediatrics Department of the Hedi Chaker Hospital in Sfax, Tunisia. As his hormonal profile indicated abnormal testosterone biosynthesis (Table 1), this patient was further investigated for 17 $\beta$ -HSD3 deficiency. Informed consent was obtained from all patients and their relatives in accordance with the ethics committee of the Hedi Chaker Hospital (Sfax, Tunisia).

### 2.2. Controls

Peripheral blood samples of 272 unrelated controls were collected. They originated from the same geographic region as the patients, their parents and grandparents (region of Sfax). Importantly, these control individuals did not have any personal or family history of 46, XY DSD.

### 2.3. Methods

#### 2.3.1. Analysis of HSD17B3 mutations

Genomic DNA was extracted from peripheral blood leukocytes following a phenol–chloroform-based method described earlier [9]. The coding regions and intron–exon boundaries of the *HSD17B3* gene were amplified by PCR (oligonucleotide primer sequences available upon request). The PCR was performed in a thermal cycler (GenAmp PCR System 9700; Applied Biosystem) in a final volume of 50  $\mu$ l containing 50 ng genomic DNA, 0.2  $\mu$ M of each primer, 1  $\times$  PCR buffer, 1.2 mM MgCl<sub>2</sub>, 0.5 mM dNTP, and 1U Taq DNA polymerase (Promega). Direct sequencing of PCR products was performed using the ABI Prism BigDye Terminator Cycle Sequencing Ready Reaction Kit (ABI PRISM/Biosystems) and the products were resolved on an ABI PRISM instrument. The mutation c.618C>A responsible for the premature stop p.C206X was found to abolish an *Hha*I endonuclease restriction site (using <http://nc2.neb.com/NEBcutter2/program>) and this characteristic was used to verify the presence or absence of this mutation via Polymerase Chain Reaction Restriction Fragment Length Polymorphism (PCR-RFLP) in the patients and in controls. The amplified exon 9 DNA product was digested by *Hha*I for 4 h at 37 °C, followed by separation of the fragments on a 3% agarose gel.

#### 2.3.2. Computational analyses

To analyze the effects of the c.54G>T variant on the splicing event, we used HSF software (<http://www.umd.be/HSF3/HSF.html>) and the ESE finder 3.0 software ([http://rulai.cshl.edu/cgi-bin/tools/ESE3/ese\\_finder.cgi?process=home](http://rulai.cshl.edu/cgi-bin/tools/ESE3/ese_finder.cgi?process=home)). The effect of the c.54G>T mutation on mRNA secondary structure was also performed by using the MFOLD program (available at <http://unafold.rna.albany.edu/?q=mfold>).

#### 2.3.3. SNP typing and microsatellite analysis

To test for a possible founder effect, we analyzed one Single Nucleotide Polymorphism (SNP) localized in intron 5 (rs408876,

**Table 1**  
Clinical investigation of patients.

	P1	P2	P3	P4	P5	P6	P7	P8
Age	2 years	27 years	7 days	7 years	14 years	15 years	14 years	11 years
Height (cm)	-	-	-	155	-	-	148	155
Weight (kg)	11	-	-	45	-	-	-	-
Tanner stage	P1B1	P5 S4	-	P1B1	P4B1	P5B1	P4B1	-
Testosterone (ng/mL)	0.9	-	0.15	0.8	3	4	3	-
hCG stimulation	T1: 0.09 T2: 0.22 A1: 0.12 ng/ml A2: 1.33 ng/ml T2/A2 = 0.165 < 0.8	-	T1: 0.04 T2: 0.44 A1: 0.2 ng/ml A2: 2.5 ng/ml T2/A2 = 0.176 < 0.8	-	-	-	-	T1: 0.10 T2: 1.7
LH (IU/L)	8.5	18.9	0.1	12.5	-	-	5.7	2.3
FSH (IU/L)	0.98	28.9	0.58	4.7	40	42	8.2	0.2
Referral reason	Sexual ambiguity; Prader IV	Primary amenorrhea and hirsutism	Discordance between 46, XY karyotype and female phenotype	Inguinal hernia	Primary amenorrhea and hirsutism	Primary amenorrhea and hirsutism	Primary amenorrhea and hirsutism	Micropenis

Reference values: Luteinizing hormone (LH): 1.24–8.62 mIU/mL; follicle stimulating hormone (FSH): 1.27–19.26 mIU/mL; testosterone: 1.75–7.61 ng/mL. hCG: human Chorionic Gonadotropin. T1: testosterone level before hCG stimulation; T2: testosterone level after hCG stimulation; A1:  $\Delta 4$ -androstene-3,17-dione before hCG stimulation; A2:  $\Delta 4$ -androstene-3,17-dione after hCG stimulation. hCG stimulation consists of an intramuscular injection of 1500 IU of hCG daily for 3 consecutive days.

c.453 + 37T > C) of the *HSD17B3* gene and the three polymorphic microsatellite markers D9S287, D9S1690 and D9S1786 consisting of tandemly repeated dinucleotide (CA) sequences. The SNP rs408876 was chosen based on available sequencing data, suggesting an association with the mutation c.618C > A. Two extragenic microsatellite markers, D9S287 and D9S1690, were selected from the panel ABI PRISM® Linkage Mapping Set version 2.5, Applied Biosystems. D9S287 and D9S1690 are located at 540,434 bp proximal and 5,093,506 bp distal from the c.618C > A mutation, respectively. The polymorphic intragenic marker D9S1786 in intron 2 was also chosen (the probes were determined according to information from the web site <http://www.ncbi.nlm.nih.gov/probe/?term=D9S1786/>). It is located at 33,364 bp from the mutation in exon 9 (Fig. 1). PCR for the microsatellite markers was performed using a fluorescence-labeled forward primer and an unlabeled reverse primer, in a 25  $\mu$ l reaction mixture containing 20 ng of genomic DNA, 1 Unit of Taq polymerase (Gotaq, Promega), 2.5 mM of MgCl<sub>2</sub>, 5  $\mu$ M of each primer, and 10 mM of dNTP. After 7 min at 95 °C, 40 cycles of amplification (95 °C for 30 s; 55 °C for 30 s; 72 °C for 40 s) were performed, followed by 5 min in at 72 °C. Then, the fluorescence-labeled alleles were analyzed on an ABI PRISM 3100-Avant automated Genetic Analyzer (Applied Biosystems). The genotypes were determined using the GenScan software (Applied Biosystems). Alleles were named using an arbitrary scale for the observed fragment length of the microsatellites. A haplotype co-segregating with the disease was derived from the segregation of the SNP and markers within the whole pedigree; in fact, the profiles of markers as well as the SNP haplotype were compared among the affected members of the six families.

### 3. Results

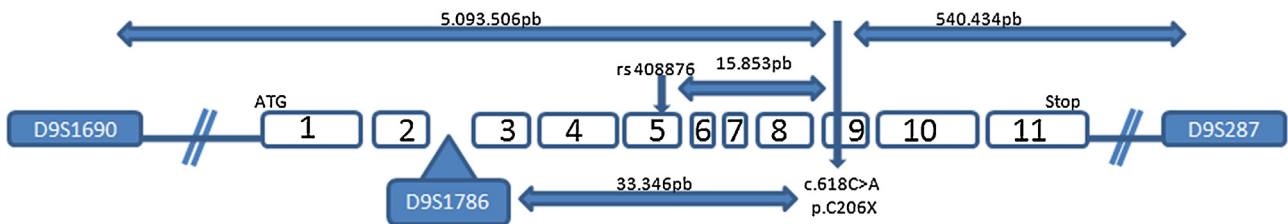
#### 3.1. Clinical investigation of the patients

17 $\beta$ -HSD3 deficiency was suspected in eight Tunisian patients of different age and that were admitted to the hospital for different reasons (Table 1). In case of P1, the hypothesis of 17 $\beta$ -HSD3 deficiency was made based on the hormonal profile revealing a testosterone/androstenedione ratio < 0.8. For patient P4, 17 $\beta$ -HSD3 deficiency was suspected due to the family history, which reported P1 as a paternal cousin. Patients P2, P5, P6 and P7 were investigated because they consulted for primary amenorrhea and hirsutism. The patient P8 presented with a male phenotype but a micropenis and a low testosterone level following hCG test, indicating abnormal steroidogenesis. The remaining patient P3 was diagnosed to be 46, XY DSD during the prenatal stage. Due to the advanced maternal age (42 years), the fetal karyotype was determined and a 46, XY formula in discordance with the female fetal phenotype was observed. Then, in the postnatal stage, the patient's hormonal profile indicated 17 $\beta$ -HSD3 deficiency.

#### 3.2. Mutational analysis of the *HSD17B3* gene and identification of three different mutations, a polymorphism and a novel silent variant

The genomic DNA of all patients was analyzed for the p.C206X mutation by PCR-RFLP using the *HhaI* restriction enzyme (data not shown), followed by sequencing of all exons and intron-exon boundaries of the *HSD17B3* gene. The mutational analysis revealed the presence of the previously described mutation c.618C > A in patients P1, P2 and P3, and in a heterozygous state in the patients P4-P7 (for representative sequences see Fig. 2A). The results of the sequencing were in accordance with those of the PCR-RFLP assay





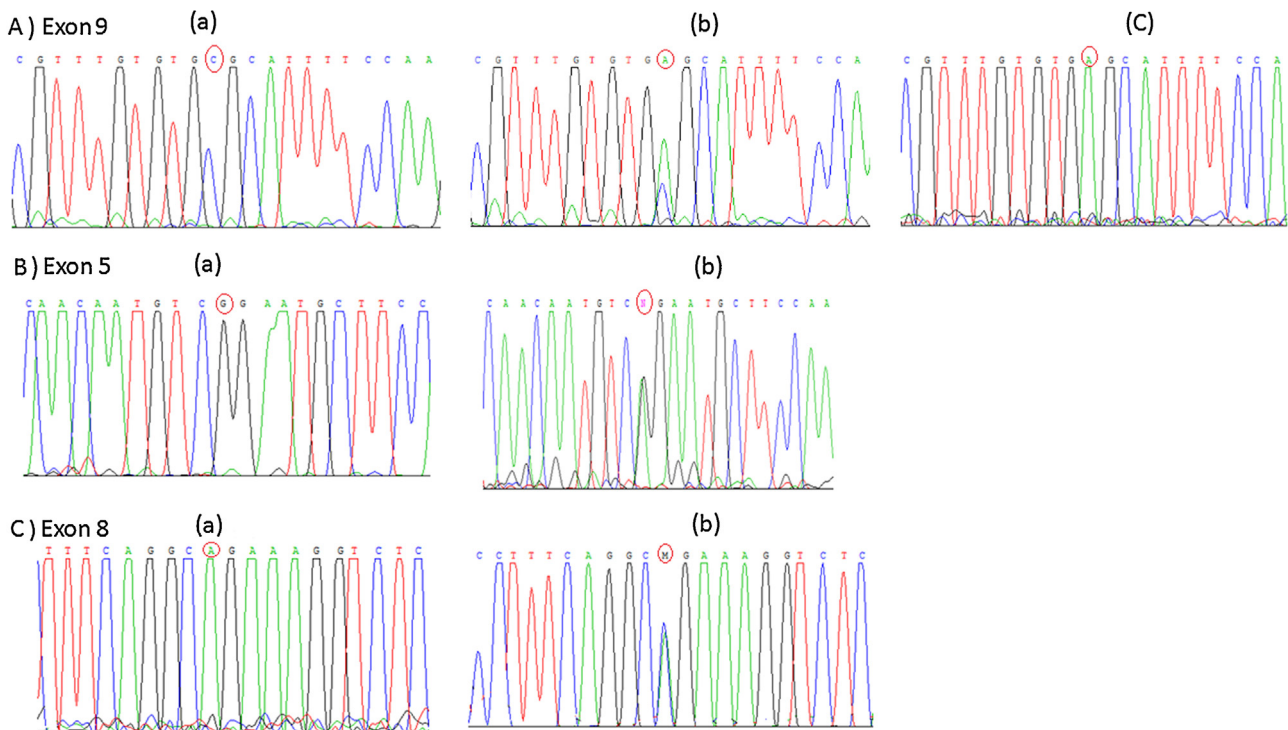
**Fig. 1.** Schematic representation of the *HSD17B3* gene. The scheme shows the intragenic SNP rs408876 in intron 5, the two extragenic microsatellite markers D9S1690 and D9S287 and the intragenic microsatellite marker D9S1786 used for haplotype analysis and their positions relative to the mutation c.618C>A.

(data not shown). The mutation c.618C>A is responsible for the generation of a premature stop codon in position 206 (p.C206X). The three patients P4, P5 and P6, presenting the mutation p.C206X in a heterozygous state, were investigated for additional mutations in the remaining 10 exons of the *HSD17B3* gene and their flanking regions. The analysis revealed a heterozygous nucleotide change in exon 5, i.e. the substitution of guanine to adenine at position 397 of the coding sequence (c.397G>A) (for representative sequences see Fig. 2B). The mutation c.397G>A results in the substitution of glycine by arginine in position 133 (p.G133R). The presence of the compound heterozygous mutations p.C206X and p.G133R explains the 17 $\beta$ -HSD3 deficiency in patients P4, P5 and P6, as reported recently [8].

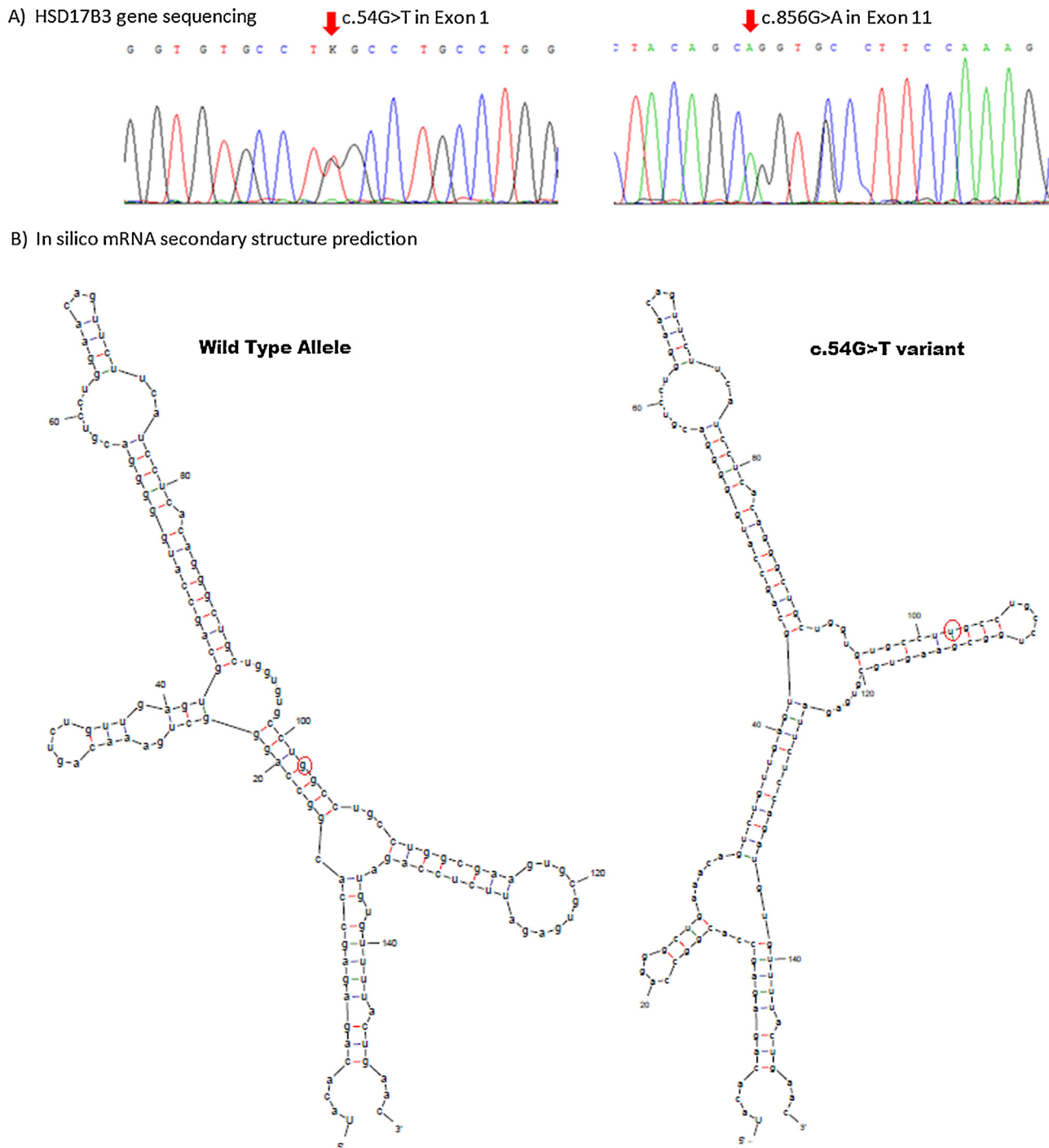
Upon sequencing the remaining exons of the *HSD17B3* gene of patient P7, the mutation c.527A>C was identified in a heterozygous state (Fig. 2C). This substitution results in the mutation p.Q176P, which was previously described by Andersson et al. to cause loss-of-function [10]. Thus, the compound heterozygous mutations

p.C206X and p.Q176P, reported here for the first time, explain the 17 $\beta$ -HSD3 deficiency in P7.

The sequencing of the *HSD17B3* gene of patient P8 revealed the previously described substitution c.856G>A resulting in the missense p.G289S in a heterozygous state (rs2066479) (Fig. 3A) [11]. In addition, sequencing of exon 1 revealed a novel substitution, i.e. c.54G>T in a heterozygous state (Fig. 3A). This substitution does not alter the leucine residue at position 18. To test whether the SNP c.54G>T might affect the splicing efficiency of the *HSD17B3* gene, we performed a more detailed analysis. The bioinformatics analysis of its neighboring region in exon 1 using ESEfinder predicted a strong recognition site for the splicing enhancer protein SRp40 for the G allele, while the T allele completely lacks any sites at this position. The abolition of the SRp40 binding site (the affinity score of the wild-type sequence is over 2.86, compared to the SRp40 binding threshold of 2.67) located further inside the exon might alter the normal assembly of the splicing factors on pre-mRNA. These results were confirmed by



**Fig. 2.** Mutational analysis of the *HSD17B3* gene in patients P1–P7. Identification of three different mutations in the *HSD17B3* gene in exon 9 (A), exon 5 (B) and exon 8 (C). Genomic DNA sequence of the *HSD17B3* gene from healthy control individuals (exon 9: A-a; exon 5: B-a and exon 8: C-a). Chromatograms showing an individual bearing the c.618C>A mutation in a heterozygous state (A-b) and in a homozygous state (A-c), respectively; an affected individual bearing the c.397G>A mutation in a heterozygous state (B-b); and finally an affected individual with the pathogenic variant c.527A>C in a heterozygous state in the *HSD17B3* gene (C-b).



**Fig. 3.** Mutational and computational analyses for the variant found in patient P8. (A) Identification of the novel synonymous variant c.54G>T in exon 1 and the c.856G>A polymorphism in exon 11 in heterozygous states. (B) Computational analyses using the Mfold program showed a modified mRNA secondary structure due to the c.54G>T variant. (a) The normal sequence contained an external closing pair between G102 and C19. (b) The c54U variant (U102) forms an external closing pair with G114.

the HSD software, which predicted a disruption of the SRp40 site in the C allele. The results of the MFOLD program showed several changes in the RNA secondary structure (Fig. 3B). In fact, the commonly conserved structure is formed by the external closing G43 and C91 with a hairpin loop between A56 and U77. The

remaining secondary structure was altered by the c.54G>T substitution. For example, in the wild-type prediction, G102 and C19 form an external closing; however, the substitution to U102 results in the formation of an external closing with G114 (Fig. 3B).



### 3.3. Haplotype reconstruction and c.618C>A frequency calculation

Because the c.618C>A mutation was detected in all patients belonging to the five unrelated families from the same geographic area in Tunisia, this could be due to a founder effect. A founder effect is expected to result in sharing of allelic sequence polymorphisms in the vicinity of the mutation or close to the gene (linkage disequilibrium due to a common ancestor). To test the presence of a founder effect, the three microsatellite markers D9S1786, D9S287 and D9S1690 together with the SNP rs408876 were analyzed (Fig. 1). The haplotype analysis was performed in the seven patients and in all available relatives. Both markers D9S287 and D9S1786 were analyzed, showing that alleles of 302 bp and 204 bp repeat length, respectively, were shared in a homozygous state by the three patients harboring the homozygote c.618C>A mutation and in a heterozygous state for patients P4–P7, as well as P1's parents, P1's brother, P2's father, and P3's mother (the genotypes obtained are shown in Fig. 4). To further strengthen this association, we analyzed SNP rs408876, revealing a common haplotype in all patients. As the patients' genotypes showed a segregation of a haplotype composed of the 301 bp repeat length allele, the 203 bp repeat length allele and the SNP rs408876 (c.453+37C) with the c.618C>A mutation (Fig. 4), we concluded that the c.618C>A mutation is not the result of separate mutations occurring independently in different individuals, but is due to a mutation occurring in a common ancestor of the autosomal recessive 17 $\beta$ -HSD3 deficiency patients in Tunisia that were identified so far.

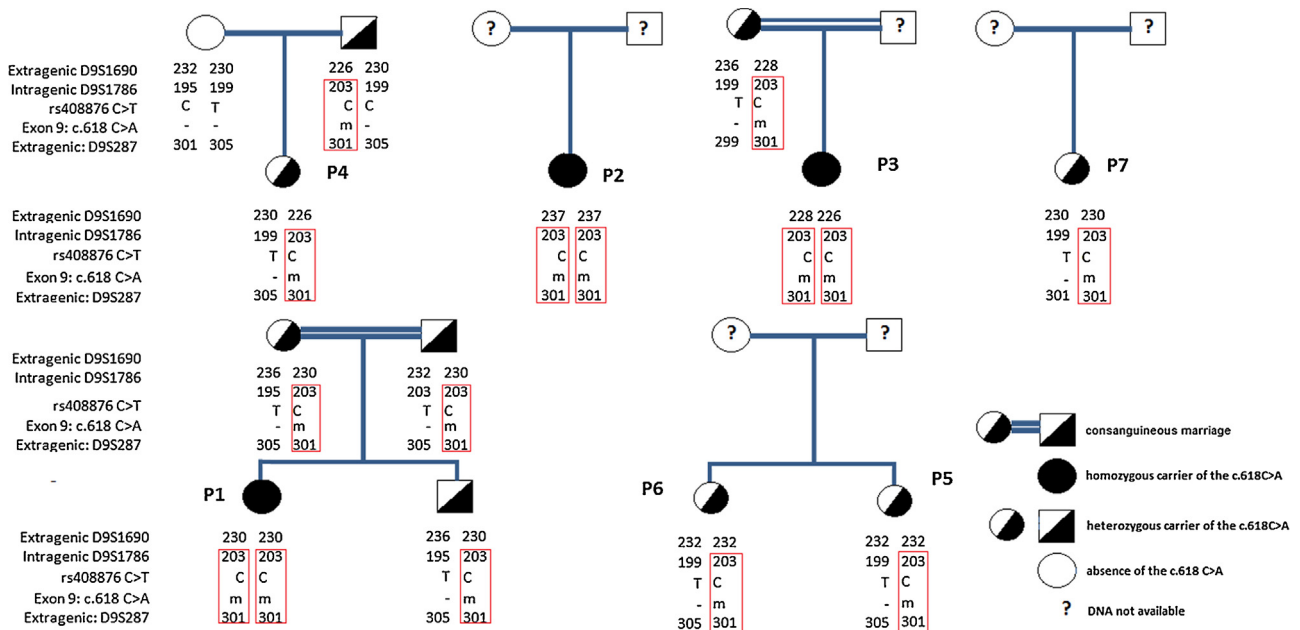
To identify the prevalence of mutation carriers in a random sample of people from the same geographic community, genomic DNA from 272 healthy individuals were screened for the c.618C>A mutation by PCR-RFLP. Fourteen individuals (5%) carrying the c.618C>A (p.C206X) mutation in a heterozygous state were

identified. Based on these observations, the p.C206X carrier frequency can be estimated approximately as 1/40 in the region of Sfax.

### 4. Discussion

Mutations in the *HSD17B3* gene that lead to abolished conversion of androstenedione to testosterone in the testes result in 46, XY DSD. This etiology of 46, XY DSD is frequently unnoticed at birth and misdiagnosed during the pediatric consultation [2]. In fact, 46, XY DSD patients with 17 $\beta$ -HSD3 deficiency may be overlooked since external genitalia observed at birth often appear female [2]. In prepubertal patients, 17 $\beta$ -HSD3 deficiency is clinically indistinguishable from other 46, XY DSD etiologies including AIS, 5 $\alpha$ -reductase type 2 deficiency, and testosterone biosynthesis disorders such as LHR defects [2]. The common clinical features of these etiologies in childhood are varying degrees of virilisation, inguinal hernia consisting of testes, and, less often, ambiguous external genitalia and male genitalia with a micropenis or hypospadias [2]. During puberty, 17 $\beta$ -HSD3 deficiency is indistinguishable from 5 $\alpha$ -reductase type 2 deficiency as virilisation is commonly observed [12]. The excessive virilisation at puberty is thought to occur by an extratesticular conversion of androstenedione to testosterone or a residual function of the mutated 17 $\beta$ -HSD3 enzyme [2,12].

17 $\beta$ -HSD3 deficiency can be diagnosed by the presence of characteristically decreased testosterone but increased androstenedione levels [2,15]. At different age, the basal concentrations of testosterone and androstenedione can vary considerably; however, in adults at baseline a testosterone/androstenedione ratio <0.8 was found to be characteristic for 17 $\beta$ -HSD3 deficiency [2]. In infants younger than six month the testosterone/androstenedione ratio <0.8 is a reliable diagnostic marker (sensitivity



**Fig. 4.** Pedigrees of the six Tunisian families showing the inheritance of the c.618C>A mutation. Haplotype analysis showed a common haplotype indicated by the framed red boxes in the seven affected individuals and the available relatives. All patients shared the same founder allele: 301 bp repeat length for marker D9S287, 203 bp repeat length for D9S1786 transmitted with the c.618C>A mutation. (m) indicates mutated allele and (–) indicates wild-type allele. (For interpretation of the references to colour in this figure legend, the reader is referred to the web version of this article.)

100%), whereas in prepubertal children a hCG stimulation test was found to increase the sensitivity from about 60% to 90% when a cutoff of  $<0.8$  is applied. Because a testosterone/androstenedione ratio  $<0.8$  might also be observed in conditions with abnormal testes, confirmation of 17 $\beta$ -HSD3 deficiency by molecular genetics analysis is necessary.

17 $\beta$ -HSD3 deficiency is considered as a rare autosomal recessive cause of 46, XY DSD [2,3,7]. In fact, a study on DSD over a 25-year period in the United States did not identify a single patient with 17 $\beta$ -HSD3 deficiency [13]. Moreover, in the United Kingdom DSD database, patients diagnosed with 17 $\beta$ -HSD3 deficiency represent only 4% of the total 46, XY DSD subjects (13/322) [14]. So far, only about 40 different mutations have been identified in the *HSD17B3* gene [5,6]. However, the incidence of 17 $\beta$ -HSD3 deficiency is likely to be underestimated because of misdiagnosis as AIS or 5 $\alpha$ -reductase type 2 deficiency. Indeed, the rate of 17 $\beta$ -HSD3 deficiency misdiagnosis was estimated earlier to be 67% [15]. The recent identification of a first Tunisian case with 17 $\beta$ -HSD3 deficiency led to an improved diagnosis and confirmation of 17 $\beta$ -HSD3 deficiency in patients who were initially misdiagnosed with LHR defect (P4) and 5 $\alpha$ -reductase type 2 deficiency (P2, P5, P6 and P7) [7,8].

The mutational analysis of *HSD17B3* of the eight Tunisian patients revealed four different mutations, i.e. the homozygous mutation p.C206X, the two compound heterozygous mutations p.C206X/p.G133R and p.C206X/p.Q176P, as well as the compound heterozygous variants p.G289S and c.54G>T. Patients P1, P2 and P3 were born from consanguineous parents and are homozygous for the mutation p.C206X. Patients P4–P7, deriving from non-consanguineous families, showed the two remaining compound heterozygous mutations [8]. The truncated p.C206X mutant enzyme lacks half of the substrate binding region and was poorly expressed and inactive [8]. Mutant p.G133R was shown to be almost completely devoid of enzymatic activity despite normal expression levels and intracellular localization [8]. Biochemical analyses and molecular modeling suggested that the loss of activity is due to steric hindrance of NADPH binding by the bulky arginine side-chain of mutant G133R. The p.Q176P variant has been shown by Andersson et al. to exhibit very low activity in transfected intact cells and no activity in cell lysates [12]. The authors hypothesized that the substitution of glutamine by proline may result in an unstable and/or incorrectly folded protein, as proline residues can cause bends in  $\alpha$ -helices of protein structures due to the inability to form hydrogen bonds with the main chain nitrogen [11]. Thus, the three mutations p.C206X, p.G133R and p.Q176P abolish the enzymatic activity, explaining the 17 $\beta$ -HSD3 deficiency in the seven Tunisian patients.

Recurrence of several mutations in multiple patients offered the opportunity for genotype/phenotype comparison. The patients homozygous for the mutation p.C206X, i.e. P1, P2 and P3, consulted for primary amenorrhea or sexual ambiguity. Thus, distinct phenotypic variation occurs for patients homozygous for this mutation. In addition, phenotypic variation in patients of compound heterozygous mutations was observed, as the two sisters P5 and P6 were thought to be normal girls during childhood, while the unrelated patient P4 carrying the same mutations consulted for inguinal hernia at age of 7. Our observation of a lack of phenotype to genotype correlation in patients with 17 $\beta$ -HSD3 deficiency is in accordance with other reports [2,3,13,14]. The phenotypic differences may be a result of the ability of some subjects to form active androgens in peripheral tissues or even in the testes by another 17 $\beta$ -HSD isoenzyme, i.e. 17 $\beta$ -HSD5 (also known as AKR1C3) [2,5,16,17].

We were the first to confirm the diagnosis of 17 $\beta$ -HSD3 deficiency in Tunisia [7,8]. The homozygous mutation p.C206X and the compound heterozygous mutations p.C206X/p.G133R and

p.C206X/p.Q176P, as well as the compound heterozygous variants G289S and c.54G>T, have, so far, only been found in the Tunisian population. The Tunisian population belongs to the Arabian population. According to the literature, p.R80Q is the most common mutation in the Mediterranean and in the Arabian population [14,15]. It was first identified in a Palestinian family from the Gaza Strip [15], then found in different regions of Israel, Lebanon, and Syria [17,18]. A second mutation p.Y287X was described in the Sudanese and Turkish population [19,20] and the novel mutation p.W192X in Oman and the Gulf region [3]. These mutations have not been detected in the Tunisian population so far, even in a heterozygous state, but three different novel mutations were found. The possibility that the mutations arising in the Middle East were introduced into the Tunisian population, following Phoenician, Banu Hilal or the Ottoman invasions, cannot not be ruled out and should thus be considered in the genetic assessment.

Patient P8 exhibits a less severe phenotype than the other patients (P1–P7), as he presented a male phenotype with a micropenis. The hormonal profile revealed a testosterone level elevation after a hCG test; however, the level was lower than 3 ng/ml and the clinical evaluation reported no adrenal insufficiency. These findings pointed to normal Leydig cell stimulation in addition to normal adrenal steroidogenesis. Sequencing of the *HSD17B3* gene revealed two substitutions in a heterozygous state. The novel identified substitution in exon 1 is a synonymous variant c.54G>T (Leu18=). According to the literature, silent substitutions could influence the efficiency and precision of splicing by altering the regulatory elements of auxiliary splicing factors [21–23], in fact, several studies have demonstrated that single point mutations in exonic splicing enhancers (ESEs) can contribute to disease development [24–26]. For example, a C/T mutation in an ESE sequence of the human mitochondrial acetoacetyl-CoA thiolase gene results in exon 10 skipping. The protein is no longer functional, causing the mitochondrial acetoacetyl-CoA thiolase (T2) deficiency disorder [25]. Two silent substitutions in the pyruvate dehydrogenase complex (*PDHA1* gene) found in most patients with PDHc deficiency cause exon 5 skipping by disruption of a putative exonic splicing enhancer [24]. Therefore, we evaluated the effect of the c.54G>T variation on the splicing event using HSF software and ESE software and provide evidence for a disruption of a SRp40 site. The SRp40 factor is a member of the arginine and serine rich protein family (SR proteins), which binds to exonic splicing enhancer elements and promotes splicing [27]. A number of other polypeptides including SF2/ASF, Sc35, SRp55 and members of the hnRNP family together with small nuclear RNAs participate in splicing by ensuring the correct recognition of exons and excision of introns from transcribed RNA [21,28]. The lack of a SRp40 factor to the region located deeper in the exon might displace the other factors and thus exert a negative effect on the spliceosome assembly, which might lead to a splicing abnormality of exon 1 and lower levels of intact mRNA. Moreover, the c.54G>T mutation may cause important changes of the pre mRNA secondary structure of the exon 1. This fact can inhibit the recruitment of spliceosome components mediating splicing in this crucial position [29]. A growing body of evidence showed that the folding of mRNA influences a diverse range of transcription events such as pre mRNA splicing, processing, translational control and regulation [30]. However, the functional significance of this synonymous variant, deduced from bioinformatics tools, needs to be defined through functional studies.

The second identified substitution was c.856G>A encoding p.G289S. It was identified earlier by Moghrabi et al. [11] and was considered as polymorphism since it is frequent in all populations reported in the screening of 1000 genomes [31]. Enzyme activity analysis showed no difference between mutant G289S and wild-type enzyme [11]. However, it was found in a female patient with

compound heterozygous mutations, also carrying the p.N130S mutation [16] and in a homozygous state in a female patient with phallus enlargement and hirsutism [31]. The authors supposed that these female patients might carry other mutations in the regulatory regions of the *HSD17B3* gene [16,31], which could cause their phenotypes. In addition, the p.G289S amino acid substitution has been associated with an increased risk of developing prostate cancer, and with hypospadias in a case where mRNA expression levels were significantly lower for the mutant p.G289S compared with the wild-type enzyme [32]. These findings indicated that the variant p.G289S may not be as neutral as it had been initially thought [16,31], and it should be reconsidered as a possible genetic contributor for 17 $\beta$ -HSD3 deficiency and 46, XY DSD. This variant together with the nonsynonymous variant c.54G>T might be responsible for the mild testosterone synthesis deficiency of patient P8. Nevertheless, additional functional analyses are required to support our hypothesis.

In the present study, we also calculated the frequency of mutation c.618C>A in the geographic area of all patients investigated. To estimate the prevalence of mutation carriers in a random sample of individuals from the same geographic community, genomic DNA from 272 healthy individuals were screened for the c.618C>A mutation by PCR-RFLP. Fourteen individuals carrying the c.618C>A (p.C206X) mutation in a heterozygous state were identified. Thus, the carrier frequency for a heterozygous mutation is about 1 in 40 in the region of Sfax. The theoretical probability of a marriage between two carriers is 1 in 1600, and that for the birth of an affected child with a homozygous mutation based on random mating is predicted as 1 in 6400. The actual number of 17 $\beta$ -HSD3 deficiency cases in Sfax was not calculated. A higher prevalence than the predicted number can be expected due to the practice of consanguinity in the town, as well as the high variability of identified mutations in the *HSD17B3* gene. In fact, although Sfax is an industrialized town and not considered as rural region where the consanguinity is spread, consanguineous marriages and endogamy in this urban region have been traditionally performed as a way of maintaining land possession and families' names.

In the present study, we provide also evidence for a founder effect associated with the mutation p.C206X in six Tunisian families. This founder effect was supported by genotyping using the intragenic microsatellite marker D9S287, located in intron 2 of the *HSD17B3* gene, and the extragenic microsatellite marker D9S1786 together with the SNP rs408876. The seven patients harboring the p.C206X mutation carried the same haplotype. Importantly, for the more distant marker D9S1690, recombination (allele 232, 236, 226, 228 and 234) had occurred, which confirmed the pedigree analysis showing no close genetic relationship between families.

The subjects carrying the p.G133R mutation in a heterozygous state belonged to two unrelated families. They share the same haplotype for the p.G133R mutation, which would support a founder effect. This finding needs to be confirmed by a greater number of both controls and subjects harboring the p.G133R mutation. For the remaining p.Q176P mutation, which was first identified by Andersson et al. in The Netherlands [10], sequencing revealed its presence in only one Tunisian case of 17 $\beta$ -HSD3 deficiency in a heterozygous state. Unfortunately, no further genotyping data was available for this mutation to compare different intra and/or interethnic haplotypes, and to conclude concerning its geographic origin or whether it occurred *de novo*.

Haplotype analysis of genetic markers flanking the *HSD17B3* gene has been performed also to establish the ancient or *de novo* occurrence of mutations described in European, North American, Latin American, Australian and Arabs' populations [13]. Dutch, German, white Australian and white American patients, carrying the 325+4,A>T mutation, share the same genetic markers and

seemed to have a common European ancestor. A founder effect was also demonstrated for the R80Q mutation that is common in Dutch, Arabian (in Gaza), white Brazilian, and white Portuguese patients [13]. As this mutation is associated with a specific haplotype, a common ancestor introduced during the Phoenician migration has been hypothesized. An additional founder effect has been suggested for the 655–1,G>T mutation found in Greek, Turk and Syrian patients that may have spread to the Mediterranean area during the Ottoman empire [12]. On the contrary, patients harboring the 326–1,G>C and the p.P282L mutations have a different marker genotype suggesting that these are *de novo* mutations [12].

To detect novel newborns with 17 $\beta$ -HSD3 deficiency, individuals should be properly evaluated by thorough physical examination, abdominal and pelvic ultrasonography, and systematic endocrine analysis. Then, the initial diagnosis should be consistently confirmed by molecular analysis. Also, all family members should be tested to identify the carriers, and they should be informed about the risk of marrying a heterozygous carrier during a pre-nuptial consulting, and the prenatal diagnosis to their progeny should be available and systematic.

Diagnosis and consequently early treatment of 17 $\beta$ -HSD3 deficiency is difficult because clinical signs are often mild or absent from birth until puberty. Moreover, 17 $\beta$ -HSD3 deficiency is clinically indistinguishable from other forms of 46, XY DSD such as AIS or 5 $\alpha$ -reductase 2 deficiency. The correct diagnosis can be reached by systematic endocrine evaluation and, most importantly, by the calculation of the testosterone/androstenedione ratio. However, the diagnostic power of biochemical parameters is not always specific, because a normal reference range has not yet been established in strictly age-matched controls and because of overlapping with other causes of 46, XY DSD due to impaired testosterone biosynthesis. Thus, molecular genetic testing by sequencing or PCR-RFLP is an efficient way to confirm the diagnosis. Founder mutations are also of particular interest because they allow a rapid molecular diagnosis and targeted screening of ethnically restricted disease mutations in the appropriate population subgroups.

## 5. Conclusion

We reported novel cases of 46, XY DSD patients with 17 $\beta$ -HSD3 deficiency in the Tunisian population. The identification of four different mutations in a cohort of eight patients confirmed the previously observed heterogeneity of 17 $\beta$ -HSD3 deficiency. Nevertheless, haplotyping revealed a founder effect for the p.C206X mutation detected in six Tunisian families, and the carrier frequency of this mutation was estimated as 1 in 40. Due to the rather difficult diagnosis, the genetic heterogeneity and consanguinity, the incidence of 17 $\beta$ -HSD3 deficiency is likely to be underestimated and molecular diagnosis is indicated in 46, XY DSD patients. The screening for the identified mutations or the common haplotype may contribute to the rapid diagnosis of 17 $\beta$ -HSD3 deficiency. The genetic confirmation of mutations in the *HSD17B3* gene provides crucial information for genetic counseling, prenatal diagnosis and quick therapeutic approaches.

## Conflict of interest

The authors declare no conflict of interest that could be perceived as prejudicing the impartiality of the research reported.

## Acknowledgments

We thank the patients and their families for their cooperation in this study and for giving informed consent. We thank Prof. Thouraya Kamoun, Prof. Mongia Hachicha (Department of

Pediatrics, Hedi Chaker Hospital, Sfax, Tunisia) and Prof. Mouna Mnif (Department of Endocrinology, Hedi Chaker Hospital, Sfax, Tunisia) who contributed to the clinical investigation.

This work was supported by the Ministry of Higher Education and Scientific Research in Tunisia.

## References

- [1] I.A. Hughes, C. Houk, S.F. Ahmed, P.A. Lee, L.C. Group, Consensus statement on management of intersex disorders, *Arch. Dis. Child.* 91 (7) (2006) 554–563.
- [2] M.M. George, M.I. New, S. Ten, C. Sultan, A. Bhangoo, The clinical and molecular heterogeneity of 17 $\beta$ -HSD3 enzyme deficiency, *Horm. Res. Paediatr.* 74 (4) (2010) 229–240.
- [3] J.M. Saez, E. De Peretti, A.M. Morera, M. David, J. Bertrand, Familial male pseudohermaphroditism with gynecomastia due to a testicular 17-ketosteroid reductase defect. I. Studies in vivo, *J. Clin. Endocrinol. Metab.* 32 (5) (1971) 604–610.
- [4] W.M. Geissler, D.L. Davis, L. Wu, K.D. Bradshaw, S. Patel, B.B. Mendonca, et al., Male pseudohermaphroditism caused by mutations of testicular 17 $\beta$ -hydroxysteroid dehydrogenase 3, *Nat. Genet.* 7 (1) (1994) 34–39.
- [5] A. Al-Sinani, W.-A. Mula-Abed, M. Al-Kindi, G. Al-Kusaibi, H. Al-Azkawi, N. Nahavandi, A novel mutation causing 17 $\beta$ -hydroxysteroid dehydrogenase type 3 deficiency in an Omani child: first case report and review of literature, *Oman Med. J.* 30 (2) (2015) 129–134.
- [6] N. Phelan, E.L. Williams, S. Cardamone, M. Lee, S.M. Creighton, G. Rumsby, et al., Screening for mutations in 17 $\beta$ -hydroxysteroid dehydrogenase and androgen receptor in women presenting with partially virilised 46, XY disorders of sex development, *Eur. J. Endocrinol.* 172 (6) (2015) 745–751.
- [7] B. Ben Rhouma, N. Belguith, M.F. Mnif, T. Kamoun, N. Charfi, M. Kamoun, et al., A novel nonsense mutation in HSD17B3 gene in a Tunisian patient with sexual ambiguity, *J. Sex Med.* 10 (2013) 2586–2589.
- [8] R.T. Engeli, B. Ben Rhouma, C.P. Sager, M. Tschacki, J. Birk, F. Fakhfakh, et al., Biochemical analyses and molecular modeling explain the functional loss of 17 $\beta$ -hydroxysteroid dehydrogenase 3 mutant G133R in three Tunisian patients with 46, XY Disorders of Sex Development, *J. Steroid Biochem. Mol. Biol.* 155 (Pt A) (2016) 147–154.
- [9] H.A. Lewin, J.A. Stewart-Haynes, A simple method for DNA extraction from leukocytes for use in PCR, *BioTechniques* 13 (4) (1992) 522–524.
- [10] S. Andersson, W.M. Geissler, L. Wu, D.L. Davis, M.M. Grumbach, M.I. New, et al., Molecular genetics and pathophysiology of 17 $\beta$ -hydroxysteroid dehydrogenase 3 deficiency, *J. Clin. Endocrinol. Metab.* 1 (1996) 130–136.
- [11] N. Moghrabi, I.A. Hughes, A. Dunaif, S. Andersson, Deleterious missense mutations and silent polymorphism in the human 17 $\beta$ -hydroxysteroid dehydrogenase 3 gene (HSD17B3), *J. Clin. Endocrinol. Metab.* 83 (8) (1998) 2855–2860.
- [12] Y.S. Lee, J.M.W. Kirk, R.G. Stanhope, D.I. Johnston, S. Harland, R.J. Auchus, et al., Phenotypic variability in 17 $\beta$ -hydroxysteroid dehydrogenase-3 deficiency and diagnostic pitfalls, *Clin. Endocrinol. (Oxf.)* 1 (2007) 20–28.
- [13] M.A. Parisi, L.A. Ramsdell, M.W. Burns, M.C. Carr, R.E. Grady, D.F. Gunther, et al., A Gender Assessment Team: experience with 250 patients over a period of 25 years, *Genet. Med.* 9 (6) (2007) 348–357.
- [14] I.A. Hughes, Disorders of sex development: a new definition and classification, *Best Pract. Res. Clin. Endocrinol. Metab.* 22 (1) (2008) 119–134.
- [15] S. Faisal Ahmed, A. Iqbal, I.A. Hughes, The testosterone:androstenedione ratio in male undermasculinization, *Clin. Endocrinol. (Oxf.)* 6 (2000) 697–702.
- [16] A.L. Boehmer, A.O. Brinkmann, L.A. Sandkuijl, D.J. Halley, M.F. Niermeijer, S. Andersson, et al., 17 $\beta$ -hydroxysteroid dehydrogenase-3 deficiency: diagnosis, phenotypic variability, population genetics, and worldwide distribution of ancient and de novo mutations, *J. Clin. Endocrinol. Metab.* 84 (12) (1999) 4713–4721.
- [17] A. Rösler, Steroid 17 $\beta$ -hydroxysteroid dehydrogenase deficiency in man: an inherited form of male pseudohermaphroditism, *J. Steroid Biochem. Mol. Biol.* 43 (8) (1992) 989–1002.
- [18] A. Rösler, S. Silverstein, D. Abeliovich, A. (R80Q) mutation in 17 $\beta$ -hydroxysteroid dehydrogenase type 3 gene among Arabs of Israel is associated with pseudohermaphroditism in males and normal asymptomatic females, *J. Clin. Endocrinol. Metab.* 81 (5) (1996) 1827–1831.
- [19] M. Ellaithi, R. Werner, F.G. Riepe, N. Krone, A.E. Kulle, T. Diab, et al., 46,XY disorder of sex development in a sudanese patient caused by a novel mutation in the HSD17B3 gene, *Sex Dev.* 4 (2014) 151–155.
- [20] H.U. Tuhani, A. Anik, G. Catli, S. Ceylaner, B. Dundar, E. Bober, et al., A novel missense mutation in HSD17B3 gene in a 46, XY adolescent presenting with primary amenorrhea and virilization at puberty, *Clin. Chim. Acta* 438 (2015) 154–156.
- [21] S.V. Kozyrev, M. Bernal-Quirós, M.E. Alarcón-Riquelme, C. Castillejo-López, The dual effect of the lupus-associated polymorphism rs10516487 on BANK1 gene expression and protein localization, *Genes Immun.* 13 (2) (2012) 129–138.
- [22] L. Cartegni, S.L. Chew, A.R. Krainer, Listening to silence and understanding nonsense: exonic mutations that affect splicing, *Nat Rev Genet.* 3 (4) (2002) 285–298.
- [23] F. Pagani, F.E. Baralle, Genomic variants in exons and introns: identifying the splicing spoilers, *Nat. Rev. Genet.* 5 (5) (2004) 389–396.
- [24] J. Kráľovicová, S. Houngininou-Molango, A. Krämer, I. Vorechovsky, Branch site haplotypes that control alternative splicing, *Hum. Mol. Genet.* 24 (2004) 3189–3202.
- [25] S. Chavanas, Y. Gache, J. Vailly, J. Kanitakis, L. Pulkkinen, J. Uitto, et al., Splicing modulation of integrin beta4 pre-mRNA carrying a branch point mutation underlies epidermolysis bullosa with pyloric atresia undergoing spontaneous amelioration with ageing, *Hum. Mol. Genet.* 8 (11) (1999) 2097–2105.
- [26] H.X. Liu, L. Cartegni, M.Q. Zhang, A.R. Krainer, A mechanism for exon skipping caused by nonsense or missense mutations in BRCA1 and other genes, *Nat. Genet.* 1 (2001) 55–58.
- [27] E.C. Ibrahim, T.D. Schaal, K.J. Hertel, R. Reed, T. Maniatis, Serine/arginine-rich protein-dependent suppression of exon skipping by exonic splicing enhancers, *Proc. Natl. Acad. Sci. U. S. A.* 14 (2005) 5002–5007.
- [28] A.J. Matlin, F. Clark, C.W.J. Smith, Understanding alternative splicing: towards a cellular code, *Nat. Rev. Mol. Cell Biol.* 6 (5) (2005) 386–398.
- [29] O. Siala, N. Belguith, H. Kammoun, B. Kammoun, N. Hmida, I. Chabchoub, et al., Two Tunisian patients with Peters plus syndrome harbouring a novel splice site mutation in the B3GALT1 gene that modulates the mRNA secondary structure, *Gene* 507 (1) (2012) 68–73.
- [30] K.J. Address, J.P. Babilion, R.D. Klausner, T.A. Rouault, A. Pardi, Structure and dynamics of the iron responsive element RNA: implications for binding of the RNA by iron regulatory binding proteins, *J. Mol. Biol.* 274 (1) (1997) 72–83.
- [31] C.C. Castro, G. Guaragna-Filho, F.L. Calais, F.B. Coeli, I.R.L. Leal, E.F. Cavalcante-Junior, et al. Clinical and molecular spectrum of patients with 17 $\beta$ -hydroxysteroid dehydrogenase type 3 (17 $\beta$ -HSD3) deficiency, *Arq. Bras. Endocrinol. Metabol.* (2012) 56 (8) 533–539.
- [32] K. Margiotti, E. Kim, C.L. Pearce, E. Spera, G. Novelli, J.K.V. Reichardt, Association of the G289S single nucleotide polymorphism in the HSD17B3 gene with prostate cancer in Italian men, *Prostate* 53 (1) (2002) 65–68.

#### 4.4 Paper 7 (Engeli et al, submitted)

### Biochemical Analysis of Four Missense Mutations in the HSD17B3 Gene associated with 46, XY DSD in Egyptian Patients

Roger T. Engeli, Maria Tsachaki, Heba A. Hassan, Christoph P. Sager, Mona L. Essawi, Yehia Z.  
Gad, Alaa K. Kamel, Inas Mazen, Alex Odermatt

Submitted manuscript

**Contribution:** Provided all data for the in vitro activity experiments (Figure 4), analyzed data (Figure 3 and 5), and drafted the manuscript.

**Aims:** Biochemical analysis of four mutations from Egyptian patients associated with 17 $\beta$ -HSD3 deficiency.

**Results:** T54A and L194P mutations completely abolished 17 $\beta$ -HSD3 activity despite normal protein expression. M164T mutation showed residual activity. G289S mutation does not alter the 17 $\beta$ -HSD3 activity. Screening for additional mutations in patients with G289S polymorphism revealed a mutation in the *SRD5A2* gene.

**Conclusion:** *In vitro* biochemical evaluation of *HSD17B3* mutations is crucial to confirm 17 $\beta$ -HSD3 deficiency.



## **Biochemical Analysis of Four Missense Mutations in the *HSD17B3* Gene associated with 46, XY Disorders of Sex Development in Egyptian Patients**

Roger T. Engeli, MSc<sup>a</sup>, Maria Tsachaki, PhD<sup>a</sup>, Heba A. Hassan, PhD<sup>b</sup>, Christoph P. Sager, MSc<sup>c</sup>, Mona L. Essawi, MD<sup>b</sup>, Yehia Z. Gad, MD<sup>b</sup>, Alaa K. Kamel, MD<sup>d</sup>, Inas Mazen, MD<sup>e</sup>, Alex Odermatt, PhD<sup>a</sup>

<sup>a</sup>Division of Molecular and Systems Toxicology, Department of Pharmaceutical Sciences, University of Basel, Basel, Switzerland; <sup>b</sup>Department of Medical Molecular Genetics, Division of Human Genetics and Genome Research, Center of Excellence for Human Genetics, National Research Centre, Cairo, Egypt; <sup>c</sup>Molecular Modeling, Department of Pharmaceutical Sciences, University of Basel, Basel, Switzerland; <sup>d</sup>Department of Human Cytogenetics, Division of Human Genetics and Genome Research, Center of Excellence for Human Genetics, National Research Centre, Cairo, Egypt; <sup>e</sup>Department of Clinical Genetics, Division of Human Genetics and Genome Research, Center of Excellence for Human Genetics, National Research Centre, Cairo, Egypt

Corresponding author: Prof. Dr. Alex Odermatt

E-Mail: [alex.odermatt@unibas.ch](mailto:alex.odermatt@unibas.ch) T: +41 (0)61 207 15 30 F: +41 (0)61 207 15 15

## **Abstract**

**Background.** Mutations in the *HSD17B3* gene are associated with a 46, XY disorder of sexual development (46, XY DSD) as a result of low testosterone production during embryogenesis.

**Aims.** Four missense mutations in *HSD17B3* (T54A, M164T, L194P, G289S) from Egyptian patients with 46, XY DSD were biochemically analyzed to elucidate the molecular basis of the disorder in these patients.

**Methods.** Expression plasmids for wild-type 17 $\beta$ -hydroxysteroid hydrogenase type 3 (17 $\beta$ -HSD3) and mutant enzymes generated by site-directed mutagenesis were transiently transfected into human HEK-293 cells. Protein expression was verified by western blotting and activity determined by measuring the conversion of radiolabeled  $\Delta^4$ -androstene-3,17-dione to testosterone (T). Application of a homology model provided an explanation for the observed effects of the mutations.

**Main Outcome Measures.** Comparison of testosterone (T) formation by wild-type and mutant 17 $\beta$ -HSD3 enzymes.

**Results.** The mutations T54A and L194P, despite normal protein expression, completely abolished 17 $\beta$ -HSD3 activity, explaining their severe 46, XY DSD phenotype. Mutant M164T was still able to produce T, albeit with significantly reduced activity compared to wild-type 17 $\beta$ -HSD3, resulting in ambiguous genitalia or a microphallus at birth. The substitution G289S represented a polymorphism exhibiting comparable activity to wild-type 17 $\beta$ -HSD3. Sequencing of the *SRD5A2* gene in three siblings bearing the *HSD17B3* G289S polymorphism revealed the homozygous Y91H mutation in the former gene, thus explaining the 46, XY DSD presentations. Molecular modeling analyses supported the biochemical observations and predicted a disruption of cofactor binding by mutations T54A and M164T and of substrate binding by L196P, resulting in the loss of enzyme activity. In contrast, the G289S substitution was predicted to neither disturb 3D structure nor enzyme activity.

**Clinical translation.** Biochemical analysis of mutant 17 $\beta$ -HSD3 enzymes is necessary to understand genotype-phenotype relationships.

**Conclusion.** The G289S substitution, previously reported in other 46, XY DSD patients, is a polymorphism not causing 46, XY DSD; thus further sequence analysis was required and revealed a mutation in *SRD5A2*, explaining the cause of 46, XY DSD in these patients.



## Introduction

17 $\beta$ -hydroxysteroid dehydrogenase type 3 (17 $\beta$ -HSD3) converts the weak androgen  $\Delta^4$ -androstene-3,17-dione (AD) into the potent androgen testosterone (T) using NADPH as a cofactor [1, 2]. This enzyme is predominantly expressed in testicular Leydig cells [3, 4]. T can be further converted into 5 $\alpha$ -dihydrotestosterone (DHT) in fetal genital tissues by 5 $\alpha$ -reductase type 2 (SRD5A2) [5]. T and DHT synthesis is crucial for the normal male genital development during embryogenesis. While T mediates the masculinization of the Wolffian ducts, seminal vesicles, and vas deferens, DHT is responsible for the growth of the prostate and external genital development [6, 7].

Mutations in the *HSD17B3* gene (9q22) can lead to a 46, XY disorder of sex development (46, XY DSD) due to the lack of T and DHT production [3]. The prevalence of 17 $\beta$ -HSD3 deficiency in European countries is rather low, representing approximately 4% of all 46, XY DSD cases [8]. A study in The Netherlands reported an incidence of 1:147,000 in newborns [9]. However, in some Arabic populations, the prevalence is much higher due to a high rate of consanguineous marriages [10-12]. To date, more than 40 different mutations in introns and exons of the *HSD17B3* gene are known [13-15]. Patients with this disorder are XY individuals that characteristically show undermasculinization. The external genitalia often appear to be female with or without clitoromegaly or labial fusion and a blind ending vagina [16, 17]. The spectrum of phenotypes can vary from ambiguous female genitalia to male microphallus, depending on T and DHT levels during development [18]. Unfortunately, the diagnosis of 46, XY DSD is sometimes missed until puberty and moreover, the clinical phenotype overlaps with that of SRD5A2 deficiency to a great extent [19]. Patients may frequently be raised as girls, and undergo sex change after puberty because of ongoing masculinization due to partial activity of the mutant 17 $\beta$ -HSD3 enzyme or extra-testicular T production by 17 $\beta$ -hydroxysteroid dehydrogenase type 5 (17 $\beta$ -HSD5, AKR1C3) [17, 20].

In this study, we biochemically investigated four missense mutations in the *HSD17B3* gene that were previously proposed to cause 46, XY DSD in Egyptian patients [13]. The mutant enzymes were biochemically analyzed to check for their expression and remaining activity. Additionally, a

17 $\beta$ -HSD3 homology model was applied in an attempt to understand the impact of the mutated amino acid residues on the enzyme activity.

## **Materials and methods**

### **Patient details and sequencing**

Blood samples were collected from seven patients with 46, XY DSD representing five unrelated families. The patients were recruited from the outpatient Clinical Genetics and Endocrinology Clinics at the Egyptian National Research Centre. Written informed consent was obtained from all patients or their guardians according to the Medical Ethics Committee at the Egyptian National Research Centre. Clinical examinations, hormonal profile and karyotyping were provisionally suggesting the diagnosis of 46, XY DSD with 17 $\beta$ -HSD3 enzyme deficiency. The age of referral differed from very young (two months) up to post pubertal stages (16-20 years) (Table 1). Post-pubertal patients presented with either primary amenorrhea or virilization, and pre-pubertal patients with ambiguous genitalia. Patients (no. 5-7) were ascertained from one family, the older siblings (no. 6 & 7) were dizygotic twins who were reared as females and seeking for sex reversal later in development. Human chorionic gonadotropin (hCG) stimulation was only performed in pre-pubertal patients. Only the short hCG stimulation protocol was performed (2500 IU hCG were administered by intramuscular injection daily for three consecutive days). Steroid hormone levels were measured before and after stimulation.

Genomic DNA extraction was performed according to a standard protocol [21]. For all patients the coding regions and flanking intron/exon boundaries of the *HSD17B3* gene were sequenced. The *SRD5A2* gene was sequenced in selected cases bearing the *HSD17B3* G289S substitution. PCR conditions and the oligonucleotide primers were described previously [13, 22].

### **Plasmids and molecular cloning**

The pcDNA3 plasmid containing the coding sequence of 17 $\beta$ -HSD3 followed by a C-terminal FLAG epitope tag (17 $\beta$ -HSD3-FLAG) was described earlier [23]. This plasmid was used as a template for

site-directed mutagenesis using the Pfu Polymerase (Promega, Madison, WI, USA) in order to introduce the corresponding mutation into the coding sequence of 17 $\beta$ -HSD3. Expression of these constructs led to the mutant 17 $\beta$ -HSD3 proteins T54A, M164T, L194P and G289S. All constructs were sequence-verified. The oligonucleotide primer sequences used for PCR are available upon request.

### **Cell culture and western blotting**

For enzymatic activity determination, the wild-type and mutant 17 $\beta$ -HSD3-FLAG constructs were transiently expressed in the HEK-293 cell line (ATCC, Manassas, VA, USA). HEK-293 cells were cultured in Dulbecco's Modified Eagle's Medium (DMEM, Sigma-Aldrich, St. Louis, MO, USA) supplemented with 10% fetal bovine serum (FBS, Connectorate, Dietikon, Switzerland), 100 U/mL penicillin, 100  $\mu$ g/mL streptomycin (Sigma-Aldrich), 10 mM HEPES buffer, pH 7.4 (Life Technologies, Grand Island, NY, USA) and non-essential amino acid solution (Sigma-Aldrich). Cells were cultivated under standard conditions (37°C, 5% CO<sub>2</sub>). Western blotting, for confirmation of proper protein expression was performed as described earlier [23]. Briefly, cells were transfected with the corresponding cDNA constructs using the calcium phosphate precipitation method, and lysed 48 h later with RIPA buffer (Sigma-Aldrich) containing protease inhibitor cocktail (Roche, Basel, Switzerland). For detection of the FLAG epitope the mouse monoclonal antibody M2 was used (Sigma-Aldrich) at a final concentration of 0.5  $\mu$ g/mL in 3% defatted milk solution. To confirm equal loading, membranes were probed with the anti-actin polyclonal antibody sc-1616 (Santa Cruz Biotechnology Inc., CA, USA), which was used at a final concentration of 1  $\mu$ g/mL.

### **Enzyme activity assay**

The procedure for enzymatic activity measurements in intact cells has been described previously [23]. Briefly, HEK-293 cells ( $2 \times 10^6$ ) were seeded into 10 cm dishes, 24 h prior to transfection. Expression plasmids (8  $\mu$ g) for wild-type and mutant enzymes were transiently transfected using the calcium phosphate precipitation method. Media was replaced with fresh media 4 h post transfection. After an incubation time of 24 h, transfected cells were seeded (15'000) into poly-L-

lysine (Sigma-Aldrich) pre-coated 96-well plates containing 100 mL media. The day after, media was replaced by 50  $\mu$ L charcoal-treated serum-free media containing 200 nM AD with 50 nCi [1,2,6,7- $^3$ H]-AD (American Radiolabeled Chemicals, St. Louis, MO, USA). Reactions were stopped after 0.5 h and 1 h by adding a mixture of 2 mM unlabeled AD and T (Sigma-Aldrich). Samples were loaded onto TLC plates (Macherey-Nagel, Oensingen, Switzerland) and steroids were separated using chloroform/ethyl acetate (4:1 ratio). Corresponding substrate and product concentrations were determined using scintillation counting (PerkinElmer, Waltham, MA, USA).

### **Molecular modeling**

The 17 $\beta$ -HSD3 homology models were generated as previously described [23]. Briefly, wild-type and mutant gene sequences were aligned together with the crystal structure of 17 $\beta$ -HSD1 (3DHE, 2.3 Å) using Modeller (Version 9.11) [24, 25]. The Multiple Sequence Viewer implemented in Maestro was used to align protein sequences [26]. Model refinement was performed using Prime, treating all residues within 8 Å of the respective mutated residue as flexible, while keeping the rest of the model rigid [27-29]. All modeling Figures were created using PyMOL [30].

## **Results**

### **Characterization of 46, XY DSD patients**

The clinical, hormonal, and molecular data of seven patients with 46, XY DSD are shown in Table 1. Sequencing data of the *HSD17B3* gene of four patients (cases no. 1, 3-5) was reported previously [13]. Like for patient no 1, sequencing of the *HSD17B3* gene in patient no. 2 revealed a homozygous T54A mutation in exon 2 (Fig. 1). Patients no. 1 and 2 had comparable age and similar hormonal and molecular profiles and they both exhibited hirsutism in body and face, developed pubic hair, had no palpable gonads, a microphallus (4 cm) and a Quigley score of 3. The genital examination of patient no. 4 revealed the presence of two palpable gonads in the labioscrotal folds, single opening, and microphallus (2 cm) [13], suggesting weak androgen-dependent sex development. Regarding patients 6 and 7, a heterozygous G289S substitution in exon 11 was detected (Fig. 2). These dizygotic twins from a consanguineous family had a clinical

phenotype similar to that of their sibling with the homozygous G289S substitution, case no 5. This implied that sequencing of the *SRD5A2* gene was necessary. A homozygous Y91H mutation was found in exon 1 in all three siblings (patients no. 5-7) (Fig. 2C).

### **Analysis of expression and activity of mutant 17 $\beta$ -HSD3 enzymes**

In order to assess the biochemical effects of the different mutations in the *HSD17B3* gene on the activity of the expressed enzymes, we first generated the corresponding mutations in the cDNA by site-directed mutagenesis. A FLAG epitope tag was inserted right after the coding region in all cDNA constructs for facilitated detection of the expressed proteins. The expression plasmids for wild-type and mutant 17 $\beta$ -HSD3 were then transfected into HEK-293 cells and protein expression was assessed by western blotting. Quantification of protein expression from three independent experiments showed that mutant and wild-type 17 $\beta$ -HSD3 were efficiently expressed and at comparable levels (Fig. 3). After confirming expression of all mutated proteins, we sought to assess their enzymatic activity in comparison to the wild-type enzyme. Cells were incubated for 60 min with 200 nM AD, followed by determination of T production. The wild-type enzyme converted approximately 30% of AD to T, whereas no conversion was detected for 17 $\beta$ -HSD3 mutants T54A and L194P (Fig. 4A). 17 $\beta$ -HSD3 mutant M164T retained weak activity but it was approximately 15-20 times less active than 17 $\beta$ -HSD3 (Fig. 4B). The substitution G289S efficiently catalyzed the conversion of AD to T, at comparable activity to wild-type 17 $\beta$ -HSD3. Comparison of activities upon incubation for 0.5 h and 1 h revealed an indistinguishable conversion rate to T for the substitution G289S and wild-type 17 $\beta$ -HSD3, indicating that G289S is a fully functional polymorphism (Fig. 4A).

### **Modeling**

The 17 $\beta$ -HSD3 homology model was used to study impacts of all investigated mutations on the activity of the enzyme (Fig. 5). The T54A mutation is located on the highly-conserved cofactor binding site among the short-chain dehydrogenase/reductase (SDR) family (Fig. 5A). The threonine to alanine mutation leads to the loss of two hydrogen bonds with the  $\beta$ 4 $\alpha$ 5-loop backbone, which could propagate to the conserved glycine region (GXXXGXG), essential for cofactor binding. A mutation (G133R) in the  $\beta$ 4 $\alpha$ 5-loop was previously elaborated as culprit of

enzyme inactivation [23] and it seems that perturbations in this loop have a huge impact on cofactor binding.

The M164T mutation is located closely to the cofactor binding site (Fig. 5B). The mutated polar threonine residue is smaller and could lead to more freedom of the  $\beta 4\alpha 5$ -loop and most likely interferes with the affinity of the cofactor binding. The mutant model also shows a slight rearrangement of the N131 side chain. However, this might be an artifact of the employed methods, and reasons of dynamic nature, not revealed by the homology model, could be the cause of a loss of affinity.

The L194P mutation most likely disrupts the arrangement of bulky, hydrophobic side-chains, such as Y195 and Y258, closely to the substrate binding site (Fig. 5C). Proline is the only cyclic amino acid and has a huge impact on secondary structures, frequently breaking  $\alpha$ -helices and  $\beta$ -sheets by introducing inflexibility. However, whether this added rigidity disturbs the binding of the substrate by negatively affecting the induced fit of the binding pocket or the substrate is hindered to enter the binding pocket at all, cannot be examined conclusively only using the obtained homology model.

The G289S substitution is located on the surface of the enzyme, more than 20 Å away from the NADPH cofactor and substrate binding site (Fig. 5D). The mutated serine residue does not have any impact on the structure of the enzyme.

## Discussion

This study describes the activity assessment of four mutations in the *HSD17B3* gene from Egyptian patients with 46, XY DSD. The enzymological consequences of the mutations were biochemically examined in transfected HEK-293 cells expressing wild-type and mutant 17 $\beta$ -HSD3 enzymes, followed by *in silico* homology modeling to visualize the structural changes caused by the mutations.

Biochemical assays showed completely abolished enzyme activity for 17 $\beta$ -HSD3 mutants T54A and L194P. The homozygous T54A state in both cases no 1 and 2 could explain the severe phenotype and their late referral to the clinician. This was also evidenced in patient no. 3 where the compound heterozygous state of L194P/c.588C>T resulted in a severe 46, XY DSD phenotype.

Molecular modeling simulations for mutant T54A predicted a disruption of the cofactor binding site (Fig. 5A). The mutated alanine residue is expected to destabilize the cofactor binding site due to the loss of hydrogen bonds formed by threonine. Amino acid residue 54 is located one residue upstream of the well-conserved GXXXGXXG motif involved in cofactor binding at the N-terminal region that is highly conserved among SDR enzymes [31]. Furthermore, two other mutations (A51V [13] and A56T [19, 32]) have been previously identified in the cofactor binding region that resulted in a similar clinical appearance in these patients. Introduction of an additional proline residue in the L194P mutation was predicted by the homology model to disrupt the substrate binding site (Fig. 5C), thus providing an explanation for the loss of function of this mutant enzyme. Regarding patient 4, the identification of microphallus and developed testes is a sign for partial androgen-dependent fetal masculinization [13]. Activity assays in transfected HEK-293 cells revealed residual T formation by mutant M164T. The mutant enzyme was able to convert AD into T; however, with 15-20 times lower activity than wild-type 17 $\beta$ -HSD3. Molecular modeling simulations revealed small changes in the 3D-structure close to the cofactor binding site that may negatively influence the binding affinity for NADPH or its positioning for the electron transfer (Fig. 5B), thereby resulting in a significantly reduced activity (Fig. 4D). M164T caused major effects on genitalia, though not complete loss of enzymatic activity. The low amounts of T produced during the critical period of fetal sexual differentiation could explain the patient's phenotype.

Molecular modeling simulations showed that the G289S substitution is located far away from the substrate and cofactor binding site (Fig. 5A). The extra hydroxy group from the introduced serine does not affect the 3D-structure nor the enzymatic activity. In the literature, contradictory data was found about the residual activity of the G289S substitution and its potential cause of 46, XY DSD. Homozygous G289S substitution was reported to cause 46, XY DSD in Italian and Brazilian patients by Bertelloni et al. [33] and Castro et al. [18]. Additionally, three patients from Egypt were also described carrying this substitution that was suspected to be responsible for 46, XY DSD [13]. Besides, an increased risk of developing hypospadias for G289S carriers was reported by Sata et al. [34]. Furthermore, an association of the G289S substitution with an increased prostate cancer risk was described by Margiotti et al. in a study on Italian men [35]. These studies highlight the actual research interest in this substitution. However, these studies did not functionally investigate the G289S substitution. In the present study, we showed that the G289S variant has



comparable enzymatic activity as wild-type 17 $\beta$ -HSD3 (Fig. 4A), consistent with an early biochemical study by Moghrabi et al. [36]. Together with the molecular modeling analysis showing no potential disruption by this substitution of substrate and cofactor binding (Fig. 5A), this data emphasizes that G289S is a fully functionally active polymorphism not causing 46, XY DSD. Thus, other causes of 46, XY DSD have to be investigated in patients homozygous for G289S, such as mutations in other genes related to androgen synthesis or mutations in the androgen receptor (AR). This was successfully demonstrated in the sibling patients no. 5-7, where further genetic analysis revealed that the homozygous mutation Y91H in *SDR5A2* is causative for the 46, XY DSD phenotype. The measured high T/DHT ratio, atypical for 17 $\beta$ -HSD3 deficiency, and the masculine gender identity led to the assumption of *SRD5A2* deficiency in these patients. Failure of hormone testing to elucidate clearly the cause of XY undervirilization may relate to the variability and lack of consensus among hCG stimulation protocols. Herein, we used the short stimulation protocol with a daily dose of 2500 units for 3 days. The protocols differ in dose and duration, ranging from 500 to 1500 units/day and extending from 2 days to a month [9, 37-41]. Furthermore; the value of AD/T ratio as a sole reliable diagnostic tool of 17 $\beta$ -HSD3 deficiency has been questioned, and a confirmation by molecular studies is highly warranted [42].

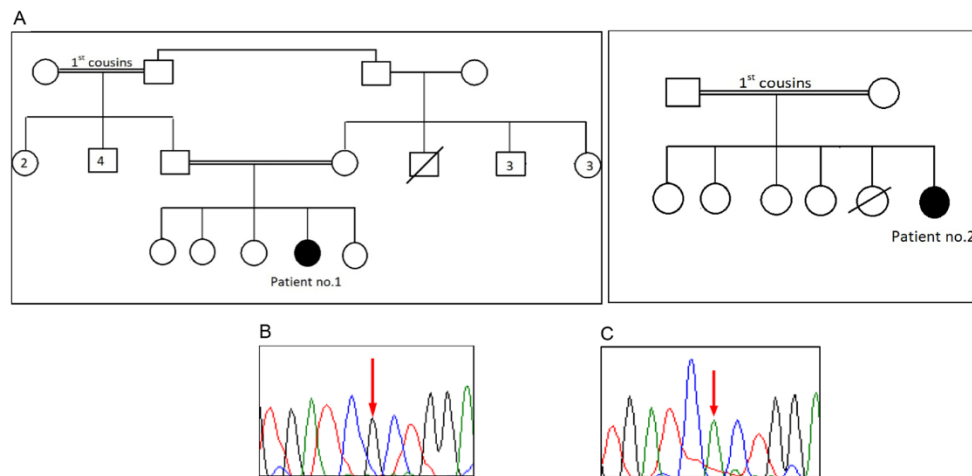
The Y91H mutation has been previously reported in Egyptian, Palestinian and Turkish 46, XY patients [37, 43], supporting that the *SRD5A2* mutation Y91H is responsible for 46, XY DSD in the three Egyptian siblings included in this study. However, biochemical confirmation that the Y91H mutation abolishes *SRD5A2* expression and/or enzyme activity is needed to exclude other causes of 46, XY DSD in these patients.

## **Conclusion**

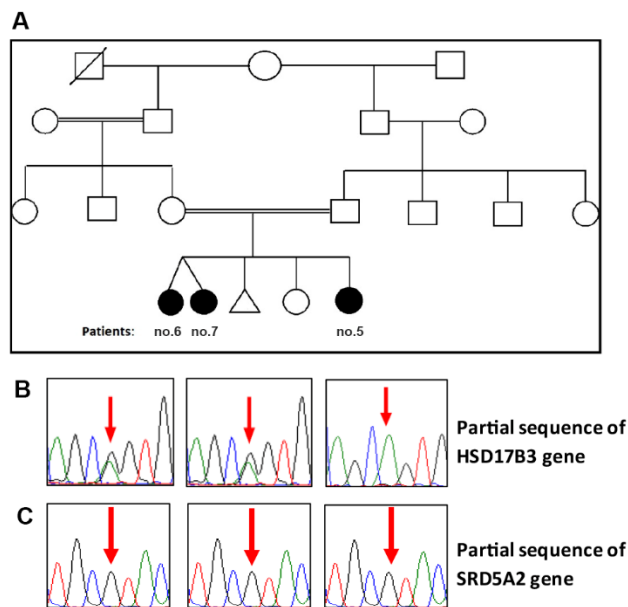
In this study, we biochemically analyzed four mutations in the *HSD17B3* gene of Egyptian patients that were suspected to cause 46, XY DSD. The missense mutations T54A and L194P completely abolished 17 $\beta$ -HSD3 activity despite normal protein expression, whereas mutant M164T exhibited low residual activity, providing an explanation for its somewhat less severe 46, XY DSD phenotype. In contrast to the functional loss of these missense mutations, we demonstrate that the G289S substitution, associated in the literature with 46, XY DSD, is a fully functional polymorphism not causing 46, XY DSD. In three siblings bearing the G289S polymorphism

(patients no 5, 6, and 7) further genetic screening led to the identification of the homozygous mutation Y91H in the *SRD5A2* gene. Molecular modeling analyses supported the biochemical observations and predicted a disruption of cofactor binding by mutations T54A and M164T and of substrate binding by L196P, resulting in the loss of enzyme activity. In contrast, the G289S substitution was predicted not to disturb the 3D structure and enzyme activity. Thus, biochemical analyses in combination with molecular modeling can provide important information on the identified mutations, helping to understand genotype-phenotype relationships.

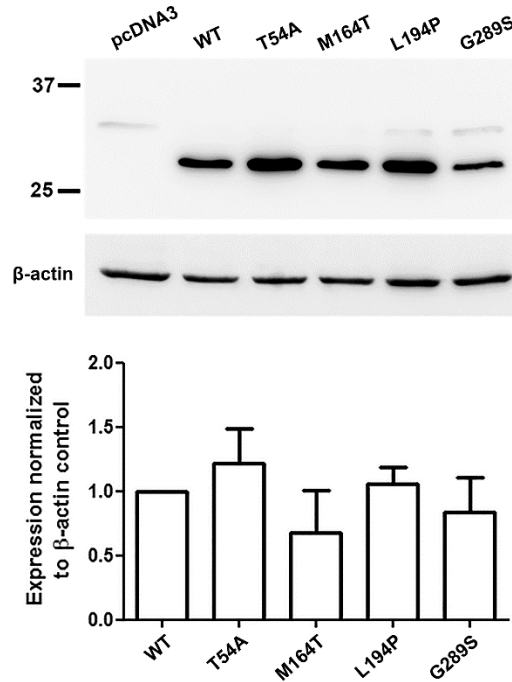
### Figure Legends



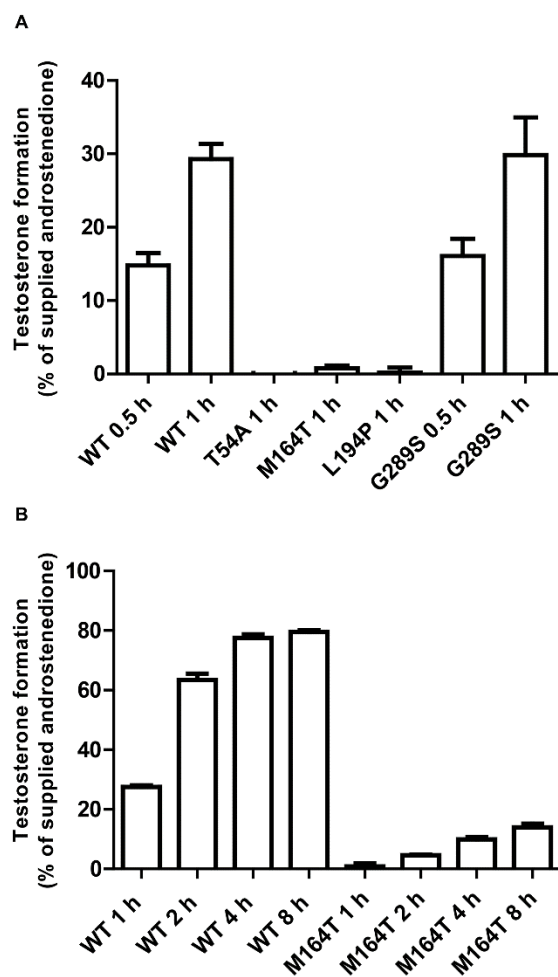
**Figure 1.** Patients with 46, XY DSD bearing the T54A mutation in the *HSD17B3* gene. (A) Pedigree charts of two families showing patients no.1 & 2. (B) Electropherogram of part of the *HSD17B3* gene sequence showing wild-type T54. (C) Electropherogram of part of the *HSD17B3* gene sequence showing the homozygous T54A mutation. The site of the mutation is denoted by the red arrow. Pedigree chart symbols: □ male, ○ female, ● affected individual, strikethrough symbols (deceased individual), number of children written inside symbol, double line indicates consanguineous marriage.



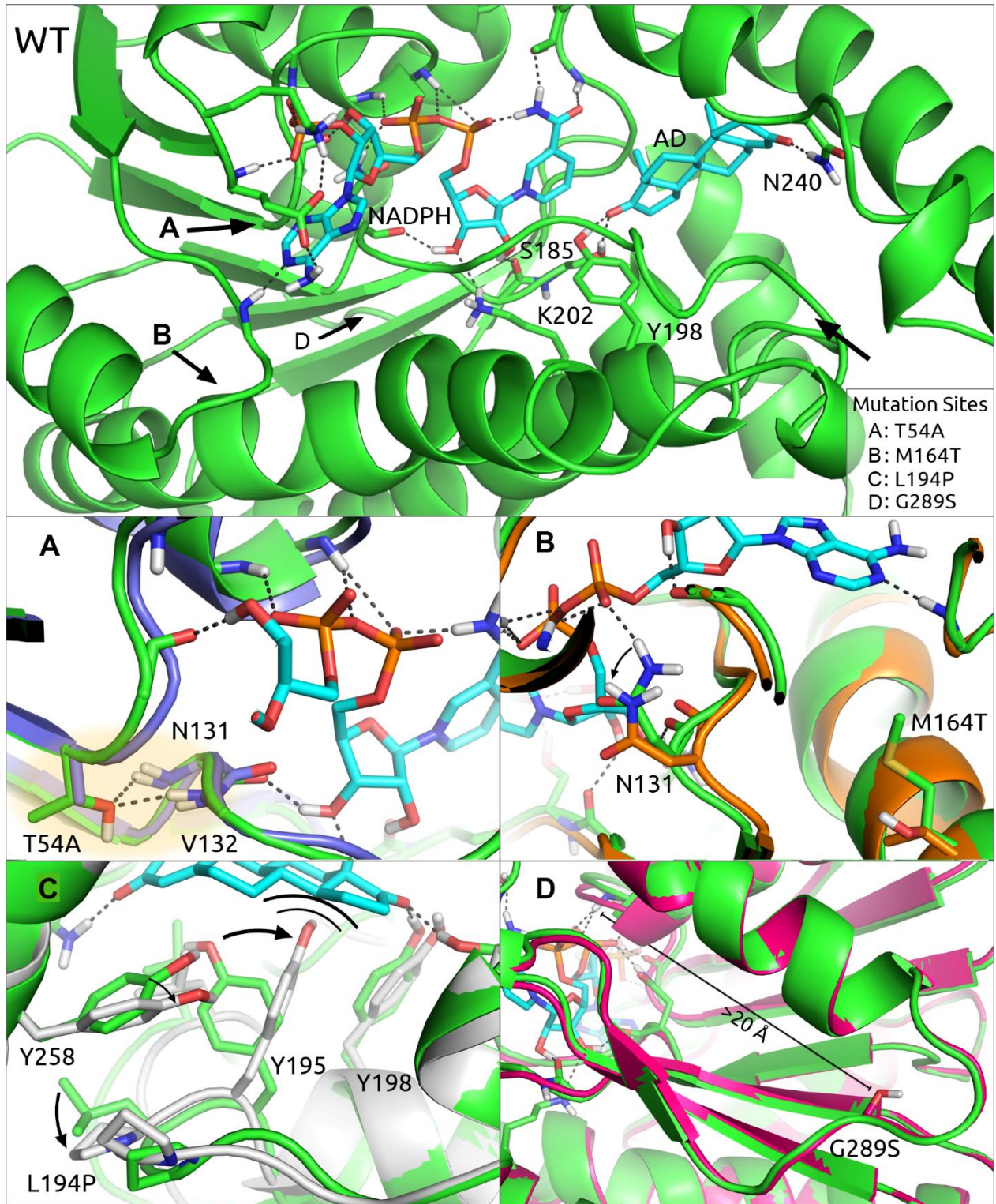
**Figure 2.** Family with three 46, XY DSD patients. (A) Pedigree chart of the family through four generations showing three affected patients (no. 5-7). (B) Electropherogram of part of the *HSD17B3* gene sequence (exon 11) showing the heterozygous G289S mutation in patients no. 6 & 7 and the homozygous mutation in patient no. 5. (C) Electropherogram of part of the *SRD5A2* gene sequence (exon 1) showing the homozygous Y91H mutation in the three siblings. The site of the mutations is denoted by the red arrow. Pedigree chart symbols: □ male, ○ female, ● affected individual, Δ spontaneous abortion, strikethrough symbols (deceased individual), double line indicates consanguineous marriage, and two diagonal lines from one point represent dizygotic twin.



**Figure 3. Expression of wild-type and mutant 17 $\beta$ -HSD3 enzymes.** HEK-293 cells were transiently transfected with C-terminally FLAG epitope-tagged plasmids for wild-type and mutant (T54A, M164T, L194P, and G289) 17 $\beta$ -HSD3 enzymes. After an incubation time of 48 h, cells were harvested and total cellular proteins subjected to SDS-polyacrylamide gel electrophoresis and western blotting. The mouse monoclonal antibody M2 was used to detect the FLAG epitope. The anti-actin polyclonal antibody sc-1616 was used as a loading control. One representative experiment out of three independently performed measurements is shown.



**Figure 4. Testosterone formation by wild-type and mutant 17 $\beta$ -HSD3 enzymes.** HEK-293 cells were transiently transfected with plasmids for wild-type and mutant 17 $\beta$ -HSD3 enzymes (T54A, M164T, L194P, and G289S). Transfected cells (15'000) were incubated at 37°C in 96-well plates with 200 nM androstenedione, containing 50 nCi [1,2,6,7-<sup>3</sup>H]-androstenedione, for different period of time. Testosterone formation was quantified after separation of steroids by TLC and scintillation counting. Results represent testosterone formation in percentage of initially supplied androstenedione. (A) Testosterone formation by mutants T54A, M164T, L194T, and G289S incubated for 0.5 h and 1 h compared with wild-type 17 $\beta$ -HSD3. Results show mean  $\pm$  SD of three independent measurements. (B) Testosterone formation by mutant M164T after 1 h, 2 h, 4 h and 8 h compared with wild-type 17 $\beta$ -HSD3 (WT). Results show mean  $\pm$  SD from four independent wells of a representative experiment.



**Figure 5. Pictures of wild-type enzyme and studied mutations.** (WT) Homology model of wild-type 17 $\beta$ -HSD3 (green) with bound NADPH (cyan) and androstenedione (cyan). Mutation sites labelled A-D correspond to the respective close-up. (A) T54A model (blue) shows the two hydrogen bonds lost compared to WT. (B) M164T model (orange) shows the void introduced by the mutation, which causes surrounding residues to gain in flexibility. (C) L194P model (gray) shows the rearrangement of hydrophobic amino acid side chains. (D) G289S model (magenta) shows the distance of >20 Å to the cofactor.



**Table 1: Clinical, hormonal and genetic results of 7 patients with 46, XY DSD**

#	Complaint	Age, Geographical origin	Consanguinity	Quigley Scoring	T (ng/ml)	AD (ng/ml)	DHT (ng/dl)	T/AD	T/DHT	Masculin-ity/ Feminin-ity index	HSD17B3 mutation	SRD5A2 mutation
1	primary amenorrhea	15 years, Giza	Positive	3	Basal: 2.1	7.8	25.3	0.27	8.3	Feminine gender identity with masculine behavioral characters	T54A	N/D
2	primary amenorrhea	16 years, Kaliobeya	Positive	3	Basal: 2.7	6.9	28.6	0.39	9.4	Masculine gender identity with undifferentiated gender role	T54A	N/D
3	virilization	20 years, NA	Positive	5	Basal: 2.5	9	48	0.28	5.2	Masculine gender identity (sex reversal was done)	L194P & c.588C>T	wild-type
4	ambiguous genitalia	2 m, Luxor	Negative	4	Basal: 1.7 Post hCG: 3.8	4.1 5.6	35 61.9	0.41 0.68	4.9 6.1	N/D	M164T	N/D
5	ambiguous genitalia	1m 2w, Kaliobeya	Positive	4	Basal: 1.3 Post hCG: 2.3	2.5 6.4	24.7 41.8	0.52 0.36	5.3 5.5	N/D	G289S	Y91H
6	virilization	11 years, Kaliobeya	Positive	4	Basal: 2.5	6.4	20.5	0.39	12.2	Masculine gender identity (arrangement for sex reversal)	G289S (heterozygous)	Y91H
7	virilization	11 years, Kaliobeya	Positive	4	Basal: 3.0	8.2	24.1	0.37	12.5	Masculine gender identity (arrangement for sex reversal)	G289S (heterozygous)	Y91H

NA = not available; N/D = not determined. Clinical and genetic analysis of patients 1, 3, 4 and 5 (except *SRD5A2* analysis) have been previously reported [13]

## References

1. Luu-The, V., et al., Structure of two in tandem human 17 beta-hydroxysteroid dehydrogenase genes. *Mol Endocrinol*, 1990. 4(2): p. 268-75.
2. Inano, H. and B. Tamaoki, Testicular 17 beta-hydroxysteroid dehydrogenase: molecular properties and reaction mechanism. *Steroids*, 1986. 48(1-2): p. 1-26.
3. Geissler, W.M., et al., Male pseudohermaphroditism caused by mutations of testicular 17 beta-hydroxysteroid dehydrogenase 3. *Nature genetics*, 1994. 7(1): p. 34-9.
4. Saez, J.M., et al., Familial male pseudohermaphroditism with gynecomastia due to a testicular 17-ketosteroid reductase defect. I. Studies in vivo. *J Clin Endocrinol Metab*, 1971. 32(5): p. 604-10.
5. Thigpen, A.E., et al., Molecular genetics of steroid 5 alpha-reductase 2 deficiency. *The Journal of clinical investigation*, 1992. 90(3): p. 799-809.
6. Tsuji, M., H. Shima, and G.R. Cunha, In vitro androgen-induced growth and morphogenesis of the Wolffian duct within urogenital ridge. *Endocrinology*, 1991. 128(4): p. 1805-11.
7. Marchetti, P.M. and J.H. Barth, Clinical biochemistry of dihydrotestosterone. *Annals of clinical biochemistry*, 2013. 50(Pt 2): p. 95-107.
8. Hughes, I.A., Disorders of sex development: a new definition and classification. *Best Pract Res Clin Endocrinol Metab*, 2008. 22(1): p. 119-34.
9. Boehmer, A.L., et al., 17Beta-hydroxysteroid dehydrogenase-3 deficiency: diagnosis, phenotypic variability, population genetics, and worldwide distribution of ancient and de novo mutations. *The Journal of clinical endocrinology and metabolism*, 1999. 84(12): p. 4713-21.
10. Rosler, A., Steroid 17beta-hydroxysteroid dehydrogenase deficiency in man: an inherited form of male pseudohermaphroditism. *The Journal of steroid biochemistry and molecular biology*, 1992. 43(8): p. 989-1002.
11. Ben Rhouma, B., et al., Novel cases of Tunisian patients with mutations in the gene encoding 17beta-hydroxysteroid dehydrogenase type 3 and a founder effect. *J Steroid Biochem Mol Biol*, 2017. 165(Pt A): p. 86-94.
12. Mazen, I., et al., Screening of genital anomalies in newborns and infants in two egyptian governorates. *Horm Res Paediatr*, 2010. 73(6): p. 438-42.
13. Hassan, H.A., et al., Mutational Profile of 10 Afflicted Egyptian Families with 17-beta-HSD-3 Deficiency. *Sexual development : genetics, molecular biology, evolution, endocrinology, embryology, and pathology of sex determination and differentiation*, 2016. 10(2): p. 66-73.
14. Mendonca, B.B., et al., 46,XY disorder of sex development (DSD) due to 17beta-hydroxysteroid dehydrogenase type 3 deficiency. *J Steroid Biochem Mol Biol*, 2017. 165(Pt A): p. 79-85.
15. Phelan, N., et al., Screening for mutations in 17beta-hydroxysteroid dehydrogenase and androgen receptor in women presenting with partially virilised 46,XY disorders of sex development. *European journal of endocrinology / European Federation of Endocrine Societies*, 2015. 172(6): p. 745-51.
16. Mendonca, B.B., et al., Male pseudohermaphroditism due to 17 beta-hydroxysteroid dehydrogenase 3 deficiency. Diagnosis, psychological evaluation, and management. *Medicine*, 2000. 79(5): p. 299-309.

17. George, M.M., et al., The clinical and molecular heterogeneity of 17betaHSD-3 enzyme deficiency. *Hormone research in paediatrics*, 2010. 74(4): p. 229-40.
18. Castro, C.C., et al., Clinical and molecular spectrum of patients with 17beta-hydroxysteroid dehydrogenase type 3 (17-beta-HSD3) deficiency. *Arquivos brasileiros de endocrinologia e metabologia*, 2012. 56(8): p. 533-9.
19. Lee, Y.S., et al., Phenotypic variability in 17beta-hydroxysteroid dehydrogenase-3 deficiency and diagnostic pitfalls. *Clinical endocrinology*, 2007. 67(1): p. 20-8.
20. Mindnich, R., G. Moller, and J. Adamski, The role of 17 beta-hydroxysteroid dehydrogenases. *Molecular and cellular endocrinology*, 2004. 218(1-2): p. 7-20.
21. Miller, S.A., D.D. Dykes, and H.F. Polesky, A simple salting out procedure for extracting DNA from human nucleated cells. *Nucleic acids research*, 1988. 16(3): p. 1215.
22. Soliman, H., Amr, K., El-Ruby, M., Mekkawy, M., Elaidy, A. and Mazen, I., Mutational pattern in the 5 $\alpha$  reductase 2 (SRD5A2) gene in 46, XY Egyptian DSD patients. *Middle East Journal of Medical Genetics*. 4(2): p. 77-82.
23. Engeli, R.T., et al., Biochemical analyses and molecular modeling explain the functional loss of 17beta-hydroxysteroid dehydrogenase 3 mutant G133R in three Tunisian patients with 46, XY Disorders of Sex Development. *The Journal of steroid biochemistry and molecular biology*, 2016. 155(Pt A): p. 147-54.
24. Sali, A., et al., Evaluation of comparative protein modeling by MODELLER. *Proteins*, 1995. 23(3): p. 318-26.
25. Biegert, A., et al., The MPI Bioinformatics Toolkit for protein sequence analysis. *Nucleic acids research*, 2006. 34(Web Server issue): p. W335-9.
26. Maestro, S.R.-. Schrödinger, LLC, New York, NY, 2016.
27. Jacobson, M.P., et al., On the role of the crystal environment in determining protein side-chain conformations. *J Mol Biol*, 2002. 320(3): p. 597-608.
28. Jacobson, M.P., et al., A hierarchical approach to all-atom protein loop prediction. *Proteins*, 2004. 55(2): p. 351-67.
29. Prime, S.R.-. Schrödinger, LLC, New York, NY, 2016.
30. The PyMOL Molecular Graphics System, V.S., LLC.
31. Persson, B., M. Krook, and H. Jornvall, Short-chain dehydrogenases/reductases. *Advances in experimental medicine and biology*, 1995. 372: p. 383-95.
32. Maestro, v., Schrödinger, LLC, New York, NY (2014).
33. Bertelloni, S., et al., 17beta-Hydroxysteroid dehydrogenase-3 deficiency: from pregnancy to adolescence. *Journal of endocrinological investigation*, 2009. 32(8): p. 666-70.
34. Sata, F., et al., Genetic polymorphisms of 17 beta-hydroxysteroid dehydrogenase 3 and the risk of hypospadias. *The journal of sexual medicine*, 2010. 7(8): p. 2729-38.
35. Margiotti, K., et al., Association of the G289S single nucleotide polymorphism in the HSD17B3 gene with prostate cancer in Italian men. *The Prostate*, 2002. 53(1): p. 65-8.
36. Moghrabi, N., et al., Deleterious missense mutations and silent polymorphism in the human 17beta-hydroxysteroid dehydrogenase 3 gene (HSD17B3). *The Journal of clinical endocrinology and metabolism*, 1998. 83(8): p. 2855-60.
37. Maimoun, L., et al., Phenotypical, biological, and molecular heterogeneity of 5alpha-reductase deficiency: an extensive international experience of 55 patients. *The Journal of clinical endocrinology and metabolism*, 2011. 96(2): p. 296-307.

38. Douglas, G., et al., Consensus in Guidelines for Evaluation of DSD by the Texas Children's Hospital Multidisciplinary Gender Medicine Team. *Int J Pediatr Endocrinol*, 2010. 2010: p. 919707.
39. Ahmed, S.F., et al., UK guidance on the initial evaluation of an infant or an adolescent with a suspected disorder of sex development. *Clin Endocrinol (Oxf)*, 2011. 75(1): p. 12-26.
40. Paris, F., et al., Disorders of sex development: neonatal diagnosis and management. *Endocr Dev*, 2012. 22: p. 56-71.
41. Chan, A.O., et al., Diagnosis of 5alpha-reductase 2 deficiency: is measurement of dihydrotestosterone essential? *Clin Chem*, 2013. 59(5): p. 798-806.
42. Khattab, A., et al., Pitfalls in hormonal diagnosis of 17-beta hydroxysteroid dehydrogenase III deficiency. *J Pediatr Endocrinol Metab*, 2015. 28(5-6): p. 623-8.
43. Akcay, T., et al., AR and SRD5A2 gene mutations in a series of 51 Turkish 46,XY DSD children with a clinical diagnosis of androgen insensitivity. *Andrology*, 2014. 2(4): p. 572-8.

## 4.5 Conclusion

Disorder of sexual development in men can be provoked by a number of causes including defects in androgen signaling, defects in androgen synthesis, defects in sex determining genes and many more[22, 130]. The most frequent causes of 46, XY DSD are; the complete androgen insensitivity syndrome (CAIS) and the partial androgen insensitivity syndrome (PAIS)[22, 131, 132]. Patients with CAIS often have a defect in androgen signaling, whereas the cause of PAIS is likely to be due to defects in AR co-regulators[132-134]. Patients with CAIS are usually raised as girls due their female genital phenotype. Despite higher androgen levels at puberty, those patients do not undergo virilization due to androgen insensitivity. Fortunately, the vast majority of affected patients are satisfied with their female gender[135]. However, this is not the case in patients with 17 $\beta$ -HSD3 deficiency, where virilization at puberty occurs due to extra testicular androgen formation. A high percentage of patients with 46, XY DSD raised a girls, change their gender to male at puberty due to pronounced virilization[128, 136]. These circumstances result in a stressful stage of life for the affected individual during puberty. If the 17 $\beta$ -HSD3 deficiency is diagnosed in early life, doctors and family members should decide whether the patient should be raised as a girl or a boy. The decision may be taken depending on phenotype of the external genitalia. Besides, it is important to recognize that every cause of 46, XY DSD is unique and requires extensive investigations[118]. Nowadays, it is possible to reconstruct genitals from both genders using plastic surgery in modern and well equipped hospitals[114, 137]. Patients raised as boys that underwent surgical correction and androgen replacement therapy can even have normal sexual intercourse[22]. If the patient is raised as a female, surgical corrections of the external and internal genitalia need to be performed. In the case of the appearance of internal gonads, they need urgently be removed to prevent excessive androgen production during puberty[22, 137]. Estrogen replacement therapy is required during puberty to develop secondary sexual characteristics[129].

Medical interventions are complicated and expensive and cannot be performed in every hospital. Unfortunately, most of the 17 $\beta$ -HSD3 deficient patients are reported in poor Arab countries and regions where the access to medical health care is limited[138]. In terms of diagnosis, 17 $\beta$ -HSD3 deficiency is a very rare disease but the actual number of affected people is very likely to be

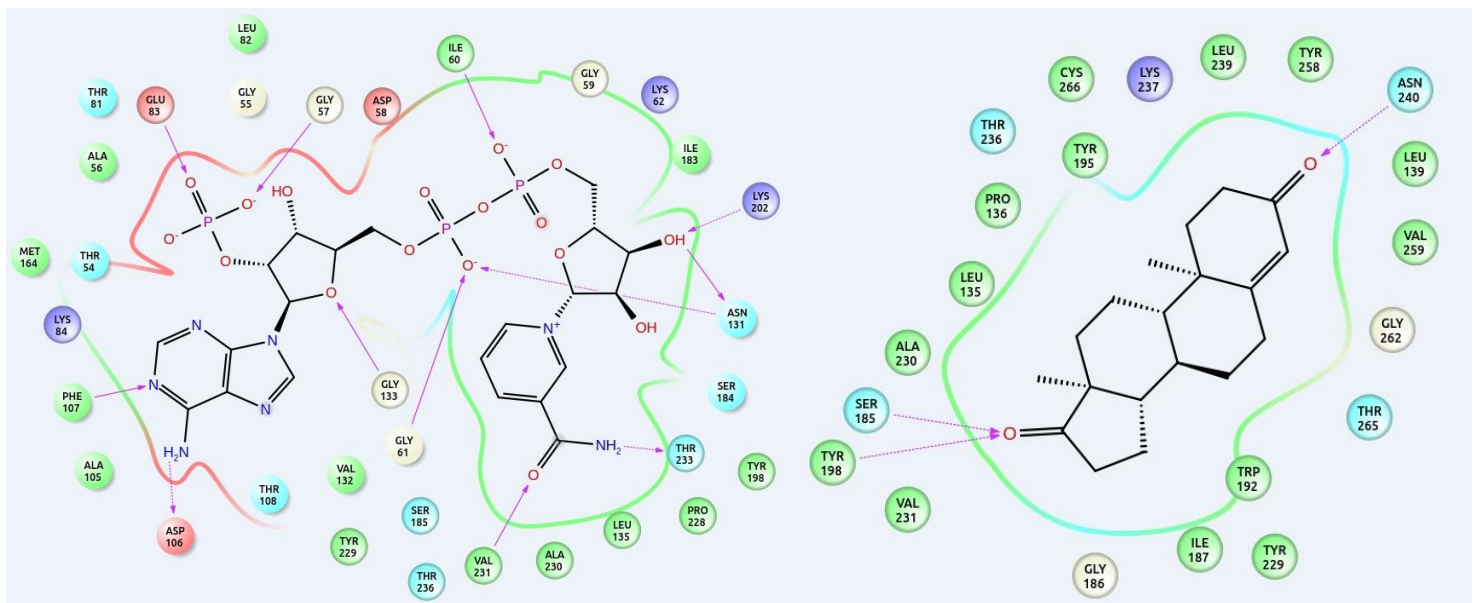
higher. Psychological, familial, and social factors prevent the patients from being open about their condition and therefore the incidence of 46, XY DSD may be underestimated[139].

Females have the same probability to inherit *HSD17B3* defective genes as men. However, so far no case is known in which 17 $\beta$ -HSD3 deficiency was diagnosed in a XX karyotype[130, 132]. Lower testosterone formation in a female embryo due to 17 $\beta$ -HSD3 deficiency seems to have no influence on female genital development or anything else resulting in a specific phenotype. Mutations in the *HSD17B3* gene in women appears not to affect genital development or fertility compared to the severe effects on male sexual development.

In this project we present a novel 17 $\beta$ -HSD3 homology model to visualize the effects of mutations on the 3-dimensional structure of the 17 $\beta$ -HSD3 enzyme. The construction of a 17 $\beta$ -HSD3 homology model, based on the 3-dimensional structure of the enzyme 17 $\beta$ -HSD1, was successful. Despite low sequence identity, the conserved cofactor binding among SDR's and their similar 3-dimensional structure resulted in a homology model with accurate cofactor and substrate binding sites[127]. NADPH (NADP<sup>+</sup> depicted) was shown to interact with the cofactor binding site through the formation of 12 hydrogen bonds (Figure 4). The catalytic triad containing Ser185, Tyr198, and Lys202 was facing the D-ring of the substrate androstenedione reinforcing the accuracy of the model (Figure 4). Due to the fact that 17 $\beta$ -HSD1 is localized in the cytosol and 17 $\beta$ -HSD3 is anchored to the ER membrane via its N-terminus, we were unable to predict the 3-dimensional structure of the amino acids in this specific region. The model allowed us to predict on a molecular level the cause of the loss of activity of 17 $\beta$ -HSD3 mutations identified in humans. In most of the cases, the mutated amino acid residues adversely affected cofactor or substrate binding of the protein. The main limitation of the applied homology model was the lack of a 17 $\beta$ -HSD3 crystal structure. Additionally, it was not possible to investigate mutations potentially affecting the induced fit of the protein as well as mutations interfering with the ER membrane binding. Our generated 17 $\beta$ -HSD3 homology model has its limitations and biochemical analyses need to be performed to confirm our predictions on enzyme activity.

However, not every mutation found in the *HSD17B3* gene abolishes the activity of the enzyme. In most clinical reports of 17 $\beta$ -HSD3 deficiency, mutated enzymes were not biochemically analyzed. Polymorphisms such as G289S[81] do not affect the protein activity. Therefore, other defects need to be inspected to understand the causes of the disorder. Taken together, five different

mutations in the *HSD17B3* gene (G133R, C206X, T54A, M164T, and L194P) and one polymorphism (G289S) were biochemically analyzed in this project. Biochemical evaluation of mutations in the *HSD17B3* gene confirm the diagnosis of  $17\beta$ -HSD3 deficiency in suspected patients. An early diagnosis of  $17\beta$ -HSD3 deficiency and sequential medical interventions are crucial to prevent patients from undergoing social and psychological stress later on in life. A fast diagnosis is beneficial for decisions regarding gender assignment by doctors and family members. Our data will help clinicians to diagnose  $17\beta$ -HSD3 deficiency more effectively.



**Figure 4.** 2-Dimensional model of the  $17\beta$ -HSD3 cofactor and substrate binding pocket. NAD<sup>+</sup> embedded in the cofactor binding pocket (left) stabilized through the formation of 12 hydrogen bonds with amino acids side chains. Androstenedione embedded in the substrate binding pocket, stabilized through hydrogen bonds by Ser185 and Tyr198 (right).



## 5. Project 3: Murine Leydig Cell Lines

### 5.1 Introduction

Testosterone plays a critical role in sexual differentiation and regulates a variety of physiological functions. These include muscle growth, bone density, and libido. In mammals, testosterone formation occurs in the Leydig cells, which are found in the interstitial compartment of the testes[140]. These cells produce the majority of systemic testosterone through *de novo* synthesis from cholesterol[141]. The dramatic phenotypic effect of loss of function mutations in the *HSD17B3* gene highlight the importance of this enzyme in male sexual development. Over the course of a life time, humans are exposed to a huge variety of chemical compounds used in personal care products or as food additives[142]. Any compound that potentially interferes with the activity or transcriptional regulation of 17 $\beta$ -HSD3 may exert toxicologically relevant effects. Therefore, research on environmental disrupting chemicals (EDC) that can interfere with androgen action in humans is of particular interest. Due to the rapid evolution of synthetic chemistry, thousands of new organic compounds entered the market in the past decades[143]. Most investigations on endocrine disrupting effects of xenobiotic compounds are limited to steroid receptor interferences[144, 145]. Little is known about the impact of xenobiotics on pre-receptor regulation or non-receptor mediated effects[142]. Therefore, the development of accurate, cheap, and rapid endocrine disrupting testing systems that test for endocrine pre-receptor regulation would be helpful. In the first study, we reviewed the literature for cell models (which include Leydig cells) currently used to investigate the disruption of steroidogenesis by xenobiotics. We identified three potential Leydig cell lines which could be further characterized. In the second study, we were focused on establishing a Leydig cell model which endogenously expresses 17 $\beta$ -HSD3, in order to examine xenobiotic compounds that potentially disrupt the formation of testosterone. Ideally, the cell model could be used to test the potential effects of xenobiotic compounds on 17 $\beta$ -HSD3 activity and on the transcriptional regulation of *Hsd17b3*. In an unpublished work carried out in our lab, we examined the influence of organotin on the activation of the human *HSD17B3* promoter. Triphenyltin (TPT) and Tributyltin (TBT) were shown to activate the human *HSD17B3* promoter at nanomolar concentrations (Fürstenberger et al., unpublished data). Since they are not commercially available human Leydig cell lines, we selected murine Leydig cell lines to study the influence of TPT and TBT on transcriptional *Hsd17b3*

messenger ribonucleic acid (mRNA) levels. In addition to transcriptional regulation, we were also interested in assessing 17 $\beta$ -HSD3 activity. In this project, three different murine Leydig cell lines (MA-10, BLTK, TM3) were used to establish a screening model able to identify compounds interfering with testosterone synthesis. Fortunately, human and murine androgen steroidogenesis are similar, indicating that murine Leydig cells could be a suitable model to study testosterone disruption that may be further extrapolated to humans.

## 5.2 Paper 8 (Odermatt et al, 2016)

### **Disruption of steroidogenesis: Cell models for mechanistic investigations and as screening tools**

Alex Odermatt, Petra Strajhar, Roger T. Engeli

Published manuscript

**Contribution:** Carefully reviewed the section on Leydig cell culture models. Collected and overviewed references about the most important Leydig cell models in the literature.

**Aims:** Provided an overview of all available gonadal and adrenal cell lines regarding their suitability as screening tools for steroidogenic disruption by xenobiotics.

**Results:** This review demonstrates the species specific differences between rodent and human cell lines, and highlights that steroidogenesis is altered in most cell lines due to their tumor origins.

**Conclusion:** The currently available cell lines are limited as screening tools for steroidogenesis. Future efforts should specifically aim to develop a human Leydig cell producing testosterone.



## Review

# Disruption of steroidogenesis: Cell models for mechanistic investigations and as screening tools



Alex Odermatt\*, Petra Strajhar, Roger T. Engeli

Swiss Center for Human Toxicology and Division of Molecular and Systems Toxicology, Department of Pharmaceutical Sciences, Pharmacenter, University of Basel, Klingelbergstrasse 50, 4056 Basel, Switzerland

## ARTICLE INFO

*Article history:*

Received 8 October 2015  
Received in revised form 31 December 2015  
Accepted 20 January 2016  
Available online 22 January 2016

*Keywords:*

Adrenal  
Testis  
Ovary  
Leydig  
Granulosa  
Endocrine disrupting chemical  
*In vitro*

## ABSTRACT

In the modern world, humans are exposed during their whole life to a large number of synthetic chemicals. Some of these chemicals have the potential to disrupt endocrine functions and contribute to the development and/or progression of major diseases. Every year approximately 1000 novel chemicals, used in industrial production, agriculture, consumer products or as pharmaceuticals, are reaching the market, often with limited safety assessment regarding potential endocrine activities. Steroids are essential endocrine hormones, and the importance of the steroidogenesis pathway as a target for endocrine disrupting chemicals (EDCs) has been recognized by leading scientists and authorities. Cell lines have a prominent role in the initial stages of toxicity assessment, *i.e.* for mechanistic investigations and for the medium to high throughput analysis of chemicals for potential steroidogenesis disrupting activities. Nevertheless, the users have to be aware of the limitations of the existing cell models in order to apply them properly, and there is a great demand for improved cell-based testing systems and protocols. This review intends to provide an overview of the available cell lines for studying effects of chemicals on gonadal and adrenal steroidogenesis, their use and limitations, as well as the need for future improvements of cell-based testing systems and protocols.

© 2016 Elsevier Ltd. All rights reserved.

## Contents

1. Introduction	9
2. Steroidogenesis	10
3. Leydig cell models to investigate steroidogenesis	11
4. Cell-based systems to study effects of EDCs on ovarian steroidogenesis	14
5. Adrenal cell models to investigate disruption of steroidogenesis	15
6. Conclusions and outlook	17
Acknowledgements	17
References	17

## 1. Introduction

There is an increasing interest in the identification of chemicals that interfere with the endocrine system. The Endocrine Society defines an endocrine disrupting chemical (EDC) as an “exogenous chemical or mixture of chemicals that can interfere with any aspect of hormone action” [1]. It is important, in our opinion, to distinguish between transient influences followed by adaptation

and disruption of endocrine functions leading to adverse health effects. This is considered by the European Union (EU) that defines an EDC as an “exogenous substance that causes adverse health effects in an intact organism, or its progeny, secondary to changes in endocrine function” [2,3]. The protection of human health and the environment is of high priority for major organizations and regulatory authorities. Regarding the large number of chemicals that need to be tested for potential endocrine disrupting effects, in programs such as REACH (Registration, Evaluation, Authorization and Restriction of Chemicals, [http://ec.europa.eu/growth/sectors/chemicals/reach/index\\_en.htm](http://ec.europa.eu/growth/sectors/chemicals/reach/index_en.htm)), the EPA’s EDSP (Environmental

\* Corresponding author.

E-mail address: [alex.odermatt@unibas.ch](mailto:alex.odermatt@unibas.ch) (A. Odermatt).

Protection Agency's Endocrine Disruptor Screening Program, <http://www.epa.gov/endo/>) or the FDA (U.S. Food and Drug Administration) guidelines for drug development (<http://www.fda.gov/Drugs/GuidanceComplianceRegulatoryInformation/Guidances/>), it is important to first evaluate the most relevant chemicals, *i.e.* chemicals with evidence of causing adverse effects and for which relevant exposure is known or can be expected. Besides chemicals used in industrial production, agriculture, electronics, and consumer products, the safety of pharmaceuticals and food constituents need to be assessed. Thus, a huge number of chemicals need to be tested for a wide range of possible adverse effects, including such caused by a disruption of steroid hormone action.

Amongst other endocrine hormones, steroids play crucial roles in the regulation of nearly all physiological processes. Several reports provided evidence for an association of disturbances of steroid hormone action caused by exogenous chemicals with developmental defects [4], infertility and reproductive dysfunctions [5,6], testicular, prostate and breast cancer [7–9], obesity and diabetes [10–12], immune disorders and neurobehavioral and learning dysfunctions [13,14]. Further research is needed to identify other chemicals disrupting steroid hormone action, to evaluate the mechanisms by which such chemicals disrupt steroid hormone action, and to assess the critical exposure windows and concentrations that are relevant regarding development and progression of diseases.

For the initial endocrine safety testing of a large number of chemicals, improved *in silico* and *in vitro* assays are needed to facilitate the prioritization of chemicals for further toxicological investigations. Cell-based steroidogenesis assays represent a suitable starting point to assess disturbances of steroid biosynthesis, induced by direct inhibition of steroidogenic enzymes or by affecting their expression. The advantage of the cell-based models is that several enzymes and receptors required for the synthesis of steroids, as well as the signaling pathways regulating their activities, may be covered in a single assay. In addition to the identification of potentially hazardous chemicals, the cell-based steroidogenesis assays allow first mechanistic insights into the mode-of-action of EDCs; however, the users need to be aware of the limitations of the system applied in order to avoid drawing inappropriate conclusions and over-interpretation of results. This review focuses on the cell lines that are available to study steroidogenesis, their advantages and limitations, and the existing

gaps for early safety testing of chemicals disrupting steroid homeostasis.

## 2. Steroidogenesis

Primary organs that are producing steroids from their precursor cholesterol include the adrenal glands and the gonads, with testes in males and ovaries in females. Additionally, in females the placenta produces high amounts of progesterone during pregnancy [15]. Other organs expressing steroidogenic enzymes include the brain [16,17], the intestinal tract [18] and the skin [19]. However, the steroids produced in these tissues seem to be restricted to affect local rather than systemic levels, and the relevance of steroidogenesis in these tissues will not be discussed.

The major steroidogenic organs synthesize steroids *de novo* from cholesterol that is either produced directly by the cell from acetyl-CoA or taken up from dietary cholesterol bound to low-density lipoproteins (LDL) in the circulation (for a comprehensive review see [20]). Cholesterol can be esterified, stored in lipid droplets and be released by the activity of hormone-sensitive lipase. The rate-limiting step in adrenal and gonadal steroidogenesis is the uptake of cholesterol into the mitochondria. The steroidogenic acute regulatory protein (StAR) facilitates the transfer of cholesterol from the outer to the inner mitochondrial membrane, and its conversion to pregnenolone by the cytochrome P450 side chain cleavage enzyme (P450<sub>sc</sub>, CYP11A1) in cooperation with adrenodoxin reductase that functions as an electron transfer protein of CYP11A1 [20]. Dependent on the organ, pregnenolone is then further converted by tissue- and cell type-specific enzymes into androgens, estrogens, glucocorticoids or mineralocorticoids.

The cortex of the adult human adrenals is responsible for the production of mineralocorticoids in the *zona glomerulosa*, glucocorticoids in the *zona fasciculata* and precursors of active androgens in the *zona reticularis* (Fig. 1). The *zona reticularis* expresses high levels of CYP17A1 [21], which possesses 17 $\alpha$ -hydroxylase activity for the formation of 17 $\alpha$ -hydroxypregnenolone and 17,20-lyase activity for the subsequent formation of dehydroepiandrosterone (DHEA). The high expression of cytochrome b5, in the presence of cytochrome P450 reductase, allows efficient 17,20-lyase activity that is needed for the production of DHEA [20,22]. Additionally, the *zona reticularis* expresses high levels of the steroid sulfotransferase SULT2A1 that is responsible

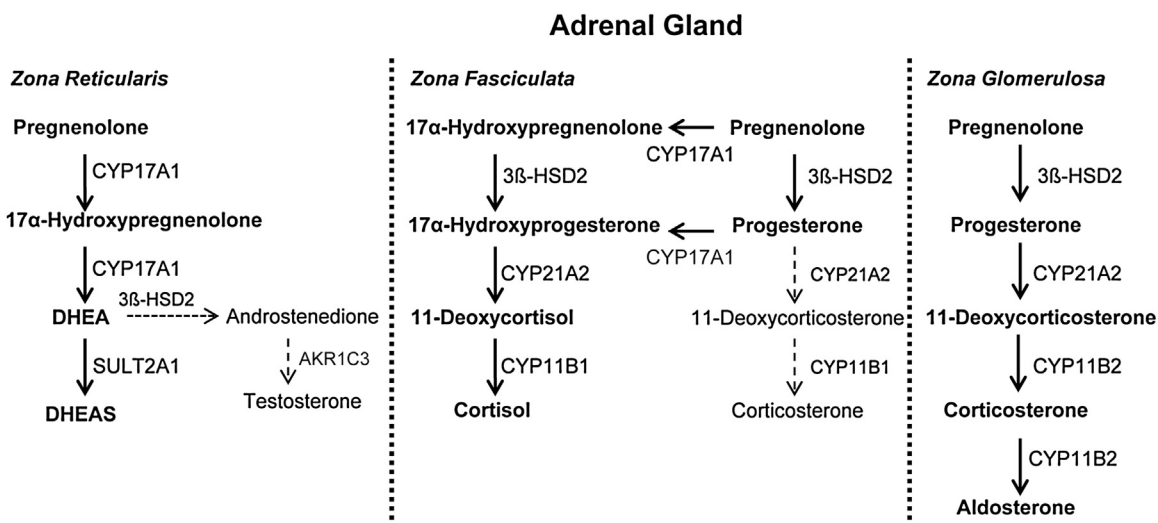


Fig. 1. Schematic overview of adrenal steroidogenesis. Major steroids produced are indicated in bold and by solid lines, minor metabolites are indicated by dashed lines.

for the formation of sulfated DHEA (DHEAS) [23], the most abundant steroid in human blood [24]. Importantly, 3 $\beta$ -hydroxysteroid dehydrogenase 2 (3 $\beta$ -HSD2) is expressed in the *zona reticularis* at very low levels, thus leading to only low amounts of  $\Delta$ 4-androstene-3,17-dione (androstenedione) production [20]. Since 17 $\beta$ -hydroxysteroid dehydrogenase type 3 (17 $\beta$ -HSD3) is absent and 17 $\beta$ -HSD5 (AKR1C3) expressed at very low levels in the *zona reticularis* [21,25], only very low levels of testosterone are produced by the adrenals [26,27]. CYP21A2 is absent in the *zona reticularis*, thus no mineralocorticoids and glucocorticoids are formed in this layer [20].

In the *zona fasciculata* pregnenolone is converted to 17 $\alpha$ -hydroxypregnenolone by CYP17A1, and pregnenolone and 17 $\alpha$ -hydroxypregnenolone are converted to progesterone and 17 $\alpha$ -hydroxyprogesterone, respectively, by 3 $\beta$ -HSD2. Most of the progesterone formed is also 17 $\alpha$ -hydroxylated. Further metabolism by CYP21A2 leads to 11-deoxycortisol and lower amounts of 11-deoxycorticosterone that are further converted by CYP11B1, which is specifically expressed in this zone, into cortisol and corticosterone, respectively [20,28]. Cytochrome b5 is expressed at background levels in the *zona fasciculata* [21], resulting in very low CYP17A1 17,20-lyase activity and thus low amounts of DHEA formation [20]. The *zona fasciculata* expresses the melanocortin-2-receptor and is therefore responsive to adrenocorticotropic hormone (ACTH) [20,28].

The *zona glomerulosa* does not express CYP17A1, and pregnenolone is converted to progesterone by 3 $\beta$ -HSD2 and further to 11-deoxycorticosterone by CYP21A2, and to corticosterone and aldosterone by CYP11B2. In the adrenals, CYP11B2 expression is restricted to the *zona glomerulosa* and the production of aldosterone is regulated by angiotensin II receptors [20].

The human fetal adrenals produce high amounts of DHEAS, which is abolished soon after birth where the adrenals mainly consist of a *zona glomerulosa* and a *zona fasciculata* and thus produce mineralocorticoids and glucocorticoids [29]. The *zona reticularis* actively starts producing adrenal androgens at adrenarche at around 6–8 years of age and reaching peak levels in the third decade of life, before declining gradually [30,31].

In the testis, steroidogenesis is restricted to the Leydig cells. They convert pregnenolone by CYP17A1 into 17 $\alpha$ -hydroxypregnenolone and further to DHEA (Fig. 2). Because of the high expression of 3 $\beta$ -HSD2 and 17 $\beta$ -HSD3 but the absence of SULT2A1, DHEA is not sulfated and therefore further converted to androstenediol, or by a lower extent to androstenedione, and subsequently to testosterone in Leydig cells [20,32]. Furthermore, CYP21A2, CYP11B1 and CYP11B2 are absent, thus no gluco- and mineralocorticoids are produced. Testicular steroidogenesis is under the control of human chorionic gonadotropin (hCG) and luteinizing hormone (LH).

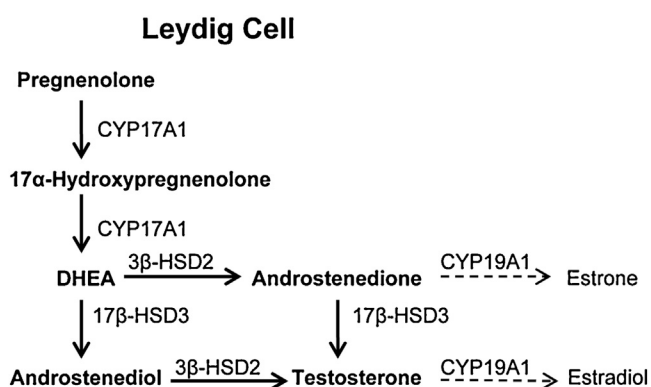


Fig. 2. Schematic overview of steroidogenesis in Leydig cells.

In the ovaries, steroidogenesis is mediated by theca and granulosa cells. The granulosa cells are located in the avascular cellular compartment surrounding the oocyte, and the theca cells reside in the ovarian stroma; these cellular compartments are separated by the basal membrane. The theca and granulosa cells both express StAR and CYP11A1 [33]. Because granulosa cells do not express CYP17A1 [34], they can synthesize pregnenolone from cholesterol and they convert it further to progesterone in the *corpus luteum* (Fig. 3) [20]. However, for the production of estrogens, pregnenolone needs to be secreted from the granulosa cells and taken up by the theca cells, or it is produced directly by the theca cells, to form DHEA. The theca cells express 3 $\beta$ -HSD2 and convert DHEA into androstenedione [35]. Androstenedione is then delivered back to the granulosa cells for the aromatase-dependent production of estrogens [34]. Granulosa cells also express 17 $\beta$ -HSD1, which is needed for the conversion of estrone into estradiol. There are cycle-dependent changes in ovarian steroidogenesis: in the luteal phase the luteinized granulosa cells are supplied with sufficient cholesterol, due to enhanced vascularization of the previously avascular compartment, and elevated LH levels enhance the expression of CYP11A1 and 3 $\beta$ -HSD2, resulting in the synthesis of high amounts of progesterone [33]. In the follicular phase, follicle stimulating hormone (FSH) enhances the expression of aromatase and 17 $\beta$ -HSD1 for the production of increased amounts of estradiol from theca cell-derived androstenedione. LH also activates LH receptors on theca cells to induce CYP17A1 expression, thereby enhancing androgen precursors for estrogen production by granulosa cells. Thus, a tight control of the cooperation of granulosa and theca cell function is essential for the appropriate regulation of estradiol synthesis.

### 3. Leydig cell models to investigate steroidogenesis

Three independent large epidemiological studies revealed a decline in male serum testosterone levels in the general population [36–38]. Obesity was identified as a contributing factor for some but not all observations [39]. Increasing evidence suggests that exposures to EDCs contribute to male reproductive diseases and that prevention of EDC exposures may reduce the burden of male reproductive health problems [40]. As an example, cryptorchidism is a typical impairment following exposure to antiandrogenic chemicals during male sexual development [41]. Evidence was provided that levels of polybrominated diphenyl ethers (PBDEs) in

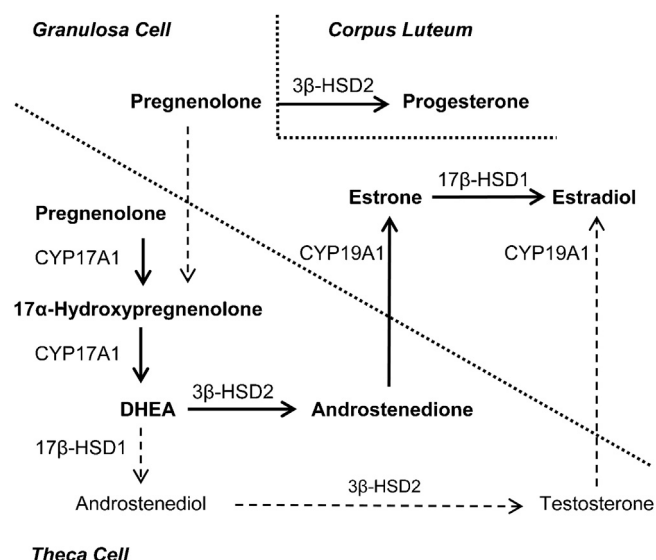


Fig. 3. Schematic overview of ovarian steroidogenesis.

human breast milk are associated with congenital cryptorchidism, although a contribution of other environmental factors cannot be excluded [42]. PDBEs have been shown in *in vitro* studies to directly antagonize AR activity (IC<sub>50</sub> of approximately 5  $\mu$ M for the mixture DE-71 in an MDA-kb2 cell model expressing an AR-dependent luciferase reporter), and PDBEs additively and/or synergistically acted with other AR antagonistic compounds [43]. In *in vivo* studies PDBEs were shown to cause diminished growth of androgen-dependent tissues and a delay in puberty in the male rat following a pubertal exposure to 60 and 120 mg/kg/day of the DE-71 mixture [44]. Although such high exposure levels are unlikely to be reached in humans, the fact that humans are exposed to a multitude of compounds that may exert additive or synergistic effects emphasizes the need for the screening of chemicals for potential antiandrogenic effects. Because of the high public demand to reduce animal testing [45], improved cell-based assays are needed that allow the identification of chemicals disrupting the biosynthesis of steroids and the gaining of insights into the mode-of-action of such chemicals.

There are several immortalized rodent Leydig cell lines available for studying the regulation of steroidogenesis and to assess the impact of substances on steroid hormone production. However, to our knowledge, no human Leydig cell model is currently available that can be used for screening purposes and for toxicological studies. The available rodent Leydig cell lines have been derived from spontaneous tumors, upon experimental induction, or by *in vitro* immortalization. All of these cell systems have their limitations, as some of the steroidogenic enzymes and regulatory pathways are expressed at very low levels, if at all, likely as a result of the selection of cell clones that rapidly proliferate and because of dedifferentiation and loss of initial phenotype during prolonged cultivation.

Probably the most widely used immortalized Leydig cell line is MA-10 [46]. MA-10, the related MA-12, and the frequently used mLTC-1 are all derived from a C57Bl/6 Leydig cell tumor (designated M5480) [47]. These cell lines express LH receptors, and incubation with LH/hCG induces cAMP-dependent steroidogenesis. MA-10 cells also express mouse epidermal growth factor receptor (EGFR), which suppresses the hCG-induced steroidogenesis [48]. In both, MA-10 and mLTC-1, progesterone was the main steroid being produced, in line with the observation that the original tumor M5480 secreted progesterone but only very low amounts of testosterone, and the two cell lines displayed similar functional characteristics [47]. These observations suggest that 3 $\beta$ -hsd1 activity is dominant over Cyp17a1; therefore, pregnenolone is mainly converted into progesterone, with only minor amounts being further converted into androstenedione and testosterone. For these reasons, we propose that, using progesterone as a read-out, MA-10 and mLTC-1 cells can serve as suitable models to detect chemicals that affect the induction of steroidogenesis, the cAMP- and PKA-dependent signaling, or that directly inhibit the activities of StAR, Cyp11a1 or 3 $\beta$ -hsd1. Due to the generation of only low amounts of testosterone by these cell lines, it is difficult to quantitatively assess the effect of chemicals that disrupt Cyp17a1 or 17 $\beta$ -hsd3 activities. Nevertheless, the mRNA expression of key steroidogenic enzymes, including StAR, Cyp11a1 and 3 $\beta$ -hsd1, and to a lesser extent that of Cyp17a1 and 17 $\beta$ -hsd3, has been detected in MA-10 and mLTC-1 cells, and has been found to be affected upon exposure to chemical modulators [49–51].

MA-10 cells are applied by many investigators to study the impact of EDCs on the regulation of steroidogenesis; only a few will be mentioned in this review as examples. Recent studies on effects of bisphenol A (BPA) and its analogs on steroidogenesis in MA-10 cells suggested that tetrabromobisphenol A (TBBPA) concentration-dependently increased testosterone production at

concentrations of 3  $\mu$ M and higher, while bisphenol S (BPS) had no effect and BPA and bisphenol F (BPF) induced testosterone secretion only at very high concentrations (30 and 100  $\mu$ M, respectively) [49,50]. Following incubation of the cells for 48 h in the presence of 10  $\mu$ M of TBBPA, BPF or BPS an increased production of progesterone, and in the case of TBBPA of 17 $\alpha$ -hydroxyprogesterone and androstenedione, was measured. Furthermore, incubation of cells with 10  $\mu$ M of BPF, BPS or TBBPA led to an elevated expression of 5 $\alpha$ -reductase 1, indicating an increased production of 5 $\alpha$ -androstenedione and dihydrotestosterone. Importantly, the authors provided evidence that the TBBPA-mediated increase in testosterone production may be due to an inhibition of the efflux of androgen precursors required for testosterone synthesis by the multidrug resistance proteins MRP1 and MRP4 [50]. These observations emphasize the need to include steroid transporters in the assessment of EDCs and provide a further explanation for the low amount of testosterone produced by MA-10 cells under basal conditions.

MA-10 cells were also used to study direct effects of mono-phthalates on testicular steroidogenesis [52]. The LH-induced production of cAMP and progesterone was significantly inhibited in MA-10 cells treated with 30  $\mu$ M of mono(2-ethylhexyl) phthalate (MEHP), whereas testosterone production was significantly lowered upon incubation of the cells with 1  $\mu$ M MEHP, 3  $\mu$ M monobutylphthalate (MBP), 10  $\mu$ M mono-*n*-octylphthalate (MnOP) or 3  $\mu$ M monebenzylphthalate (MBEP) but not in the presence of monoethylphthalate (MEP) or monomethylphthalate (MMP) [52]. At the high concentration of 100  $\mu$ M MEHP the mRNA expression levels of StAR, Cyp11A1 and Cyp17A1 were down regulated. Interestingly, in mLTC-1 cells (not induced by LH) the phthalates di-*n*-butyl phthalate (DBP), MBP, di(2-ethylhexyl) phthalate (DEHP) and MEHP seemed to increase testosterone production at low concentrations of 0.001 to 0.1  $\mu$ M but inhibited at high concentrations of 100  $\mu$ M. Interestingly, the mRNA expression levels of Cyp11A1, Cyp17 and 3 $\beta$ -HSD1 were decreased even at concentrations as low as 0.1  $\mu$ M [53,54]. Also, the impact of the major metabolites of MEHP and DEHP on the expression of steroidogenic genes has been analyzed, suggesting that the metabolite 2-ethylhexanal might inhibit Leydig cell testosterone formation, although this effect was only observed at high concentrations of 100  $\mu$ M [55]. The human relevance of such high concentrations are questionable and further research using lower concentrations is needed. Also, it should be noted that progesterone and testosterone were measured by ELISA in this study. Furthermore, a possible effect of phthalates on the efflux of androgen precursors or on cholesterol flux in MA-10 or in mLTC-1 cells has not been investigated.

Other studies focused on initial steps of steroidogenesis. Incubation of MA-10 and mLTC-1 cells with an organochlorine compound mixture resulted in a decreased expression of StAR, CYP11A1 and the adrenodoxin reductase, enzymes crucial for the production of pregnenolone from cholesterol [56]. The cAMP- and hCG-induced production of progesterone tended to be lower at 1  $\mu$ g/ml and was significantly lower at 10  $\mu$ g/ml of organochlorine mixture. Also, the UV-filter chemical 2,2',4,4'-tetrahydroxybenzophenone (BP2), applied at 30  $\mu$ M, was found to alter the expression of StAR, 3 $\beta$ -hsd and Cyp17a1 and had opposite effects on Leydig cell steroidogenesis than thyroid hormone signaling [57]. Moreover, MA-10 cells were employed to test pesticide formulations that are widely used in agriculture. The pesticide mixture Roundup, a broad-spectrum systemic herbicide containing glyphosate (N-phosphonomethyl-glycine), inhibited the cAMP analog-induced progesterone production at subcytotoxic concentrations of 25  $\mu$ g/ml by decreasing the expression of the StAR protein [58]. Furthermore, the benzodiazepine midazolam was found to stimulate progesterone and testosterone production, measured



by radio-immunoassay, at the subcytotoxic concentrations of 30 and 150  $\mu\text{M}$  in primary mouse Leydig cells and in MA-10 cells by an induction of the expression of the peripheral-type benzodiazepine receptor and StAR, probably via a pathway involving protein kinase A (PKA) and protein kinase C (PKC) [59]. Murine mLTC-1 Leydig cells were used to further investigate the reproductive toxicity of perfluorooctanoic acid (PFOA) that was observed in mice treated by gavage [60]. Exposure of mLTC-1 cells with 100  $\mu\text{M}$  PFOA decreased Cyp11a1 mRNA and protein expression and at 300  $\mu\text{M}$  PFOA progesterone production was significantly decreased. Also, StAR protein seemed to be decreased, likely as a result of oxidative stress caused by PFOA exposure [60,61]. The mycotoxin zearalenone at concentrations of 5  $\mu\text{M}$  was suggested to affect steroidogenesis in mLTC-1 cells by disrupting lipid metabolism and inducing endoplasmic reticulum stress-mediated apoptosis [62,63]. Furthermore, the polybrominated diphenyl ether BDE-47 at a concentration of 1  $\mu\text{M}$  was found to decrease progesterone production via cAMP-PKA-dependent downregulation of CYP11a1 [64]. Thus, a multitude of chemicals were shown to affect initial steps of steroidogenesis by different mechanisms. It should be noted that in order to judge on the human relevance of the findings described above further investigations are required, as in most if these *in vitro* studies the concentrations applied were either much higher than concentrations measured in humans or data on such concentrations are not yet available.

Another mouse Leydig cell line, designated TTE1, was derived from transgenic mice, upon immortalization using a temperature-sensitive simian virus 40 (SV40) large T-antigen [65]. These cells can be grown at 33 °C and differentiated at a non-permissive temperature of 39 °C. The cell model was used to study genes involved in Leydig cell differentiation characteristics, and the expression of the terminal enzyme of testosterone synthesis, 17 $\beta$ -hsd3, was confirmed at least on the mRNA level [66]. TTE1 cells were only used in very few studies, so for example to investigate the impact of diethylstilbestrol on the expression of steroidogenic genes [67,68]. Diethylstilbestrol at concentrations of 50 nM or higher decreased Cyp11a1 expression and, furthermore, diminished apoptotic cell death pathways and DNA repair capability, suggesting an increased carcinogenic potential of the exposed cells.

Mice transgenic for the SV40 T-antigen under the control of the inhibin- $\alpha$  promoter were used to establish the steroidogenic Leydig cell line BLT-1 [69]. BLT-1 cells responded well to LH and hCG by increased cAMP levels and enhanced production of progesterone. As observed for MA-10 and mLTC-1, BLT-1 cells are only producing very low amounts of testosterone, as measured by enzyme immunoassay. Regarding investigations into EDCs, the BLT-1 derived cell clone BLTK1 was used to study several environmental toxicants [70]. BLTK1 cells seem to express all key steroidogenic proteins such as StAR, Cyp11a1, Cyp17a1, 3 $\beta$ -hsd1, 17 $\beta$ -hsd3 and 5 $\alpha$ -reductase 1. These cells were shown to respond to hCG and forskolin, which resulted in enhanced cAMP production and expression of steroidogenic genes. An elevated production of progesterone and testosterone was indicated by enzyme immuno assays measurements. The antifungals prochloraz (30  $\mu\text{M}$ ) and triclosan (30  $\mu\text{M}$ ) seemed to decrease the hCG-induced testosterone production, whereas MEHP (300  $\mu\text{M}$ ) and atrazine (at concentrations of 30  $\mu\text{M}$  or higher) promoted basal testosterone formation but inhibited the hCG-dependent testosterone synthesis. Furthermore, the triazine herbicides atrazine, simazine, propazine and terbuthylazine were reported to enhance progesterone and testosterone production in BLTK1 cells at high concentrations (with significant effects observed at 100  $\mu\text{M}$  or higher), effects explained by the altered expression of steroidogenic genes [71]. However, in these studies very high concentrations of questionable human relevance were used.

The non-tumor mouse epithelial Leydig cell line TM3 was originally derived from the testis of an immature Balb/c mouse [72]. TM3 cells respond to LH, but not FSH, with an increased cAMP production [73]. Evidence was provided that LH and EGF are involved in the regulation of cyclin-dependent kinase 5 (Cdk5) expression and activity, and that this signaling pathway modulates hormonally stimulated testicular steroidogenesis [74]. Furthermore, LRH-1 was found to regulate Cyp19a1 expression via promoter II in multiple testis cell types [75]. Additionally, a role for hypoxia-inducible factor-1 $\alpha$  by mediating hypoxia-dependent changes on steroidogenesis by regulating the transcriptional expression of 3 $\beta$ -hsd1 was reported [76]. The C1q and tumor necrosis factor-related protein (CTRP3) was found to induce testosterone production by increasing cAMP and phosphorylation of cAMP response element-binding protein (CREB) by PKA and subsequently enhancing the expression of StAR and Cyp11a1 [77]. TM3 cells express V1 type arginine vasopressin receptors that seem to act independent of the adenylate cyclase system [78] and calcitonin receptors, which mediate calcium influx and stimulate cAMP formation and testosterone secretion [79]. They also express inhibin/activin  $\beta$ -A subunits and activin receptors II and IIB [80]. A role for the Src tyrosine kinase in the regulation of phosphodiesterase PDE4 activity and the production of cAMP was reported [81]. TM3 cells mainly produce progesterone, and only minor amounts of testosterone (own observations), suggesting that they can serve as a model to study early steps of the regulation of steroidogenesis and direct inhibition of the activities of StAR, Cyp11a1 and 3 $\beta$ -hsd1.

The TM3 mouse Leydig cell line is frequently used to study the impact of environmental pollutants on testicular toxicity and on alterations in steroidogenesis. A study on gap junctional intercellular communication in TM3 cells showed inhibitory effects by estradiol and diethylstilbestrol via an estrogen receptor (ER)-dependent mechanism [82]. Interestingly, similar effects were observed at 10 pM and 10  $\mu\text{M}$  concentrations for both diethylstilbestrol and estradiol, and these effects were fully reversed in the presence of an ER antagonist. Incubation of TM3 cells with diesel exhaust particles led to a reduced expression of ER $\alpha$  (at 0.1  $\mu\text{g}/\text{ml}$  particle concentration) and an induction of Cyp11a1 (at 1  $\mu\text{g}/\text{ml}$ ) [83]. A transcriptomics analysis was performed on the impact of 1 and 5 mM methoxyacetic acid, the active metabolite of the industrial chemical ethylene glycol monomethyl ether, on TM3 cells revealing alterations in steroidogenesis, inflammation reactions and metabolic functions [84]. It needs to be noted that these concentrations are very high, and thus the human relevance is questionable. Two recent studies provided evidence for a protective role of the activation of the transcription factor Nrf2 toward the toxicity caused by the phthalate DBP, indicating the importance of the antioxidant defence system to protect Leydig cells from toxic chemicals [85,86]. Studies on chemicals affecting testosterone production in TM3 cells are rather uncertain, since these cells produce very low amounts. Furthermore, results on changes in testosterone production obtained using ELISA kits should be confirmed using quantification by GC-MS or LC-MS.

I-10 clonal Leydig cells were originally obtained from a spontaneous mouse testicular tumor [87]. Like other mouse Leydig cell lines described above, I-10 were reported to mainly produce progesterone, which was stimulated by cAMP [88], although not as efficient as in MA-10 and mLTC-1 cells. I-10 Leydig cancer cells were scarcely used for the assessment of EDCs. A study on PCBs showed enhanced CYP19a1 expression in mouse I-10 Leydig and human H295R adrenal cells following incubation for 24 h with the high concentration of 10  $\mu\text{M}$  PCB126 [89]. Interestingly, this effect was blunted in hCG and cAMP analog-treated cells, and the authors proposed a role for AhR in these effects. Similarly, the mouse Leydig tumor cell line K28 was applied

only in a few studies, including the investigation of the time-dependent induction of StAR mRNA expression and progesterone production by 9-cis and all-trans of retinoic acid (increases at concentrations greater than 10 nM) [90], the impact of LH on the expression of Nur77 (NR4A1) [91], the effect of 1  $\mu$ M BPA under serum-free conditions for 24 h on the induction of Nur77 expression and the production of progesterone [92], as well as the stimulating effects of 30  $\mu$ M cadmium chloride on CREB protein phosphorylation and StAR expression [93].

The rat Leydig tumor interstitial cell line R2C displays high StAR expression and produces high amounts of progesterone [94–96]. The high expression of StAR, Cyp11a1 and 3 $\beta$ -hsd1 was confirmed by RT-PCR and Western blot [97] and the production of progesterone was detected by ELISA and RIA measurements [98,99]. The expression of Cyp17a1 and the production of testosterone have been reported [97–99]; however, a general problem with antibody-based quantification of proteins and steroids remains the often limited specificity of the antibodies used [100]. Thus, testosterone production by R2C cells should be confirmed using quantification by GC–MS or LC–MS. An interesting property of R2C cells is that they are insensitive to cAMP regulation and do not require trophic stimulation to produce progesterone, which might be explained by a constitutively activated downstream signaling pathway [95,101]. Because of the constitutive production of progesterone, these cells are suitable to test chemicals that directly inhibit the activity of StAR, Cyp11a1 or 3 $\beta$ -hsd1. On the other side, this cell line is not suitable to study chemicals affecting the induction of steroidogenesis due to the lack of sensitivity of the involved signaling pathways.

R2C cells were used in a comparative study with MA-10 cells to assess effects of various phthalates on testosterone production measured by ELISA [98]. The phthalates MBP and MEHP significantly inhibited testosterone synthesis at concentrations of 1 and 3  $\mu$ M, with IC<sub>50</sub> values of 3 and 6  $\mu$ M respectively. Phthalates with shorter alkyl side chains were found to be less active or inactive. Interestingly, R2C cells express substantial levels of Cyp19a1, and this cell line has been applied to characterize aromatase inhibitors [102,103]. A study on effects of BPA (concentrations of 0.1–10 nM) on steroidogenesis suggested an up regulation of Cyp19a1 protein expression and activity, whereas testosterone synthesis was decreased [104]. Testosterone was measured by ELISA. Using R2C cells the anabolic androgenic steroids nandrolone and stanozolol (at 1  $\mu$ M concentration) were shown to increase Cyp19a1 expression as well as estradiol production [105]. Further, these authors provided evidence for an additive effect of androgens and IGF-1 on R2C cell proliferation and aromatase expression. In contradiction, a recent study showed that treatment of R2C cells with the androgen mibolerone up regulated the transcription factor DAX-1 and inhibited the expression and activity of Cyp19a1, in line with observations in old Fischer rats with spontaneous Leydig cell tumors where AR and DAX-1 were down regulated and Cyp19a1 was up regulated [106]. The reason for the discrepancies of the above studies remains unclear and requires further research.

A major limitation for mechanistic investigations into the regulation of steroidogenesis in Leydig cells and the assessment of the impact of potential EDCs is the fact that currently no human Leydig cell model is available. There are considerable species differences in the functions of Leydig cells. For example, it has been shown that the expression level of LH receptors is an order of magnitude higher in rat compared with human Leydig cells, and that rat Leydig cells respond with hyperplasia to hCG, whereas human Leydig cells become hypertrophic [107–110]. Furthermore, rat Leydig cells express gonadotropin-releasing hormone, whereas mouse and human Leydig cells do not [111,112].

Additionally, several studies demonstrated species-specific inhibition of testicular steroidogenesis by EDCs. Using organotypic primary culture systems, the phthalate MEHP at a concentration of 10  $\mu$ M was shown to decrease testosterone production in rat but not in human fetal testis explants [113,114]. Further support for species-specific effects of phthalates was provided by studies where rat and human fetal testes were xenografted into a host mouse or rat [115,116]. Treatment with di-*n*-butylphthalate (500 mg/kg per day for four days) inhibited steroidogenesis in animals with rat but not human xenografts. Also, diethylstilbestrol did not affect human fetal testicular steroidogenesis in the xenograft model [117] and in human fetal testis explants, in contrast to rat and mouse testis cultures [118,119], a difference explained by the fact that ER $\alpha$  is expressed in rat and mouse but not in human fetal Leydig cells [117]. Moreover, the anti-diabetic drug metformin inhibited testosterone production at an order of magnitude higher concentrations in human compared with mouse testis explants [120]. In contrast, it was shown that BPA inhibited testosterone synthesis at 100 times lower concentrations in human compared with rat and mouse fetal testis explants [118]. These studies demonstrate important species-specific differences in the susceptibility of human, rat and mouse testes to xenobiotics and further emphasize the need to establish a human Leydig cell model for the investigations into the molecular mechanisms of steroidogenesis disruption.

#### 4. Cell-based systems to study effects of EDCs on ovarian steroidogenesis

In the industrialized countries, there is an increasing incidence of reproductive disorders such as polycystic ovary syndrome (PCOS) [121], which is characterized by chronic anovulation and hyperandrogenism and results in hirsutism, infertility and menstrual disturbances. As with male infertility, there is evidence for the contribution of EDCs from consumer products or environmental pollutants to the increasing incidence of female reproductive disorders (for a recent comprehensive review see [122]). Several EDCs and potential EDCs have been detected in human samples, including follicular fluid, from the general population [123–127]. Exposure to EDCs likely contributes to sub-fecundity, ovarian failure and infertility, and affects reproductive behavior. Exposure to EDCs may contribute to ovulatory dysfunction by decreasing estradiol biosynthesis in granulosa cells or as abortifacients by disrupting progesterone production in luteal cells [128].

*In vivo* testing of EDCs for reproductive toxicity is mostly conducted in rodents, with fertility as a primary endpoint [129]. Alteration in serum steroid levels may indicate an adverse effect but it may also represent an adaptive response, thus often not providing sufficient information on the toxicity of a given chemical. Also, changes in circulating steroid levels may be due to a direct effect on steroidogenesis or an altered feedback regulatory system. *Ex vivo* tissue samples, e.g. whole ovaries or isolated individual follicles, can be used to study follicular development, ovulation and steroidogenesis, and assays using such samples can provide results on multiple fertility-related endpoints [130]. In order to allow high throughput analyses and to gain mechanistic insight into the action of EDCs, cultured cells are advantageous. Isolated primary theca and granulosa cells can be applied for functional studies, and they retain the normal responses and steroidogenic pathways [131]. Porcine and bovine primary cells can be isolated from ovaries obtained from the slaughterhouse or from ovaries of rodent animal models; however, there are significant species-specific differences in the steroidogenic pathways, which need to be taken into account when trying to extrapolate results to the human system. Human granulosa cells

are mostly obtained from women undergoing *in vitro* fertilization; however, these cells are usually subjected to supraphysiological concentrations of hCG and FSH, and these cells can only be cultivated for a relatively short time [132]. For these reasons, there is a great demand for suitable human theca and granulosa cell lines to investigate a large number of individual EDCs at various concentrations and incubation time as well as mixtures of EDCs. The establishment of a theca cell line was not successful so far; in contrast, several granulosa cell lines are available for investigating effects of chemicals on steroidogenesis.

Granulosa cell lines are useful to study the impact of potential EDCs on progesterone synthesis as well as on the aromatase- and 17 $\beta$ -HSD1-dependent production of estradiol upon incubation of these cells with androstenedione. There is a large number of human ovarian cancer cell lines available (for a recent review see [133]). Most of them express CYP19A1 and 17 $\beta$ -HSD1 and their proliferation is stimulated by estrogens. Additionally, immortalized granulosa cell lines from various animal species and of human origin have been described [134].

Among the rodent granulosa cell lines, KK-1, GRM01 and GRM02 were found to produce progesterone, and retain responsiveness to cAMP, FSH and LH/hCG [134]. KK-1 cells were derived from mice bearing an SV40 T-antigen driven by the inhibin- $\alpha$  promoter, and treatment of these cells with hCG, forskolin and FSH increased cAMP 10-fold, 40-fold and 2.6-fold, respectively, indicating enhanced steroidogenesis [135]. KK-1 cells were shown to express Cyp19a1 and 17 $\beta$ -hsd1 and convert androstenedione to estradiol. The KK-1 cell line was used, for example, to study effects of phthalates on the stimulation of steroidogenesis [136]. The phthalate MEHP at high concentrations of 20–100  $\mu$ M stimulated basal steroid production in KK-1 granulosa cells, a finding confirmed in mLTC-1 Leydig cells. The expression of StAR and cAMP-mediated signaling did not seem to be affected, and the authors suggested that MEHP may stimulate steroidogenesis by enhanced cholesterol supply. Thus, KK-1 represents a mouse cell system to study granulosa steroidogenesis. GRM01 and GRM02 granulosa cell lines were established by transfection of murine granulosa cells with v-myc [137]. Both cell lines retained steroidogenic activity and were shown to express 3 $\beta$ -hsd2 and 17 $\beta$ -hsd1 [138]. GRM01 was able to produce both progesterone and estradiol *de novo*, whereas GRM02 produced progesterone but not estradiol [139]. However, aromatase activity was also demonstrated in GRM02 upon the addition of androstenedione or testosterone to the culture medium. Steroid production was induced in both GRM01 and GRM02 by LH/hCG, FSH, forskolin and cAMP analogs. Both cell lines also express inhibin- $\alpha$ , which has a role in feedback regulation by inhibiting pituitary FSH secretion. They represent alternative murine cell models to study the impact of potential EDCs that act as direct inhibitors of enzymes involved in progesterone or estradiol production or of the signaling pathways involved in steroidogenesis in granulosa cells.

There are several human granulosa cell lines that are useful for the investigation of endogenous regulators of steroidogenesis as well as pathways involved in metabolic regulation, the regulation of cell proliferation and apoptotic pathways. The cell lines HGP53, HO23, HGL5, HTOG and SVOG were primarily used to study signaling pathways, which are involved in the regulation of steroidogenesis and effects on apoptosis as well as cell proliferation [140–145]. The immortalized human granulosa cell line COV434, initially isolated from a primary granulosa cell tumor, was shown to express FSH receptor and CYP19A1. In FSH supplemented medium COV434 was able to produce estradiol from androstenedione [146]. FSH and forskolin both stimulated steroidogenesis by induction of cAMP. Pharmacological inhibition of the FSH receptor was found to inhibit COV434 cell proliferation [147]. Furthermore, incubation of COV434 cells with soy isoflavones, considered to act

as phytoestrogens, promoted cell proliferation [148]. Incubation with 5–50  $\mu$ M genistein led to increased expression of ER $\alpha$  and enhanced cell proliferation by repressing proapoptotic genes. The human relevance of these observations remain uncertain because of the low bioavailability of oral intake of isoflavones.

The most widely used human ovarian granulosa-like tumor cell line is KGN. Progesterone production as well as CYP19A1- and 17 $\beta$ -HSD1-dependent estradiol formation from androstenedione supplemented culture medium was found to be induced by FSH *via* induction of IGF-1 in KGN granulosa cells [149]. Additionally, several endogenous regulators, such as steroidogenic factor-1 (SF-1) [150], liver receptor homolog-1 (LRH-1) [151], AMP-kinase (AMPK)/sirtuin-1 (SIRT1) [152], oocyte-derived growth differentiation factor and bone morphogenic protein 15 [153], the Notch signaling pathway [154] and the Hippo pathway [155], were shown to affect progesterone production and CYP19A1- and 17 $\beta$ -HSD1-dependent estradiol synthesis.

Several investigators used the KGN granulosa cell line to address the impact of xenobiotics on steroid synthesis. Bisphenol-A (BPA) was found to activate peroxisome proliferator-activated receptor (PPAR) $\gamma$  and inhibit the FSH-stimulated insulin-like growth factor-1 (IGF1)-dependent induction of CYP19A1 expression and estradiol synthesis in KGN cells and in primary granulosa cells [156]. A significant blunting of the FSH-induced CYP19A1 expression was seen at 40  $\mu$ M whereas estradiol production was reduced after treatment with 80  $\mu$ M of BPA. The BPA concentrations applied are very high and human relevance of this findings remains uncertain. Another study found that BPA concentration-dependently down regulated CYP19A1 expression in KGN cells as well as in human fetal osteoblastic cells, with significant effects seen at 5  $\mu$ M [157]. Additionally, DEHP (5  $\mu$ M) and TCDD (10 nM) were found to inhibit the FSH-induced estradiol synthesis and to enhance the AhR expression in a PPAR-dependent manner [158]. Another study found that atrazine and simazine at 10  $\mu$ M enhanced the stimulatory effect of transfected SF-1 on aromatase mRNA expression and activity in KGN cells [159]. Recently, the pesticide simazine was found to shorten anogenital distance and to decrease whole body, ovarian and uterine weights in offspring of pregnant mice treated with 5–500  $\mu$ g/kg of this pesticide [160]. Simazine at a concentration of 1 nM diminished the viability and proliferation of KGN granulosa cells. Interestingly, a U-shaped curve was observed, whereby concentrations of 100–1000 nM no longer inhibited cell viability and proliferation.

Currently, most studies on EDCs affecting ovarian steroidogenesis are conducted using tumor cell lines of granulosa origin, where several pathways may be altered compared with normal granulosa cells. This limitation needs to be considered in the interpretation of results. Also, most cell lines are cultivated in medium containing high glucose concentrations and fetal bovine serum as well as under hyperoxia, a situation clearly distinct from that of the physiological context and likely to affect metabolic pathways and steroid production. Another limitation is that currently no suitable human theca cell line is available. Since the production of steroids by the ovaries requires a tight cooperation of granulosa and theca cells, ideally a co-culture system of granulosa and theca cells should be applied for the investigation of ovarian steroidogenesis.

## 5. Adrenal cell models to investigate disruption of steroidogenesis

The adrenal glands play an essential role in the regulation of electrolyte and energy homeostasis [161]. An over production of glucocorticoids by the adrenal glands ultimately causes Cushing's syndrome, which is characterized by increased visceral adipose tissue, insulin resistance, skin and skeletal muscle atrophy, and impaired wound healing. In contrast, insufficient glucocorticoid



production causes Addison's disease, characterized by hypotension, fatigue, muscle weakness, loss of body weight and depression. The clinical observations emphasize the importance of including the assessment of chemicals applied to humans (drugs, chemicals in food and personal care products) or released at high amounts into the environment for potential adrenal toxicity. In this respect, fatal adrenal insufficiency, due to unexpected severe adverse drug effects [162–165], is a known clinical problem that has been recognized by the FDA [166]. In contrast to the investigations of the safety of chemicals regarding reproductive and developmental endpoints, with a major focus on the disruption of sex steroid hormone action, the adrenal gland has been neglected in EDCs regulatory testing strategy, as recently discussed by Harvey [167]. However, there are several chemicals, e.g. drugs, chemicals contained in consumer products and environmental pollutants, that were shown to cause adrenal toxicity (for reviews see [163,167,168]), further emphasizing the necessity of testing chemicals for potential adrenal toxicity.

Nevertheless, regarding the use of cell-based testing systems, there is a widely used human adrenal cell line, i.e. H295R. The OECD (Organization for Economic Cooperation and Development) published a guideline for the testing of chemicals using this cell line [169]. The H295R cell line was derived from the NCI-H295 cell line that was established from an adrenocortical carcinoma of a female patient [170]. The use of NCI-H295 cells was limited by the slow proliferation and the fact that they formed cell clusters in culture. Using GC-MS analysis and radio-immuno assays (RIA) NCI-H295 cells were shown to produce about 30 different steroids [170–174]. Importantly, this cell line was shown to express most of the major steroidogenic genes; it also expresses CYP11B2 and has the ability to produce aldosterone, mainly upon stimulation with angiotensin II or potassium. The parental NCI-H295 cells were used to derive the H295A cells [175] as well as the H295R cells [173]. H295R cells can further be distinguished as H295R-S1, H295R-S2 and H295R-S3 clones, depending on the cultivation conditions. H295R-S1 are cultivated in a medium containing Nu-serum, H295R-S2 in a medium with the serum substitute Ultrosor-G and H295R-S3 in a medium containing Cosmic calf serum [176]. Furthermore, three additional clones were derived from NCI-H295, namely HAC13, HAC15 and HAC50 [176–178]. The NCI-H295 derived clonal cell lines all grow as adherent monolayers but show significant differences in the expression of steroidogenic enzymes, the response to endogenous regulators and the amounts of steroids synthesized, emphasizing the importance of the culture medium composition. Nevertheless, the NCI-H295 cell lines respond to angiotensin II and potassium by increased aldosterone production; however, their response to ACTH is either absent or very weak [179]. Besides the NCI-H295 clonal cell lines, no other human adrenal cell line with substantial steroidogenic properties has been reported to date.

Based on the secreted steroids and mRNA analyses the NCI-H295 clonal cell lines appeared to express all of the adrenocortical enzymes that were present in the original tumor including StAR, 3 $\beta$ -HSD2, CYP11A1, CYP17A1, CYP21A1, CYP11B1, CYP11B2, 3 $\beta$ -hydroxysteroid sulfotransferase and low levels of CYP19A1 [173,178]. The expression pattern and steroids produced indicates that these cells represent characteristics of the different adrenal zones. It needs to be noted that the basal production of cortisol and aldosterone in H295R cells is low, indicating a low expression of CYP11B1 and CYP11B2 in the absence of inducers. However, treatment with endogenous regulators can enhance some zone-specific effects. Forskolin and cAMP analogs enhance the production of adrenal androgens (DHEA, DHEAS, androstenedione) and glucocorticoids (cortisol, 11-deoxycortisol, corticosterone), whereas angiotensin II, the primary regulator of the renin-angiotensin-aldosterone system, and potassium induce the production of

aldosterone in H295R cells [171,172,180,181]. It was shown that H295R cells mediate angiotensin II effects through angiotensin receptor 1 (AT1) [172,179,182–184]. In contrast, H295A do not express substantial levels of AT1 and lack sensitivity to angiotensin II [185]. NCI-H295 clonal cell lines show weak or absent response to ACTH due to the very low expression of melanocortin 2 receptor (MC2R) [177]. Interestingly, in H295R cells ACTH induced a transient increase in aldosterone but not in cortisol production. Thus, depending on whether the cells are used in the basal state or upon stimulation with various effective agonists, the adrenal cell lines may be used to study the effect of EDCs on the functions of the different adrenocortical zones.

Besides the human NCI-H295 clonal cell lines, mouse adrenal cell lines have been used in several studies on adrenal steroidogenesis. The mouse Y-1 cells were reported to exhibit characteristics of both *zona fasciculata* and *zona glomerulosa*, and they are able to produce corticosterone and aldosterone [173,186–188]. Y-1 cells were shown to respond to ACTH with increased expression of steroidogenic genes and enhanced corticosterone production; however, the stimulatory effect was rather modest compared with that of isolated primary mouse adrenal cells [179,189]. Later, two other cell lines, designated ATC1 and ATC7-L, established from adrenal tumors of two transgenic mice expressing the SV40 large T-antigen under the control of the *akr1b7* promoter, have been described [190]. Both cell lines exhibited a typical phenotype of the *zona fasciculata*. They produced high amounts of corticosterone and retained responsiveness to ACTH. Incubation of these cells with ACTH increased SF-1 and decreased DAX-1 expression, providing an explanation for the observed stimulation of corticosterone production. Thus, ATC1 and ATC7-L represent useful cell models to study *zona fasciculata* specific function.

In contrast to the testicular and ovarian cell models, there is a human adrenal cell model (H295R) that has been recognized by the regulators for toxicity screening and resulted in an OECD test guideline for the evaluation of EDCs [169]. Therefore, a large number of studies applied the H295R cell model for the assessment of chemicals that cause disturbances of steroidogenesis, including pharmaceuticals, consumer products, food constituents and environmental pollutants [191–198], and it is out of the scope of this review to cover the findings of these studies. Currently, the OECD guideline only focuses on the use of H295R cells in their basal state and on the production of estradiol and testosterone as endpoints [199], two hormones not typically produced by the adrenals. Thus, there are limitations of the current protocol as well as in the use of the H295R cells and the exploitation of this cell model could be significantly extended. Interestingly, the measurement of the main adrenal steroids, i.e. adrenal androgens, glucocorticoids and mineralocorticoids, is currently not covered by the OECD guideline and an extended protocol to include the quantification of DHEA, cortisol and aldosterone needs to be validated [200,201]. Other important steroids such as progesterone, 17 $\alpha$ -hydroxyprogesterone, 11-deoxycorticosterone and 11-deoxycortisol should also be determined simultaneously with the major adrenal steroids in order to obtain a broader picture of disturbances caused by a given chemical.

Since in their basal state H295R cells produce only low amounts of cortisol and aldosterone, the cells should be used in the basal state to detect chemicals that induce steroidogenesis and upon treatment with specific agonists such as ACTH, angiotensin II and potassium [202] in order to detect chemicals that inhibit steroidogenesis. For the latter, the time point of adding a chemical is important. The pre-incubation or simultaneous addition of a chemical with an inducer may allow to identify chemicals that disrupt regulatory pathways of steroidogenesis. Incubation of a chemical following stimulation of the cells will allow to identify

compounds that directly inhibit steroidogenic enzymes. Thus, different protocols need to be applied depending on the mode-of-action of a given compound. Also, inclusion of appropriate reference compounds (positive and negative controls) and time course analysis of the steroid production would aid the interpretation of the data. Another important issue is the inclusion of measurements of the steroid concentrations in the complete medium at the time of the start of the experiment, as the amounts of these steroids are influenced by the composition of the serum used. Furthermore, the availability of LC–MS based methods allows to simultaneously quantify several steroid hormones and specific steroid pattern analysis can be performed for reference compounds and individual EDCs [201,203–205]. In many recent studies antibody-based detection methods have still been used for quantification of steroids. These methods often are lacking specificity due to cross-reactivity of the antibodies. Thus, GC–MS and LC–MS methods should not only allow more accurate quantification but allow the simultaneous assessment of multiple steroids.

A major limitation of the H295R cell system is the insensitivity toward ACTH. Thus, the establishment of an additional human adrenal cell line is required. Regarding ACTH response, murine ATC1 and ATC7-L cells may represent useful alternatives for testing until a suitable human cell system is available; however, species-specific differences in signaling pathways need to be taken into account.

## 6. Conclusions and outlook

Cell-based steroidogenesis models are highly valuable for mechanistic studies of chemicals disrupting steroidogenesis and allow an initial medium to high throughput assessment of the potential endocrine toxicity of chemicals. In contrast, to adrenal steroidogenesis, there is no commonly used cell line or standardized procedure to assess effects of chemicals on steroidogenesis in Leydig cells and ovarian cells. Future efforts should therefore aim at establishing a human Leydig cell line with the capability to respond to LH and produce testosterone. To investigate ovarian steroidogenesis, a human theca cell model is needed and, ideally, a theca granulosa co-culture cell system responding to FSH should ideally be established, with the capability for *de novo* steroid synthesis up to the final step of estradiol production. Moreover, there is a need for an ACTH-sensitive human adrenal cell line.

In order to extend and improve the current cell-based testing protocols for studying chemicals that disrupt steroidogenesis and to facilitate the comparison of results from different laboratories, several general issues should be considered: (1) the description of experiments using steroidogenic cell lines should include passage number, cell density, incubation time and the composition of the complete medium used, including glucose concentration, possible use of antibiotics, amount of serum as well as the amount of steroids contained in the complete medium. Cells should only be used within certain passage numbers to guarantee comparable steroidogenic activity and responsiveness of the involved signaling pathways; (2) Ideally, the same positive and negative controls should be included in every experiment to verify the responsiveness of the cell batch used; (3) The cells should be used in the basal state as well as upon stimulation with specific inducers. Ideally, the same inducers, concentrations and conditions should be applied in different laboratories and experiments to allow a direct comparison of the results. The chemicals to be tested should be added prior to stimulation or simultaneously with the inducer in order to investigate whether the response to an inducer is blunted or potentiated, as well as following stimulation in order to detect direct effects on steroidogenic enzymes; (4) The quantification of steroid metabolites should be performed by GC–MS or LC–MS to

assure specificity of the results. The major steroids should be quantified rather than a single steroid; and (5) another key issue remains the experimental concentration of a given chemical to be tested. A drawback of cell-based studies is the short duration of the incubation compared with humans who might be exposed for a long period of time. Also, often human exposure data is not available and concentrations of a given compound can vary significantly from its tissue concentration. Usually concentrations chosen for *in vitro* experiments are higher than those observed in humans. Nevertheless, it has to be distinguished between studies aiming at providing mechanistic information and studies for risk assessment. For the latter, it is crucial to choose concentrations that realistically can be reached after occupational exposure or in case of environmental toxicants after exposure in the general population. As suggested by Teeguarden and Hanson-Drury toxicity study exposures should be directly compared to human exposure if such data are available and qualification of a study as “low dose” in the absence of reliable human exposure data should be avoided [206].

Thus, there is still considerable room for improvement of the currently available cellular testing systems and the protocols for measurements of chemical-induced disturbances of steroidogenesis.

## Acknowledgements

This work was supported by the Swiss National Science Foundation (31003A\_159454), the Swiss Center for Applied Human Toxicology, and the Novartis Research Foundation.

## References

- [1] R.T. Zoeller, T.R. Brown, L.L. Doan, A.C. Gore, N.E. Skakkebaek, A.M. Soto, T.J. Woodruff, F.S. Vom Saal, Endocrine-disrupting chemicals and public health protection: a statement of principles from The Endocrine Society, *Endocrinology* 153 (2012) 4097–4110.
- [2] G.J. Nohynek, C.J. Borgert, D. Dietrich, K.K. Rozman, Endocrine disruption: fact or urban legend? *Toxicol. Lett.* 223 (2013) 295–305.
- [3] Global Assessment of the State-of-the-Science of Endocrine Disruptors, International Programme on Chemical Safety, in: S. Damstra, A. Barlow, R.J. Bergman (Eds.), World Health Organization, Geneva, Switzerland, 2002 WHO publication no. WHO/PCS/EDC/02.2.
- [4] R.E. Chapin, J. Adams, K. Boekelheide, L.E. Gray Jr., S.W. Hayward, P.S. Lees, B.S. McIntyre, K.M. Portier, T.M. Schnorr, S.G. Selevan, J.G. Vandenberg, S.R. Woskie, NTP-CERHR expert panel report on the reproductive and developmental toxicity of bisphenol A, *Birth Defects Res. B Dev. Reprod. Toxicol.* 83 (2008) 157–395.
- [5] R. Hauser, The environment and male fertility: recent research on emerging chemicals and semen quality, *Semin. Reprod. Med.* 24 (2006) 156–167.
- [6] D.C. Luccio-Camelo, G.S. Prins, Disruption of androgen receptor signaling in males by environmental chemicals, *J. Steroid Biochem. Mol. Biol.* 127 (2011) 74–82.
- [7] B.A. Cohn, M.S. Wolff, P.M. Cirillo, R.I. Sholtz, DDT and breast cancer in young women: new data on the significance of age at exposure, *Environ. Health Perspect.* 115 (2007) 1406–1414.
- [8] S. De Coster, N. van Larebeke, Endocrine-disrupting chemicals: associated disorders and mechanisms of action, *J. Environ. Public Health* 2012 (2012) 713696.
- [9] M. Fucic, Z. Gamulin, J. Ferencic, A. Kraymer von Krauss, D.F. Merlo, Environmental exposure to xenoestrogens and oestrogen related cancers: reproductive system, breast, lung, kidney, pancreas, and brain, *Environ. Health* 11 (Suppl. 1) (2012) S8.
- [10] J.L. Carwile, K.B. Michels, Urinary bisphenol A and obesity: NHANES 2003–2006, *Environ. Res.* 111 (2011) 825–830.
- [11] L. Trasande, T.M. Attina, J. Blustein, Association between urinary bisphenol A concentration and obesity prevalence in children and adolescents, *JAMA* 308 (2012) 1113–1121.
- [12] B.A. Neel, R.M. Sargis, The paradox of progress: environmental disruption of metabolism and the diabetes epidemic, *Diabetes* 60 (2011) 1838–1848.
- [13] M. Kajta, A.K. Wojtowicz, Impact of endocrine-disrupting chemicals on neural development and the onset of neurological disorders, *Pharmacol. Rep.* 65 (2013) 1632–1639.
- [14] B. Weiss, The intersection of neurotoxicology and endocrine disruption, *Neurotoxicology* 33 (2012) 1410–1419.
- [15] W.L. Miller, Steroid hormone biosynthesis and actions in the materno-feto-placental unit, *Clin. Perinatol.* 25 (1998) 799–817.

- [16] N.A. Compagnone, S.H. Mellon, Neurosteroids: biosynthesis and function of these novel neuromodulators, *Front. Neuroendocrinol.* 21 (2000) 1–56.
- [17] S.H. Mellon, C.F. Deschepper, Neurosteroid biosynthesis: genes for adrenal steroidogenic enzymes are expressed in the brain, *Brain Res.* 629 (1993) 283–292.
- [18] G. Bouguen, L. Dubuquoy, P. Desreumaux, T. Brunner, B. Bertin, Intestinal steroidogenesis, *Steroids* 103 (2015) 64–71.
- [19] A. Slominski, B. Zbytek, G. Nikolakis, P.R. Manna, C. Skobowiat, M. Zmijewski, W. Li, Z. Janjetovic, A. Postlethwaite, C.C. Zouboulis, R.C. Tuckey, Steroidogenesis in the skin: implications for local immune functions, *J. Steroid Biochem. Mol. Biol.* 137 (2013) 107–123.
- [20] W.L. Miller, R.J. Auchus, The molecular biology, biochemistry, and physiology of human steroidogenesis and its disorders, *Endocr. Rev.* 32 (2011) 81–151.
- [21] T. Suzuki, H. Sasano, J. Takeyama, C. Kaneko, W.A. Freije, B.R. Carr, W.E. Rainey, Developmental changes in steroidogenic enzymes in human postnatal adrenal cortex: immunohistochemical studies, *Clin. Endocrinol. (Oxf.)* 53 (2000) 739–747.
- [22] R.J. Auchus, T.C. Lee, W.L. Miller, Cytochrome b5 augments the 17,20-lyase activity of human P450c17 without direct electron transfer, *J. Biol. Chem.* 273 (1998) 3158–3165.
- [23] R.J. Auchus, W.E. Rainey, Adrenarche—physiology, biochemistry and human disease, *Clin. Endocrinol. (Oxf.)* 60 (2004) 288–296.
- [24] J. Rege, Y. Nakamura, T. Wang, T.D. Merchen, H. Sasano, W.E. Rainey, Transcriptome profiling reveals differentially expressed transcripts between the human adrenal zona fasciculata and zona reticularis, *J. Clin. Endocrinol. Metab.* 99 (2014) E518–527.
- [25] J.S. Gell, B. Atkins, L. Margraf, J.I. Mason, H. Sasano, W.E. Rainey, B.R. Carr, Adrenarche is associated with decreased 3 beta-hydroxysteroid dehydrogenase expression in the adrenal reticularis, *Endocr. Res.* 22 (1996) 723–728.
- [26] J. Rege, Y. Nakamura, F. Satoh, R. Morimoto, M.R. Kennedy, L.C. Layman, S. Honma, H. Sasano, W.E. Rainey, Liquid chromatography–tandem mass spectrometry analysis of human adrenal vein 19-carbon steroids before and after ACTH stimulation, *J. Clin. Endocrinol. Metab.* 98 (2013) 1182–1188.
- [27] Y. Nakamura, P.J. Hornsby, P. Casson, R. Morimoto, F. Satoh, Y. Xing, M.R. Kennedy, H. Sasano, W.E. Rainey, Type 5 17beta-hydroxysteroid dehydrogenase (AKR1C3) contributes to testosterone production in the adrenal reticularis, *J. Clin. Endocrinol. Metab.* 94 (2009) 2192–2198.
- [28] P. Mulatero, K.M. Curnow, B. Appetit-Faisant, M. Foekling, C. Gomez-Sanchez, F. Veglioni, X. Jeunemaitre, P. Corvol, L. Pascoe, Recombinant CYP11B genes encode enzymes that can catalyze conversion of 11-deoxycortisol to cortisol, 18-hydroxycortisol, and 18-oxocortisol, *J. Clin. Endocrinol. Metab.* 83 (1998) 3996–4001.
- [29] W.L. Miller, Androgen synthesis in adrenarche, *Rev. Endocr. Metab. Disord.* 10 (2009) 3–17.
- [30] S. Dharia, A. Slane, M. Jian, M. Conner, A.J. Conley, R.M. Brissie, C.R. Parker Jr., Effects of aging on cytochrome b5 expression in the human adrenal gland, *J. Clin. Endocrinol. Metab.* 90 (2005) 4357–4361.
- [31] L.N. Parker, Adrenarche, *Endocrinol. Metab. Clin. North Am.* 20 (1991) 71–83.
- [32] C.E. Fluck, W.L. Miller, R.J. Auchus, The 17, 20-lyase activity of cytochrome p450c17 from human fetal testis favors the delta5 steroidogenic pathway, *J. Clin. Endocrinol. Metab.* 88 (2003) 3762–3766.
- [33] M. Jamnongjit, S.R. Hammes, Ovarian steroids: the good, the bad, and the signals that raise them, *Cell Cycle* 5 (2006) 1178–1183.
- [34] R. Voutilainen, J. Tapanainen, B.C. Chung, K.J. Matteson, W.L. Miller, Hormonal regulation of P450scc (20,22-desmolase) and P450c17 (17 alpha-hydroxylase/17,20-lyase) in cultured human granulosa cells, *J. Clin. Endocrinol. Metab.* 63 (1986) 202–207.
- [35] I. Hanukoglu, Steroidogenic enzymes: structure, function, and role in regulation of steroid hormone biosynthesis, *J. Steroid Biochem. Mol. Biol.* 43 (1992) 779–804.
- [36] A.M. Andersson, T.K. Jensen, A. Juul, J.H. Petersen, T. Jorgensen, N.E. Skakkebaek, Secular decline in male testosterone and sex hormone binding globulin serum levels in Danish population surveys, *J. Clin. Endocrinol. Metab.* 92 (2007) 4696–4705.
- [37] A. Perheentupa, J. Makinen, T. Laatikainen, M. Vierula, N.E. Skakkebaek, A.M. Andersson, J. Toppari, A cohort effect on serum testosterone levels in Finnish men, *Eur. J. Endocrinol.* 168 (2013) 227–233.
- [38] T.G. Travison, A.B. Araujo, A.B. O'Donnell, V. Kupelian, J.B. McKinlay, A population-level decline in serum testosterone levels in American men, *J. Clin. Endocrinol. Metab.* 92 (2007) 196–202.
- [39] C. Wang, G. Jackson, T.H. Jones, A.M. Matsumoto, A. Nehra, M.A. Perelman, R.S. Swerdloff, A. Traish, M. Zitzmann, G. Cunningham, Low testosterone associated with obesity and the metabolic syndrome contributes to sexual dysfunction and cardiovascular disease risk in men with type 2 diabetes, *Diabetes Care* 34 (2011) 1669–1675.
- [40] A. Bergman, J.J. Heindel, T. Kasten, K.A. Kidd, S. Jobling, M. Neira, R.T. Zoeller, G. Becher, P. Bjerregaard, R. Bormann, I. Brandt, A. Kortenkamp, D. Muir, M.N. Drisse, R. Ochieng, N.E. Skakkebaek, A.S. Bylehn, T. Iguchi, J. Toppari, T.J. Woodruff, The impact of endocrine disruption: a consensus statement on the state of the science, *Environ. Health Perspect.* 121 (2013) A104–106.
- [41] L.E. Gray, Jr., V.S. Wilson, T. Stoker, C. Lambright, J. Furr, N. Noriega, K. Howdeshell, G.T. Ankley, L. Guillette, Adverse effects of environmental antiandrogens and androgens on reproductive development in mammals, *Int. J. Androl.* 29 (2006) 96–104 discussion 105–108.
- [42] K.M. Main, H. Kiviranta, H.E. Virtanen, E. Sundqvist, J.T. Tuomisto, J. Tuomisto, T. Vartiainen, N.E. Skakkebaek, J. Toppari, Flame retardants in placenta and breast milk and cryptorchidism in newborn boys, *Environ. Health Perspect.* 115 (2007) 1519–1526.
- [43] F. Orton, S. Ermler, S. Kugathas, E. Rosivatz, M. Scholze, A. Kortenkamp, Mixture effects at very low doses with combinations of anti-androgenic pesticides antioxidants, industrial pollutant and chemicals used in personal care products, *Toxicol. Appl. Pharmacol.* 278 (2014) 201–208.
- [44] T.E. Stoker, R.L. Cooper, C.S. Lambright, V.S. Wilson, J. Furr, L.E. Gray, In vivo and in vitro anti-androgenic effects of DE-71, a commercial polybrominated diphenyl ether (PBDE) mixture, *Toxicol. Appl. Pharmacol.* 207 (2005) 78–88.
- [45] T. Hartung, Toxicology for the twenty-first century, *Nature* 460 (2009) 208–212.
- [46] M. Ascoli, D. Puett, Gonadotropin binding and stimulation of steroidogenesis in Leydig tumor cells, *Proc. Natl. Acad. Sci. U. S. A.* 75 (1978) 99–102.
- [47] R.V. Rebois, Establishment of gonadotropin-responsive murine leydig tumor cell line, *J. Cell Biol.* 94 (1982) 70–76.
- [48] M. Ascoli, Regulation of gonadotropin receptors and gonadotropin responses in a clonal strain of Leydig tumor cells by epidermal growth factor, *J. Biol. Chem.* 256 (1981) 179–183.
- [49] M.J. Roelofs, M. Berg, T.F. Bovee, A.H. Piersma, M.B. Duursen, Structural bisphenol analogues differentially target steroidogenesis in murine MA-10 Leydig cells as well as the glucocorticoid receptor, *Toxicology* 329 (2015) 10–20.
- [50] A.C. Dankers, M.J. Roelofs, A.H. Piersma, F.C. Sweep, F.G. Russel, M. van den Berg, M.B. van Duursen, R. Masereeuw, Endocrine disruptors differentially target ATP-binding cassette transporters in the blood–testis barrier and affect Leydig cell testosterone secretion in vitro, *Toxicol. Sci.* 136 (2013) 382–391.
- [51] M.T. Dyson, M.P. Kowalewski, P.R. Manna, D.M. Stocco, The differential regulation of steroidogenic acute regulatory protein-mediated steroidogenesis by type I and type II PKA in MA-10 cells, *Mol. Cell. Endocrinol.* 300 (2009) 94–103.
- [52] R.A. Clewell, J.L. Campbell, S.M. Ross, K.W. Gaido, H.J. Clewell, 3rd, M.E. Andersen assessing the relevance of in vitro measures of phthalate inhibition of steroidogenesis for in vivo response, *Toxicol. In Vitro* 24 (2010) 327–334.
- [53] X. Chen, Q.H. Zhou, L. Leng, Z.R. Sun, N.J. Tang, Effects of di(n-butyl) and monobutyl phthalate on steroidogenesis pathways in the murine Leydig tumor cell line MLTC-1, *Environ. Toxicol. Pharmacol.* 36 (2013) 332–338.
- [54] X. Chen, Y.N. Liu, Q.H. Zhou, L. Leng, Y. Chang, N.J. Tang, Effects of low concentrations of di-(2-ethylhexyl) and mono-(2-ethylhexyl) phthalate on steroidogenesis pathways and apoptosis in the murine leydig tumor cell line MLTC-1, *Biomed. Environ. Sci.* 26 (2013) 986–989.
- [55] C.D. Piche, D. Sauvageau, M. Vanlian, H.C. Erythropel, B. Robaire, R.L. Leask, Effects of di-(2-ethylhexyl) phthalate and four of its metabolites on steroidogenesis in MA-10 cells, *Ecolotoxicol. Environ. Saf.* 79 (2012) 108–115.
- [56] A.N. Enangue Njembele, J.L. Bailey, J.J. Tremblay, In vitro exposure of Leydig cells to an environmentally relevant mixture of organochlorines represses early steps of steroidogenesis, *Biol. Reprod.* 90 (2014) 118.
- [57] Y. Kim, J.C. Ryu, H.S. Choi, K. Lee, Effect of 2,2',4,4'-tetrahydroxybenzophenone (BP2) on steroidogenesis in testicular Leydig cells, *Toxicology* 288 (2011) 18–26.
- [58] L.P. Walsh, C. McCormick, C. Martin, D.M. Stocco, Roundup inhibits steroidogenesis by disrupting steroidogenic acute regulatory (STAR) protein expression, *Environ. Health Perspect.* 108 (2000) 769–776.
- [59] E.C. So, Y.T. Chang, C.H. Hsing, P.W. Poon, S.F. Leu, B.M. Huang, The effect of midazolam on mouse Leydig cell steroidogenesis and apoptosis, *Toxicol. Lett.* 192 (2010) 169–178.
- [60] H. Zhang, Y. Lu, B. Luo, S. Yan, X. Guo, J. Dai, Proteomic analysis of mouse testis reveals perfluorooctanoic acid-induced reproductive dysfunction via direct disturbance of testicular steroidogenic machinery, *J. Proteome Res.* 13 (2014) 3370–3385.
- [61] Z. Shi, Y. Feng, J. Wang, H. Zhang, L. Ding, J. Dai, Perfluorododecanoic acid-induced steroidogenic inhibition is associated with steroidogenic acute regulatory protein and reactive oxygen species in cAMP-stimulated Leydig cells, *Toxicol. Sci.* 114 (2010) 285–294.
- [62] Y. Li, B. Zhang, K. Huang, X. He, Y. Luo, R. Liang, H. Luo, X.L. Shen, W. Xu, Mitochondrial proteomic analysis reveals the molecular mechanisms underlying reproductive toxicity of zearalenone in MLTC-1 cells, *Toxicology* 324 (2014) 55–67.
- [63] P. Lin, F. Chen, J. Sun, J. Zhou, X. Wang, N. Wang, X. Li, Z. Zhang, A. Wang, Y. Jin, Mycotoxin zearalenone induces apoptosis in mouse Leydig cells via an endoplasmic reticulum stress-dependent signalling pathway, *Reprod. Toxicol.* 52 (2015) 71–77.
- [64] R. X. Han, X. Tang, B. Chen, Y. Xu, W. Qin, Y. Wu, L. Hu, Y. Song, X. Wang Xia, 2,2',4,4'-Tetrabromodiphenyl ether (BDE-47) decreases progesterone synthesis through cAMP-PKA pathway and P450scc downregulation in mouse Leydig tumor cells, *Toxicology* 302 (2012) 44–50.
- [65] S. Ohta, Y. Tabuchi, N. Yanai, S. Asano, H. Fuse, M. Obinata, Establishment of Leydig cell line TTE1, from transgenic mice harboring temperature-sensitive simian virus 40 large T-antigen gene, *Arch. Androl.* 48 (2002) 43–51.
- [66] S. Ohta, H. Fuse, Y. Tabuchi, DNA microarray analysis of genes involved in the process of differentiation in mouse Leydig cell line TTE1, *Arch. Androl.* 48 (2002) 203–208.
- [67] K. Warita, T. Mitsuhashi, Y. Tabuchi, K. Ohta, S. Suzuki, N. Hoshi, T. Miki, Y. Takeuchi, Microarray and gene ontology analyses reveal downregulation of



- DNA repair and apoptotic pathways in diethylstilbestrol-exposed testicular Leydig cells, *J. Toxicol. Sci.* 37 (2012) 287–295.
- [68] K. Warita, T. Mitsuhashi, T. Sugawara, Y. Tabuchi, T. Tanida, Z.Y. Wang, Y. Matsumoto, T. Yokoyama, H. Kitagawa, T. Miki, Y. Takeuchi, N. Hoshi, Direct effects of diethylstilbestrol on the gene expression of the cholesterol side-chain cleavage enzyme (P450<sub>sc</sub>) in testicular Leydig cells, *Life Sci.* 87 (2010) 281–285.
- [69] K. Kananen, M. Markkula, T. el-Hefnawy, F.P. Zhang, T. Paukku, J.G. Su, A.J. Hsueh, I. Huhtaniemi, The mouse inhibin alpha-subunit promoter directs SV40 T-antigen to Leydig cells in transgenic mice, *Mol. Cell. Endocrinol.* 119 (1996) 135–146.
- [70] A.L. Forgacs, Q. Ding, R.G. Jaremba, I.T. Huhtaniemi, N.A. Rahman, T.R. Zacharewski, BLTK1 murine Leydig cells: a novel steroidogenic model for evaluating the effects of reproductive and developmental toxicants, *Toxicol. Sci.* 127 (2012) 391–402.
- [71] A.L. Forgacs, M.L. D'Souza, I.T. Huhtaniemi, N.A. Rahman, T.R. Zacharewski, Triazine herbicides and their chlorometabolites alter steroidogenesis in BLTK1 murine Leydig cells, *Toxicol. Sci.* 134 (2013) 155–167.
- [72] J.P. Mather, Establishment and characterization of two distinct mouse testicular epithelial cell lines, *Biol. Reprod.* 23 (1980) 243–252.
- [73] J.P. Mather, L.Z. Zhuang, V. Perez-Infante, D.M. Phillips, Culture of testicular cells in hormone-supplemented serum-free medium, *Ann. N. Y. Acad. Sci.* 383 (1982) 44–68.
- [74] F.R. Musa, I. Takenaka, R. Konishi, M. Tokuda, Effects of luteinizing hormone, follicle-stimulating hormone, and epidermal growth factor on expression and kinase activity of cyclin-dependent kinase 5 in Leydig TM3 and Sertoli TM4 cell lines, *J. Androl.* 21 (2000) 392–402.
- [75] V. Pezzi, R. Sirianni, A. Chimento, M. Maggolini, S. Bourguiba, C. Delalande, S. Carreau, S. Ando, E.R. Simpson, C.D. Clyne, Differential expression of steroidogenic factor-1/adrenal 4 binding protein and liver receptor homolog-1 (LRH-1)/fetoprotein transcription factor in the rat testis: LRH-1 as a potential regulator of testicular aromatase expression, *Endocrinology* 145 (2004) 2186–2196.
- [76] J.J. Lysiak, J.L. Kirby, J.J. Tremblay, R.I. Woodson, M.A. Reardon, L.A. Palmer, T.T. Turner, Hypoxia-inducible factor-1 $\alpha$  is constitutively expressed in murine Leydig cells and regulates  $\beta$ 3-hydroxysteroid dehydrogenase type 1 promoter activity, *J. Androl.* 30 (2009) 146–156.
- [77] M. Otani, M. Kogo, S. Furukawa, S. Wakisaka, T. Maeda, The adiponectin paralog C1q/TNF-related protein 3 (CTRP3) stimulates testosterone production through the cAMP/PKA signaling pathway, *Cytokine* 58 (2012) 238–244.
- [78] M. Maggi, P.L. Morris, S. Kassis, D. Rodbard, Identification and characterization of arginine vasopressin receptors in the clonal murine Leydig-derived TM3 cell line, *Int. J. Androl.* 12 (1989) 65–71.
- [79] A.M. Nakhla, C.W. Bardin, Y. Salomon, J.P. Mather, O.A. Janne, The actions of calcitonin on the TM3 Leydig cell line and on rat Leydig cell-enriched cultures, *J. Androl.* 10 (1989) 311–320.
- [80] C. Ying, Z. Zhang, S.Y. Ying, Expression and localization of activin beta A-subunit and activin receptors in TM3, a mouse Leydig cell line, *Endocr. Res.* 21 (1995) 815–824.
- [81] C.C. Taylor, D. Limback, P.F. Terranova, Src tyrosine kinase activity in rat thecal-interstitial cells and mouse TM3 Leydig cells is positively associated with cAMP-specific phosphodiesterase activity, *Mol. Cell. Endocrinol.* 126 (1997) 91–100.
- [82] Y. Iwase, H. Fukata, C. Mori, Estrogenic compounds inhibit gap junctional intercellular communication in mouse Leydig TM3 cells, *Toxicol. Appl. Pharmacol.* 212 (2006) 237–246.
- [83] S. Yoshida, S. Hirano, K. Shikagawa, S. Hirata, S. Rokuta, H. Takano, T. Ichinose, K. Takeda, Diesel exhaust particles suppress expression of sex steroid hormone receptors in TM3 mouse Leydig cells, *Environ. Toxicol. Pharmacol.* 24 (2007) 292–296.
- [84] G. Bagchi, Y. Zhang, D.J. Waxman, Impact of methoxyacetic acid on mouse Leydig cell gene expression, *Reprod. Biol. Endocrinol.* 8 (2010) 65.
- [85] B. Shen, W. Wang, L. Ding, Y. Sao, Y. Huang, Z. Shen, Y. Zhuo, Z. Wei, W. Zhang, Nuclear factor erythroid 2-related factor 2 rescues the oxidative stress induced by di-N-butylphthalate in testicular Leydig cells, *Hum. Exp. Toxicol.* 34 (2015) 145–152.
- [86] B. Shen, W. Wang, L. Ma, S. Wang, L. Ding, Z. Chen, Y. Sao, H. Shen, Z. Wei, W. Zhang, Sulforaphane restores oxidative stress induced by di-N-butylphthalate in testicular Leydig cells with low basal reactive oxygen species levels, *Urology* 84 (2014) 850–856.
- [87] Y. Yasamura, A.H. Tashjian Jr., G.H. Sato, Establishment of four functional, clonal strains of animal cells in culture, *Science* 154 (1966) 1186–1189.
- [88] S.I. Shin, Studies on interstitial cells in tissue culture: steroid biosynthesis in monolayers of mouse testicular interstitial cells, *Endocrinology* 81 (1967) 440–448.
- [89] L.A. Li, Polychlorinated biphenyl exposure and CYP19 gene regulation in testicular and adrenocortical cell lines, *Toxicol. In Vitro* 21 (2007) 1087–1094.
- [90] H.K. Lee, M.S. Yoo, H.S. Choi, H.B. Kwon, J. Soh, Retinoic acids up-regulate steroidogenic acute regulatory protein gene, *Mol. Cell. Endocrinol.* 148 (1999) 1–10.
- [91] K.H. Song, J.I. Park, M.O. Lee, J. Soh, K. Lee, H.S. Choi, LH induces orphan nuclear receptor Nur77 gene expression in testicular Leydig cells, *Endocrinology* 142 (2001) 5116–5123.
- [92] K.H. Song, K. Lee, H.S. Choi, Endocrine disrupter bisphenol A induces orphan nuclear receptor Nur77 gene expression and steroidogenesis in mouse testicular Leydig cells, *Endocrinology* 143 (2002) 2208–2215.
- [93] S.Y. Park, C. Gomes, S.D. Oh, J. Soh, Cadmium up-regulates transcription of the steroidogenic acute regulatory protein (StAR) gene through phosphorylated CREB rather than SF-1 in K28 cells, *J. Toxicol. Sci.* 40 (2015) 151–161.
- [94] S.I. Shin, Y. Yasumura, G.H. Sato, Studies on interstitial cells in tissue culture. II. Steroid biosynthesis by a clonal line of rat testicular interstitial cells, *Endocrinology* 82 (1968) 614–616.
- [95] D.A. Freeman, Constitutive steroidogenesis in the R2C Leydig tumor cell line is maintained by the adenosine 3',5'-cyclic monophosphate-independent production of a cycloheximide-sensitive factor that enhances mitochondrial pregnenolone biosynthesis, *Endocrinology* 120 (1987) 124–132.
- [96] R.M. Rao, Y. Jo, M. Babb-Tarbox, P.J. Syapin, D.M. Stocco, Regulation of steroid hormone biosynthesis in R2C and MA-10 Leydig tumor cells: role of the cholesterol transfer proteins StAR and PBR, *Endocr. Res.* 28 (2002) 387–394.
- [97] R. Barone, F. Macaluso, P. Catanese, A. Marino Gammazza, L. Rizzuto, P. Marozzi, G. Lo Giudice, T. Stampono, F. Cappello, G. Morici, G. Zummo, F. Farina, V. Di Felice, Endurance exercise and conjugated linoleic acid (CLA) supplementation up-regulate CYP17A1 and stimulate testosterone biosynthesis, *PLoS One* 8 (2013) e79686.
- [98] P. Balbuena, J. Campbell Jr., H.J. Clewell 3rd., R.A. Clewell, Evaluation of a predictive in vitro Leydig cell assay for anti-androgenicity of phthalate esters in the rat, *Toxicol. In Vitro* 27 (2013) 1711–1718.
- [99] Q. Zhang, P. Zou, H. Zhan, M. Zhang, L. Zhang, R.S. Ge, Y. Huang, Dihydroipoamide dehydrogenase and cAMP are associated with cadmium-mediated Leydig cell damage, *Toxicol. Lett.* 205 (2011) 183–189.
- [100] T.L. Rizner, H. Sasano, M.H. Choi, A. Odermatt, J. Adamski, Recommendations for description and validation of antibodies for research use, *J. Steroid Biochem. Mol. Biol.* 156 (2015) 40–42.
- [101] D.M. Stocco, W. Chen, Presence of identical mitochondrial proteins in unstimulated constitutive steroid-producing R2C rat Leydig tumor and stimulated nonconstitutive steroid-producing MA-10 mouse Leydig tumor cells, *Endocrinology* 128 (1991) 1918–1926.
- [102] K.M. Doody, B.A. Murry, J.I. Mason, The use of rat Leydig tumor (R2C) and human hepatoma (HEPG2) cells to evaluate potential inhibitors of rat and human steroid aromatase, *J. Enzyme Inhib.* 4 (1990) 153–158.
- [103] M. Heneweer, M. van den Berg, J.T. Sanderson, A comparison of human H295R and rat R2C cell lines as in vitro screening tools for effects on aromatase, *Toxicol. Lett.* 146 (2004) 183–194.
- [104] J.Y. Kim, E.H. Han, H.G. Kim, K.N. Oh, S.K. Kim, K.Y. Lee, H.G. Jeong, Bisphenol A-induced aromatase activation is mediated by cyclooxygenase-2 up-regulation in rat testicular Leydig cells, *Toxicol. Lett.* 193 (2010) 200–208.
- [105] A. Chimento, R. Sirianni, F. Zolea, A. De Luca, M. Lanzino, S. Catalano, S. Ando, V. Pezzi, Nandrolone and stanozolol induce Leydig cell tumor proliferation through an estrogen-dependent mechanism involving IGF-I system, *J. Cell. Physiol.* 227 (2012) 2079–2088.
- [106] P. Maris, A. Campana, I. Barone, C. Giordano, C. Morelli, R. Malivindi, D. Sisci, S. Aquila, V. Rago, D. Bonfiglio, S. Catalano, M. Lanzino, S. Ando, Androgens inhibit aromatase expression through DAX-1: insights into the molecular link between hormone balance and Leydig cancer development, *Endocrinology* 156 (2015) 1251–1262.
- [107] T. Wahlstrom, I. Huhtaniemi, O. Hovatta, M. Seppala, Localization of luteinizing hormone, follicle-stimulating hormone, prolactin, and their receptors in human and rat testis using immunohistochemistry and radioreceptor assay, *J. Clin. Endocrinol. Metab.* 57 (1983) 825–830.
- [108] A.K. Christensen, K.C. Peacock, Increase in Leydig cell number in testes of adult rats treated chronically with an excess of human chorionic gonadotropin, *Biol. Reprod.* 22 (1980) 383–391.
- [109] C.G. Heller, D.R. Leach, Quantification of Leydig cells and measurement of Leydig-cell size following administration of human chorionic gonadotrophin to normal men, *J. Reprod. Fertil.* 25 (1971) 185–192.
- [110] B.J. Simpson, F.C. Wu, R.M. Sharpe, Isolation of human Leydig cells which are highly responsive to human chorionic gonadotropin, *J. Clin. Endocrinol. Metab.* 65 (1987) 415–422.
- [111] R.N. Clayton, I.T. Huhtaniemi, Absence of gonadotropin-releasing hormone receptors in human gonadal tissue, *Nature* 299 (1982) 56–59.
- [112] N.G. Wang, K. Sundaram, S. Pavlou, J. Rivier, W. Vale, C.W. Bardin, Mice are insensitive to the antitesticular effects of luteinizing hormone-releasing hormone agonists, *Endocrinology* 112 (1983) 331–335.
- [113] R. Habert, V. Muczynski, T. Grisin, D. Moison, S. Messiaen, R. Frydman, A. Benachi, G. Delbes, R. Lambrot, A. Lehraki, T. N'Tumba-Byn, M.J. Guerin, C. Levacher, V. Rouiller-Fabre, G. Livera, Concerns about the widespread use of rodent models for human risk assessments of endocrine disruptors, *Reproduction* 147 (2014) R119–129.
- [114] R. Lambrot, V. Muczynski, C. Lecureuil, G. Angenard, H. Coffigny, C. Pairault, D. Moison, R. Frydman, R. Habert, V. Rouiller-Fabre, Phthalates impair germ cell development in the human fetal testis in vitro without change in testosterone production, *Environ. Health Perspect.* 117 (2009) 32–37.
- [115] N.E. Heger, S.J. Hall, M.A. Sandrof, E.V. McDonnell, J.B. Hensley, E.N. McDowell, K.A. Martin, K.W. Gaido, K.J. Johnson, K. Boekelheide, Human fetal testis xenografts are resistant to phthalate-induced endocrine disruption, *Environ. Health Perspect.* 120 (2012) 1137–1143.
- [116] R.T. Mitchell, A.J. Childs, R.A. Anderson, S. van den Driesche, P.T. Saunders, C. McKinnell, W.H. Wallace, C.J. Kelnar, R.M. Sharpe, Do phthalates affect steroidogenesis by the human fetal testis? Exposure of human fetal testis



- xenografts to di-*N*-butyl phthalate, *J. Clin. Endocrinol. Metab.* 97 (2012) E341–348.
- [117] R.T. Mitchell, R.M. Sharpe, R.A. Anderson, C. McKinnell, S. Macpherson, L.B. Smith, W.H. Wallace, C.J. Kelnar, S. van den Driesche, Diethylstilbestrol exposure does not reduce testosterone production in human fetal testis xenografts, *PLoS One* 8 (2013) e61726.
- [118] T. N'Tumba-Byn, D. Moison, M. Lacroix, C. Lecureuil, L. Lesage, S.M. Prud'homme, S. Pozzi-Gaudin, R. Frydman, A. Benachi, G. Livera, V. Rouiller-Fabre, R. Habert, Differential effects of bisphenol A and diethylstilbestrol on human, rat and mouse fetal Leydig cell function, *PLoS One* 7 (2012) e51579.
- [119] G. Delbes, C. Duquenne, J. Szenker, J. Taccoen, R. Habert, C. Levacher, Developmental changes in testicular sensitivity to estrogens throughout fetal and neonatal life, *Toxicol. Sci.* 99 (2007) 234–243.
- [120] P. Tartarin, D. Moison, E. Guibert, J. Dupont, R. Habert, V. Rouiller-Fabre, N. Frydman, S. Pozzi, R. Frydman, C. Lecureuil, P. Froment, Metformin exposure affects human and mouse fetal testicular cells, *Hum. Reprod.* 27 (2012) 3304–3314.
- [121] E.K. Barthelmeß, R.K. Naz, Polycystic ovary syndrome: current status and future perspective, *Front. Biosci. (Elite Ed.)* 6 (2014) 104–119.
- [122] A. Mlynarcikova, M. Fickova, S. Scsukova, Impact of endocrine disruptors on ovarian steroidogenesis, *Endocr. Regul.* 48 (2014) 201–224.
- [123] A.M. Calafat, X. Ye, L.Y. Wong, J.A. Reidy, L.L. Needham, Exposure of the U.S. population to bisphenol A and 4-tertiary-octylphenol: 2003–2004, *Environ. Health Perspect.* 116 (2008) 39–44.
- [124] B.L. Sprague, A. Trentham-Dietz, C.J. Hedman, J. Wang, J.D. Hemming, J.M. Hampton, D.S. Buist, E.J. Aiello Bowles, G.S. Sisney, E.S. Burnside, Circulating serum xenoestrogens and mammographic breast density, *Breast Cancer Res.* 15 (2013) R45.
- [125] Y. Ikezuki, O. Tsutsumi, Y. Takai, Y. Kamei, Y. Taketani, Determination of bisphenol A concentrations in human biological fluids reveals significant early prenatal exposure, *Hum. Reprod.* 17 (2002) 2839–2841.
- [126] E. De Felip, A. di Domenico, R. Miniero, L. Silvestroni, Polychlorobiphenyls and other organochlorine compounds in human follicular fluid, *Chemosphere* 54 (2004) 1445–1449.
- [127] J.D. Meeker, S.A. Missmer, L. Altshul, A.F. Vitonis, L. Ryan, D.W. Cramer, R. Hauser, Serum and follicular fluid organochlorine concentrations among women undergoing assisted reproduction technologies, *Environ. Health* 8 (2009) 32.
- [128] E.L. Gregoraszczuk, Dioxin exposure and porcine reproductive hormonal activity, *Cad. Saude Publica* 18 (2002) 453–462.
- [129] W.S. Stokes, Selecting appropriate animal models and experimental designs for endocrine disruptor research and testing studies, *ILAR J.* 45 (2004) 387–393.
- [130] S. Lenie, J. Smitz, Steroidogenesis-disrupting compounds can be effectively studied for major fertility-related endpoints using in vitro cultured mouse follicles, *Toxicol. Lett.* 185 (2009) 143–152.
- [131] A. Mlynarcikova, M. Fickova, S. Scsukova, The effects of selected phenol and phthalate derivatives on steroid hormone production by cultured porcine granulosa cells, *Altern. Lab. Anim.* 35 (2007) 71–77.
- [132] M. Breckwoldt, N. Selvaraj, D. Aharoni, A. Barash, I. Segal, V. Insler, A. Amsterdam, Expression of Ad4-BP/cytochrome P450 side chain cleavage enzyme and induction of cell death in long-term cultures of human granulosa cells, *Mol. Hum. Reprod.* 2 (1996) 391–400.
- [133] F. Jacob, S. Nixdorf, N.F. Hacker, V.A. Heinzlmann-Schwarz, Reliable in vitro studies require appropriate ovarian cancer cell lines, *J. Ovarian Res.* 7 (2014) 60.
- [134] J.C. Havelock, W.E. Rainey, B.R. Carr, Ovarian granulosa cell lines, *Mol. Cell. Endocrinol.* 228 (2004) 67–78.
- [135] K. Kananen, M. Markkula, E. Rainio, J.G. Su, A.J. Hsueh, I.T. Huhtaniemi, Gonadal tumorigenesis in transgenic mice bearing the mouse inhibin alpha-subunit promoter/simian virus T-antigen fusion gene: characterization of ovarian tumors and establishment of gonadotropin-responsive granulosa cell lines, *Mol. Endocrinol.* 9 (1995) 616–627.
- [136] D. Gunnarsson, P. Leffler, E. Ekwurtzel, G. Martinsson, K. Liu, G. Selstam, Mono-(2-ethylhexyl) phthalate stimulates basal steroidogenesis by a cAMP-independent mechanism in mouse gonadal cells of both sexes, *Reproduction* 135 (2008) 693–703.
- [137] T.W. Briers, A. van de Voorde, H. Vanderstichele, Characterization of immortalized mouse granulosa cell lines, *In Vitro Cell. Dev. Biol. Anim.* 29A (1993) 847–854.
- [138] H. Vanderstichele, B. Delaey, J. de Winter, F. de Jong, L. Rombauts, G. Verhoeven, C. Dello, A. van de Voorde, T. Briers, Secretion of steroids, growth factors, and cytokines by immortalized mouse granulosa cell lines, *Biol. Reprod.* 50 (1994) 1190–1202.
- [139] P.K. Kreeger, T.K. Woodruff, L.D. Shea, Murine granulosa cell morphology and function are regulated by a synthetic Arg-Gly-Asp matrix, *Mol. Cell. Endocrinol.* 205 (2003) 1–10.
- [140] K. Tajima, K. Hosokawa, Y. Yoshida, A. Dantes, R. Sasson, F. Kotsuji, A. Amsterdam, Establishment of FSH-responsive cell lines by transfection of pre-ovulatory human granulosa cells with mutated p53 (p53val135) and H-ras genes, *Mol. Hum. Reprod.* 8 (2002) 48–57.
- [141] R. Sasson, K. Tajima, A. Amsterdam, Glucocorticoids protect against apoptosis induced by serum deprivation, cyclic adenosine 3',5'-monophosphate and p53 activation in immortalized human granulosa cells: involvement of Bcl-2, *Endocrinology* 142 (2001) 802–811.
- [142] S.M. Salihi, M. Jamaluddin, S.A. Salama, A.A. Fadl, M. Nagamani, A. Al-Hendy, Regulation of catechol O-methyltransferase expression in granulosa cells: a potential role for follicular arrest in polycystic ovary syndrome, *Fertil. Steril.* 89 (2008) 1414–1421.
- [143] S.S. Patel, V.E. Beshay, J.C. Escobar, T. Suzuki, B.R. Carr, Molecular mechanism for repression of 17alpha-hydroxylase expression and androstenedione production in granulosa cells, *J. Clin. Endocrinol. Metab.* 94 (2009) 5163–5168.
- [144] K. Hosokawa, A. Dantes, C. Schere-Levy, A. Barash, Y. Yoshida, F. Kotsuji, I. Vlodavsky, A. Amsterdam, Induction of Ad4BP/SF-1, steroidogenic acute regulatory protein, and cytochrome P450scc enzyme system expression in newly established human granulosa cell lines, *Endocrinology* 139 (1998) 4679–4687.
- [145] I. Ishiwata, C. Ishiwata, M. Soma, N. Kobayashi, H. Ishikawa, Establishment and characterization of an estrogen-producing human ovarian granulosa tumor cell line, *J. Natl. Cancer Inst.* 72 (1984) 789–800.
- [146] H. Zhang, M. Vollmer, M. De Geyter, Y. Litzistorf, A. Ladewig, M. Durrenberger, R. Guggenheim, P. Miny, W. Holzgreve, C. De Geyter, Characterization of an immortalized human granulosa cell line (COV434), *Mol. Hum. Reprod.* 6 (2000) 146–153.
- [147] R.M. Navalakhe, D.D. Jagtap, S.U. Nayak, T.D. Nandedkar, S.D. Mahale, Effect of FSH receptor-binding inhibitor-8 on FSH-mediated granulosa cell signaling and proliferation, *Chem. Biol. Drug Des.* 82 (2013) 178–188.
- [148] N. Mansouri-Attia, R. James, A. Ligon, X. Li, S.A. Pangas, Soy promotes juvenile granulosa cell tumor development in mice and in the human granulosa cell tumor-derived COV434 cell line, *Biol. Reprod.* 91 (2014) 100.
- [149] L. Cloix, M. Reverchon, M. Cornuau, P. Froment, C. Rame, C. Costa, G. Froment, P. Lecomte, W. Chen, D. Royere, F. Guerif, J. Dupont, Expression and regulation of INTELECTIN1 in human granulosa-lutein cells: role in IGF-1-induced steroidogenesis through NAMPT, *Biol. Reprod.* 91 (2014) 50.
- [150] T. Mizutani, Y. Ju, Y. Imamichi, T. Osaki, T. Yazawa, S. Kawabe, S. Ishikane, T. Matsumura, M. Kanno, Y. Kamiki, K. Kimura, N. Minamino, K. Miyamoto, C/EBPbeta (CCAAT/enhancer-binding protein beta) mediates progesterone production through transcriptional regulation in co-operation with SF-1 (steroidogenic factor-1), *Biochem. J.* 460 (2014) 459–471.
- [151] S. Kawabe, T. Yazawa, M. Kanno, Y. Usami, T. Mizutani, Y. Imamichi, Y. Ju, T. Matsumura, M. Orisaka, K. Miyamoto, A novel isoform of liver receptor homolog-1 is regulated by steroidogenic factor-1 and the specificity protein family in ovarian granulosa cells, *Endocrinology* 154 (2013) 1648–1660.
- [152] M. Reverchon, M. Cornuau, L. Cloix, C. Rame, F. Guerif, D. Royere, J. Dupont, Visfatin is expressed in human granulosa cells: regulation by metformin through AMPK/SIRT1 pathways and its role in steroidogenesis, *Mol. Hum. Reprod.* 19 (2013) 313–326.
- [153] H.M. Chang, J.C. Cheng, C. Klausen, P.C. Leung, BMP15 suppresses progesterone production by down-regulating StAR via ALK3 in human granulosa cells, *Mol. Endocrinol.* 27 (2013) 2093–2104.
- [154] G. Irusta, M.C. Pazos, D. Abramovich, I. De Zuniga, F. Parborelli, M. Tesone, Effects of an inhibitor of the gamma-secretase complex on proliferation and apoptotic parameters in a FOXL2-mutated granulosa tumor cell line (KGN), *Biol. Reprod.* 89 (2013) 9.
- [155] D. Fu, X. Lv, G. Hua, C. He, J. Dong, S.M. Lele, D.W. Li, Q. Zhai, J.S. Davis, C. Wang, YAP regulates cell proliferation, migration, and steroidogenesis in adult granulosa cell tumors, *Endocr. Relat. Cancer* 21 (2014) 297–310.
- [156] J. Kwintkiewicz, Y. Nishi, T. Yanase, L.C. Giudice, Peroxisome proliferator-activated receptor-gamma mediates bisphenol A inhibition of FSH-stimulated IGF-1, aromatase, and estradiol in human granulosa cells, *Environ. Health Perspect.* 118 (2010) 400–406.
- [157] M. Watanabe, S. Ohno, S. Nakajin, Effects of bisphenol A on the expression of cytochrome P450 aromatase (CYP19) in human fetal osteoblastic and granulosa cell-like cell lines, *Toxicol. Lett.* 210 (2012) 95–99.
- [158] J. Ernst, J.C. Jann, R. Biemann, H.M. Koch, B. Fischer, Effects of the environmental contaminants DEHP and TCDD on estradiol synthesis and aryl hydrocarbon receptor and peroxisome proliferator-activated receptor signalling in the human granulosa cell line KGN, *Mol. Hum. Reprod.* 20 (2014) 919–928.
- [159] W. Fan, T. Yanase, H. Morinaga, S. Gondo, T. Okabe, M. Nomura, T. Komatsu, K. Morohashi, T.B. Hayes, R. Takayanagi, H. Nawata, Atrazine-induced aromatase expression is SF-1 dependent: implications for endocrine disruption in wildlife and reproductive cancers in humans, *Environ. Health Perspect.* 115 (2007) 720–727.
- [160] S. Park, S. Kim, H. Jin, K. Lee, J. Bae, Impaired development of female mouse offspring maternally exposed to simazine, *Environ. Toxicol. Pharmacol.* 38 (2014) 845–851.
- [161] W.L. Miller, A brief history of adrenal research: steroidogenesis—the soul of the adrenal, *Mol. Cell. Endocrinol.* 371 (2013) 5–14.
- [162] P.W. Harvey, D.J. Everett, The adrenal cortex and steroidogenesis as cellular and molecular targets for toxicity: critical omissions from regulatory endocrine disrupter screening strategies for human health? *J. Appl. Toxicol.* 23 (2003) 81–87.
- [163] P.W. Harvey, D.J. Everett, C.J. Springall, Adrenal toxicology: a strategy for assessment of functional toxicity to the adrenal cortex and steroidogenesis, *J. Appl. Toxicol.* 27 (2007) 103–115.
- [164] P.W. Harvey, C. Sutcliffe, Adrenocortical hypertrophy: establishing cause and toxicological significance, *J. Appl. Toxicol.* 30 (2010) 617–626.
- [165] J.P. Hinson, P.W. Raven, Effects of endocrine-disrupting chemicals on adrenal function, *Best Pract. Res. Clin. Endocrinol. Metab.* 20 (2006) 111–120.

- [166] FDA, Endocrine disruption potential of drugs: nonclinical evaluation, Draft Guidance, Federal Register 78, 183 (2013) 57859.
- [167] P.W. Harvey, Adrenocortical endocrine disruption, *J. Steroid Biochem. Mol. Biol.* 155 (2016) 199–206.
- [168] D.B. Martinez-Arguelles, V. Papadopoulos, Mechanisms mediating environmental chemical-induced endocrine disruption in the adrenal gland, *Front. Endocrinol. (Lausanne)* 6 (2015) 29.
- [169] O.g.f.t.t.o. chemicals., Test No. 456: H295R Steroidogenesis Assay, OECD Guidelines for the Testing of Chemicals, Section 4: Health Effects, (2011).
- [170] A.F. Gazdar, H.K. Oie, C.H. Shackleton, T.R. Chen, T.J. Triche, C.E. Myers, G.P. Chrousos, M.F. Brennan, C.A. Stein, R.V. La Rocca, Establishment and characterization of a human adrenocortical carcinoma cell line that expresses multiple pathways of steroid biosynthesis, *Cancer Res.* 50 (1990) 5488–5496.
- [171] W.E. Rainey, I.M. Bird, J.I. Mason, The NCI-H295 cell line: a pluripotent model for human adrenocortical studies, *Mol. Cell. Endocrinol.* 100 (1994) 45–50.
- [172] W.E. Rainey, I.M. Bird, C. Sawetawan, N.A. Hanley, J.L. McCarthy, E.A. McGee, R. Wester, J.I. Mason, Regulation of human adrenal carcinoma cell (NCI-H295) production of C19 steroids, *J. Clin. Endocrinol. Metab.* 77 (1993) 731–737.
- [173] W.E. Rainey, K. Saner, B.P. Schimmer, Adrenocortical cell lines, *Mol. Cell. Endocrinol.* 228 (2004) 23–38.
- [174] B. Staels, D.W. Hum, W.L. Miller, Regulation of steroidogenesis in NCI-H295 cells: a cellular model of the human fetal adrenal, *Mol. Endocrinol.* 7 (1993) 423–433.
- [175] H. Rodriguez, D.W. Hum, B. Staels, W.L. Miller, Transcription of the human genes for cytochrome P450sc and P450c17 is regulated differently in human adrenal NCI-H295 cells than in mouse adrenal Y1 cells, *J. Clin. Endocrinol. Metab.* 82 (1997) 365–371.
- [176] T. Wang, J.G. Rowland, J. Parmar, M. Nesterova, T. Seki, W.E. Rainey, Comparison of aldosterone production among human adrenocortical cell lines, *Horm. Metab. Res.* 44 (2012) 245–250.
- [177] J. Parmar, R.E. Key, W.E. Rainey, Development of an adrenocorticotropic-responsive human adrenocortical carcinoma cell line, *J. Clin. Endocrinol. Metab.* 93 (2008) 4542–4546.
- [178] T. Wang, W.E. Rainey, Human adrenocortical carcinoma cell lines, *Mol. Cell. Endocrinol.* 351 (2012) 58–65.
- [179] Y. Xing, M.A. Edwards, C. Ahlem, M. Kennedy, A. Cohen, C.E. Gomez-Sanchez, W.E. Rainey, The effects of ACTH on steroid metabolomic profiles in human adrenal cells, *J. Endocrinol.* 209 (2011) 327–335.
- [180] I.M. Bird, N.A. Hanley, R.A. Word, J.M. Mathis, J.L. McCarthy, J.I. Mason, W.E. Rainey, Human NCI-H295 adrenocortical carcinoma cells: a model for angiotensin-II-responsive aldosterone secretion, *Endocrinology* 133 (1993) 1555–1561.
- [181] B.J. Clark, S.C. Soo, K.M. Caron, Y. Ikeda, K.L. Parker, D.M. Stocco, Hormonal and developmental regulation of the steroidogenic acute regulatory protein, *Mol. Endocrinol.* 9 (1995) 1346–1355.
- [182] H. Otani, F. Otsuka, K. Inagaki, J. Suzuki, T. Miyoshi, Y. Kano, J. Goto, T. Ogura, H. Makino, Aldosterone breakthrough caused by chronic blockage of angiotensin II type 1 receptors in human adrenocortical cells: possible involvement of bone morphogenetic protein-6 actions, *Endocrinology* 149 (2008) 2816–2825.
- [183] E.F. Nogueira, W.B. Bollag, W.E. Rainey, Angiotensin II regulation of adrenocortical gene transcription, *Mol. Cell. Endocrinol.* 302 (2009) 230–236.
- [184] E.F. Nogueira, C.A. Vargas, M. Otis, N. Gallo-Payet, W.B. Bollag, W.E. Rainey, Angiotensin-II acute regulation of rapid response genes in human, bovine, and rat adrenocortical cells, *J. Mol. Endocrinol.* 39 (2007) 365–374.
- [185] E. Samandari, P. Kempna, J.M. Nuoffer, G. Hofer, P.E. Mullis, C.E. Fluck, Human adrenal corticocarcinoma NCI-H295R cells produce more androgens than NCI-H295A cells and differ in 3beta-hydroxysteroid dehydrogenase type 2 and 17, 20 lyase activities, *J. Endocrinol.* 195 (2007) 459–472.
- [186] S.H. Mellon, N. Compagnone, M. Sander, C. Cover, D. Ganten, B. Djavidani, Rodent models for studying steroids and hypertension: from fetal development to cells in culture, *Steroids* 60 (1995) 59–64.
- [187] S.H. Mellon, W.L. Miller, S.R. Bair, C.C. Moore, J.L. Vigne, R.I. Weiner, Steroidogenic adrenocortical cell lines produced by genetically targeted tumorigenesis in transgenic mice, *Mol. Endocrinol.* 8 (1994) 97–108.
- [188] N.A. Compagnone, S.R. Bair, S.H. Mellon, Characterization of adrenocortical cell lines produced by genetically targeted tumorigenesis in transgenic mice, *Steroids* 62 (1997) 238–243.
- [189] B.P. Schimmer, M. Cordova, H. Cheng, A. Tsao, A.B. Goryachev, A.D. Schimmer, Q. Morris, Global profiles of gene expression induced by adrenocorticotropic in Y1 mouse adrenal cells, *Endocrinology* 147 (2006) 2357–2367.
- [190] B. Ragazzon, A.M. Lefrancois-Martinez, P. Val, I. Sahut-Barnola, C. Tournaire, C. Chambon, J.L. Gachancard-Bouya, R.J. Begue, G. Veyssiere, A. Martinez, Adrenocorticotropic-dependent changes in SF-1/DAX-1 ratio influence steroidogenic genes expression in a novel model of glucocorticoid-producing adrenocortical cell lines derived from targeted tumorigenesis, *Endocrinology* 147 (2006) 1805–1818.
- [191] K. Hilscherova, P.D. Jones, T. Gracia, J.L. Newsted, X. Zhang, J.T. Sanderson, R.M. Yu, R.S. Wu, J.P. Giesy, Assessment of the effects of chemicals on the expression of ten steroidogenic genes in the H295R cell line using real-time PCR, *Toxicol. Sci.* 81 (2004) 78–89.
- [192] A. Oskarsson, E. Ulleras, K.E. Plant, J.P. Hinson, P.S. Goldfarb, Steroidogenic gene expression in H295R cells and the human adrenal gland: adrenotoxic effects of lindane in vitro, *J. Appl. Toxicol.* 26 (2006) 484–492.
- [193] T. Gracia, K. Hilscherova, P.D. Jones, J.L. Newsted, E.B. Higley, X. Zhang, M. Hecker, M.B. Murphy, R.M. Yu, P.K. Lam, R.S. Wu, J.P. Giesy, Modulation of steroidogenic gene expression and hormone production of H295R cells by pharmaceuticals and other environmentally active compounds, *Toxicol. Appl. Pharmacol.* 225 (2007) 142–153.
- [194] T. Gracia, K. Hilscherova, P.D. Jones, J.L. Newsted, X. Zhang, M. Hecker, E.B. Higley, J.T. Sanderson, R.M. Yu, R.S. Wu, J.P. Giesy, The H295R system for evaluation of endocrine-disrupting effects, *Ecotoxicol. Environ. Saf.* 65 (2006) 293–305.
- [195] D.M. Rotroff, D.J. Dix, K.A. Houck, T.B. Knudsen, M.T. Martin, K.W. McLaurin, D. M. Reif, K.M. Crofton, A.V. Singh, M. Xia, R. Huang, R.S. Judson, Using in vitro high throughput screening assays to identify potential endocrine-disrupting chemicals, *Environ. Health Perspect.* 121 (2013) 7–14.
- [196] M.W. van den Dungen, J.C. Rijk, E. Kampman, W.T. Steegenga, A.J. Murk, Steroid hormone related effects of marine persistent organic pollutants in human H295R adrenocortical carcinoma cells, *Toxicol. In Vitro* 29 (2015) 769–778.
- [197] E. Ulleras, A. Ohlsson, A. Oskarsson, Secretion of cortisol and aldosterone as a vulnerable target for adrenal endocrine disruption—screening of 30 selected chemicals in the human H295R cell model, *J. Appl. Toxicol.* 28 (2008) 1045–1053.
- [198] J.M. Maglich, M. Kuhn, R.E. Chapin, M.T. Pletcher, More than just hormones: H295R cells as predictors of reproductive toxicity, *Reprod. Toxicol.* 45 (2014) 77–86.
- [199] M. Hecker, J.L. Newsted, M.B. Murphy, E.B. Higley, P.D. Jones, R. Wu, J.P. Giesy, Human adrenocarcinoma (H295R) cells for rapid in vitro determination of effects on steroidogenesis: hormone production, *Toxicol. Appl. Pharmacol.* 217 (2006) 114–124.
- [200] C.S. Winther, F.K. Nielsen, M. Hansen, B. Styrisshave, Corticosteroid production in H295R cells during exposure to 3 endocrine disrupters analyzed with LC-MS/MS, *Int. J. Toxicol.* 32 (2013) 219–227.
- [201] D. Tonoli, C. Furstenberger, J. Bocard, D. Hochstrasser, F. Jeanneret, A. Odermatt, S. Rudaz, Steroidomic fingerprinting based on ultra-high performance liquid chromatography coupled with qualitative and quantitative high-resolution mass spectrometry for the evaluation of endocrine disrupting chemicals in H295R cells, *Chem. Res. Toxicol.* 28 (2015) 955–966.
- [202] N.G. Hattangady, L.O. Olala, W.B. Bollag, W.E. Rainey, Acute and chronic regulation of aldosterone production, *Mol. Cell. Endocrinol.* 350 (2012) 151–162.
- [203] J.C. Rijk, A.A. Peijnenburg, M.H. Blokland, A. Lommen, R.L. Hoogenboom, T.F. Bovee, Screening for modulatory effects on steroidogenesis using the human H295R adrenocortical cell line: a metabolomics approach, *Chem. Res. Toxicol.* 25 (2012) 1720–1731.
- [204] M. Reitsma, T.F. Bovee, A.A. Peijnenburg, P.J. Hendriksen, R.L. Hoogenboom, J. C. Rijk, Endocrine-disrupting effects of thioxanthone photoinitiators, *Toxicol. Sci.* 132 (2013) 64–74.
- [205] F.K. Nielsen, C.H. Hansen, J.A. Fey, M. Hansen, N.W. Jacobsen, B. Halling-Sorensen, E. Bjorklund, B. Styrisshave, H295R cells as a model for steroidogenic disruption: a broader perspective using simultaneous chemical analysis of 7 key steroid hormones, *Toxicol. In Vitro* 26 (2012) 343–350.
- [206] J.G. Teeguarden, S. Hanson-Drury, A systematic review of Bisphenol A “low dose” studies in the context of human exposure: a case for establishing standards for reporting “low-dose” effects of chemicals, *Food Chem. Toxicol.* 62 (2013) 935–948.

### 5.3 Paper 9 (Engeli et al, in preparation)

## Characterization of murine Leydig Cells as Potential Screening Tools for Androgen Synthesis Disruption by Xenobiotics

Roger T. Engeli, Cornelia Fürstenberger, Denise Kratschmar, Alex Odermatt

Manuscript in preparation (data complete)

**Contribution:** Conducted all *in vitro* cell experiments in MA-10, BLTK, and TM3 cells. Analyzed and provided all real time-PCR data. Drafted the paper manuscript.

**Aims:** To characterize and select a murine Leydig cell model to develop an *in vitro* screening tool for disruption of androgens synthesis.

**Results:** All tested cell lines were not able to produce detectable levels of testosterone without stimulation. Stimulated cells were able to dose-dependently increase testosterone synthesis but to a lesser extent compared to other steroids, such as progesterone and androsterone. Gene expression studies revealed low levels of endogenous 17 $\beta$ -HSD3, an absence of 17 $\beta$ -HSD5, and significant levels of 17 $\beta$ -HSD1 in all of the tested cell lines.

**Conclusion:** This study emphasizes the need to use of LC-MS to quantitatively analyze steroids secreted by Leydig cells and shows that MA-10 and BLTK1 cells produce a variety of steroids but only low amounts or no testosterone.

## **Characterization of Murine Leydig Cell Lines as Potential Screening Tools for Androgen Synthesis Disruption by Xenobiotics**

Roger T. Engeli,<sup>†</sup> Cornelia Fürstenberger,<sup>†</sup> Denise Kratschmar,<sup>†</sup> Alex Odermatt<sup>†</sup>

<sup>†</sup> Division of Molecular & Systems Toxicology, University of Basel, Klingelbergstr. 50, 4056 Basel, Switzerland

Corresponding author:

Alex Odermatt, Division of Molecular & Systems Toxicology, University of Basel, Klingelbergstr. 50, 4056 Basel, Switzerland

E-mail: [alex.odermatt@unibas.ch](mailto:alex.odermatt@unibas.ch); Phone: +41 (0)61 207 1530 ; Fax: +41 (0)61 207 1515

### Abbreviations

DMEM, Dulbecco's modified Eagle's medium; LC-MS, liquid chromatography-mass spectrometry; T, testosterone; ADT, androsterone; AD, androstenedione; DHT, 5 $\alpha$ -dihydrotestosterone; P, progesterone; FBS; fetal bovine serum, HS; horse serum,

## **Abstract**

Mammalian Leydig cells produce the majority of the systemic levels of the primary male sex hormone testosterone (T). T plays a crucial role during development of male reproductive tissues, onset of puberty, and maintaining health state. Disruption of T synthesis has been associated with several diseases. The final step of T synthesis is catalyzed by 17 $\beta$ -hydroxysteroid dehydrogenase 3 (17 $\beta$ -HSD3). Due to the lack of a human Leydig cell model, murine cell lines (MA-10, BLTK1, TM3) were assessed for their suitability to investigate substances interfering with T production. Endogenous 17 $\beta$ -HSD3 expression and the ability to convert  $\Delta$ 4-androstene-3,17-dione (AD) into T was studied in these murine cell lines. Furthermore, cells were stimulated using br-8-cAMP and forskolin to study the effects on steroidogenesis. Cell supernatants were analyzed using LC-MS/MS. The results revealed that the unstimulated murine Leydig cell lines incubated with AD produced very low T but substantial amounts of the inactive metabolite androsterone. Further characterization showed that stimulated MA-10 cells generated low but concentration-dependent amounts of AD and T but high amounts of progesterone. Gene expression analyses revealed very low or background 17 $\beta$ -HSD3 levels, absence of 17 $\beta$ -HSD5 (Akr1c6), but substantial 17 $\beta$ -HSD1 expression. In conclusion, murine MA-10, BLTK1 and TM3 Leydig cells are not suitable to study 17 $\beta$ -HSD3 activity. The low T produced by these cells may be due to 17 $\beta$ -HSD1, accepting AD as substrate. This study emphasizes the necessity of quantitatively analyzing steroids using LC-MS/MS or related methods and shows that MA-10 and BLTK1 cells produce a variety of steroids but only low amounts or no T.

## **Keywords**

Leydig cells, androgens, endocrine disrupters, MA-10, screening

## Introduction

Steroid hormones are involved in the regulation of essential physiological processes. Systemic levels of steroids are mainly produced by the adrenal glands, synthesizing mineralocorticoids, glucocorticoids and precursors of active androgens, and the gonads, synthesizing active sex steroids [1]. Disruption of steroidogenesis by genetic defects or environmental influences, including the exposure to synthetic chemicals, has been associated with developmental disturbances [2], impaired reproduction [3, 4], cancer [5-7], metabolic disorders [8-10], immune and neurologic diseases [11, 12].

For the identification of substances interfering with steroidogenesis and for mechanistic investigations cell lines derived from the adrenals or from testicular Leydig cells represent ethically accepted, low-cost and rapid testing systems and alternatives to primary cells and animal experimentation. Nevertheless, cell-based models must be well characterized and they should be used only for well-defined applications for which they have proven useful. In contrast to the adrenals, where a human adrenal adenoma cell line (H295R) has been validated according to the Organization for Economic Cooperation and Development (OECD) guideline to detect substances disrupting steroid production [13], currently no human Leydig cell line to study testicular steroidogenesis is available. Primary human Leydig cells are difficult to obtain due to low yield, and there are large inter-individual differences; similarly, the preparation of primary rodent Leydig cells is laborious and the yield rather low. There are, however, several commercially available rodent Leydig cell lines to study testicular steroidogenesis (reviewed in [14, 15]).

Human and rodent *de novo* androgen production from cholesterol differs regarding androstenedione (AD) synthesis. In humans AD is produced via the  $\Delta^5$  metabolic steroid intermediates pregnenolone (Preg) and  $17\alpha$ -hydroxypregnenolone ( $17\text{OH-Preg}$ ). The human enzyme CYP17A1 efficiently converts  $17\text{OH-Preg}$  to dehydroepiandrosterone (DHEA) but has low affinity to  $17\alpha$ -hydroxy progesterone ( $17\text{OH-P}$ ). In rodents, CYP17 is able to convert  $\Delta^4$  and  $\Delta^5$  steroids, but in contrast to humans it prefers the  $\Delta^4$  intermediates progesterone (P) and  $17\text{OH-P}$  [16]. Importantly, in both species AD is converted in the last step into T by  $17\beta$ -hydroxysteroid dehydrogenase type 3 ( $17\beta\text{-HSD3}$ ) [17].

Several reports describe the use of mouse Leydig cell lines to investigate the interference of xenobiotics with steroidogenesis, especially focusing on the disruption of T production (reviewed



in [15]). Many studies have chosen a single steroid as a read-out, mostly T, and using antibody-based detection methods. Such methods often suffer from limited specificity [18-21], and it cannot be excluded that other steroid metabolites might interfere with the read-out due to lack of selectivity.

An initial aim of the present project was to find a mouse Leydig cell model expressing substantial levels of 17 $\beta$ -HSD3 in order to investigate the impact of substances on the last step of testicular T formation. Three mouse Leydig cell lines, MA-10, BLTK1 and TM3 were investigated by assessing the conversion of exogenous AD to T, the basal production of T, as well as the production of T and additional steroids following stimulation by br-8-cAMP and forskolin. The mRNA expression levels of key genes involved in androgen production was measured by quantitative RT-PCR, providing an explanation for the observed steroid production by these cells.

## **Material and Methods**

### **Cultivation of MA-10, BLTK+ and TMR cell lines**

The mouse Leydig cell line MA-10 (ATCC, Manassas, VA, USA) was cultivated as described previously [22]. Cell culture materials and chemicals were obtained from Gibco, Carlsbad, CA, USA, and Sigma-Aldrich, St. Louis, MO, USA, unless otherwise stated. Briefly, cells were grown on 0.1% gelatin-coated cell culture dishes in DMEM/F12 media containing 20 mM HEPES, pH 7.4, 15% horse serum, and 50  $\mu$ g/mL gentamicin. The BLTK1 mouse Leydig cell line (kindly provided by Prof. Ilpo Huhtaniemi and Dr. Nafis Rahman, University of Turku, Turku, Finland [23]) was maintained in DMEM/F12 media with 10% fetal bovine serum (FBS), 100 U/mL penicillin and 100  $\mu$ g/mL streptomycin. The mouse Leydig cell line TM3 was cultivated in DMEM/F12 media, containing 15 mM HEPES, pH 7.4, 100 U/mL penicillin and 100  $\mu$ g/mL streptomycin, 2.5 mM L-glutamine, 5% horse serum and 2.5% FBS. All cell lines were incubated under standard conditions (5% CO<sub>2</sub>, 37°C). For ultra-pressure liquid chromatography-tandem mass spectrometry (UPLC-MS/MS) measurements phenol red-free medium containing overnight charcoal/dextran-treated FBS or horse serum.

### **Determination of mRNA expression**

Total RNA from mouse Leydig cells (300'000 cells seeded in 6-well plates) was extracted using Trizol reagent, followed by reverse transcription using the Superscript III reverse transcriptase. The mRNA levels from different genes were analyzed using a Rotor-Gene 6000 light cycler (Corbett, Sydney, Australia). Reactions were performed in a total volume of 10  $\mu$ L reaction buffer containing KAPA SYBR master mix (Kapasystems, Boston, MA, USA), 10 ng cDNA and specific oligonucleotide primers (Table 1). Relative gene expression was compared to the internal control cyclophilin A (PPIA).

### **Determination of androstenedione metabolism**

The conversion of radiolabeled AD by BLTK1 cells (10'000 grown in 24-well plates) was measured using a modified protocol from Legeza et al. [22]. Briefly, cells were incubated in serum free DMEM/F12 medium containing 200 nM radiolabeled 50 nCi [1, 2, 6, 7-<sup>3</sup>H]-AD (GE Healthcare, Little Chalfont, UK). The enzymatic reactions were terminated by adding 2 mM unlabeled AD and T dissolved in methanol. The steroids were separated on UV-sensitive silica TLC plates (Macherey-Nagel, Oensingen, Switzerland) using a chloroform-methanol solvent system at a ratio of 9:1. Bands migrating with an R<sub>f</sub> of AD and T as well as two fractions in between AD and T were scraped off the TLC plate and transferred to tubes containing scintillation cocktail. Radioactive decay of AD and corresponding metabolites were analyzed using a scintillation counter (PerkinElmer, Waltham, MA, USA). For UPLC-MS/MS analysis unlabeled AD (250 nM) was used, and steroids analyzed after extraction from bands of TLC plates by UPLC-MS/MS. Alternatively, for experiments where steroids were directly analyzed by UPLC-MS/MS MA-10 (100'000), BLTK1 (200'000) and TM3 (75'000) cells were seeded in 12-well plates and cultivated for 24 h. Cells were washed with phosphate buffered saline (PBS) and incubated with charcoal/dextran-treated FBS/horse serum phenol red-free complete DMEM/F12 medium containing 200 nM AD, cAMP analogue or forskolin. Cells were incubated for 24 h, followed by collection of culture supernatants. Samples were stored at -20°C prior to UPLC-MS/MS analysis.

### **Assessment of cross-reactivity of the enzyme immunoassay (EIA) kit for testosterone**

The EIA kit for testosterone (Cayman Chemical Company, MI, USA) was applied according to the manufacturer's instructions. DHT and 5 $\beta$ -dihydrotestosterone, androstenediol, 5 $\alpha$ -androstanedione, ADT, eticholanolone and dihydroepiandrosterone were purchased from Steraloids (Newport, RI, USA). All tested metabolites were dissolved in ethanol, diluted in the buffer provided with the kit and measured at three different concentrations (150 pg/mL, 75 pg/mL and 37.5 pg/mL) in duplicates. Cross-reactivity was calculated in percentage of the recovery rate of the corresponding metabolite.

### **Ultra-pressure liquid chromatography-tandem mass spectrometry**

Stock solutions were prepared in methanol for deuterium labeled internal standards (IS) (Steraloids) at a concentration of 10 mM. Thereafter, standards and deuterium labeled IS working solutions were prepared by mixing each individual stock solution to obtain a working concentration of 100  $\mu$ M. Calibration curves were prepared by serial dilution of the working solutions of standards in DMEM/F12 phenol red-free medium in the range of 0.975 nM to 1000 nM. Cell supernatant was taken at the appropriate time point and IS at a final concentration of 0.1  $\mu$ M in protein precipitation solution (zinc sulfate 0.8 M in water/methanol 50/50 v/v) were added. After shaking vigorously for 10 min at 4°C, the samples were centrifuged for 10 min at 10'000  $\times$  g. Samples were transferred onto Oasis HBL SPE columns (Waters, Milford, MA, USA) that were preconditioned with methanol and water. Samples were washed twice with water, eluted with methanol and evaporated at a vacuum evaporator. Samples were reconstituted in 100  $\mu$ L methanol by vigorously shaking for 30 min at 4°C.

The samples were analyzed by an Agilent 1290 UPLC coupled to an Agilent 6490 triple quadruple mass spectrometer equipped with an electrospray ionization (ESI) source (Agilent Technologies, Basel, Switzerland). Analytes were separated by using a reversed-phase column (ACQUITY UPLC BEH C<sub>18</sub>, 1.7  $\mu$ m, 2.1  $\times$  150 mm, Waters, Wexford, Ireland), heated to 70°C. Data acquisition and analysis was performed using Mass Hunter software (Agilent Technologies). The mobile phase consisted of water-acetonitrile-formic acid (A) (95/5/0.1; v/v/v) and (B) (5/95/0.1; v/v/v). The eluent gradients were set from 25 - 75% of B during 0- 20 min, and 100% of B at 22 min onwards.

The run was stopped at 24 min, including washing and re-equilibration of the column. The flow rate was set to 0.650 mL/min. Ionization was performed using an ESI source operated in the positive ion modes (Table 2). Fragmentation was tuned for each compound using Optimizer software (Agilent Technologies). Optimal conditions are shown in Table 2. The source parameters were set to gas temperature 290°C, gas flow 14 L/min, nebulizer pressure 15 psi, sheath gas temperature 300°C, sheath gas flow 11 L/min, capillary voltage 6000 V (positive), nozzle voltage 1500 V and cell accelerator voltage 4 V. Ion funnel parameters for positive and negative high pressure were set to 200 and 110, respectively.

## Results

### Rapid metabolism of AD to androsterone by BLTK1 cells

The initial aim of this study was to identify a mouse Leydig cell line suitable for assessing 17 $\beta$ -HSD3 expression and enzyme activity in order to investigate xenobiotics interfering with the last step of testosterone synthesis. Based on a previous study reporting the expression of 17 $\beta$ -HSD3 and detecting T production using an antibody-based quantification method [23], the mouse Leydig cell line BLTK1 was first chosen as a cell model. As mRNA levels often do not provide sufficient information on protein expression and a suitable anti-17 $\beta$ -HSD3 antibody was not available, we attempted to measure 17 $\beta$ -HSD3 enzyme activity by incubating BLTK1 cells with 200 nM of radiolabeled AD and determining its metabolism by subjecting the culture supernatants to steroid separation by TLC and scintillation counting. Four distinct fractions were collected: fraction 1 migrating with the R<sub>f</sub> of AD, fraction 2 migrating with the R<sub>f</sub> of T and fractions 3 and 4 with R<sub>f</sub> between AD and T. The results suggested a time-dependent metabolism of AD and the formation of one major metabolite migrating with the R<sub>f</sub> of T and two minor metabolites (Fig. 1A). T was expected to be the main product because of the rapid conversion of AD into T by 17 $\beta$ -HSD3 in adult Leydig cells. However, the formation of this metabolite could not be blocked by the potent 17 $\beta$ -HSD3 inhibitor BP1 at concentrations of 1  $\mu$ M and 10  $\mu$ M (Fig. 1B), suggesting that it might not be T. Therefore, the fraction migrating with the R<sub>f</sub> of T was extracted from the TLC plate and subjected to LC-MS/MS analysis, revealing the absence of T.

Next, supernatants of BLTK1 cells incubated with 250 nM AD for different time periods were analyzed using LC-MS/MS. The main metabolite produced by BLTK1 cells was identified as androsterone (ADT). The time-dependent loss of AD over time was proportional to the increase of ADT in the culture supernatants. 5 $\alpha$ -Dihydrotestosterone (DHT) was below the detection limit and only very low amounts of T were measured (Fig. 2).

### Discrepancy to earlier work due to lack of specificity of antibody-based steroid quantification

An earlier study reporting T production by BLTK1 cells applied an EIA kit for T quantification [23]. Radioimmuno (RIA) and enzymes-linked immunosorbent assays (ELISA) are methods that have

been used to detect very low amounts of steroids for decades. However, all steroids share a common backbone and therefore it is important to assess the cross-reactivity rates between the key steroids produced by the system that is used in a corresponding experiment [19, 20, 24]. Thus, the recovery rates of eight androgenic steroids were tested using the T detection EIA kit (Cayman Chemical, Ann Arbor, MI, USA) used in the earlier study reporting T production by BLTK1 cells [23]. The highest mean recovery rate was detected for DHT (59%) (Table 3). Other androgens showed recovery rates between 5-36%. Most importantly, cross-contamination was found for 5 $\alpha$ -androstane-3-one (21%), AD (25%) and ADT (16%). Thus, the high amounts of ADT formed by BLTK1 cells from AD shown in the present study suggest that ADT might have been detected instead of T in the earlier study using quantification by EIA. These results emphasize the use of mass spectrometry-based steroid quantification methods when analyzing complex biological systems.

#### **Comparison of the conversion of androstenedione to testosterone and androsterone in MA-10 and BLTK1 cells**

Next, BLTK1 and the more widely used MA-10 cells were incubated with 200 nM AD for 4.5 h to compare their capacity to catalyze the last step of T synthesis (Fig. 3). AD concentrations dropped to about 50% after 4.5 h of incubation with both MA-10 and BLTK1 cells (Fig. 3 A, D). BLTK1 cells did not produce AD *de novo* (Fig. 3A), compared to MA-10 cells, where low amounts of AD could be detected (Fig. 3D). AD was absent from the medium control (Fig. 3 A, D), indicating that it was completely removed by charcoal treatment. In contrast, T could not be completely removed from the BLTK1 culture medium, which contains charcoal treated FBS (Fig. 3B), whereas it was completely removed from horse serum containing MA-10 culture medium (Fig. 3E). Thus, higher amounts of T were measured in BLTK1 cell supernatants due to T contamination contributed by the serum. However, T concentrations in supernatants of both cell lines were increased after incubation with AD compared to the medium control (Fig. 3 B, E). ADT was a major metabolite formed upon incubation of both cell lines with AD (Fig. 3 C, F). Both cell lines produced similar amounts of ADT from AD. Importantly, BLTK1 cells incubated with AD produced approximately 100 times more ADT than T, whereas MA-10 cells produced about 20 times more ADT than T (Fig. 3 C, F). Furthermore, MA-10 and BLTK1 cells both produced low amounts of ADT *de novo*. No ADT



was detected in the medium controls. However, regarding the mass balance, in both cell lines not all of the AD metabolized was converted into ADT, indicating that ADT is further metabolized (for example by conjugation) or that other metabolites were formed from AD. This finding was further supported by the fact that Hsd17b3 mRNA is 1000 times lower expressed in BLTK1 and MA-10 cells compared to mice testis (Table 4). This finding confirms that the endogenous expression of 17 $\beta$ -HSD3 in BLTK1 cells is too low to sufficiently convert AD into T. Therefore, BLTK1 is not a suitable model to the T regulation. Despite the high levels of Srd5a mRNA within the cells (data not shown), DHT is not produced due to the lack of functional 17 $\beta$ -HSD3.

### **Effects of steroidogenesis inducing compounds 8-Br-cAMP and forskolin**

Forskolin and 8-Br-cAMP are well known inducers of steroidogenesis. Two different concentrations of each compound (10  $\mu$ M and 50  $\mu$ M) were used to stimulate androgen synthesis in MA-10 cells. Cells were treated once with 10 and 50  $\mu$ M of 8-Br-cAMP and forskolin for 24 hours. Steroid concentrations were analyzed in cell supernatant using LC-MS. Result shown is a single representative experiment from three independent measurements. Cells without any stimulation (vehicle control) produced 3 nM of P. Progesterone levels were significantly increased in supernatant of cells stimulated with 8-Br-cAMP and forskolin (Fig.4A). 17OH-P levels were significantly increased in supernatant of cells stimulated with 8-Br-cAMP (50  $\mu$ M). The stimulation of 8-Br-cAMP (10  $\mu$ M) and forskolin (10  $\mu$ M and 50  $\mu$ M) did not significantly alter detectable concentrations of 17OH-P (Fig.4B).

Results in Fig.5A showed significant dose dependent induction of AD in 8-Br-cAMP treated cells. These results were reproduced independently four times. Similar trends were observed in all experiments. Nevertheless, high standard deviation occurred in different passages of the cells. Stimulation of 8-Br-cAMP did not have the same strong inducible effect in different cell passages but dose dependent increase of AD was observed in every experiment (data not shown). Forskolin did not have a significant effect on AD levels measured in the supernatant. Compared to the amount of AD detected in the supernatant, T level were much lower (Fig.5B). Despite low

concentrations detected, T was significantly increased in both concentrations of both treatments. Though, the 50  $\mu$ M 8-Br-cAMP treatment was 4 times more efficient in comparison to the 50  $\mu$ M forskolin treatment. MA-10 cells produced less than 100 pM of T in DMSO control (0.5%) without any stimulation. ADT was produced by MA-10 cells in DMSO treated cells in quantities up to 3 nM (Fig.5C). Both treatments decreased the levels of ADT in serum after 24 hrs, but only the 50  $\mu$ M forskolin treatment was able to decrease the ADT concentrations significantly. Despite of a very similar mechanism of steroid stimulation, 8-Br-cAMP and forskolin trigger androgen production completely diverse. Significance for all treatments was always compared to the DMSO control.

## Discussion

Mice Leydig cells were used to establish a model to study disruption of gonadal steroidogenesis and regulation of involved steroidogenic enzymes. Enzyme of interest was the 17 $\beta$ -HSD3 because of its importance for male genital development during embryogenesis. Mutations in that gene lead to severe disorders of sexual development due to lack of AD into T conversion [25, 26]. It was shown that confluent seeded BLTK1 cells (100'000 per 96 well) almost completely converted radiolabeled AD into an unknown metabolite. AD and T were added in excess into the supernatant to visualize the radiolabeled steroids under UV light on the TLC plate after separating them using a chloroform/ethyl acetate mixture. Four spots were chosen to analyze the radioactive contents. The AD fraction, T fraction and two spots in-between those to two visible spots. Results showed time dependent increase of a metabolite in the T fraction of the TLC plate indicating the presence of T. Low amounts of radiolabeled products were detected in the TLC fraction 1 and 2. Those detected products could be other produced steroids or degradation products. However, further studies with the 17 $\beta$ -HSD3 inhibitor BP1[27] showed no significant decrease in the amount of the product in the T fraction. We concluded that the unknown metabolite found in the T fraction was most likely not T itself. Involvement of other enzymes able to convert of AD to T such as 17 $\beta$ -HSD5 was excluded because due to the absence of its corresponding mRNA. Another steroid with similar R/f values as T was suspected to be produced in BLTK1 cells. Indeed, after validation of

many potential metabolites of AD using LC-MS analysis, ADT was identified as main product (Fig. 2). In Fig. 2 the concentrations of ADT at time point 270 min were higher than the originally added AD concentration due to ADT which was produced by the cells itself. Whereas in the Fig. 1 only radiolabeled ADT was detected by scintillation counting that has been originally converted from radiolabeled AD. Amounts of ADT produced by the cells were not able to be detected using scintillation counting.

Using LC-MS we could proof that T barely was formed in BLTK1 cells incubated with 200 nM AD for 4.5 hrs. We hypothesized that AD is converted into 5 $\alpha$ -androstane-3-one by Srd5a1 and further converted into ADT by Akr1c14 [28-30]. Both genes are highly expressed in MA-10 and BLTK1 cells and play a crucial role in the steroidogenic backdoor pathway (Fig.6). Unfortunately, 8-Br-cAMP stimulation did not increase AD or T concentrations in supernatant of BLTK1 cells in three independent measurements. This is not in line with the literature. Three papers show increasing amounts of T in supernatant of BLTK1 cells stimulated with recombinant human chorionic gonatropin (rhCH) [23, 31, 32]. However, BLTK1 cells produce more P than T, which is consistent with our data (data not shown). Unfortunately, these groups do not mention if they use serum free media or char coal treated media for the experiments. Additionally, no data are shown about cross reactivity of the ELISA kit with other steroids.

RT-PCR measurements of the most important steroidogenic enzymes involved in T synthesis were performed in MA-10 cells. Results showed lack of Hsd17b3 mRNA compared to healthy adult wild type black six mice. Hsd3b1 mRNA levels were not altered. No change of mRNA expression was expected to be found in Star and Cyp11 genes, because of high levels of progesterone in supernatant of MA-10 cells. Nevertheless, mRNA levels of Cyp17 were decreased compared to adult mice, leading to an accumulation of P in the supernatant. Progesterone is the main steroid produced in MA-10 cells and that's in line with what Ascoli observed 30 years after establishing the MA-10 cell line[33]. Decrease expression levels of Cyp17 and increased expression levels of Srd5a1 and Akr1c14 clearly support the production of steroids involved in the backdoor pathway.

Stimulation of MA-10 cells with 8-Br-cAMP for 24 hours lead to significant increase of AD and T detection in cell supernatant. Similar trends were observed in four independent experiments. However, stimulation of AD and T differed in all experiment despite of same treatment and similar

passages of the cells. It is possible to stimulate AD and T production in MA-10 cells using 8-Br-cAMP. Though, reproducibility of experiments is challenging. The pro steroidogenic effects of forskolin were much lower compared to 8-Br-cAMP, although forskolin increases intracellular cAMP concentrations and should anyhow stimulate steroidogenesis similar to 8-Br-cAMP. It could be that forskolin somehow blocks enzymatic activities in steroidogenic enzymes due to its chemical structure. Used concentration of forskolin and 8-Br-cAMP were nontoxic but lead to visible differences of the cell morphology. However, forskolin was able to significantly decrease ADT concentrations in supernatant of MA-10 cells. We hypothesized that forskolin stimulates production of steroids involved in backdoor pathway leading to accumulation of 3 $\alpha$ -androstenediol (3 $\alpha$ -diol) (Fig.6). A huge peak was detected in supernatant of forskolin treated cells using LC-MS that is suspected to be 3 $\alpha$ -diol. Further studies have to be done to proof that this peak is indeed 3 $\alpha$ -diol. ADT is the precursor of 3 $\alpha$ -diol and the synthesis of high amounts of 3 $\alpha$ -diol could explain the significant decrease in ADT levels. However, under basal conditions MA-10 cells produce very low amounts of T. AD and ADT were produced by cells, indicating that Cyp17, Srd5a1, and Akr1c14 are still enzymatically active. Only very low amounts of T could be formed in MA-10 cells due to very low expression of Hsd17b3. MA-10 cells are not applicable to investigate T disruption without any stimulation of the steroidogenesis. Besides that we have to take into account that MA-10 cells produce several steroids under basal and stimulated condition. Steroid found in supernatant of cells that are able to produce several different steroids, need to be separated using HPLC before getting quantifiably analyzed by EIA kits. EIA kits are great to quantify very low amounts of steroids. But all steroids share a basic structure and are very likely to be under or overestimated in terms of detected quantities. Despite its expensive use, LC-MS should be the gold standard method to quantify steroids measured in supernatants of cell with intact steroidogenesis.

The use of long term culture murine Leydig cells to test disruption of androgen synthesis is challenging. The three established mice Leydig cell lines BLTK1, MA-10, and TM3 showed altered steroid enzyme expression compared to adult Leydig cells. All three tested cell lines showed fetal Leydig cell (FLC) like behavior due to the lack of 17 $\beta$ -HSD3. Shima et al. showed that FLC produce and secrete AD, while T is further produced in Sertoli cells. Yet, fetal testis produce much less T

under co-incubation of FLC and Sertoli cells compared to adult Leydig cells[34, 35]. Immature mice testis minces incubated with 2 and 5  $\mu\text{M}$  [ $^3\text{H}$ ]progesterone showed less T conversion compared to 16,17 days old embryonic mouse testes[36]. Additionally, O'Shaughnessy et al. showed that  $17\beta\text{-HSD3}$  was expressed in seminiferous tubules (Sertoli cells) up to day 20 and later on the expression of  $17\beta\text{-HSD3}$  was limited to the interstitial tissues (Leydig cells)[37]. It can be concluded that FLC produce higher amounts of AD but low amounts of T. Mice do undergo a certain puberty process which leads to adult Leydig cells producing T as main androgen. Unfortunately, the progesterone variant of the Leydig cell tumor (M5480), adapted for serial transplantation by Dr. W. F. Dunning (Miami) was used to establish the MA-10 cell line[38]. M5480P variant was known to produce high amounts of P and very low amounts of T do to the lack of  $17\beta\text{-HSD3}$  and low amounts of Cyp17[39]. There exists a variant of the M5480 Leydig cell tumor (M5480A) that produces similar amounts of P and T at basal levels. This variant could be used to develop a Leydig cell line producing T to investigate T disruption and to study gene regulation of endogenous  $17\beta\text{-HSD3}$  [39].

## **Conclusion**

Mice Leydig cells remain an indispensable *in vitro* model to investigate T disruption as long as no human cell line will be available. The simple handling and cheap maintaining of cell cultures enables high throughput screening of potential endocrine disrupting chemicals. However, steroidogenesis in mammalian testes changes during development. Unfortunately, most available murine Leydig cell lines are fetal like and do not produce T as main steroid due to the low expression of  $17\beta\text{-HSD3}$ . The stimulation of MA-10 cells with 8-Br-cAMP leads to the production of detectable amounts of T. Using LC-MS methods, MA-10 cells are a usable model to test T interference by xenobiotics. Using ELISA or RIA kits to quantify steroids in supernatant of cells is not recommended anymore. Unknown metabolites and unspecific binding of antibodies do not allow an accurate measurement of steroids. LC-MS should be used as gold standard to quantify steroids in supernatant of cells capable of synthesizing complex steroid profiles.

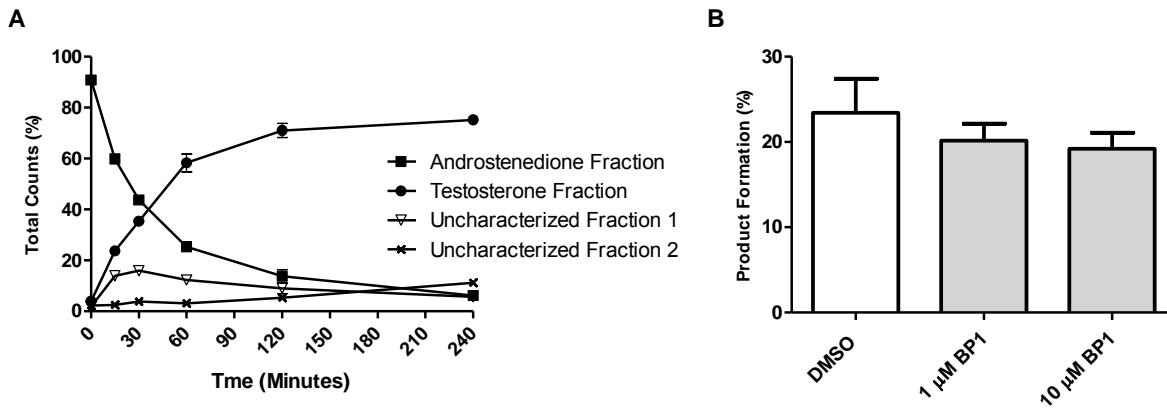
**Conflict of interests**

The authors declare no conflict of interest.

**Acknowledgments**

We are grateful for the financial support by the Swiss National Foundation (31003A-159454) and the Novartis Research Foundation.

## Figure Legends

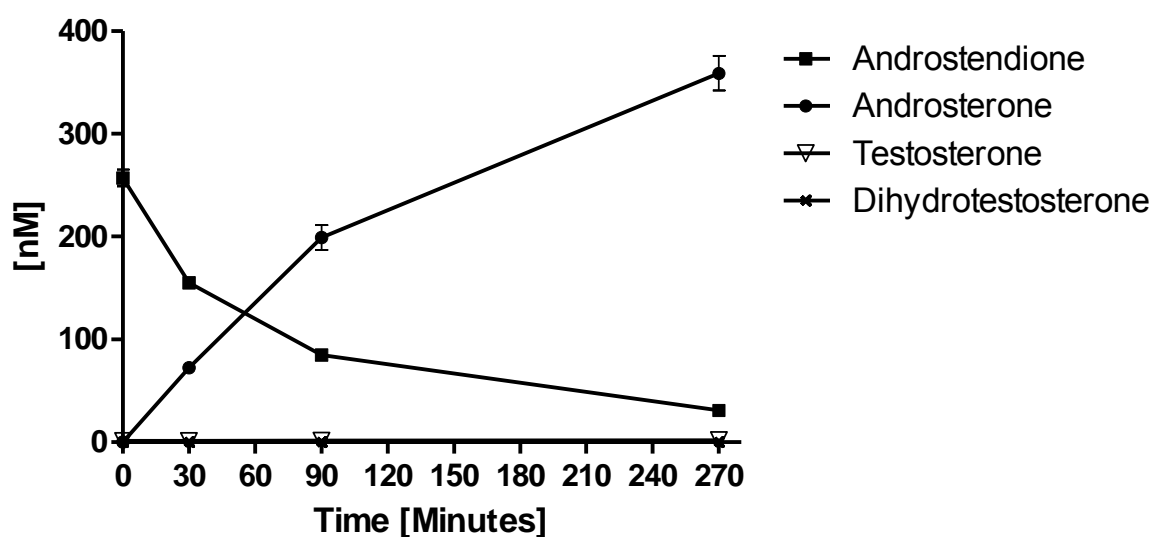


**Fig.1. Endogenous activity assays in MA-10 and BLTK1 cells using radiolabeled androstenedione as a substrate.** Formation of unknown metabolites by BLTK1 cells after incubation of 200 nM 50 nCi [1,2,6,7-<sup>3</sup>H]-androstenedione for several time points up to 180 minutes. The main formed product was found in the testosterone TLC fraction. Minor amounts of formed products were detected in TLC fraction 1 and 2. Data are represented as  $\pm$ SD from two independent experiments (A). Product formation by BLTK1 cells after 30 min exposure to 200 nM radiolabeled androstenedione and the 17 $\beta$ -HSD3 inhibitor benzophenone 1 (1  $\mu$ M and 10  $\mu$ M) compared to the DMSO (0.1%) control. Data are represented as  $\pm$ SD from three independent measurements (B). In all experiments, the supernatant of cells was collected and analyzed. Analytes were separated using thin layer chromatography. Samples were quantified using scintillation counting.

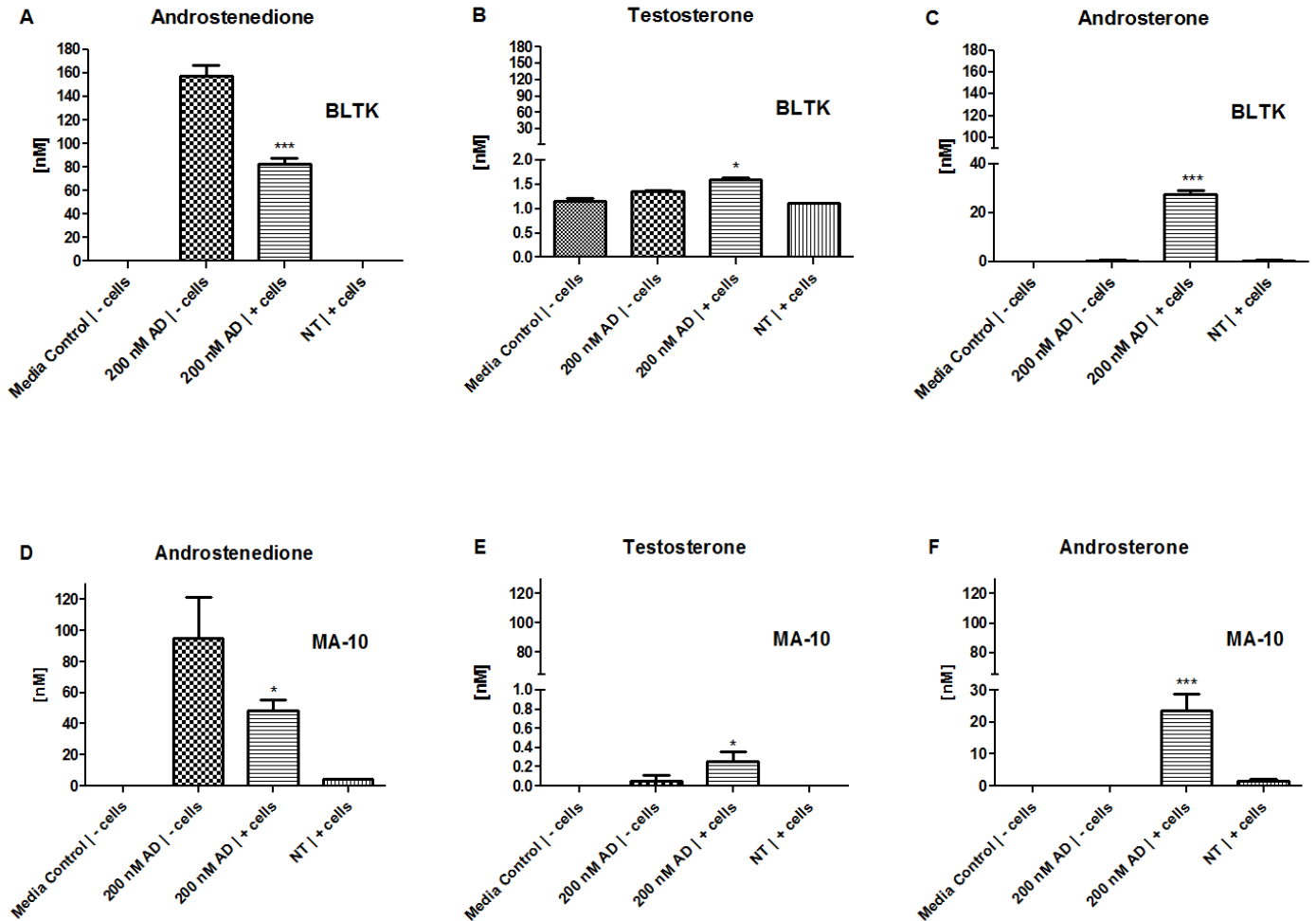


	Mean recovery rate (cross reactivity)
Testosterone	98.33 ± 9.57
5α-Androstenedione	20.55 ± 8.40
5α-Dihydrotestosterone	58.55 ± 8.83
5β-Dihydrotestosterone	28.46 ± 4.94
Androstendione	25.37 ± 6.16
Androstenediol	36.42 ± 2.80
Androsterone	16.43 ± 10.90
Dihydroepiandrosterone	5.45 ± 2.99
Etiocholanolone	18.33 ± 0.57

**Table 3. Cross reactivity of a commercially available ELISA kit (Cayman Chemical) tested on several steroids.** Experiments were performed according to the manufacturer protocol. Data show mean recovery rate of three tested steroid concentrations (150 pg/μL, 75 pg/μL, 37.5 pg/μL) from a single representative experiment. Results were conformed in a second independent measurement. Mean recovery rates from several tested steroids interacting with the testosterone antibody varied from 5% up to 60%.

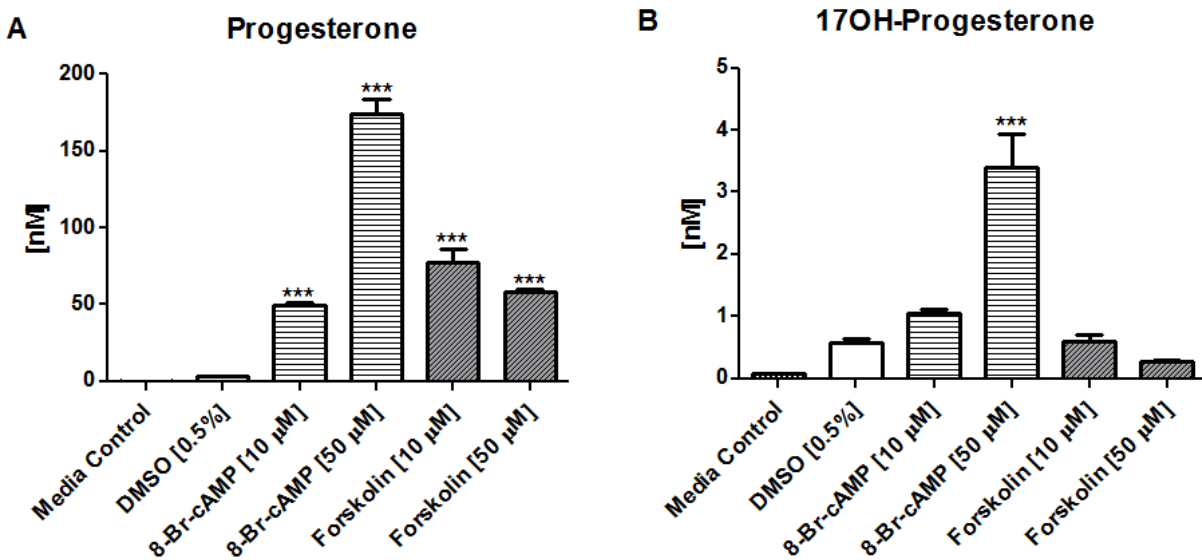


**Fig.2. Time depended decrease and increase of androstenedione and androsterone quantified using LC-MS.** Androsterone, testosterone and dihydrotestosterone formation by BLTK1 cells after incubation of 250 nM androstenedione. Supernatant was collected for different time points (0, 30, 90, and 270 min) and analyzed using LC-MS. Data are shown as  $\pm$ SD in technical triplicates.

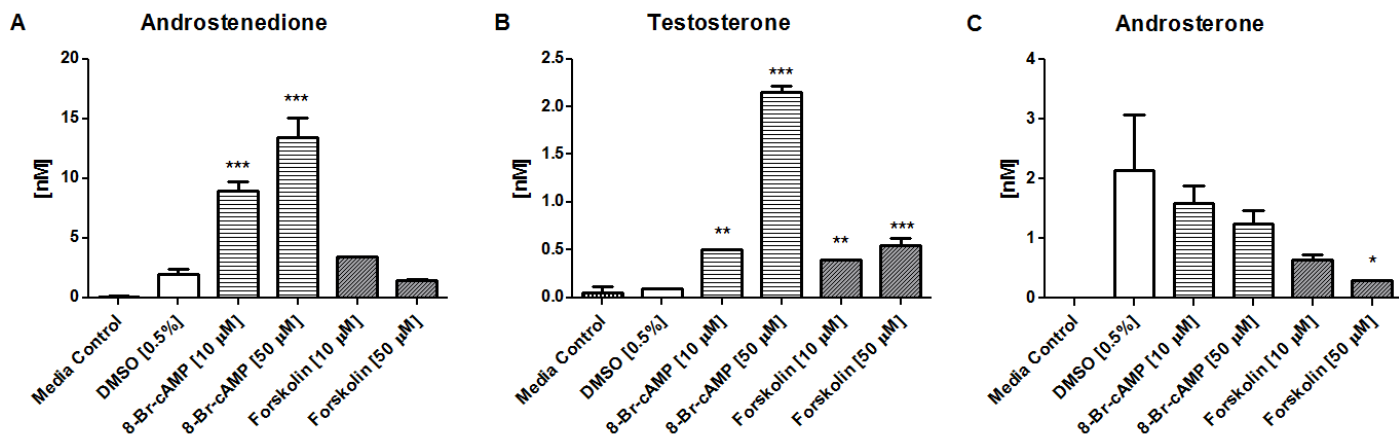


**Fig. 3. Formation of testosterone and androsterone in BLTK1 and MA-10 Leydig cells after exposure to 200 nM androstenedione.** Steroids were quantified by UPLC-MS/MS in supernatants of BLTK1 (A-C) and MA-10 Leydig cells (D-F) incubated for 4.5 h with 200 nM AD in charcoal treated medium. Results represent steroid concentrations (in nM) in supernatants of medium control (-

cells), treatment control (200 nM AD, - cells), cells exposed to AD (200 nM AD, + cells), and cells incubated in medium in the absence of AD (medium only, + cells). Statistical significance was assessed using one-way ANOVA analysis followed by a post Tukey test. Data of BLTK1 cells represent mean  $\pm$  S.D. from two independent experiments. MA-10 data represent mean  $\pm$  S.D. from three independent experiments.



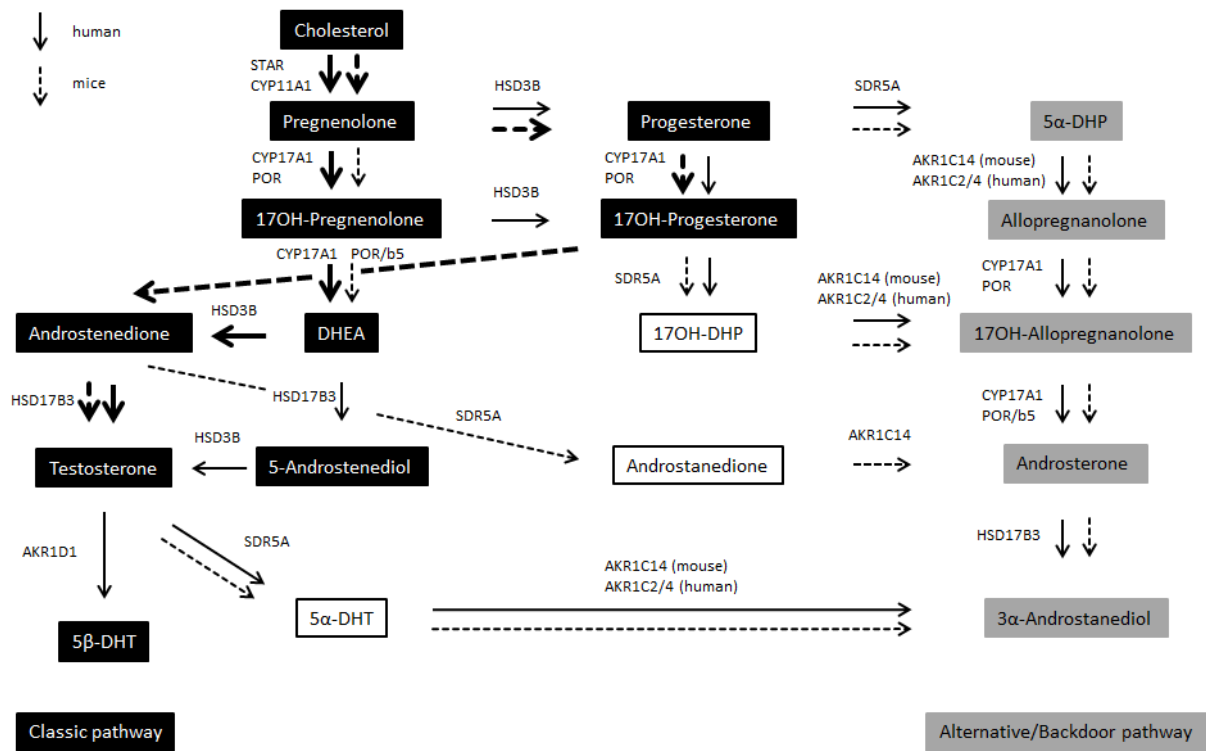
**Fig. 5. Quantification of de novo production of progesterone and 17-hydroxyprogesterone by MA-10 cells.** Progesterone and 17-hydroxyprogesterone levels were quantified by UPLC-MS/MS in medium and supernatants of MA-10 cells stimulated for 24 h with 8-Br-cAMP (10  $\mu$ M and 50  $\mu$ M) or forskolin (10  $\mu$ M and 50  $\mu$ M). DMSO (0.5%) and medium served as controls. Statistical differences to the DMSO control were assessed using one-way ANOVA analysis followed by a post Tukey test. Data represent mean  $\pm$  S.D. from one out of three independent experiments performed in duplicate. \*\*\*  $p < 0.001$



**Fig. 4. Quantification of de novo synthesis of androstenedione, testosterone and androsterone by MA-10 cells.** Steroids were quantified by UPLC-MS/MS in MA-10 cell supernatants following stimulation for 24 h with 8-Br-cAMP (10  $\mu$ M and 50  $\mu$ M) or forskolin (10  $\mu$ M and 50  $\mu$ M). DMSO (0.5%) and medium served as controls. Medium contained charcoal/dextran-treated serum. Statistically significant difference to DMSO control was assessed using one-way ANOVA analysis followed by a post Tukey test. Data represent mean  $\pm$  S.D. from one out of four independent experiments performed in duplicate.

	MA-10 (1)	MA-10 (2)	MA-10 (3)	Testis (1)	Testis (2)
<b>Hsd3b1</b>	19.33	18.29	18.36	18.17	19.13
<b>Cyp17a1</b>	24.03	24.18	21.97	16.33	17.33
<b>Hsd17b3</b>	-	31.47	31.22	21.35	22.4
<b>Akr1c6</b>	-	-	-	27	33.98
<b>Srd5a1</b>	21.04	20.38	19.99	21.91	22.47
<b>Akr1c14</b>	17.48	17.24	17.00	23.8	24.61
<b>Hsd17b1</b>	26.01	26.6	25.5	27.97	27.6
<b>Ppia</b>	13.7	13.59	13.33	14.17	14.55

**Table 4. Messenger RNA expression levels of steroidogenic enzymes in MA-10 Leydig cells and mice (black six) testes.** MA-10 cells were grown confluent in 6-well plates and lysed using TRI-reagent. Mice testes were lysed in TRI-reagent using a stirring homogenizer. Messenger RNA was isolated and converted into cDNA. CT-values were determined using 10 ng of cDNA. Significant changes of mRNA expression in MA-10 cells compared to mice testes are shown in red. MA-10 (1-3) data are represented from three independent experiments in technical triplicates. Testis 1 and 2 data are represented in technical triplicates from two different mice (11 weeks old) testis.



**Fig. 6. Murine and human androgen steroidogenesis.** Classic murine and human biosynthesis pathways of T in testes (black). Alternative/Backdoor pathway of 3α-androstanediol in human and mice (grey). Intermediate steroids are pictured in white. Murine pathways are pictured in dotted and human pathways in black arrows. Main human biosynthesis pathway of T via DHEA (bold black arrow). Preferred murine pathways of T via P and 17OH-P (bold dotted arrow)[28, 40].

## Tables

**Table 1. Oligonucleotide primers used for quantitative RT-PCR.**

Gene	Oligonucleotide Forward Primers	Oligonucleotide Reverse Primers
<i>Hsd3b1</i>	5'-GTCACAGGTGTCATTCCCAG-3'	5'-TTCTTGACGAGTTGGGCC-3'
<i>Cyp17a1</i>	5'-AGAGTTTGCCATCCCGAAG-3'	5'-AACTGGGTGTGGGTGTAATG-3'
<i>Hsd17b3</i>	5'-ACAATGGGCAGTGATTAC-3'	5'-GTGGTCCTCTCAATCTCTTC-3'
<i>Akr1C6</i>	5'-TCCGAAGCAAGATAGCAGATG-3'	5'-GTTGGACTATGTGGACCTGTAC-3'
<i>Srd5a1</i>	5'-TCACCTTTGTCTTGGCCTTC-3'	5'-TTATCACCATGCCCACTAACC-3'
<i>Akr1c14</i>	5'-GTACAAGCAAACACCAGCAC-3'	5'-ATGCCTCTGAAGCCAAGT-3'
<i>Hsd17b1</i>	5'-GCTGTGTTGGATGTGAATGTG-3'	5'-ACTTCGTGGAATGGCAGTC-3'
<i>Ppia</i>	5'-CAAATGCTGGACCAAACACAAACG-3'	5'-GTTTCATGCCTTCTTTCACCTTCC-3'

**Table 2. Parameters for the androgens measured and mass spectrometer properties**

Steroid	RT [min]	Precursor Ion (m/z)	Product ion (m/z)	Collision energy (V)	Polarity	Internal Standard
Androsterone	18.1	273.2	255.2	12	Positive	Testosterone-d2
Testosterone	8.1	289.2	97.1	28	Positive	Testosterone-d2
Androstenedione	9.5	287.2	97.1	20	Positive	Testosterone-d2
5 $\alpha$ -DHT	12.5	291.2	159.1	24	Positive	Testosterone-d2
Testosterone-d2	8.1	291.5	111.1	24	Positive	



## References

1. Miller, W.L. and R.J. Auchus, The molecular biology, biochemistry, and physiology of human steroidogenesis and its disorders. *Endocrine reviews*, 2011. 32(1): p. 81-151.
2. Chapin, R.E., et al., NTP-CERHR expert panel report on the reproductive and developmental toxicity of bisphenol A. *Birth defects research. Part B, Developmental and reproductive toxicology*, 2008. 83(3): p. 157-395.
3. Hauser, R., The environment and male fertility: recent research on emerging chemicals and semen quality. *Seminars in reproductive medicine*, 2006. 24(3): p. 156-67.
4. Luccio-Camelo, D.C. and G.S. Prins, Disruption of androgen receptor signaling in males by environmental chemicals. *The Journal of steroid biochemistry and molecular biology*, 2011. 127(1-2): p. 74-82.
5. Cohn, B.A., et al., DDT and breast cancer in young women: new data on the significance of age at exposure. *Environmental health perspectives*, 2007. 115(10): p. 1406-14.
6. De Coster, S. and N. van Larebeke, Endocrine-disrupting chemicals: associated disorders and mechanisms of action. *Journal of environmental and public health*, 2012. 2012: p. 713696.
7. Fucic, A., et al., Environmental exposure to xenoestrogens and oestrogen related cancers: reproductive system, breast, lung, kidney, pancreas, and brain. *Environmental health : a global access science source*, 2012. 11 Suppl 1: p. S8.
8. Carwile, J.L. and K.B. Michels, Urinary bisphenol A and obesity: NHANES 2003-2006. *Environmental research*, 2011. 111(6): p. 825-30.
9. Trasande, L., T.M. Attina, and J. Blustein, Association between urinary bisphenol A concentration and obesity prevalence in children and adolescents. *JAMA*, 2012. 308(11): p. 1113-21.
10. Neel, B.A. and R.M. Sargis, The paradox of progress: environmental disruption of metabolism and the diabetes epidemic. *Diabetes*, 2011. 60(7): p. 1838-48.
11. Kajta, M. and A.K. Wojtowicz, Impact of endocrine-disrupting chemicals on neural development and the onset of neurological disorders. *Pharmacological reports : PR*, 2013. 65(6): p. 1632-9.
12. Weiss, B., The intersection of neurotoxicology and endocrine disruption. *Neurotoxicology*, 2012. 33(6): p. 1410-9.
13. chemicals., O.g.f.t.t.o., Test No. 456: H295R Steroidogenesis Assay. *OECD Guidelines for the Testing of Chemicals, Section 4: Health Effects*, 2011.
14. Rahman, N.A. and I.T. Huhtaniemi, Testicular cell lines. *Molecular and cellular endocrinology*, 2004. 228(1-2): p. 53-65.
15. Odermatt, A., P. Strajhar, and R.T. Engeli, Disruption of steroidogenesis: Cell models for mechanistic investigations and as screening tools. *The Journal of steroid biochemistry and molecular biology*, 2016. 158: p. 9-21.
16. Scott, H.M., J.I. Mason, and R.M. Sharpe, Steroidogenesis in the fetal testis and its susceptibility to disruption by exogenous compounds. *Endocrine reviews*, 2009. 30(7): p. 883-925.

17. Inano, H. and B. Tamaoki, Testicular 17 beta-hydroxysteroid dehydrogenase: molecular properties and reaction mechanism. *Steroids*, 1986. 48(1-2): p. 1-26.
18. Haisenleder, D.J., et al., Estimation of estradiol in mouse serum samples: evaluation of commercial estradiol immunoassays. *Endocrinology*, 2011. 152(11): p. 4443-7.
19. Handelsman, D.J., et al., Measurement of testosterone by immunoassays and mass spectrometry in mouse serum, testicular, and ovarian extracts. *Endocrinology*, 2015. 156(1): p. 400-5.
20. Handelsman, D.J. and L. Wartofsky, Requirement for mass spectrometry sex steroid assays in the *Journal of Clinical Endocrinology and Metabolism*. *J Clin Endocrinol Metab*, 2013. 98(10): p. 3971-3.
21. Rosner, W., et al., Position statement: Utility, limitations, and pitfalls in measuring testosterone: an Endocrine Society position statement. *J Clin Endocrinol Metab*, 2007. 92(2): p. 405-13.
22. Legeza, B., et al., The microsomal enzyme 17beta-hydroxysteroid dehydrogenase 3 faces the cytoplasm and uses NADPH generated by glucose-6-phosphate dehydrogenase. *Endocrinology*, 2013. 154(1): p. 205-13.
23. Forgacs, A.L., et al., BLTK1 murine Leydig cells: a novel steroidogenic model for evaluating the effects of reproductive and developmental toxicants. *Toxicological sciences : an official journal of the Society of Toxicology*, 2012. 127(2): p. 391-402.
24. Buttler, R.M., et al., Measurement of dehydroepiandrosterone sulphate (DHEAS): a comparison of Isotope-Dilution Liquid Chromatography Tandem Mass Spectrometry (ID-LC-MS/MS) and seven currently available immunoassays. *Clin Chim Acta*, 2013. 424: p. 22-6.
25. Engeli, R.T., et al., Biochemical analyses and molecular modeling explain the functional loss of 17beta-hydroxysteroid dehydrogenase 3 mutant G133R in three Tunisian patients with 46, XY Disorders of Sex Development. *The Journal of steroid biochemistry and molecular biology*, 2016. 155(Pt A): p. 147-54.
26. Ben Rhouma, B., et al., Novel cases of Tunisian patients with mutations in the gene encoding 17beta-hydroxysteroid dehydrogenase type 3 and a founder effect. *The Journal of steroid biochemistry and molecular biology*, 2017. 165(Pt A): p. 86-94.
27. Nashev, L.G., et al., The UV-filter benzophenone-1 inhibits 17beta-hydroxysteroid dehydrogenase type 3: Virtual screening as a strategy to identify potential endocrine disrupting chemicals. *Biochemical pharmacology*, 2010. 79(8): p. 1189-99.
28. Bellemare, V., F. Labrie, and V. Luu-The, Isolation and characterization of a cDNA encoding mouse 3alpha-hydroxysteroid dehydrogenase: an androgen-inactivating enzyme selectively expressed in female tissues. *The Journal of steroid biochemistry and molecular biology*, 2006. 98(1): p. 18-24.
29. Preslocsk, J.P., Steroidogenesis in the mammalian testis. *Endocrine reviews*, 1980. 1(2): p. 132-9.
30. Normington, K. and D.W. Russell, Tissue distribution and kinetic characteristics of rat steroid 5 alpha-reductase isozymes. Evidence for distinct physiological functions. *The Journal of biological chemistry*, 1992. 267(27): p. 19548-54.

31. Karmaus, A.L. and T.R. Zacharewski, Atrazine-Mediated Disruption of Steroidogenesis in BLTK1 Murine Leydig Cells. *Toxicological sciences : an official journal of the Society of Toxicology*, 2015. 148(2): p. 544-54.
32. Forgacs, A.L., et al., Triazine herbicides and their chlorometabolites alter steroidogenesis in BLTK1 murine Leydig cells. *Toxicological sciences : an official journal of the Society of Toxicology*, 2013. 134(1): p. 155-67.
33. Ascoli, M., Characterization of Several Clonal Lines of Cultured Leydig Tumor Cells: Gonadotropin Receptors and Steroidogenic Responses. *Endocrine Society*, 1981. 108(1).
34. Shima, Y., et al., Contribution of Leydig and Sertoli cells to testosterone production in mouse fetal testes. *Molecular endocrinology*, 2013. 27(1): p. 63-73.
35. O'Shaughnessy, P.J., P.J. Baker, and H. Johnston, The foetal Leydig cell-- differentiation, function and regulation. *International journal of andrology*, 2006. 29(1): p. 90-5; discussion 105-8.
36. Mahendroo, M., et al., Steroid 5alpha-reductase 1 promotes 5alpha-androstane-3alpha,17beta-diol synthesis in immature mouse testes by two pathways. *Molecular and cellular endocrinology*, 2004. 222(1-2): p. 113-20.
37. O'Shaughnessy, P.J., et al., Localization of 17beta-hydroxysteroid dehydrogenase/17-ketosteroid reductase isoform expression in the developing mouse testis-- androstenedione is the major androgen secreted by fetal/neonatal leydig cells. *Endocrinology*, 2000. 141(7): p. 2631-7.
38. Ascoli, M., Characterization of several clonal lines of cultured Leydig tumor cells: gonadotropin receptors and steroidogenic responses. *Endocrinology*, 1981. 108(1): p. 88-95.
39. Lacroix, A., et al., Steroidogenesis in HCG-responsive Leydig cell tumor variants. *Journal of steroid biochemistry*, 1979. 10(6): p. 669-75.
40. Fluck, C.E., et al., Why boys will be boys: two pathways of fetal testicular androgen biosynthesis are needed for male sexual differentiation. *American journal of human genetics*, 2011. 89(2): p. 201-18.

## 5.4 Conclusion

In conclusion, three different murine Leydig cell lines (MA-10, BLTK1, TM3) were selected based on exhaustive literature review (Odermatt et al., 2016), to establish a model to study the regulation and activity of the enzyme 17 $\beta$ -HSD3.

In 1980, Mario Ascoli used a variant of the M5480 Leydig cell tumor, which was initially described to produce low levels of testosterone but high levels of progesterone, to establish the MA-10 cell line[146]. The progesterone Leydig cell tumor variant responded better to human chorionic gonadotropin (hcG) and LH stimulation and was therefore further established as a steroidogenesis activation read-out model[147]. However, reviewing the available literature revealed the frequent use of MA-10 cells as a standard model for testosterone disruption. This led to the assumption that low amounts of testosterone were still produced[148]. And indeed, stimulation with 8-Br-cAMP and forskolin did increase testosterone formation but had no effect on the mRNA levels of *Hsd17b3* (Figure 1 Appendix). We showed the mRNA levels of *Hsd17b3* were low and close to the limit of detection using real-time PCR. It seems that the endogenous regulation of 17 $\beta$ -HSD3 is lost in this cell line and the detected testosterone concentrations are most likely due to the conversion of androstenedione to testosterone by the enzyme 17 $\beta$ -HSD1. This hypothesis is substantiated by low to moderate expression of *Hsd17b1* mRNA levels in MA-10 cells and the fact that mouse 17 $\beta$ -HSD1 has a similar affinity for androstenedione as to estrone[149]. The MA-10 cell line is therefore not useful to further study the regulation or activity of endogenous 17 $\beta$ -HSD3.

BLTK1 cells were recently established and were reported to express *Hsd17b3* mRNA and produce very low amounts of testosterone when stimulated with forskolin and recombinant hCG. Enzyme protein expression could not be shown due to the lack of a specificity of the commercially available antibody[150]. However, we were not able to detect significant amounts of *Hsd17b3* mRNA levels using real-time PCR. Furthermore, testosterone formation was not inducible using 8-Br-cAMP in our hands. In conclusion, the promising cell line BLTK1 was not adequate to investigate endogenous *Hsd17B3* expression or its enzyme activity. Comparing *Hsd17b3* mRNA expression in MA-10 and BLTK1 cells with *Hsd17b3* mRNA expression in a minced mouse testis, revealed a 1000-fold higher expression in a freshly isolated testis. This finding explains the low formation of testosterone in both cell lines. Yet, incubation of androstenedione in both cell lines

resulted in a loss of androstenedione and the formation of huge amounts of androsterone, indicating the expression of several enzymes involved in the backdoor pathway that have been originally described by Richard J. Auchus in testes of young pouch of the tammar wallaby[151]. Real-time PCR studies confirmed high expression of enzymes involved in the backdoor pathway[152]. In both cell lines the mRNA expression of Srd5a1 and Akr1c14 were upregulated compared to mice testes. High expression of Srd5a1 and Akr1c14 might explain the rapid conversion of androstenedione to androsterone through the intermediate metabolite 5 $\alpha$ -androstenedione observed in these experiments.

Real-time PCR studies in TM3 cells revealed similar expression levels of Hsd17b3 mRNA compared to MA-10 and BLTK1 cells, indicating that Hsd17b3 expression is also absent in TM3 cells. All tested cell lines failed to express substantial levels of endogenous 17 $\beta$ -HSD3, and therefore cannot be used as a screening model for testosterone disruption. Unfortunately, so far there is no conventional *in vitro* model expressing endogenous levels of 17 $\beta$ -HSD3 available to confirm the findings from the established *HSD17B3* promoter transactivation assays. In the future, it is essential to establish primary mouse Leydig cells, or preferably human Leydig cells to investigate 17 $\beta$ -HSD3 disruption. However, when using primary cells, inter individual differences have to be taken into account. The isolating procedure is challenging and expensive also.

The section which described the Leydig cell models in the review, pointed out the importance of using accurate detection methods to measure steroids. Leydig cell lines express a huge variety of endogenous enzymes able to convert many steroids. It is of great relevance to fully understand the diversity of endogenous enzymes expressed in the applied cell system. Enzyme-linked immunosorbent assays (ELISA) are regularly used as a standard method to measure steroids in cell supernatants. In my opinion, based on the evidence in this project, only liquid chromatography-mass spectrometry (LC-MS) or gas chromatography-mass spectrometry (GC-MS) methods should be used for the detection of steroids in cell supernatants. This is due to the questionable specificity of antibodies used in commercially available ELISA kits.

Furthermore, *Hsd17b3* regulation studies could not be carried out in MA-10, BLTK, or TM3 cells due to a lack of endogenous expression of the enzyme. However, potential xenobiotics that interfere with human 17 $\beta$ -HSD3 can be examined using transfected HEK-293 cells (intact cells and lysates). In a recently initiated study we used several nonsteroidal 17 $\beta$ -HSD3 inhibitors as query

molecules for a 2D similarity-based search of an environmental chemical database. Several hits will be further tested in a newly established activity assay using HEK-293 cell lysates transfected with human 17 $\beta$ -HSD3 expression plasmids. Additionally, it would also be possible to use the established 17 $\beta$ -HSD3 homology model to support the 2D similarity-based approach. Unfortunately, the previously created ligand based pharmacophore 17 $\beta$ -HSD3 model by Daniela Schuster did not perform well. All hits identified by this pharmacophore model were inactive (Figure 2 Appendix). However, this model and the established lysate 17 $\beta$ -HSD3 assay allows us to screen and test a huge number of chemicals in a short period of time (high throughput) and at relatively low costs. We are confident that further research and further rounds of improvement of the available pharmacophore models will lead to the identification of chemicals interfering with the activity of the enzyme 17 $\beta$ -HSD3. Positive hits can then further be used to validate the applied models. The ultimate goal is to establishing a model with a high positive hit rate that can help in the prediction of toxicologically relevant effects due to the inhibition of 17 $\beta$ -HSD3.

## 6. Acknowledgments

With all my respect, I would like to thank Prof. Dr. Alex Odermatt for the continuous support during the time I conducted my Master and PhD thesis in his lab. I would like to thank Prof. Dr. Rik Eggen for co-refereeing my PhD thesis as well as being a part of the thesis committee. Further I want to express my gratitude to both master students Susanne Leugger and Simona Rohrer. Their tremendous work helped me to push many projects to publication. A special thanks goes to Dr. Daniela Schuster and Dr. Anna Vuorinen for their very successful collaboration. I also want to gratefully thank Dr. Denise Kratschmar for analyzing hundreds of LC-MS samples and Dr. Adam Lister for proofreading my thesis. Furthermore, I would also like to thank Christoph Sager for creating the 17 $\beta$ -HSD3 homology model. Many thanks go to all the people that have collaborated with me on different projects, all the members of the Molecular & Systems Toxicology group for many stimulation discussions, their support, and the good times we all had together. Finally, I would like to thank my parents and family for their continuous support through all my endeavors.

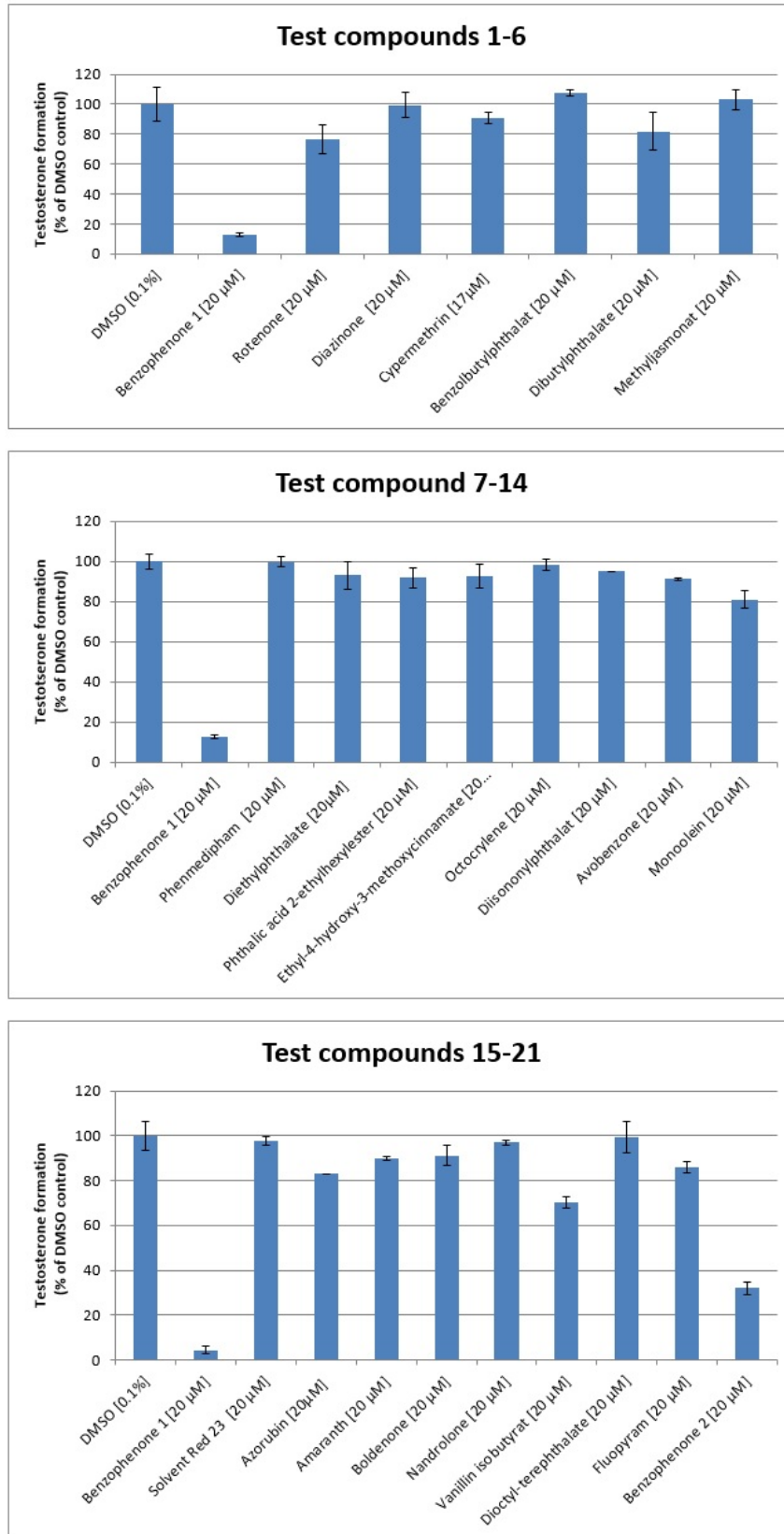
## 7. Appendix

### Results: (MA-10) mRNA Ct Values 10 ng cDNA

	24h 48h	DMSO [0.5%]	cAMP [10 $\mu$ M]	DMSO [0.5%]	cAMP [10 $\mu$ M]
<i>Hsd17b3</i>		n.d	n.d	n.d	n.d

**Figure 1.** Real-time PCR results on Hsd17b3 levels after 8-Br-cAMP (cAMP) stimulation in MA-10 cells. N.d = not detected





**Figure 2:** Testosterone formation in cells transfected with human 17 $\beta$ -HSD3 expression plasmids. Tested compounds were identified by the 17 $\beta$ -HSD3 pharmacophore model as potential inhibitors.

## 8. References

1. Beato, M., et al., Gene regulation by steroid hormones. *Journal of steroid biochemistry*, 1987. 27(1-3): p. 9-14.
2. Falkenstein, E., et al., Multiple actions of steroid hormones--a focus on rapid, nongenomic effects. *Pharmacological reviews*, 2000. 52(4): p. 513-56.
3. Duax, W.L., J.F. Griffin, and D. Ghosh, The fascinating complexities of steroid-binding enzymes. *Current opinion in structural biology*, 1996. 6(6): p. 813-23.
4. Levin, E.R. and S.R. Hammes, Nuclear receptors outside the nucleus: extranuclear signalling by steroid receptors. *Nat Rev Mol Cell Biol*, 2016. 17(12): p. 783-797.
5. Carson-Jurica, M.A., W.T. Schrader, and B.W. O'Malley, Steroid receptor family: structure and functions. *Endocrine reviews*, 1990. 11(2): p. 201-20.
6. Losel, R. and M. Wehling, Nongenomic actions of steroid hormones. *Nature reviews. Molecular cell biology*, 2003. 4(1): p. 46-56.
7. Beato, M. and J. Klug, Steroid hormone receptors: an update. *Human reproduction update*, 2000. 6(3): p. 225-36.
8. IUPAC-IUB Joint Commission on Biochemical Nomenclature (JCBN). The nomenclature of steroids. Recommendations 1989. *European journal of biochemistry*, 1989. 186(3): p. 429-58.
9. Miller, W.L., Molecular biology of steroid hormone synthesis. *Endocrine reviews*, 1988. 9(3): p. 295-318.
10. Edgren, R.A. and F.Z. Stanczyk, Nomenclature of the gonane progestins. *Contraception*, 1999. 60(6): p. 313.
11. Fahy, E., et al., A comprehensive classification system for lipids. *J Lipid Res*, 2005. 46(5): p. 839-61.
12. Mangelsdorf, D.J., et al., The nuclear receptor superfamily: the second decade. *Cell*, 1995. 83(6): p. 835-9.
13. Penning, T.M., Human hydroxysteroid dehydrogenases and pre-receptor regulation: insights into inhibitor design and evaluation. *J Steroid Biochem Mol Biol*, 2011. 125(1-2): p. 46-56.
14. Spencer, T.E. and F.W. Bazer, Biology of progesterone action during pregnancy recognition and maintenance of pregnancy. *Frontiers in bioscience : a journal and virtual library*, 2002. 7: p. d1879-98.
15. Arai, K. and G.P. Chrousos, Aldosterone Deficiency and Resistance, in *Endotext*, L.J. De Groot, et al., Editors. 2000: South Dartmouth (MA).
16. Rhen, T. and J.A. Cidlowski, Antiinflammatory action of glucocorticoids--new mechanisms for old drugs. *The New England journal of medicine*, 2005. 353(16): p. 1711-23.
17. Holst, J.P., et al., Steroid hormones: relevance and measurement in the clinical laboratory. *Clin Lab Med*, 2004. 24(1): p. 105-18.
18. Magomedova, L. and C.L. Cummins, Glucocorticoids and Metabolic Control. *Handb Exp Pharmacol*, 2016. 233: p. 73-93.
19. Rupprecht, R., et al., Transactivation and synergistic properties of the mineralocorticoid receptor: relationship to the glucocorticoid receptor. *Mol Endocrinol*, 1993. 7(4): p. 597-603.

20. Mooradian, A.D., J.E. Morley, and S.G. Korenman, Biological actions of androgens. *Endocrine reviews*, 1987. 8(1): p. 1-28.
21. Roy, A.K., et al., Regulation of androgen action. *Vitamins and hormones*, 1999. 55: p. 309-52.
22. Mendonca, B.B., et al., 46,XY disorders of sex development (DSD). *Clin Endocrinol (Oxf)*, 2009. 70(2): p. 173-87.
23. Gruber, C.J., et al., Production and actions of estrogens. *The New England journal of medicine*, 2002. 346(5): p. 340-52.
24. Jefcoate, C.R., et al., Regulation of cholesterol movement to mitochondrial cytochrome P450<sub>sc</sub> in steroid hormone synthesis. *J Steroid Biochem Mol Biol*, 1992. 43(8): p. 751-67.
25. Cigorruga, S.B., M.L. Dufau, and K.J. Catt, Regulation of luteinizing hormone receptors and steroidogenesis in gonadotropin-desensitized leydig cells. *J Biol Chem*, 1978. 253(12): p. 4297-304.
26. Richards, J.S., Maturation of ovarian follicles: actions and interactions of pituitary and ovarian hormones on follicular cell differentiation. *Physiol Rev*, 1980. 60(1): p. 51-89.
27. Santen, R.J., Feedback control of luteinizing hormone and follicle-stimulating hormone secretion by testosterone and estradiol in men: physiological and clinical implications. *Clin Biochem*, 1981. 14(5): p. 243-51.
28. Santen, R.J. and C.W. Bardin, Episodic luteinizing hormone secretion in man. Pulse analysis, clinical interpretation, physiologic mechanisms. *J Clin Invest*, 1973. 52(10): p. 2617-28.
29. Vale, W., et al., Characterization of a 41-residue ovine hypothalamic peptide that stimulates secretion of corticotropin and beta-endorphin. *Science*, 1981. 213(4514): p. 1394-7.
30. Axelrod, J. and T.D. Reisine, Stress hormones: their interaction and regulation. *Science*, 1984. 224(4648): p. 452-9.
31. Honour, J.W., Hypothalamic-pituitary-adrenal axis. *Respir Med*, 1994. 88 Suppl A: p. 9-13; discussion 13-5.
32. Odermatt, A., et al., Why is 11beta-hydroxysteroid dehydrogenase type 1 facing the endoplasmic reticulum lumen? Physiological relevance of the membrane topology of 11beta-HSD1. *Mol Cell Endocrinol*, 2006. 248(1-2): p. 15-23.
33. Rainey, W.E., et al., Dissecting human adrenal androgen production. *Trends in endocrinology and metabolism: TEM*, 2002. 13(6): p. 234-9.
34. Habert, R., H. Lejeune, and J.M. Saez, Origin, differentiation and regulation of fetal and adult Leydig cells. *Molecular and cellular endocrinology*, 2001. 179(1-2): p. 47-74.
35. Nelson, L.R. and S.E. Bulun, Estrogen production and action. *Journal of the American Academy of Dermatology*, 2001. 45(3 Suppl): p. S116-24.
36. Labrie, F., et al., DHEA and the intracrine formation of androgens and estrogens in peripheral target tissues: its role during aging. *Steroids*, 1998. 63(5-6): p. 322-8.
37. Labrie, F., et al., Intracrinology: role of the family of 17 beta-hydroxysteroid dehydrogenases in human physiology and disease. *J Mol Endocrinol*, 2000. 25(1): p. 1-16.
38. Selby, C., Sex hormone binding globulin: origin, function and clinical significance. *Ann Clin Biochem*, 1990. 27 ( Pt 6): p. 532-41.
39. Rosner, W., The functions of corticosteroid-binding globulin and sex hormone-binding globulin: recent advances. *Endocr Rev*, 1990. 11(1): p. 80-91.

40. Manni, A., et al., Bioavailability of albumin-bound testosterone. *J Clin Endocrinol Metab*, 1985. 61(4): p. 705-10.
41. Taylor, W., The excretion of steroid hormone metabolites in bile and feces. *Vitam Horm*, 1971. 29: p. 201-85.
42. Payne, A.H. and D.B. Hales, Overview of steroidogenic enzymes in the pathway from cholesterol to active steroid hormones. *Endocr Rev*, 2004. 25(6): p. 947-70.
43. Mikael Häggström, S., Hoffmeier, Settersr, Richfield, Diagram of the pathways of human steroidogenesis. *WikiJournal of Medicine*, 2014. 1(1).
44. Hanukoglu, I., Steroidogenic enzymes: structure, function, and role in regulation of steroid hormone biosynthesis. *J Steroid Biochem Mol Biol*, 1992. 43(8): p. 779-804.
45. Thomas, J.L., et al., Structure/function relationships responsible for coenzyme specificity and the isomerase activity of human type 1 3 beta-hydroxysteroid dehydrogenase/isomerase. *J Biol Chem*, 2003. 278(37): p. 35483-90.
46. Thomas, J.L., et al., An NADH-induced conformational change that mediates the sequential 3 beta-hydroxysteroid dehydrogenase/isomerase activities is supported by affinity labeling and the time-dependent activation of isomerase. *J Biol Chem*, 1995. 270(36): p. 21003-8.
47. Curnow, K.M., et al., The product of the CYP11B2 gene is required for aldosterone biosynthesis in the human adrenal cortex. *Molecular endocrinology*, 1991. 5(10): p. 1513-22.
48. Mornet, E., et al., Characterization of two genes encoding human steroid 11 beta-hydroxylase (P-450(11) beta). *J Biol Chem*, 1989. 264(35): p. 20961-7.
49. Amor, M., et al., Mutation in the CYP21B gene (Ile-172----Asn) causes steroid 21-hydroxylase deficiency. *Proc Natl Acad Sci U S A*, 1988. 85(5): p. 1600-4.
50. Swart, P., et al., Progesterone 16 alpha-hydroxylase activity is catalyzed by human cytochrome P450 17 alpha-hydroxylase. *J Clin Endocrinol Metab*, 1993. 77(1): p. 98-102.
51. Lisurek, M. and R. Bernhardt, Modulation of aldosterone and cortisol synthesis on the molecular level. *Mol Cell Endocrinol*, 2004. 215(1-2): p. 149-59.
52. Auchus, R.J., T.C. Lee, and W.L. Miller, Cytochrome b5 augments the 17,20-lyase activity of human P450c17 without direct electron transfer. *J Biol Chem*, 1998. 273(6): p. 3158-65.
53. Geissler, W.M., et al., Male pseudohermaphroditism caused by mutations of testicular 17 beta-hydroxysteroid dehydrogenase 3. *Nat Genet*, 1994. 7(1): p. 34-9.
54. Russell, D.W. and J.D. Wilson, Steroid 5 alpha-reductase: two genes/two enzymes. *Annu Rev Biochem*, 1994. 63: p. 25-61.
55. Simpson, E.R., et al., Aromatase cytochrome P450, the enzyme responsible for estrogen biosynthesis. *Endocr Rev*, 1994. 15(3): p. 342-55.
56. Labrie, F., Extragonadal synthesis of sex steroids: intracrinology. *Annales d'endocrinologie*, 2003. 64(2): p. 95-107.
57. Blouin, K., et al., Androgen metabolism in adipose tissue: recent advances. *Mol Cell Endocrinol*, 2009. 301(1-2): p. 97-103.
58. Luu-The, V., A. Belanger, and F. Labrie, Androgen biosynthetic pathways in the human prostate. *Best Pract Res Clin Endocrinol Metab*, 2008. 22(2): p. 207-21.
59. Labrie, F., et al., Intracrinology and the skin. *Horm Res*, 2000. 54(5-6): p. 218-29.

60. Mensah-Nyagan, A.G., et al., Neurosteroids: expression of steroidogenic enzymes and regulation of steroid biosynthesis in the central nervous system. *Pharmacol Rev*, 1999. 51(1): p. 63-81.
61. Bouguen, G., et al., Intestinal steroidogenesis. *Steroids*, 2015. 103: p. 64-71.
62. Luu-The, V., Assessment of steroidogenesis and steroidogenic enzyme functions. *J Steroid Biochem Mol Biol*, 2013. 137: p. 176-82.
63. Miller, W.L. and R.J. Auchus, The molecular biology, biochemistry, and physiology of human steroidogenesis and its disorders. *Endocr Rev*, 2011. 32(1): p. 81-151.
64. Jez, J.M., et al., Comparative anatomy of the aldo-keto reductase superfamily. *Biochem J*, 1997. 326 ( Pt 3): p. 625-36.
65. Penning, T.M., et al., Human 3alpha-hydroxysteroid dehydrogenase isoforms (AKR1C1-AKR1C4) of the aldo-keto reductase superfamily: functional plasticity and tissue distribution reveals roles in the inactivation and formation of male and female sex hormones. *Biochem J*, 2000. 351(Pt 1): p. 67-77.
66. Jornvall, H., et al., Short-chain dehydrogenases/reductases (SDR). *Biochemistry*, 1995. 34(18): p. 6003-13.
67. Hanukoglu, I., Proteopedia: Rossmann fold: A beta-alpha-beta fold at dinucleotide binding sites. *Biochem Mol Biol Educ*, 2015. 43(3): p. 206-9.
68. Marchais-Oberwinkler, S., et al., 17beta-Hydroxysteroid dehydrogenases (17beta-HSDs) as therapeutic targets: protein structures, functions, and recent progress in inhibitor development. *J Steroid Biochem Mol Biol*, 2011. 125(1-2): p. 66-82.
69. Bhatia, C., et al., Towards a systematic analysis of human short-chain dehydrogenases/reductases (SDR): Ligand identification and structure-activity relationships. *Chem Biol Interact*, 2015. 234: p. 114-25.
70. Luu-The, V. and F. Labrie, The intracrine sex steroid biosynthesis pathways. *Prog Brain Res*, 2010. 181: p. 177-92.
71. Prehn, C., G. Moller, and J. Adamski, Recent advances in 17beta-hydroxysteroid dehydrogenases. *J Steroid Biochem Mol Biol*, 2009. 114(1-2): p. 72-7.
72. Wang, J., et al., Activity of human 11-cis-retinol dehydrogenase (Rdh5) with steroids and retinoids and expression of its mRNA in extra-ocular human tissue. *Biochem J*, 1999. 338 ( Pt 1): p. 23-7.
73. Dufort, I., et al., Characteristics of a highly labile human type 5 17beta-hydroxysteroid dehydrogenase. *Endocrinology*, 1999. 140(2): p. 568-74.
74. Lukacik, P., K.L. Kavanagh, and U. Oppermann, Structure and function of human 17beta-hydroxysteroid dehydrogenases. *Mol Cell Endocrinol*, 2006. 248(1-2): p. 61-71.
75. Moeller, G. and J. Adamski, Integrated view on 17beta-hydroxysteroid dehydrogenases. *Mol Cell Endocrinol*, 2009. 301(1-2): p. 7-19.
76. Haller, F., et al., Molecular framework of steroid/retinoid discrimination in 17beta-hydroxysteroid dehydrogenase type 1 and photoreceptor-associated retinol dehydrogenase. *J Mol Biol*, 2010. 399(2): p. 255-67.
77. Agarwal, A.K. and R.J. Auchus, Minireview: cellular redox state regulates hydroxysteroid dehydrogenase activity and intracellular hormone potency. *Endocrinology*, 2005. 146(6): p. 2531-8.

78. Maser, E., Xenobiotic carbonyl reduction and physiological steroid oxidoreduction. The pluripotency of several hydroxysteroid dehydrogenases. *Biochem Pharmacol*, 1995. 49(4): p. 421-40.
79. Matsunaga, T., S. Shintani, and A. Hara, Multiplicity of mammalian reductases for xenobiotic carbonyl compounds. *Drug Metab Pharmacokinet*, 2006. 21(1): p. 1-18.
80. Rotinen, M., J. Villar, and I. Encio, Regulation of 17beta-hydroxysteroid dehydrogenases in cancer: regulating steroid receptor at pre-receptor stage. *J Physiol Biochem*, 2012. 68(3): p. 461-73.
81. Moghrabi, N., et al., Deleterious missense mutations and silent polymorphism in the human 17beta-hydroxysteroid dehydrogenase 3 gene (HSD17B3). *J Clin Endocrinol Metab*, 1998. 83(8): p. 2855-60.
82. Miller, W.L., Steroidogenic enzymes. *Endocrine development*, 2008. 13: p. 1-18.
83. Wu, L., et al., Expression cloning and characterization of human 17 beta-hydroxysteroid dehydrogenase type 2, a microsomal enzyme possessing 20 alpha-hydroxysteroid dehydrogenase activity. *The Journal of biological chemistry*, 1993. 268(17): p. 12964-9.
84. Labrie, Y., et al., The human type II 17 beta-hydroxysteroid dehydrogenase gene encodes two alternatively spliced mRNA species. *DNA and cell biology*, 1995. 14(10): p. 849-61.
85. Durocher, F., et al., Mapping of the HSD17B2 gene encoding type II 17 beta-hydroxysteroid dehydrogenase close to D16S422 on chromosome 16q24.1-q24.2. *Genomics*, 1995. 25(3): p. 724-6.
86. Tsachaki, M., et al., Determination of the topology of endoplasmic reticulum membrane proteins using redox-sensitive green-fluorescence protein fusions. *Biochim Biophys Acta*, 2015. 1853(7): p. 1672-82.
87. Puranen, T., et al., Characterization of structural and functional properties of human 17 beta-hydroxysteroid dehydrogenase type 1 using recombinant enzymes and site-directed mutagenesis. *Molecular endocrinology*, 1997. 11(1): p. 77-86.
88. Dumont, M., et al., Expression of human 17 beta-hydroxysteroid dehydrogenase in mammalian cells. *The Journal of steroid biochemistry and molecular biology*, 1992. 41(3-8): p. 605-8.
89. Peltoketo, H., et al., Complete amino acid sequence of human placental 17 beta-hydroxysteroid dehydrogenase deduced from cDNA. *FEBS letters*, 1988. 239(1): p. 73-7.
90. Takeyama, J., et al., 17beta-hydroxysteroid dehydrogenase type 1 and 2 expression in the human fetus. *The Journal of clinical endocrinology and metabolism*, 2000. 85(1): p. 410-6.
91. Sawetawan, C., et al., Compartmentalization of type I 17 beta-hydroxysteroid oxidoreductase in the human ovary. *Molecular and cellular endocrinology*, 1994. 99(2): p. 161-8.
92. Poutanen, M., et al., Immunological analysis of 17 beta-hydroxysteroid dehydrogenase in benign and malignant human breast tissue. *International journal of cancer*, 1992. 50(3): p. 386-90.
93. Hernlund, E., et al., Osteoporosis in the European Union: medical management, epidemiology and economic burden. A report prepared in collaboration with the International Osteoporosis Foundation (IOF) and the European Federation of Pharmaceutical Industry Associations (EFPIA). *Arch Osteoporos*, 2013. 8: p. 136.
94. Glaser, D.L. and F.S. Kaplan, Osteoporosis. Definition and clinical presentation. *Spine*, 1997. 22(24 Suppl): p. 12S-16S.

95. Compston, J.E., Sex steroids and bone. *Physiological reviews*, 2001. 81(1): p. 419-447.
96. Riggs, B.L., S. Khosla, and L.J. Melton, 3rd, A unitary model for involutinal osteoporosis: estrogen deficiency causes both type I and type II osteoporosis in postmenopausal women and contributes to bone loss in aging men. *Journal of bone and mineral research : the official journal of the American Society for Bone and Mineral Research*, 1998. 13(5): p. 763-73.
97. Chin, K.Y. and S. Ima-Nirwana, Sex steroids and bone health status in men. *International journal of endocrinology*, 2012. 2012: p. 208719.
98. Michael, H., et al., Estrogen and testosterone use different cellular pathways to inhibit osteoclastogenesis and bone resorption. *Journal of bone and mineral research : the official journal of the American Society for Bone and Mineral Research*, 2005. 20(12): p. 2224-32.
99. Lewiecki, E.M., Current and emerging pharmacologic therapies for the management of postmenopausal osteoporosis. *Journal of women's health*, 2009. 18(10): p. 1615-26.
100. Khan, M., A.M. Cheung, and A.A. Khan, Drug-Related Adverse Events of Osteoporosis Therapy. *Endocrinology and metabolism clinics of North America*, 2017. 46(1): p. 181-192.
101. Bagi, C.M., et al., Effect of 17beta-hydroxysteroid dehydrogenase type 2 inhibitor on bone strength in ovariectomized cynomolgus monkeys. *Journal of musculoskeletal & neuronal interactions*, 2008. 8(3): p. 267-80.
102. Wolber, G., A.A. Dornhofer, and T. Langer, Efficient overlay of small organic molecules using 3D pharmacophores. *Journal of computer-aided molecular design*, 2006. 20(12): p. 773-88.
103. Wolber, G. and T. Langer, LigandScout: 3-D pharmacophores derived from protein-bound ligands and their use as virtual screening filters. *Journal of chemical information and modeling*, 2005. 45(1): p. 160-9.
104. Routledge, E.J., et al., Some alkyl hydroxy benzoate preservatives (parabens) are estrogenic. *Toxicol Appl Pharmacol*, 1998. 153(1): p. 12-9.
105. Pugazhendhi, D., G.S. Pope, and P.D. Darbre, Oestrogenic activity of p-hydroxybenzoic acid (common metabolite of paraben esters) and methylparaben in human breast cancer cell lines. *J Appl Toxicol*, 2005. 25(4): p. 301-9.
106. Okubo, T., et al., ER-dependent estrogenic activity of parabens assessed by proliferation of human breast cancer MCF-7 cells and expression of ERalpha and PR. *Food Chem Toxicol*, 2001. 39(12): p. 1225-32.
107. Darbre, P.D., et al., Oestrogenic activity of benzylparaben. *J Appl Toxicol*, 2003. 23(1): p. 43-51.
108. Daniel, J.W., Metabolic aspects of antioxidants and preservatives. *Xenobiotica*, 1986. 16(10-11): p. 1073-8.
109. Final amended report on the safety assessment of Methylparaben, Ethylparaben, Propylparaben, Isopropylparaben, Butylparaben, Isobutylparaben, and Benzylparaben as used in cosmetic products. *Int J Toxicol*, 2008. 27 Suppl 4: p. 1-82.
110. Wetzal, M., S. Marchais-Oberwinkler, and R.W. Hartmann, 17beta-HSD2 inhibitors for the treatment of osteoporosis: Identification of a promising scaffold. *Bioorganic & medicinal chemistry*, 2011. 19(2): p. 807-15.
111. Schuster, D., et al., Discovery of nonsteroidal 17beta-hydroxysteroid dehydrogenase 1 inhibitors by pharmacophore-based screening of virtual compound libraries. *J Med Chem*, 2008. 51(14): p. 4188-99.



112. Soni, M.G., I.G. Carabin, and G.A. Burdock, Safety assessment of esters of p-hydroxybenzoic acid (parabens). *Food Chem Toxicol*, 2005. 43(7): p. 985-1015.
113. Byne, W., Developmental endocrine influences on gender identity: implications for management of disorders of sex development. *Mt Sinai J Med*, 2006. 73(7): p. 950-9.
114. Evaluation of the newborn with developmental anomalies of the external genitalia. American Academy of Pediatrics. Committee on Genetics. *Pediatrics*, 2000. 106(1 Pt 1): p. 138-42.
115. Wilson, J.D., Sexual differentiation. *Annu Rev Physiol*, 1978. 40: p. 279-306.
116. Tong, S.Y., J.M. Hutson, and L.M. Watts, Does testosterone diffuse down the wolffian duct during sexual differentiation? *J Urol*, 1996. 155(6): p. 2057-9.
117. Josso, N., et al., Testicular anti-Mullerian hormone: history, genetics, regulation and clinical applications. *Pediatr Endocrinol Rev*, 2006. 3(4): p. 347-58.
118. Mendonca, B.B., et al., 46,XY Disorders of Sexual Development, in *Endotext*, L.J. De Groot, et al., Editors. 2000: South Dartmouth (MA).
119. Hassan, H.A., et al., Mutational Profile of 10 Afflicted Egyptian Families with 17-beta-HSD-3 Deficiency. *Sex Dev*, 2016. 10(2): p. 66-73.
120. Mendonca, B.B., et al., 46,XY disorder of sex development (DSD) due to 17beta-hydroxysteroid dehydrogenase type 3 deficiency. *J Steroid Biochem Mol Biol*, 2017. 165(Pt A): p. 79-85.
121. Samtani, R., et al., SRD5A2 gene mutations--a population-based review. *Pediatr Endocrinol Rev*, 2010. 8(1): p. 34-40.
122. Luu-The, V., Analysis and characteristics of multiple types of human 17beta-hydroxysteroid dehydrogenase. *J Steroid Biochem Mol Biol*, 2001. 76(1-5): p. 143-51.
123. Inano, H. and B. Tamaoki, Testicular 17 beta-hydroxysteroid dehydrogenase: molecular properties and reaction mechanism. *Steroids*, 1986. 48(1-2): p. 1-26.
124. Saez, J.M., et al., Familial male pseudohermaphroditism with gynecomastia due to a testicular 17-ketosteroid reductase defect. I. Studies in vivo. *J Clin Endocrinol Metab*, 1971. 32(5): p. 604-10.
125. George, M.M., et al., The clinical and molecular heterogeneity of 17betaHSD-3 enzyme deficiency. *Horm Res Paediatr*, 2010. 74(4): p. 229-40.
126. Castro, C.C., et al., Clinical and molecular spectrum of patients with 17beta-hydroxysteroid dehydrogenase type 3 (17-beta-HSD3) deficiency. *Arq Bras Endocrinol Metabol*, 2012. 56(8): p. 533-9.
127. Engeli, R.T., et al., Biochemical analyses and molecular modeling explain the functional loss of 17beta-hydroxysteroid dehydrogenase 3 mutant G133R in three Tunisian patients with 46, XY Disorders of Sex Development. *J Steroid Biochem Mol Biol*, 2016. 155(Pt A): p. 147-54.
128. Rosler, A. and G. Kohn, Male pseudohermaphroditism due to 17 beta-hydroxysteroid dehydrogenase deficiency: studies on the natural history of the defect and effect of androgens on gender role. *J Steroid Biochem*, 1983. 19(1B): p. 663-74.
129. Cheon, C.K., Practical approach to steroid 5alpha-reductase type 2 deficiency. *Eur J Pediatr*, 2011. 170(1): p. 1-8.
130. Barbaro, M., A. Wedell, and A. Nordenstrom, Disorders of sex development. *Semin Fetal Neonatal Med*, 2011. 16(2): p. 119-27.

131. Morris, J.M., The syndrome of testicular feminization in male pseudohermaphrodites. *Am J Obstet Gynecol*, 1953. 65(6): p. 1192-1211.
132. Hughes, I.A., Disorders of sex development: a new definition and classification. *Best Pract Res Clin Endocrinol Metab*, 2008. 22(1): p. 119-34.
133. Liao, G., et al., Regulation of androgen receptor activity by the nuclear receptor corepressor SMRT. *J Biol Chem*, 2003. 278(7): p. 5052-61.
134. Hughes, I.A., A novel explanation for resistance to androgens. *N Engl J Med*, 2000. 343(12): p. 881-2.
135. Melo, K.F., et al., Clinical, hormonal, behavioral, and genetic characteristics of androgen insensitivity syndrome in a Brazilian cohort: five novel mutations in the androgen receptor gene. *J Clin Endocrinol Metab*, 2003. 88(7): p. 3241-50.
136. Wilson, J.D., Androgens, androgen receptors, and male gender role behavior. *Horm Behav*, 2001. 40(2): p. 358-66.
137. Houk, C.P., et al., Summary of consensus statement on intersex disorders and their management. International Intersex Consensus Conference. *Pediatrics*, 2006. 118(2): p. 753-7.
138. Rosler, A., Steroid 17beta-hydroxysteroid dehydrogenase deficiency in man: an inherited form of male pseudohermaphroditism. *J Steroid Biochem Mol Biol*, 1992. 43(8): p. 989-1002.
139. de Vries, A.L., T.A. Doreleijers, and P.T. Cohen-Kettenis, Disorders of sex development and gender identity outcome in adolescence and adulthood: understanding gender identity development and its clinical implications. *Pediatr Endocrinol Rev*, 2007. 4(4): p. 343-51.
140. Pelliniemi, L.J. and M. Niemi, Fine structure of the human foetal testis. I. The interstitial tissue. *Z Zellforsch Mikrosk Anat*, 1969. 99(4): p. 507-22.
141. Hou, J.W., D.C. Collins, and R.L. Schleicher, Sources of cholesterol for testosterone biosynthesis in murine Leydig cells. *Endocrinology*, 1990. 127(5): p. 2047-55.
142. Maqbool, F., et al., Review of endocrine disorders associated with environmental toxicants and possible involved mechanisms. *Life Sci*, 2016. 145: p. 265-73.
143. Andersson, A.M., et al., Endocrine disrupters: we need research, biomonitoring and action. *Andrology*, 2016. 4(4): p. 556-60.
144. Luccio-Camelo, D.C. and G.S. Prins, Disruption of androgen receptor signaling in males by environmental chemicals. *J Steroid Biochem Mol Biol*, 2011. 127(1-2): p. 74-82.
145. Kiyama, R. and Y. Wada-Kiyama, Estrogenic endocrine disruptors: Molecular mechanisms of action. *Environ Int*, 2015. 83: p. 11-40.
146. Ascoli, M. and D. Puett, Gonadotropin binding and stimulation of steroidogenesis in Leydig tumor cells. *Proc Natl Acad Sci U S A*, 1978. 75(1): p. 99-102.
147. Ascoli, M., Characterization of several clonal lines of cultured Leydig tumor cells: gonadotropin receptors and steroidogenic responses. *Endocrinology*, 1981. 108(1): p. 88-95.
148. Roelofs, M.J., et al., Structural bisphenol analogues differentially target steroidogenesis in murine MA-10 Leydig cells as well as the glucocorticoid receptor. *Toxicology*, 2015. 329: p. 10-20.
149. Nokelainen, P., et al., Molecular cloning of mouse 17 beta-hydroxysteroid dehydrogenase type 1 and characterization of enzyme activity. *Eur J Biochem*, 1996. 236(2): p. 482-90.

150. Forgacs, A.L., et al., BLTK1 murine Leydig cells: a novel steroidogenic model for evaluating the effects of reproductive and developmental toxicants. *Toxicol Sci*, 2012. 127(2): p. 391-402.
151. Auchus, R.J., The backdoor pathway to dihydrotestosterone. *Trends Endocrinol Metab*, 2004. 15(9): p. 432-8.
152. Fluck, C.E., et al., Why boys will be boys: two pathways of fetal testicular androgen biosynthesis are needed for male sexual differentiation. *Am J Hum Genet*, 2011. 89(2): p. 201-18.